Bulletin 656

BLASTING VIBRATIONS AND THEIR EFFECTS ON STRUCTURES

By Harry R. Nicholls, Charles F. Johnson, and Wilbur I. Duvall

US Department of Interior
Office of Surface Mining
Reclamation and Enforcement

Kenneth K. Eltschlager
Mining/Explosives Engineer
3 Parkway Center
Pittsburgh, PA 15220

Phone 412.937.2169
Fax 412.937.3012
Keltschl@osmre.gov

UNITED STATES DEPARTMENT OF THE INTERIOR

BUREAU OF MINES

CONTENTS

ILLUSTRATIONS

Fig.		Page

TABLES

LIST OF SYMBOLS

A	— Amplitude of vibration for displacement, velocity, or acceleration.
A_a	— Trace deflection for acceleration.
A_d	— Trace deflection for displacement.
A_v	— Trace deflection for particle velocity.
a	— Peak acceleration.
a_h	— Peak horizontal acceleration.
a_v	— Peak vertical acceleration.
b	— Exponent of charge weight in general propagation law.
D	— Distance.
E. R.	— Energy Ratio.
F	— Driving force.
F_v	— Vertical force.
f	— Frequency.
g	— Acceleration of gravity.
H	— Particle velocity intercept for scaled propagation equation.
K	— Intercept of regression line.
k	— Constant or intercept of regression line.
k_a	— Proportionality constant or magnification for acceleration seismograph.
k_d	— Proportionality constant or magnification for displacement seismograph.
k_v	— Proportionality constant or magnification for velocity seismograph.
m	— Mass.
n	— Exponent.
P	— Peak overpressure.
R	— Radial component of motion.
r	— Damping factor.
r_c	— Critical damping factor.
s	— Spring constant.
T	— Transverse component of motion.
t	— Time.
u	— Peak displacement.
v	— Peak velocity.
V	— Vertical component of motion.
W	— Charge weight.
x	— Instantaneous amplitude of indicated displacement.
x_1, x_2, x_3	— x coordinates.
x_c	— x coordinate for center of gravity.
y_1, y_2, y_3	— y coordinates.
y_c	— y coordinate for center of gravity.
α	— Exponent of charge weight in scaled propagation law.
β	— Exponent in scaled propagation law.
θ	— Angle.
μ	— Coefficient of friction.
σ	— Standard deviation about the regression line.
Φ	— Phase angle.
ω	— Angular frequency.

BLASTING VIBRATIONS AND THEIR EFFECTS ON STRUCTURES

by

Harry R. Nicholls,[1] Charles F. Johnson,[2] and Wilbur I. Duvall[3]

ABSTRACT

This report presents the results of the Bureau of Mines 10-year program to study the problem of air blast and ground vibrations generated by blasting. The program included an extensive field study of ground vibrations; a consideration of air blast effects; an evaluation of instrumentation to measure vibrations; establishment of damage criteria for residential structures; determination of blasting parameters which grossly affected vibrations; empirical safe blasting limits; and the problem of human response. While values of 2.0 in/sec particle velocity and 0.5 psi air blast overpressure are recommended as safe blasting limits not to be exceeded to preclude damage to residential structures, lower limits are suggested to minimize complaints. Millisecond-delay blasting is shown to reduce vibration levels as compared to instantaneous blasting, and electric cap delay blasts offer a slight reduction in vibration levels as compared to Primacord delay blasts. Vibration levels of different blasts may be compared at common scaled distances, where scaled distance is the distance divided by the square root of the maximum charge weight per delay. Geology, rock type, and direction affect vibration level within limits. Empirically, a safe blasting limit based on a scaled distance of 50 ft/lb$^{1/2}$ may be used without instrumentation. However, a knowledge of the particle velocity propagation characteristics of a blasting site determined from instrumented blasts at that site are recommended to insure that the safe blasting limit of 2.0 in/sec is not exceeded.

CHAPTER 1.—GENERAL INTRODUCTION

1.1—INTRODUCTION

Using explosives to break rock generates air- and ground-borne vibrations which may have detrimental effects on nearby structures. A variety of complaints attributable to vibrations from blasting have always been received by the quarrying industry, producing stone or aggregate from surface excavations, the mining industry producing ore from open-pit mines, and the construction industry producing road cuts, pipe line, and foundation excavations. Blasting operations associated with underground mining and excavation work are relatively immune to these complaints, but if large-scale nuclear devices are used for mining purposes, complaints from underground blasting operations will become a major problem. This problem is currently being investigated by the Atomic Energy Commission (AEC).

Some complaints registered are legitimate claims of damage from vibrations generated by blasting. However, other complaints are not valid, and the reported damage has resulted from natural settling of building, poor construction, et cetera. In general, complaints have been sufficiently numerous to constitute a major problem for operators engaged in blasting and emphasize the need for technological data to evaluate vibration problems associated with blasting. Both the

[1] Supervisory geophysicist.
[2] Geophysicist.
[3] Supervisory research physical scientist. All authors are with the Denver Mining Research Center, Bureau of Mines, Denver, Colo.

operators and the general public need adequate safeguards based upon factual data to protect their specific interests. Industry needs a reliable basis on which to plan and conduct blasting operations to minimize or abolish legitimate damage claims and eliminate the nuisance variety of complaint. The public would benefit by the absence of conditions which would create damage. The problem has been of major concern to Federal, State, and local governments, industries engaged in blasting, explosive manufacturers, insurance companies, and scientists.

During the post World War II period, the growth in population, urbanization, new highway programs, and the need for more construction materials increased the problem of complaints from blasting. In addition, the need for quarries and construction near urban centers and the simultaneous urban sprawl acted to bring operators engaged in blasting and the public into a closer physical contact. In many cases, housing and public buildings were actually built on property adjoining quarries. Naturally, the number of complaints increased drastically. During the same time period, rapid advancements and improvements were made in applicable instrumentation, primarily seismic gages, amplifiers, and recording equipment. There was also extensive research in closely related fields. The Defense Department and other groups studied damage to structures from explosive and other impulse-type loading. The Bureau of Mines and other investigators studied both empirically and theoretically, the generation and propagation of seismic waves in rock and other media.

In 1958 the Bureau of Mines decided to reinvestigate blasting vibration phenomena because of the pressing need for additional blasting vibration information, the availability of improved seismic instrumentation, and the availability of applicable seismic information from investigators in other disciplines. To assure that the research effort was directed toward the solution of the most urgent problems, industry support was solicited and obtained to establish a cooperative research program.

1.2 INDUSTRY MEETING

In 1959 representatives of the cooperating groups, quarry operators, scientists from industry and educational institutions, and members of the Bureau of Mines technical staff engaged in blasting research attended a conference, held at the Bureau of Mines facility at College Park, Maryland. As a result, a comprehensive research program on blasting vibrations and their effects on structures was developed and initiated by the Bureau. The major objectives of this program were

1. To establish reliable damage criteria, i.e., the relationship between the magnitude of the ground vibrations and the damage produced in a structure and

2. To establish a propagation law for ground-borne surface vibrations that could be used to predict the relationship between the magnitude of the ground vibration and the size of the explosive charge, the effect of shot-to-measurement point distance, and the other variables which have a major effect on the magnitude or character of the ground vibrations. The other variables might include explosive type, method of initiation, geology, and directional effects.

Additional objectives were to evaluate the vibration measuring equipment currently used and to develop specifications for new instrumentation, if warranted. The degree of significance of air blast in causing damage to structures was also to be established.

1.3 HISTORY

Many investigations had been conducted both in the U.S. and other countries on the effects of air and ground vibrations from blasting on residential and other type structures. One of the first such studies reported in this country was made in 1927 by Rockwell (*8*).[4] From blast-effect studies instrumented with displacement seismographs and falling-pin gauges, Rockwell concluded that quarry blasting, as normally conducted, would not produce damage to residential structures if they were more than 200 to 300 feet distant from the quarry. He also pointed out the need for "securing accurate quantitative measurements of the vibrations produced by blasting".

The Bureau of Mines conducted an extensive investigation of the problem of seismic effects of quarry blasting during the period 1930 to 1940. This study represented the first major effort to establish damage criteria for residential structures and to develop a generalized propagation law for ground vibrations (*11*). The recommended criteria of damage were based upon the resultant acceleration experienced by the structures. Consideration of all data indicated an acceleration of 1.0 g was the best index of damage. Accelerations ranging between 0.1 g and 1.0 g

[4] Italic numbers in parentheses refer to references at the end of each chapter.

resulted in slight damage. Accelerations of less than 0.1 g resulted in no damage. A propagation law relating displacement amplitude, charge weight, and distance was developed empirically from data from many quarry blasts, but its use was recommended only within specified distances and charge weights.

In 1943 the Bureau published the results of a study on the effect of air blast waves on structures (*12*). The results indicated that windows were always the first portion of a structure to be damaged. An overpressure of 0.7 psi or less would result in no window damage, while overpressures of 1.5 psi or more would definitely produce damage. The main conclusion of this study was that damage from air blast was not a major problem in normal quarry operations.

Damage criteria for structures subjected to vibration were advanced by Crandell in 1949 (*1*) and were based upon measured vibration levels in the ground near the structure. A consideration of the energy transmitted through the ground resulted in his use of the quantity identified as Energy Ratio (E.R.) and defined as the ratio of the square of the acceleration in feet per second squared and the square of the frequency in cycles per second. His tests showed that when the Energy Ratio in the ground was less than 3.0, 3.0 to 6.0, and greater than 6.0, nearby structures were in damage zones considered safe, caution, and danger, respectively. Crandell pointed out that displacement and frequency could also be used to determine the Energy Ratio.

In 1950 Sutherland reported (*9*) the results of a study of vibrations produced in structures by passing vehicles. No harmful effects on the structures were associated with vibrations from the nearby movement of heavy vehicles. It was shown that people perceived vibrations at much lower levels than would cause any damage to structures and that vibrations causing extreme discomfort to a person would barely cause plaster damage in a structure. Two additional published papers (*3, 4*) discussed the relationship of seismic amplitude and explosive charge size. Both established a propagation law for a specific site with little application elsewhere. In 1956 Jenkins (*5*) discussing the data of Reiher and Meister (*7*) on human response to vibratory motion and the response to blasting vibrations, stated that the public should be made aware of the fact that the average person can feel vibrations from one-hundredth to one-thousandth of the magnitude necessary to damage structures.

Several states and organizations adopted damage criteria during the period 1949 to 1960. For example, New Jersey and Massachusetts specified an Energy Ratio of 1.0 as the allowable limit for blasting operations. Pennsylvania adopted a displacement amplitude of 0.03 inch as a safe blasting limit. Blasting operations conducted by or for the U.S. Corps of Engineers and the New York State Power Authority specify a damage criterion based on an Energy Ratio of 1.0.

In 1957 Teichmann and Westwater (*10*) presented a brief but informative state-of-the-art summary on the subject of blasting vibrations, including ground movement, air blast, human susceptibility, legal aspects, and other topics.

In 1958, as the result of an extensive series of tests to study vibrations from blasting, Langefors, Kihlström, and Westerberg proposed damage criteria based on particle velocity in the ground near a structure (*6*). A particle velocity of 2.8 in/sec was cited as a damage threshold above which damage might begin to occur. In 1960 Edwards and Northwood presented the results of their study in which six structures were subjected to damage from vibrations due to blasting (*2*). From the evaluation of data obtained from an assortment of instrumentation, including acceleration, particle velocity, and displacement measurements, they concluded that particle velocity was the most reliable quantity on which to base damage criteria, and they proposed a safe limit of 2 in/sec particle velocity.

1.4 GENERAL APPROACH TO THE PROBLEM

The available data as discussed in section 1.3 and the general state of the art of the blasting vibration technology represented the starting point for the Bureau study. The first objective of the program was the development of reliable damage criteria. Since the acquisition of sufficient and reliable vibration damage data would be a long and costly process and since a considerable effort had been expended on this subject by the Bureau and other investigators, it was believed that the most profitable approach would be to conduct a comprehensive study to evaluate the published experimental data pertaining to damage. This study would determine if published data relating vibration amplitudes and frequencies to damage could be pooled to establish one set of reliable damage criteria. If the data could not be pooled, results would indicate the direction of further investigation to establish reliable damage criteria. Additional data involving damage from blasting vibrations would be obtained if possible. The determination of which quantity (displacement, particle velocity, or acceleration) was most closely associated with damage to structures would provide optimum selection of gages and instrumentation.

The use of three-component seismographs or gage stations enabling the recording of motion in three mutually perpendicular directions was considered a necessity, because seismic quantities, such as displacement, particle velocity, and acceleration are vector quantities. Examination of published vibration data from blasting revealed the serious limitation in the data that results when only one or two three-component stations were employed to record seismic data from any one shot. It was decided to use six to eight three-component gage stations as an array to record data from each quarry blast to overcome this limitation.

In the determination of a propagation law that would be useful at any site and to avoid considering the nearly infinite variety of structures, damage criteria were based on the vibration levels observed in the ground near the structure rather than on exposed rock or in structures. A comprehensive program to evaluate existing instrumentation was planned which included shaking table tests to study linearity, useful amplitude and frequency range, and a sensitivity calibration as a function of frequency and amplitude.

Most published data indicated that damage from air blast was insignificant in routine blasting operations. Evaluation of air blast effects was to be initiated after the major factors contributing to ground vibrations had been studied, rather than divide the recording capabilities to study the two phenomena simultaneously.

This report reviews and summarizes the Bureau program to restudy the problem of vibrations from quarry blasting. Data from 171 blasts at 26 different sites are presented. Published data from many other investigators have been considered in the analysis. The results include an evaluation of instrumentation, recommended instrumentation specifications, and gage placement procedures.

Recommendations for safe levels of vibration permissible in structures, safe levels of airblast overpressure, and human response and the resulting problems are discussed in Chapter 3. The generation and propagation of air blast and ground vibrations and the variables which grossly affect them are discussed in Chapters 4 and 5 and a general propagation law derived. Chapter 6 is devoted to the problem of estimating safe vibration levels.

1.5 REFERENCES[5]

1. Crandell, F. J. Ground Vibration Due to Blasting and Its Effects Upon Structures. J. Boston Soc. Civil Engineers, April 1949, pp. 222–245.
2. Edwards, A. T., and T. D. Northwood. Experimental Studies of the Effects of Blasting on Structures. The Engineer, v. 210, Sept. 30, 1960, pp. 538–546.
3. Habberjam, G. M., and J. R. Whetton. On the Relationship Between Seismic Amplitude and Charge of Explosive Fired in Routine Blasting Operations. Geophysics, v. 17, No. 1, January 1952, pp. 116–128.
4. Ito, Ichiro. On the Relationship Between Seismic Ground Amplitude and the Quantity of Explosives in Blasting. Reprint from Memoirs of the Faculty of Eng., Kyoto Univ., v. 15, No. 11, April 1953, pp. 579–587.
5. Jenkins, J. E. Human Response to Industrial Blasting Vibrations. AIME Trans., Mining Engineering, May 1956, pp. 535–538.
6. Langefors, U., Kihlström, B., and H. Westerberg. Ground Vibrations in Blasting. Water Power v. 10, February 1958, pp. 335–338, 390–395, 421–424.
7. Reiher, H., and F. J. Meister. Die Empfindlichkeit des Menschen gegen Erschuetterungen (Sensitivity of Human Beings to Vibration). Forschung auf dem Gebert des Ingenieurwesens (Berlin), v. 2, February 1931, pp. 381–386.
8. Rockwell, E. H. Vibrations Caused by Quarry Blasting and Their Effect on Structures. Rock Products, vol. 30, 1927, pp. 58–61.
9. Sutherland, H. B. A Study of Vibrations Produced in Structures by Heavy Vehicles. Proc. of the Thirtieth Annual Meeting of the Highway Research Board, Ottawa, December 1950, pp. 406–419.
10. Teichman, G. A., and R. Westwater. Blasting and Associated Vibrations. Engineering, April 12, 1957, pp. 460–465.
11. Thoenen, J. R., and S. L. Windes. Seismic Effects of Quarry Blasting. BuMines Bull. 442, 1942, 83 pp.
12. Windes, S. L. Damage From Air Blast. BuMines Rept. of Inv. 3708, 1943, 50 pp.

[5] Titles enclosed in parentheses are translations from the language in which the item was originally published.

CHAPTER 2.—INSTRUMENTATION

2.1—INTRODUCTION

The Bureau of Mines program of research in the field of vibrations from quarry blasting included objectives to evaluate currently used vibration-measuring equipment and to develop instrumentation for use in the research program. The instrumentation then widely used to monitor blast vibrations was of the portable seismograph type with three adjustable feet. These instruments were designed to measure displacement or acceleration and to record the components of motion along with timing lines on a moving strip of light sensitive paper. The tripod-like feet permitted easy leveling of the machines. However, some instability of the machines was noted, and a theoretical study of the stability of three-point mounted portable seismographs was made by Duvall (*1*). Calibration studies of three portable displacement seismographs and a portable acceleration seismograph were made (*4, 8*).

The instrumentation developed by the Bureau of Mines for measuring blasting vibrations was housed in a mobile van-type laboratory and consisted of particle velocity gages, amplifiers, and a direct writing oscillograph to record either particle velocity or displacement by integrating the particle velocity. Because airborne vibrations were recognized as a major factor in the complaints presented to agencies involved in blasting, gages to measure the airborne vibrations were included in the instrumentation. Mounting of particle velocity gages was subjected to critical examination, and a standard technique for coupling the gages to soil was devised (*6*).

The dynamic response of a seismic transducer is presented to provide the mathematical basis for a brief description of the three types of seismographs. The stability of three-point mounted seismographs and calibration studies of two types of portable seismographs are included to complete the objective of evaluating vibration measuring equipment. The instrumentation developed for use in the research program and the technique for coupling gages to the soil are briefly described.

2.2—THE DYNAMIC RESPONSE OF A SEISMIC TRANSDUCER

The typical portable seismograph consists of a seismic transducer, a timer, and a recording system. The recording system may be a peak-reading volt meter, a photographic paper recorder, or a direct-writing paper recorder. The timer is an accurate frequency generator which puts timing lines on the paper record. The seismic transducer is a device for converting ground motion to a varying voltage or to a similar motion of a spot of light which is recorded on a moving strip of light sensitive paper. Seismic transducers can be designed to respond linearly to either particle displacement, velocity, or acceleration.

A seismic transducer can be modeled by a mass-spring-dashpot system as shown in figure 2.1. The differential equation for such a system under forced vibration conditions is

$$m\frac{d^2x}{dt^2} + r\frac{dx}{dt} + sx = F \cos \omega t \qquad (2.1)$$

where t = time

x = instantaneous amplitude of indicated displacement

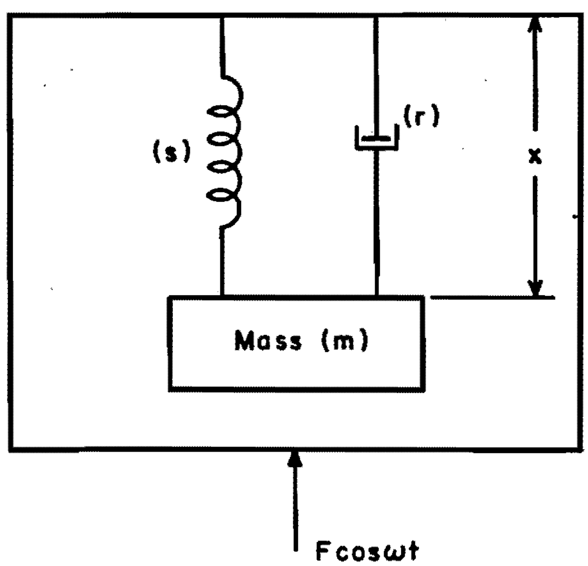

Figure 2.1.—Mass-spring-dashpot model of a seismic transducer.

m = inertial mass
r = damping factor
s = restoring force or spring constant
F = driving force acting on the system
ω = $2\pi f$ = angular frequency
f = frequency.

A solution to equation 2.1 is

$$x = \frac{F \cos(\omega t - \Phi)}{[r^2\omega^2 + (s - m\omega^2)^2]^{1/2}} \tag{2.2}$$

where the phase angle Φ is given by

$$\Phi = \tan^{-1} \frac{r\omega}{s - m\omega^2}. \tag{2.3}$$

The resonant frequency of the undamped system ($r = 0$) is

$$\omega_0 = 2\pi f_0 = \sqrt{s/m}. \tag{2.4}$$

The critical damping factor r_c is given by

$$r_c = 2m\omega_0. \tag{2.5}$$

From equations 2.4 and 2.5, equations 2.2 and 2.3 become

$$x = \frac{F \cos(\omega t - \Phi)}{m\omega^2[4(\frac{r}{r_c})^2(\frac{\omega_0}{\omega})^2 + (\frac{\omega_0^2}{\omega^2} - 1)^2]^{1/2}} \tag{2.6}$$

and

$$\Phi = \tan^{-1} \frac{2(\frac{\omega}{\omega_0})(\frac{r}{r_c})}{1 - (\frac{\omega}{\omega_0})^2}. \tag{2.7}$$

For a sinusoidal driving force the peak acceleration, a, is related to the peak velocity, v, and the peak displacement, u, by

$$a = \omega v = \omega^2 u \tag{2.8}$$

and the force required to drive the system is

$$F = ma. \tag{2.9}$$

Seismic transducers can be designed to measure the particle displacement, velocity, or acceleration of the driving force. Therefore, three basic transducer types are of interest.

2.2.1—Displacement Transducer

For a displacement transducer the driving force is represented by the peak displacement, u, and the trace deflection, A_u, on the record is proportional to the indicated displacement, x. Thus,

$$A_u = k_u x \tag{2.10}$$

where k_u is the proportionality constant. From equations 2.6, 2.8, and 2.9, equation 2.10 becomes

$$A_u = \frac{k_u u \cos(\omega t - \Phi)}{[4(\frac{r}{r_c})^2(\frac{\omega_0}{\omega})^2 + (\frac{\omega_0^2}{\omega^2} - 1)^2]^{1/2}}. \tag{2.11}$$

From equation 2.11, it is evident that as the driving frequency decreases from ω_0 to 0, that the trace amplitude decreases toward zero and that for driving frequencies large compared to ω_0, that the trace amplitude is proportional to the driving displacement and the constant k_u becomes the magnification constant for the transducer. Thus, an ideal displacement transducer should have a low resonant frequency which requires a low restoring force or spring constant and a large mass, and the useful operating frequency range is above the resonant frequency of the system. Typical theoretical response curves for a displacement transducer are shown in figure 2.2.

2.2.2—Velocity Transducer

For a velocity transducer the driving force is represented by the peak velocity, v, and the trace deflection is proportional to the rate of change of the indicated displacement. Thus,

$$A_v = k_v \frac{dx}{dt} \tag{2.12}$$

where k_v is the proportionality constant. From equations 2.6, 2.8, and 2.9, equation 2.12 becomes

$$A_v = -\frac{k_v v \sin(\omega t - \Phi)}{[4(\frac{r}{r_c})^2(\frac{\omega_0}{\omega})^2 + (\frac{\omega_0^2}{\omega^2} - 1)^2]^{1/2}}. \tag{2.13}$$

Equation 2.13 shows that as the driving frequency decreases from ω_0 to 0, the trace deflection decreases toward zero, and as the driving frequency becomes large compared to the resonant frequency, the trace amplitude becomes proportional to the driving velocity and the proportionality constant k_v becomes the magnification constant for the transducer. Thus, the theoretical response curves for a velocity transducer are identical in shape to those for a displacement transducer as given in figure 2.2.

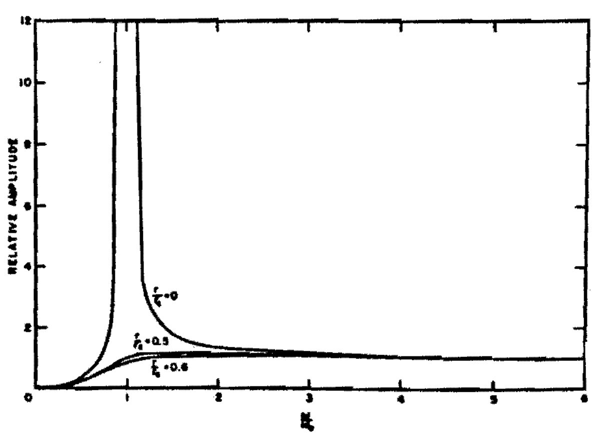

Figure 2.2.—Theoretical response curves for a typical displacement or velocity transducer.

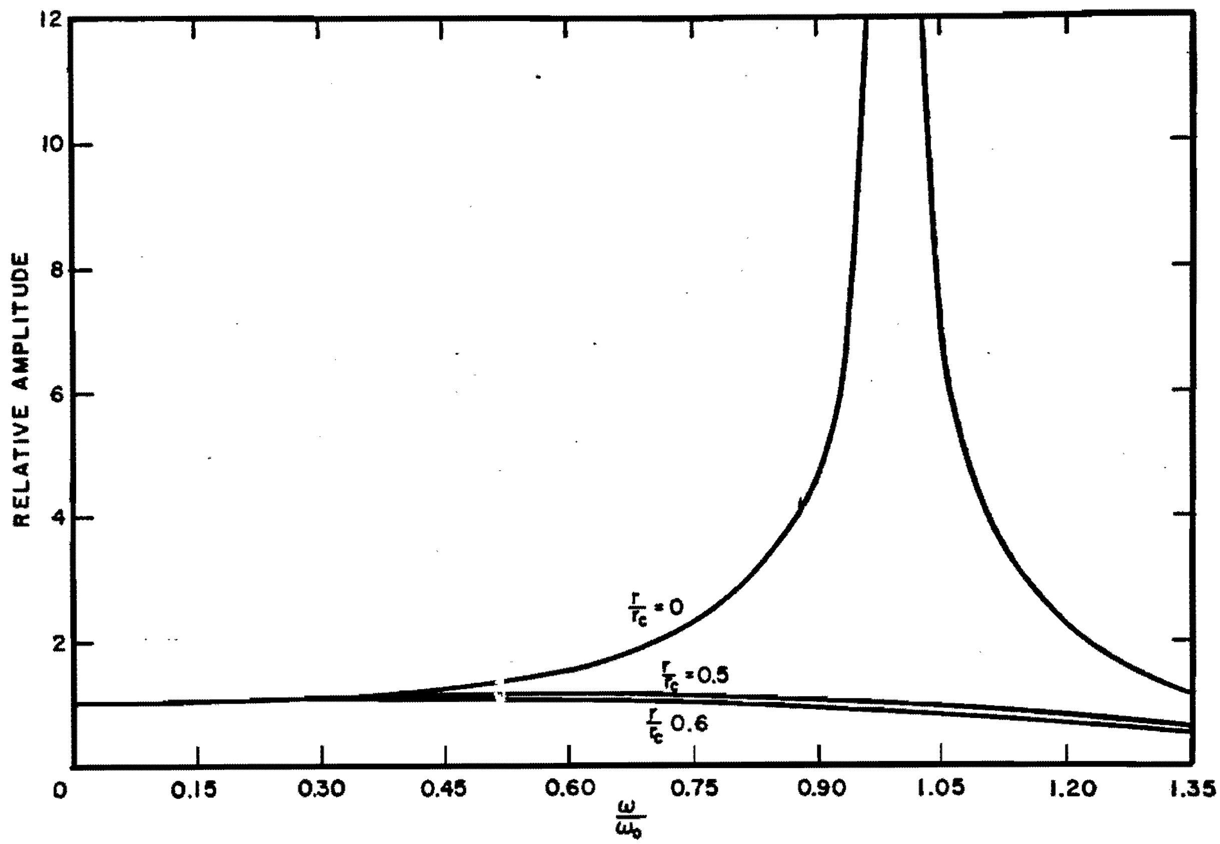

Figure 2.3.—Theoretical response curves for a typical acceleration transducer.

Therefore, an ideal velocity transducer should have a low resonant frequency, which implies a low spring constant and a large mass, and the useful operating frequency range lies above the resonant frequency of the system.

2.2.3—Acceleration Transducer

For an acceleration transducer, the driving force is represented by the peak acceleration, a, and the trace deflection is proportional to the indicated displacement. Thus,

$$A_a = k_a x \qquad (2.14)$$

where k_a is the proportionality constant. From equations 2.4, 2.6, 2.8, and 2.9, equation 2.14 becomes

$$A_a = \frac{k_a a \frac{m}{s} \cos(\omega t - \Phi)}{\left[4\left(\frac{r}{r_c}\right)^2\left(\frac{\omega}{\omega_o}\right)^2 + \left(1-\frac{\omega^2}{\omega_o^2}\right)^2\right]^{1/2}} \,. \qquad (2.15)$$

Equation 2.15 shows that as ω increases above ω_o, the trace deflection decreases to zero and as ω decreases from ω_o to 0, the trace deflection becomes proportional to the driving acceleration. The magnification of the transducer is $(k_a m)/s$. Typical theoretical response curves for an acceleration transducer are shown in figure 2.3. Thus, an ideal acceleration transducer should have a high resonant frequency which implies a large spring constant and a small mass, and the useful operating frequency range is below the resonant frequency of the system.

2.3—DESCRIPTIONS OF TYPICAL SEISMOGRAPHS

The typical portable displacement seismograph consists of a rigid case, with a three-point mount and leveling screws, which houses a timing mechanism, a recording mechanism, and three inertial pendulums having axes that are mutually perpendicular and oriented so that the motion of one is vertical and the other two are horizontal. Motions with respect to the inertial masses of the pendulums are indicated by the deflection of light beams on a strip of photographic paper. The beams of light are deflected by mirrors attached to the arms of the pendulums. The displacement of the case is magnified optically and mechanically so that the deflection of the light beam on the strip chart is 25 to 150 times greater than the case motion. The response of the displacement seismograph is described by equation 2.11. The resonant frequency is low (1–4 cps), and the trace deflection is proportional to the displacement. The dynamic range of the instrument is defined as the ratio of the largest usable deflection of the trace to the smallest that can be meaningfully measured. The dynamic range is limited by the slipping or tilting of the instrument and the width of the trace on the strip chart. Because the magnification of these instruments is fixed, the dynamic range is limited to about 20. Thus, a seismograph with a minimum trace deflection of 0.1 inch and a magnification of 150 would be capable of measuring displacements ranging from 0.000667 inch to 0.0133 inch at frequencies ranging from 5 to 40 cps.

The typical portable velocity seismograph system consists of two units. Three orthogonal gages are contained in a case. Electronic amplifiers, batteries, a light source, a timing device, galvanometers, and a recording camera are contained in a separate case. The case containing the gages is designed to match the soil density so it can be coupled firmly to the soil (*6*). Thus, it does not have the same limitation of dynamic range as do the three points or tripod-mounted displacement seismographs. The three gages measure the vertical and horizontal components of particle velocity. Each gage can be represented by a mass-spring-dashpot system whose response is described by equation 2.13. The resonant frequency of the gage is low, typically between 2 and 5 cps. Thus, the mass of the system is large, and the spring is soft. Because the magnification of the seismograph is variable and is dependent upon the electronic circuits, the dynamic range of the seismograph is large. Through the use of stable electronic circuits, the particle velocity output of the gages can be recorded directly or integrated to record displacement or differentiated to record acceleration. The camera records the light traces from the galvanometers on a moving strip of light sensitive paper along with timing marks generated by the timing device. These seismographs have a near-linear frequency response from about 2 to 250 cps.

The typical portable acceleration seismograph uses three external gages that can be positioned to measure the vertical and horizontal components of acceleration. Each gage can be modeled by a mass-spring-dashpot system, and its output is proportional to the gage displacement as shown by equation 2.15. The resonant frequency of the gage is high, usually 10 to 100 times the measured frequency. Thus, the mass is small, and the spring constant is large.

There are two general types of indicating and recording systems. Suitable electronic circuits may be employed to either cause a meter to deflect and indicate the peak vector output of the gages relative to standard gravity, or a light source and a galvanometer may be used to expose a moving strip of light sensitive paper. The latter system preserves the wave form, while the former indicates only the peak acceleration. Because the gages are not physically located in the case of the instrument, they can be attached to a type of mount that is not subject to the same limitations of acceleration as the three-point-mount displacement seismographs. As the magnification of this kind of seismograph is variable, the dynamic range is broad and is limited by the linear response of the electronics and indicating circuits, cables, and components. These seismographs have a useful operating frequency range from about 2 to 250 cps.

2.4—SEISMOGRAPH STABILITY

A seismograph which sits on the ground or the floor of a building can give false records if the instrument slips or tilts. The vibration level at which instability occurs is determined by the friction between the feet and the surface, the spacing of the feet, and the distribution of mass above them.

The rigid body motions of portable seismographs were theoretically investigated by Duvall (*1*). The rigid body motions of a portable seismograph are completely described when the translational and rotational motions are specified. The first condition for dynamic equilibrium is that there must be no rotation of the seismograph about a vertical axis, assuming that the three feet are frictionless. Figure 2.4 shows a cartesian coordinate system containing a lamina with three equal forces, F, acting at points (x_1, y_1), (x_2, y_2), and (x_3, y_3) at an angle θ from the axis. The center of gravity is at point (x_c, y_c). If there is to be no rotation about a vertical axis, the sum of the moments about the center of gravity must be zero. Thus:

$$(y_c - y_1) F \cos \theta + (y_c - y_2) F \cos \theta + (y_c - y_3) F \cos \theta + (x_c - x_1) F \sin \theta + (x_c - x_2) F \sin \theta + (x_c - x_3) F \sin \theta = 0. \tag{2.16}$$

If equation 2.16 is to be true for all values of θ,

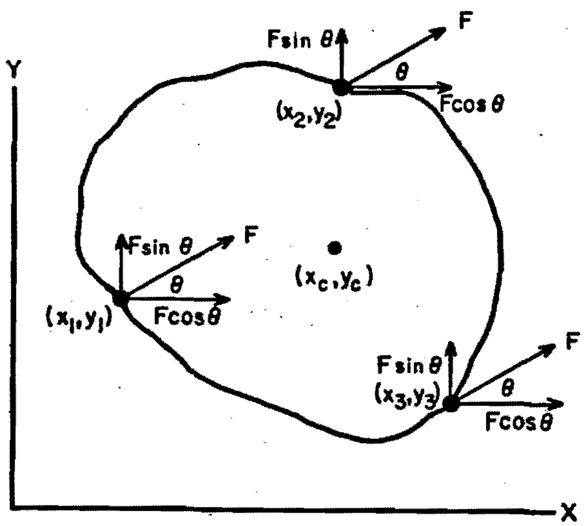

Figure 2.4.—Horizontal location of center of gravity of a lamina.

the sum of the coefficients of cos θ and sin θ must be zero.

Therefore,

$$x_c = \frac{x_1+x_2+x_3}{3}$$

and (2.17)

$$y_c = \frac{y_1+y_2+y_3}{3}.$$

Thus, the condition for no rotation about a vertical axis is that the center of gravity of the seismograph must be located at the centroid of the feet.

If the center of gravity of the seismograph were located at the centroid and in the plane of the feet, the same type of solution would hold for rotation about a horizontal axis. However, all portable seismographs have a center of gravity that is located some distance above the plane of the feet. This configuration is shown in figure 2.5.

The feet of the seismograph are located at points A, B, and C. Point 0 is the centroid of the triangle ABC. Because tilting will normally occur by the raising of one of the feet, the rotation axis will lie along the lines between two of the feet. For convenience, line AB has been selected for a rotation axis. The center of gravity of the seismograph is located above the plane of the feet at point G.

A motion of the surface in a direction normal to the line AB will cause a force to be generated to accelerate the mass. This force will be distributed among the feet so that each foot will

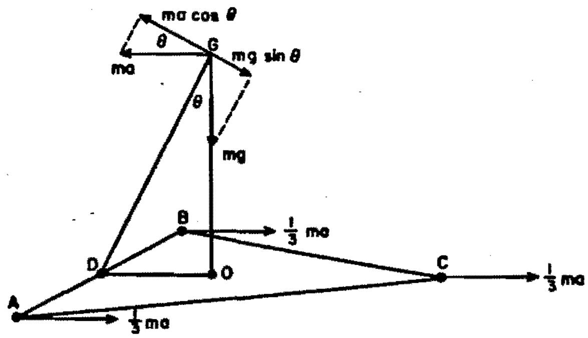

Figure 2.5.—Vertical location of center of gravity of a Seismograph.

contribute one-third of the total horizontal accelerating force ma_h, where m is the mass of the instrument and a_h is the horizontal acceleration. The inertial force resisting the driving force is then equal to it and opposite in direction. A second force mg due to gravity acting on the mass is directed downward.

The condition of no rotation about the axis AB is that the moment of the force ma_h be less than the moment of the force mg. Thus,

$$\overline{DG}\, ma_h \cos \Theta \leq \overline{DG}\, mg \sin \Theta$$

or (2.18)

$$a_h \leq g \tan \Theta.$$

The sliding of a seismograph is resisted by the friction between the feet and the surface. This frictional force is dependent upon the coefficient of friction, μ, and the mass of the machine, m. The condition of no slippage is that the inertial force must not exceed the frictional force. Thus,

$$ma_h \leq \mu\, mg. \quad (2.19)$$

Because the coefficient of friction is usually less than unity, slipping may occur at less than 1 g. When the seismograph is subjected to vibratory motion, the vertical force, F_v, may be thought of as oscillating about some steady value,

$$F_v = mg + ma_v \sin \omega t$$

where a_v is the vertical acceleration.

Therefore, the minimum vertical force is

$$F_v \min = m(g-a_v). \quad (2.20)$$

Thus, from equations 2.19 and 2.20, the maximum horizontal acceleration before slipping occurs is

$$a_h \max \leq \mu\ (g-a_v). \quad (2.21)$$

Equation 2.21 shows that horizontal accelerations of 1 g cannot be measured with a seismograph simply resting on a surface when it is subjected to vibratory motion. If the seismograph is spring loaded to the ground with an additional vertical force, accelerations greater than 1 g can be measured (7).

2.5—SEISMOGRAPH CALIBRATION

Three portable displacement seismographs and one acceleration measuring seismograph were calibrated in accordance with the objectives of the research program. The four seismographs that were tested were the Seismolog,[1] Sprengnether, Leet, and Blastcorder instruments (4, 8). The calibrations were performed by subjecting each component of measurement of each instrument to a sinusoidal motion on a shaking table.

Tests of the displacement seismographs were performed with two conditions of coupling:

1. The instruments were vibrated while simply sitting on emery cloth cemented to a driven plate.
2. The instruments were vibrated while bolted by the feet to the driven plate.

Each component of motion was studied separately. The frequency and amplitude of motion were independently varied to test the frequency response and the linearity of each instrument for both coupling conditions. The usable frequency range for the seismographs tested was found to lie between 5 and 40 cps. None of the instruments exhibited a linear response above 0.4 g for the unbolted coupling condition.

Magnifications for the displacement seismographs are summarized in table 2.1 which shows

Table 2.1.—Average magnification of displacement seismograph

Seismograph	Dynamic magnification [1]	Static magnification [2]
Seismolog	54 ± 10	50
Sprengnether	89 ± 10	75
Leet	31 ± 11	50

[1] Average for all components measured.
[2] Manufacturer's value.

the average dynamic magnification measured for all components for each machine, as well as the static magnification listed by each manufacturer. Throughout the operating frequency range the magnification of the instruments tended to increase with frequency. Within the limits of reliability of the measurements, the dynamic magnification of the Seismolog showed good agreement with the static magnification for all components and both coupling conditions. The dynamic magnification of the Sprengnether and Leet instruments tended to depart from the static magnification values.

All three displacement seismographs displayed an objectionable (20 percent) amount of crosstalk (that is, measured motion in the nondriven directions after subtraction of the table motion in the nondriven directions). This crosstalk increased with frequency in the same manner as dynamic magnification increased with frequency.

The centers of mass of the three displacement seismographs tested were found to be considerably removed from the centroids of the triangles formed by the feet of the three point mounts. This resulted in instability of the machines at low vibration levels and severely limited the dynamic range of the recordings.

The Blastcorder made use of external gages which were calibrated separately. Double-back tape was used to affix each gage to the shaking table. The results of the calibration showed that the usable frequency range was 12 to 30 cps. In this range, the average accuracy of measurement was ± 0.1 g. The internal calibration gave consistent results with a standard deviation of 1 percent. The three gages exhibited different sensitivity and varied as much as 9 percent. Because the output of the Blastcorder indicated the output directly in terms of standard gravity, no determination of magnification was made.

The calibration studies of portable seismographs disclosed inherent dynamic instability of the machines as the vibration levels approached 0.4 g. To provide guidelines for the improvement of the stability of portable seismographs and to update the machines, design requirements for a portable seismograph to measure particle velocity were presented by Duvall (2). At least two manufacturers have remodeled their displacement seismographs, and at least one manufacturer has built and marketed a portable seismograph to measure particle velocity.

2.6—INSTRUMENTATION USED BY THE BUREAU OF MINES

The instrumentation requirements for the Bureau program were determined by a study of the variables involved in the measurement of blast-induced vibration in the ground, in the air, and in structures. A preliminary study of vibration damage to structures showed that the degree of damage to a structure was more closely related to particle velocity than to the displacement or acceleration of the ground vibration that caused the damage (3). Also as particle velocity

[1] Reference to specific company or brand names is made to facilitate understanding and does not imply endorsement by the Bureau of Mines.

could be recorded directly or converted to either displacement or acceleration by a single integration or differentiation, particle velocity was selected as the quantity to measure in the ground.

The measurement of air-blast waves by the Bureau of Mines was initially done with microphone-type devices *(5, 11)*. During World War II, these studies were taken over by the armed forces, and their results showed that dynamic pressure was the best quantity to measure in the air and to correlate with damage to structures *(9)*.

Using these guidelines, instrumentation was developed for use with a mobile laboratory housed in a 2½-ton van-body truck. To provide sufficient instrumentation for the study of progagation of seismic waves and their loss of amplitude with distance, a 36-channel direct-writing oscillograph, 24 linear-integrating amplifiers, and 12 carrier-type amplifiers, along with velocity gages and accelerometers, were provided. The carrier-type amplifiers were replaced later with linear-integrating amplifiers. Power to operate the equipment was provided by a gasoline-driven AC power plant housed in a trailer.

Six pressure gages with mounting mechanisms, tripods, and preamplifiers were provided for the measurement of air waves resulting from the blasts. The pressure gages were calibrated at the Naval Ordnance Laboratory, White Oak, Md. An auxiliary 12-channel direct-writing oscillograph was used to augment the recording capability and to allow portable operation when used in conjunction with a small auxiliary power plant. Two-conductor shielded cables on reels were provided with waterproof connectors to connect the gages to the amplifiers through an input panel located in the side of the van-body.

The 36-channel direct-writing oscillograph contained fluid damped galvanometers that directed light beams on a 12-inch wide light sensitive recording paper which was driven at the rate of 17½ inches per second. Ten-millisecond timing lines were produced on the paper by a light beam passing through a slotted rotating cylinder. Because the accuracy of these timing lines was dependent upon the frequency of the portable power plant, a secondary means of time control was maintained by recording the output of a 100-cps tuning fork controlled oscillator. This provided a timing accuracy of about 1 percent. The fluid damped galvanometers had a resonant frequency of 3,500 cps and maintained a flat frequency response (within ± 5 percent) from 0 to 2,100 cps.

The linear-integrating amplifiers were selected for ruggedness and simplicity of operation. Velocity output from the gages could be recorded directly or integrated to furnish displacement data. Acceleration could be recorded directly or integrated to provide velocity data. The frequency response of the amplifiers was flat (within ± 5 percent) from 5 to 5,000 cps as shown in figure 2.6. Step attenuators on each amplifier provided control of the output signal level. Calibration of the amplifiers for each recorded blast was performed by using a variable frequency oscillator and a microvolter to provide a known input signal which was then recorded by the system with the controls set for the blast recording.

The velocity gages were adjustable to operate in either vertical or horizontal positions. The resonant frequency of the gages was 4.75 cps, and they were damped at 65 per cent critical. The frequency response of the gages is shown in figure 2.7. The gages were periodically calibrated on a shaking table to maintain them within 2 percent of the manufacturer's specifications. Defective gages were returned to the manufacturer for repair.

The problem of coupling the gages to the soil for making measurements at or near the soil surface was studied. Several different coupling methods were compared *(6)*. The following criteria were established for a satisfactory gage mount:

1. There should be no evidence of "ringing" or resonance in the output of a velocity gage from the vibration produced by a sharp hammer blow to the surface of the soil at a distance of 10 feet.

2. The velocity record should resemble the velocity wavelet shapes that are predicted by Ricker's theory *(10)*.

3. Good reproducibility should be obtained from repeated hammer blow tests.

4. Good reproducibility should be obtained from repeated mounting of the gage.

Four types of gage mounts were tested:

1. A single gage was attached to a steel plate welded to a steel pin which could be driven into the bottom or the sides of a square hole in the soil. One mount was required for each component of the vibration.

2. Three gages were attached to the sides of a cube of metal welded to a steel pin driven into the soil.

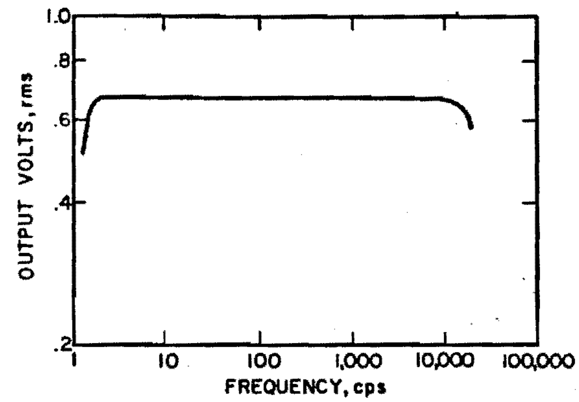

Figure 2.6.—Frequency response curve of linear amplifier.

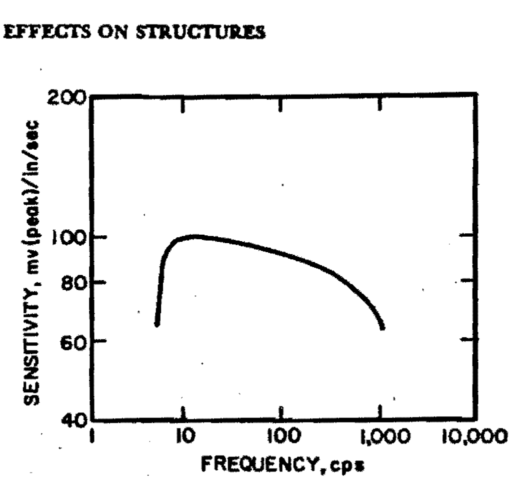

Figure 2.7.—Frequency response curve of velocity gage.

3. Three gages at right angles were attached to an angle bracket welded to a steel pin driven into the soil.

4. Three gages were attached to the inside of an aluminum box at right angles to one another. The box was buried in the soil. The box mount was designed to approximately match the soil density.

A designed test randomized the variables that could not be controlled. The test results showed that the mounts carrying three gages on a cube or an angle bracket resonated or "rang" with each hammer blow. The single gage mounts and the box mounts produced identical wave forms that satisfied the four gage criteria for a satisfactory gage mount. However, because it is not possible to drive pins firmly into all types of soil, the box mount was selected for use in the research program.

The gage system used by the Bureau and other investigators consists of three mutually perpendicular gages representing two horizontal and one vertical component which are commonly referred to as radial, vertical, and transverse. Radial signifies a horizontal gage, oriented radial to the source if the source is projected vertically to the horizontal plane of the gage.

2.7—REFERENCES

1. Duvall, Wilbur I. Design Criteria for Portable Seismographs. BuMines Rept. of Inv. 5708, 1961, 6 pp.
2. ———. Design Requirements for Instrumentation To Record Vibrations Produced by Blasting. BuMines Rept. of Inv. 6487, 1964, 7 pp.
3. Duvall, Wilbur I., and David E. Fogelson. Review of Criteria for Estimating Damage to Residences From Blasting Vibrations. BuMines Rept. of Inv. 5968, 1962, 19 pp.
4. Fogelson, David E., and Charles F. Johnson. Calibration Studies of Three Portable Seismographs. BuMines Rept. of Inv. 6009, 1962, 21 pp.
5. Ireland, A. T. Design of Air-Blast Meter and Calibrating Equipment. BuMines Tech. Paper 635, 1942, 20 pp.
6. Johnson, Charles F. Coupling Small Vibration Gages to Soil, Earthquake Notes, v. 33, September 1962, pp. 40–47.
7. Langefors, U., and B. Kihlström. Rock Blasting. John Wiley and Sons, Inc., New York, 1963, pp. 262–264.
8. Meyer, Alfred V. C., and Wilbur I. Duvall. Calibration Study of a Peak-Reading Accelerograph. BuMines Rept. of Inv. 6026, 1962, 6 pp.
9. Perkins, Beauregard, Jr. Forecasting the Focus of Air Blasts Due to Meteorological Conditions in the Lower Atmosphere. Ballistic Research Laboratories Rept. No. 1118, October 1960, 72 pp.
10. Ricker, Norman. The Form and Nature of Seismic Waves and the Structure of Seismograms, Geophysics, vol. 5, No. 4, October 1940, pp. 348–366.
11. Thoenen, J. R., and S. L. Windes. Seismic Effects of Quarry Blasting, BuMines Bull. 442, 1942, 83 pp.

CHAPTER 3.—SAFE VIBRATION LEVELS FOR RESIDENTIAL STRUCTURES

3.1—INTRODUCTION

One of the primary objectives of this research program was to establish reliable damage criteria for structures subjected to blasting vibrations. Of the literature reviewed, only five papers contained specific data on the amplitude and frequency of vibrations associated with damage evaluation of structures (*3–4, 7, 13–14*). The data from these investigations have been comprehensively studied to provide a set of damage criteria and to establish a safe vibration level for residential structures. The analysis shows that particle velocity is more directly related to structural damage than displacement or acceleration. The effect of air blast waves and their effects on structures does not generally create a damage problem in normal blasting operations. The magnitudes of safe and damaging overpressures for structures are discussed and methods of reducing overpressures are considered in this chapter. This chapter also discusses the human response to blasting operations, its psychological aspects, and its relation to vibration levels.

3.2—STATISTICAL STUDY OF PUBLISHED DATA ON GROUND VIBRATIONS AND DAMAGE

A statistical study has been made of the data presented by Thoenen and Windes (*13*), Langefors, Kihlström and Westerberg (*7*), and Edwards and Northwood (*4*). These three papers provide sufficient amplitude and frequency data from blasting vibrations and an assessment of damage to structures for detailed analysis. In addition, the instrumentation in these three investigations was adequate to record the amplitudes and frequencies observed. Test conditions, while not ideal, were adequate, and the procedures used were good.

3.2.1—Investigations by the Bureau of Mines

From 1930 to 1942, the Bureau of Mines conducted an extensive research program to study the seismic effects of quarry blasting. The first 5 years were spent in developing instrumentation and techniques needed for field measurements. Field tests were conducted from 1935 to 1940. Assembly and analysis of data was completed, and a summary bulletin published in 1942 (*13*).

Vibration amplitudes were measured with variable capacitance displacement seismometers. Horizontal and vertical seismometers were used so that motion in three orthogonal directions could be measured at each station. The outputs of up to 12 seismometers were recorded simultaneously on a 12-channel oscillograph.

Vibration amplitudes were recorded from many quarry blasts. A major difficulty was encountered in locating buildings suitable in all respects for determining blast-induced damage. Structures available for damage tests generally fell into two categories: 1. those in such a state of disrepair as to be useless for testing, 2. those adjacent to other buildings which precluded testing. These same conditions prevailed in the Bureau's current test series.

On Bureau-operated property, one house was available for testing. Blasts were set off in a mine adit some 75 feet beneath the structure with instrumentation near and in the structure. Successively larger shots (from 10 to 195 pounds) were fired until damage (cracking of plaster) was observed. A review of previous recordings made in houses during quarry blasting which resulted in no damage indicated that displacements at damage were 5 to 20 times those experienced in normal blasting operations with explosive charges ranging from 1 to 17,000 pounds.

Because these tests indicated that damage occurred at greater displacements than those occurring from ordinary quarry blasts, a renewed attempt was made to obtain structures to be blast-loaded to damage. Again, no suitable structures were located. Therefore, damage was induced by mechanical means. The mechanical vibrator was of the unbalanced rotor type driven by an electric motor. Both force and frequency were adjustable with upper limits of 1,000 pounds and 40 cps, respectively. A total of 14 structures near quarries were tested to determine building response, damage indices, and comparative effect of quarry blasting. Construction was frame, brick, or stone, and the height ranged from one to three stories. Recordings of vibrations were made from vibrating the building as a whole, vibrating individual wall or floor panels, and from quarry shots. As the buildings or building members were taken to damage, examinations for damage were made as well as recordings of vibrations in and near the buildings. Apart from the data included in the present analysis, two very interesting features were pointed out by the results. First, for ordinary residential structures, the vibration level necessary to produce damage is much greater than that resulting from most quarry blasts. Second, vibrating structures at resonance, in the amplitude and frequency range of Thoenen and Windes' tests, is no more destructive than at any other frequency.

In six of the 14 buildings tested, 160 mechanical vibrator tests were made about the damage point as defined by the failure of plaster. Amplitudes ranged from 1 to 500 mils and frequencies from 4 to 40 cps. To relate vibration amplitudes and frequencies to damage, three classifications of damage were proposed based upon the degree of failure of plaster. These indices of damage were:

1. Major damage (fall of plaster, serious cracking)
2. Minor damage (fine plaster cracks, opening of old cracks)
3. No damage.

In modern dry wall construction similar evidence would probably be observed in the spackling at joints and corners. It should be noted that any index of damage is gradational between degrees of severity of damage. There is no sharp distinction between classifications. It should also be noted that many other factors, including aging, settling, and shrinkage, result in similar failure. The amplitude, frequency, and damage data are shown in figure 3.1. The Bureau report of these data (*13*) recommended an index of damage based upon acceleration. If accelerations were less than 0.1 g, no damage was expected; from 0.1 to 1.0 g, minor damage; and greater than 1.0 g, major damage. Duvall and Fogelson showed statistically (*2*) that these data gave contradictory results, because major damage correlated with particle velocity, while minor damage correlated with acceleration.

3.2.2—Investigations by Langefors, Kihlström, and Westerberg

A report (*7*) by Langefors, Kihlström, and Westerberg, published in 1958, described extensive studies of the relationship between damage and ground vibrations from nearby blasting. The data were obtained during a reconstruction project in Stockholm which required the use of explosives near buildings. The amplitude of vibrations attenuated very little with distance from the blast since both the charge location and the buildings were set in rock. This seemed to dictate the use of small explosive charges. However, larger blasts were desirable to improve the economy of the operation. The principle of using larger blasts resulting in minor damage which could be repaired at moderate cost was therefore adopted. This procedure enabled the investigators to record and analyze a large amount of data on damage to buildings from blasting.

A Cambridge vibrograph was used to record vibrations in and near the buildings. This instrument is a mass-spring displacement seismograph system that records on celluloid strips. The instrument was weighted or clamped to the supporting surface whenever accelerations greater than 1 g were expected to prevent the base of the instrument from leaving the surface at high accelerations. Because early tests indicated that the level of vibrations in horizontal and vertical directions were of similar magnitude, later tests involved only vertical measurements.

Results from more than 100 tests were analyzed. Vertical ground displacements ranged from 0.8 to 20 mils; frequencies, from 50 to 500 cps. The investigators were aware that the frequencies observed were generally higher than those reported elsewhere. After studying the instrumentation and test conditions, they concluded that the higher frequencies were real and not a consequence of instrumental difficulties.

A damage severity classification based upon failure of plaster similar to that used by the Bureau of Mines but with four degrees of severity was proposed. However, they concluded that particle velocity was the best criterion of damage and related particle velocity and damage as follows:

1. 2.8 in/sec, no noticeable damage
2. 4.3 in/sec, fine cracking and fall of plaster
3. 6.3 in/sec, cracking
4. 9.1 in/sec, serious cracking.

For purposes of comparison these data have been divided into three classes—major, minor, and no damage—and are shown in figure 3.2. Statistical analyses of these data show that the degree of damage, both major and minor, correlates with particle velocity.

3.2.3—Investigations by Edwards and Northwood

Edwards and Northwood (*4*) conducted a series of controlled blasting tests on six resi-

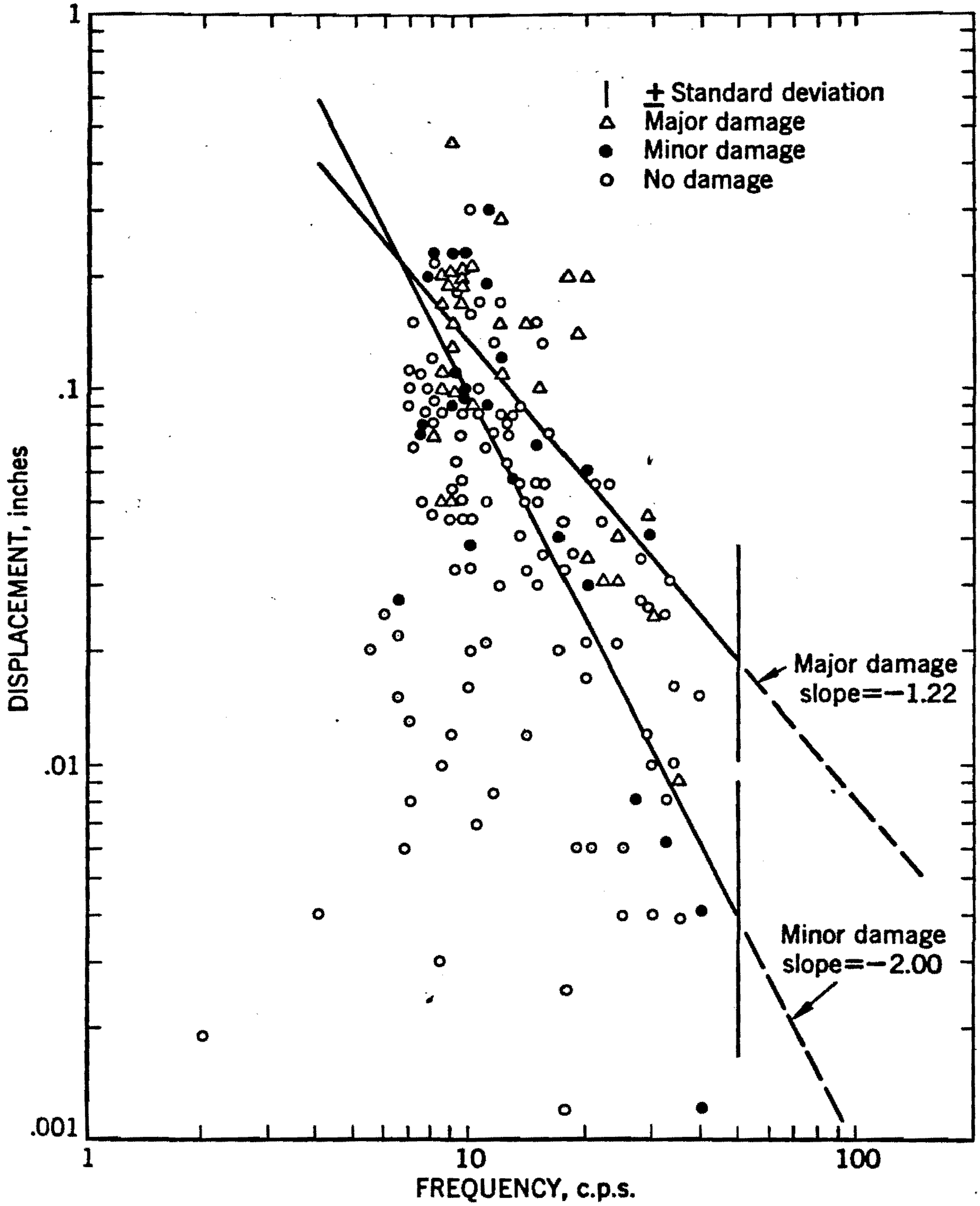

Figure 3.1.—Displacement versus frequency for observed damage, Bureau of Mines.

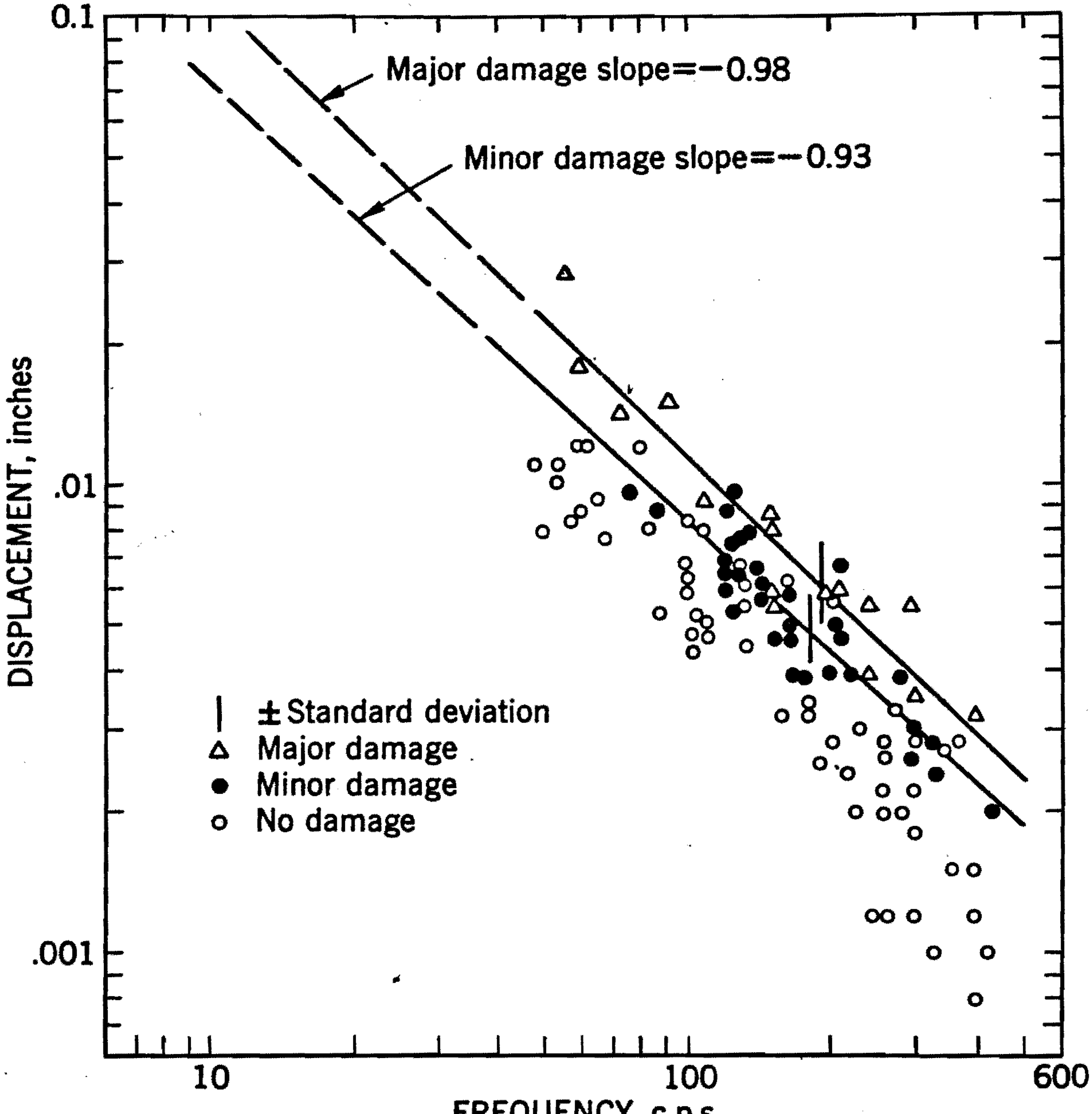

Figure 3.2.—Displacement versus frequency for observed damage, Langefors and others.

dential structures slated for removal at the St. Lawrence Power Project. The buildings selected were old but in good condition with frame or brick construction on heavy stone masonry foundations. In contrast to the buildings in the Swedish tests which were located on rock, three of the buildings were on a soft sand-clay material, and three were on a well-consolidated glacial till.

To determine which quantity was most useful in indicating damage risk, acceleration, particle velocity, and displacement were all measured. The instrumentation included: unbonded strain gage-type accelerometers, Willmore-Watt velocity

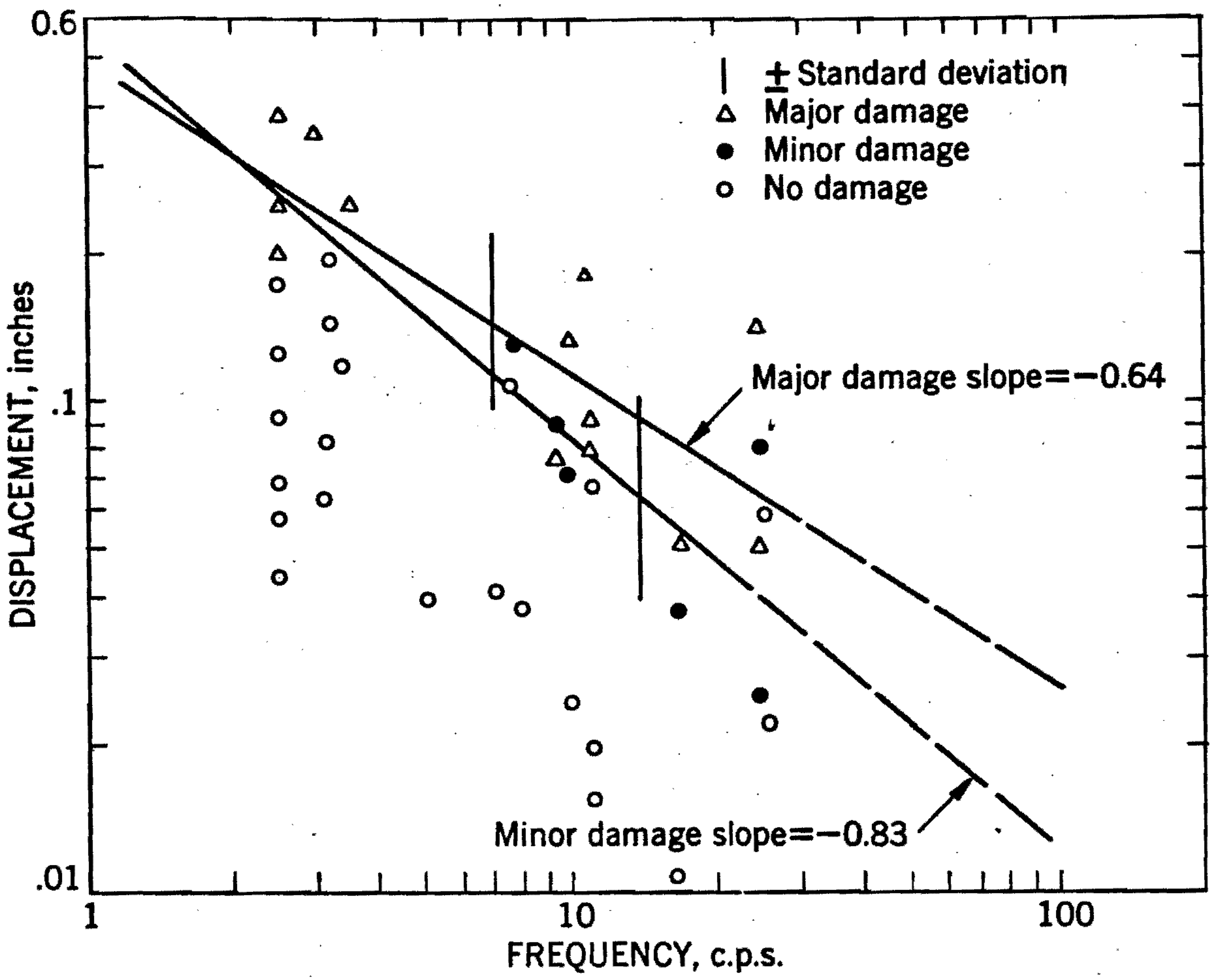

Figure 3.3.—Displacement versus frequency for observed damage, Edwards and Northwood.

seismometers, and Leet and Sprengnether seismographs. Precautions were taken to insure that true ground motion was measured. The displacement seismographs were secured to their bearing surface with chains to insure reliable operation when accelerations exceeded 1.0 g. Records from velocity gages and accelerometers were obtained on photographic or direct-writing oscillographs. Gages were installed in or near the structures. Some difficulty was experienced in recording particle velocity, because the particle motions often exceeded the limit of the seismometers. Therefore, most of the observations were displacements or accelerations.

Charges, buried at depths of 15 to 30 feet, were detonated progressively closer to the buildings until damage occurred. Charge sizes ranged from 47 to 750 pounds. Special precautions insured that the soil between individual charges and the structure being tested was undisturbed. Recordings from 22 blasts showed displacements ranging from 10 to 350 mils and frequencies, from 3 to 30 cps. The data are presented in figure 3.3.

Edwards and Northwood classified damage into three categories:

1. Threshold—opening of old cracks and formation of new plastic cracks.
2. Minor—superficial, not affecting the strength of the structure.
3. Major—resulting in serious weakening of the structure.

They concluded that damage was more closely related to particle velocity than to displacement or acceleration and that damage was likely to occur with a particle velocity of 4 to 5 in/sec. A safe vibration limit of 2 in/sec was recommended.

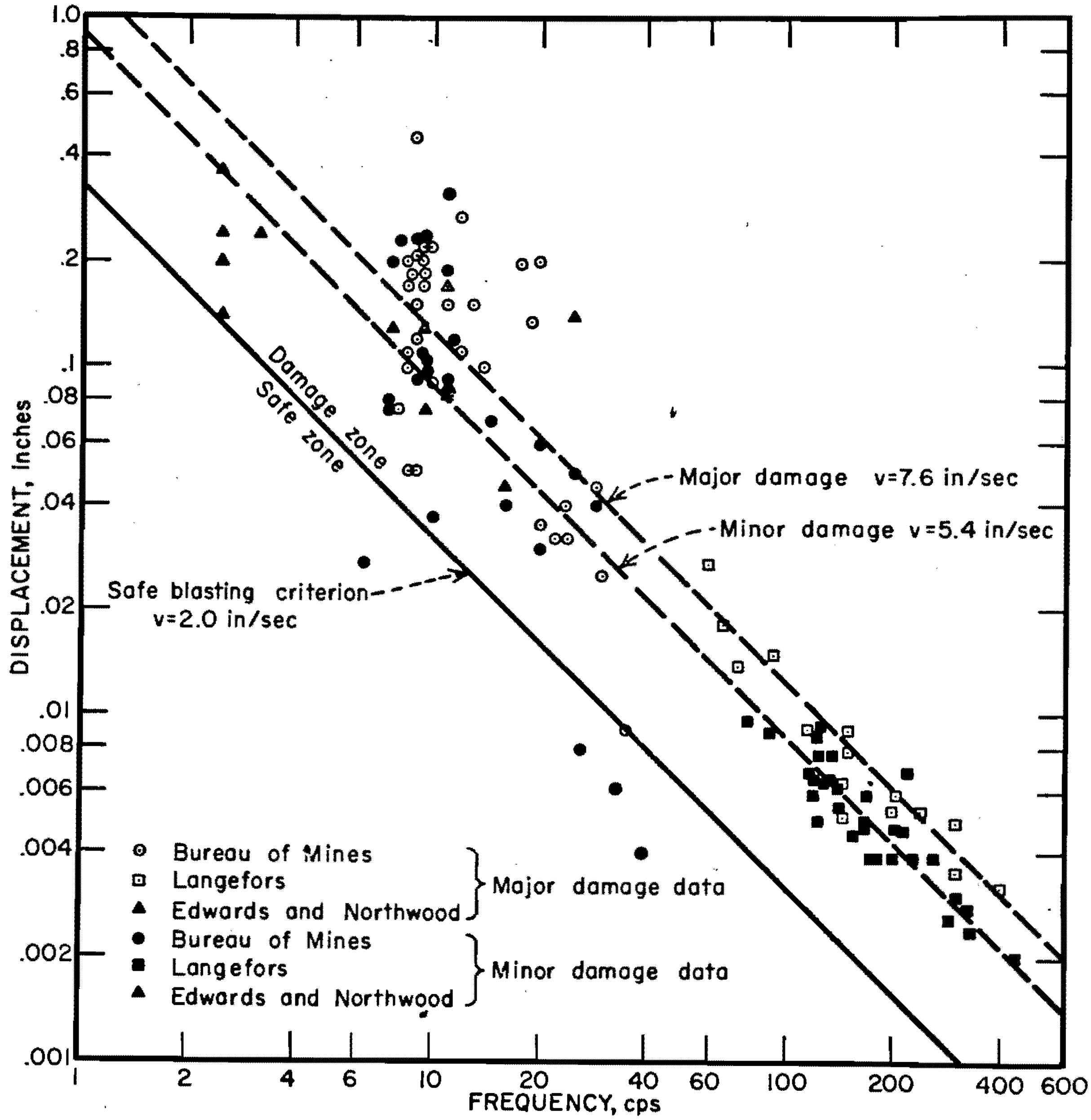

Figure 3.4.—Displacement versus frequency, combined data with recommended safe blasting criterion.

As in section 3.2.2, these data have been divided into three classes—major, minor, and no damage—and are shown in figure 3.3.

Statistical analyses of their data showed that particle velocity correlated with major damage data. For minor damage data, the statistical analyses were inconclusive.

3.2.4—Statistical Study of Damage Data

Figure 3.4 shows a composite plot of displacement amplitude versus frequency data. Three degrees of damage severity are considered; no damage, minor damage, and major damage. Minor damage is classified as the formation of new fine cracks either in plaster or dry wall joints or the opening of old cracks. Major damage is serious cracking of plaster or dry wall and fall of material, and it may indicate structural damage. The data presented individually in the three previously discussed papers have all been converted to displacement and plotted versus frequency.

Statistical tests on the individual sets of data related to major damage indicate that a slope of -1 on a displacement-frequency plot on log-log coordinates must be accepted. A slope of -1 corresponds to a constant particle velocity. Using standard statistical analysis techniques, these data can be pooled, and a single regression line used to represent all the major damage data. Moreover, it can be shown that the slope of the regression line must be -1, rather than 0, or -2. This result indicates that the regression line, representing all major damage data considered, corresponds to a constant particle velocity rather than constant displacement or acceleration, respectively. The magnitude of this particle velocity is 7.6 in/sec and is shown as a dashed line in figure 3.4.

Statistical tests of the individual sets of minor damage data are inconclusive. Only the data of Langefors show that a slope of -1, indicating a constant particle velocity, is acceptable while rejecting hypothetical slopes of 0 and -2 representing constant displacement or acceleration. However, statistical tests show that the three sets of data can be pooled and represented by a single regression line. Statistical tests of the pooled minor damage data indicate that a slope of -1, representing a constant particle velocity, cannot be rejected and that slopes of 0 and -2 can be rejected. Thus, the pooled minor damage data correspond to a constant particle velocity with a value of 5.4 in/sec as shown in figure 3.4.

Analysis of the pooled major and minor damage data show that both sets of data are statistically correlated with constant particle velocity. It is significant that these data were obtained by different investigators using different instrumentation, procedures, and sources and a wide variety of house structures on different types of foundation material. Therefore, a damage criterion based on particle velocity should be applicable to a wide variety of physical conditions.

Other investigators have proposed damage criteria and defined three or more zones of damage. Because the data did not have homogeneous variance when pooled, the outer limits of the damage zones could not be determined statistically. Therefore, Duvall and Fogelson (*2*) recommended a safe zone and a damage zone. A particle velocity of 2 in/sec was proposed as a reasonable separation between the safe and damage zones.

3.3—DATA FROM OTHER INVESTIGATORS

In 1949 Crandell (*1*) reported results from a study of damage to structures. Insufficient data were published to permit inclusion of these results in the analysis of section 3.2.4. Vibrations from blasting, pile driving, and industrial machinery were recorded on accelerographs. Crandell introduced a quantity which he called Energy Ratio, or E. R., which is defined as:

$$
\begin{aligned}
\text{E. R.} &= \frac{a^2}{f^2} \\
\text{E. R.} &= 16\pi^4 f^2 u^2 \qquad (3.1)\\
\text{E. R.} &= 4\pi^2 v^2
\end{aligned}
$$

where a = peak acceleration, ft/sec^2,
u = peak displacement, ft,
v = peak velocity, ft/sec,
and f = frequency associated with peak amplitude, cps.

The first two terms he derived from a consideration of kinetic energy, and the relationship between a, u, and v if simple harmonic motions are assumed (see equation 2.8, where ω is equal to $2\pi f$). Although not used by Crandell, the third equation of 3.1 is presented to illustrate that Energy Ratio is proportional to particle velocity squared. He concluded that a value of E. R. equal to 3.0 was the threshold limit of damage to structures, below 3.0 was a safe zone, between 3.0 and 6.0 was a caution zone, and an E. R. of 6.0 or greater was defined as the danger zone. An E. R. of 3.0 is equivalent to a particle velocity of 3.3 in/sec, and 6.0 is equivalent to 4.7 in/sec. These zones are in good agreement with Bureau results.

In 1962 Dvorak (*3*) published results from studies of damage caused by the seismic effects of blasting. Explosive charges ranging from 2 to 40 pounds were detonated at distances of 16 to 100 feet from the buildings. The ground was a semihardened clay containing lenses of sand, usually water-bearing. The buildings were one to two stories of ordinary brick construction.

The shots were instrumented with mechanical-optical displacement seismographs of three types: Cambridge, Somet, and Geiger. These were placed in or near the structures. The natural frequencies of these instruments were within the range of the observed frequencies. The Cambridge system with natural frequencies of 3.5 cps for the horizontal and 5.5 cps for the vertical direction presented the most serious problem. The observed frequencies of the seismic data were in the range of 1.5 to 15 cps. An additional source of trouble, not discussed by Dvorak, may have been the tendency of these instruments to leave their supporting surface at accelerations of 1.0 g or more. Edwards and Northwood (*4*) and Langefors and others (*7*) recognized this problem and weighted or clamped their instruments.

Displacements of 6 to 260 mils were measured at frequencies ranging from 1.5 to 15 cps. The four degrees of severity of damage, considered and correlated with plaster or structural damage, were

1. No damage,
2. Threshold—minor plaster cracking,
3. Minor—loosening and falling of plaster, minor cracking in masonry, and
4. Major—serious structural cracking and weakening.

Dvorak correlated damage with particle velocity; threshold damage occurring at particle velocities between 0.4 to 1.2 in/sec, minor damage from 1.2 to 2.4 in/sec, and major damage above 2.4 in/sec. He stated that these limits are conservative compared to other investigators.

The observed frequency range is lower than would be expected from the charge sizes and distances involved. This may have been a result of the instrumentation problem previously pointed out. Consequently, because of the instrumentation problem and the low frequencies reported, the results have not been included by pooling with other data.

In 1967 Wall (*14*) reported on seismic-induced damage to masonry structures at Mercury, Nev. Two of the objectives of the study were to determine the validity of particle velocity as a damage criterion and the level of velocity at damage. The buildings were generally of concrete block construction and less than 3 years old. The buildings were inspected for cracking before and after nuclear detonations at the Nevada Test Site. Charge sizes are not listed but must be assumed to be greater than normally encountered in other blasting operations. The detonations were at distances ranging from 100,000 to 290,000 feet from the buildings.

The instrumentation consisted of three-component moving coil seismometers, responsive to particle velocity, and accessory recording equipment (not described). The seismometers were placed on the ground near the buildings. The particle velocity used was the vector sum of the three components.

The buildings were experiencing cracks due to natural reasons (use, settling, shrinkage, temperature cycling, etc.). Therefore, the damage study consisted of examining cracks, establishing natural cracking rates, and correlating any increase in rates after a nuclear detonation with observed particle velocities. The peak particle velocities at selected sites within the complex of 43 buildings under study were within a factor of 2. No frequencies were reported. The particle velocities observed when the rate of cracking was above normal were in the range of 0.04 to 0.12 in/sec. Wall noted that the cracks at these low levels were no more severe than those occurring naturally and may represent an acceleration of normal cracking. He concluded that "it appears that this cracking would have occurred naturally in a matter of time."

The size of explosion, distance, and assessment of damage (increase in rate of cracking) may place these results in a domain different from the usual blasting operations. The results may be valid but only applicable to very large blasts.

3.4—ADDITIONAL BUREAU OF MINES DATA

In October 1969, the Bureau participated in a test program, sponsored by the American Society of Civil Engineers (ASCE), to study the response of a residential structure to blast loading. Previously described instrumentation (see section 2.6) was used to record ground and house vibrations from a series of 10 explosive blasts detonated in glacial till. Shot-to-house distances ranged from 200 to 35 feet. Charge weights ranged from 1 to 85 pounds. Particle velocities in the ground varied from 0.091 to 11.6 in/sec. Particle velocities in and on the house at ground or floor level agreed generally with those measured in the ground outside the house. Measurements at the roof level of the house show an amplification of up to a factor of 2.0 compared to ground response. Frequencies ranged from 5 to 40 cps and were higher in the vertical component than in the radial and transverse component.

The structure investigated was more substantial than most present-day residences due to a massive field-stone foundation and to 1-inch planking on the studs under the dry wall in some rooms. Through the eighth blast in the series there had been no observable damage. Maximum particle velocities recorded at the house in the ground through test 8 were: radial, 5.36 in/sec; vertical, 6.86 in/sec; and transverse, 1.71 in/sec. The vibrations from test 9 opened new cracks in the walls and ceiling of an upstairs room. Maximum particle velocities in the ground at the edge

Table 3.1.—Vibrations from normal activities

Activity	Particle velocity in room			Particle velocity in adjacent room		
	Radial in/sec	Vertical in/sec	Transverse in/sec	Radial in/sec	Vertical in/sec	Transverse in/sec
Walking	0.00914	0.187	0.372	0.00129	—	0.00102
	—	.0578	.0155	.00167	0.0281	.00227
	—	.00770	.00210	.00229	.0626	.00462
	.0600	.120	.0300	—	—	—
	.0100	.0600	.007	—	—	—
	.00600	.0110	.00400	—	—	—
	.00800	.0200	.00700	—	—	—
Door closing	.0110	.0558	.0149	.00170	—	.00153
	—	.0150	.00500	.0125	.0970	.00963
	.008	.0100	.00800	—	—	—
Jumping	.0524	4.03	1.05	.120	.219	.551
	.120	.219	.551	.0153	.0239	.0101
	1.00	2.500	1.70	.00450	.0100	.0045
	.500	5.00	1.10	—	—	—
Automatic washer	.00340	.00400	.00340	—	—	—
Clothes dryer	.00500	.00500	.00500	—	—	—
Heel drops	.0100	.0100	.0100	—	—	—
	.0800	.600	.0300	—	—	—
	.0200	.200	.0200	.006	.0100	.006
	.900	3.500	.400	—	—	—
	.0500	.450	.0700	.009	.014	.008
	.0100	.200	.00900	—	—	—

of the house from test 9 were radial, 12.7 in/sec; vertical, 22.2 in/sec; and transverse, 3.0 in/sec.

Although particle velocities were in excess of the 2.0 in/sec safe blasting limit, no damage was observed through test 8. The vertical velocity in the ground from test 9 was 11 times the safe blasting limit. The fact that particle velocities generated prior to damage exceeded the safe blasting limit is probably attributable to the substantial construction of the house. Although the 2.0 in/sec particle velocity criterion is obviously conservative for construction of this type, it is a satisfactory and reliable criterion that can be used for all types of residential structures.

3.5—BUILDING VIBRATIONS FROM NORMAL ACTIVITIES

The normal activities associated with living in and maintaining a home give rise to vibrations that are, in some instances, capable of causing minor damage to plaster walls and ceilings in localized sections of the structure. To complete the study of vibrations from quarry blasting and their effects on structures, instrumentation was placed in several homes to record the vibrations from walking, door closing, jumping, and operating mechanical devices, such as an automatic washing machine and a clothes dryer. The vibration levels of some of these activities are listed in table 3.1.

The data in table 3.1 indicate that walking, door closing, and the operation of an automatic clothes washing machine and dryer do not normally generate vibrations that approach a damaging level. It is interesting to note that the vibrations from these sources are approximately the same as those generated by a quarry blast and felt at a scaled distance of 100 ft/lb$^{1/2}$ (see sections 4.3 and 6.4).

Jumping in a room generates vibrations that are potentially damaging. "Heel drops," made by standing on the toes and suddenly dropping full weight on the heels, can also be potentially damaging. However, the large amplitude vibrations resulting from these more violent activities are localized and do not affect the entire structure as do ground vibrations. Thus, although the potential for causing damage is present, it is confined to a small specific area within the structure, and the probability of damage is thereby reduced.

3.6—RELIABILITY OF PARTICLE MOTION CALCULATIONS

Analysis of particle motion amplitudes, whether in terms of displacement, particle velocity, or acceleration, often leads investigators to calculate one or more of these quantities from the others. The mathematical relationships are

$$u = \int v dt \quad \text{or} \quad v = du/dt \qquad (3.2)$$

$$v = \int a dt \quad \text{or} \quad a = dv/dt \qquad (3.3)$$

where

u = displacement,
v = particle velocity,
a = acceleration, and
t = time.

The integration or differentiation can be done either electronically or mathematically. Neither of these techniques could be applied to the published data, because the original records were not available.

An alternative procedure permits calculation of the other quantities from a given recorded quantity using the relationships of equation 2.8:

$$u = v/2\pi f \quad \text{or} \quad v = 2\pi f u \qquad (3.4)$$

$$v = a/2\pi f \quad \text{or} \quad a = 2\pi f v \qquad (3.5)$$

where f is the frequency of the seismic trace, where the peak amplitude is observed. Equations 3.4 and 3.5 may be used if the motion is simple harmonic. This is not the case with seismic motion which is generally aperiodic. The authors of the published papers used these relationships either directly or indirectly. Duvall and Fogelson (*2*) used this treatment directly or indirectly when analyzing the data from the three published papers. The need to establish the reliability of using equations 3.4 and 3.5 on aperiodic data was pressing, particularly when the data were being used to establish damage criteria.

Particle velocity records obtained during the current test series were used to evaluate the use of equations 3.4 and 3.5. Data from several shots of different charge size and distribution were selected for analysis. The data used included radial, vertical, and transverse components and represented a cross section of the data available. The peak amplitude and its associated frequency were read for the selected velocity-time records. Equation 3.4 was used to calculate the displacement for these data. The same velocity-time records were digitized, input to a computer, and the velocity amplitude spectra calculated. These spectra were integrated in the frequency domain to provide displacement amplitude spectra from which displacement-time records were synthesized. The peak displacement could then be determined for each recording. This is the same as applying equation 3.2 to the original data to determine displacement, except that the integration is done in the frequency domain. Figure 3.5 shows the plot of displacement integrated from velocity versus displacement computed from velocity and frequency, as the abscissa and ordinate, respectively. The line with slope of 1.0 indicates the locus of points which would result if the displacements calculated by the two methods were identical. The bulk of the points falling below the line indicates that displacements calculated by assuming simple harmonic motion are generally less than displacements from integrated velocities which are mathematically correct.

Because most calculations treating the published data were from displacement or acceleration to particle velocity, the next step was to take the synthesized displacement-time records, read the peak amplitude and associated frequency. These values were used to calculate particle velocities assuming simple harmonic motion. The calculated particle velocities were plotted versus recorded particle velocities for the same traces as shown in figure 3.6. Again, the line with a slope of 1.0 shows the relationship of calculated and recorded values if they have a 1:1 ratio. Since most of the points fall below the line, calculated values are generally less than recorded velocities.

It should be noted that the calculation of displacements as shown in figure 3.5 is directly analogous to the calculation of particle velocity data from recorded acceleration data. The results, shown in figures 3.5 and 3.6, indicate that particle velocities calculated from either displacement or acceleration data assuming simple harmonic motion will generally be less than particle velocities recorded directly. It is obvious that a damage criterion of particle velocity calculated from displacement and acceleration has a built-in safety factor. If the data of figures 3.5 and 3.6 fell above the lines, a risk factor would have resulted.

3.7—RECOMMENDED SAFE GROUND VIBRATION LEVELS

On the basis of the statistical study of published data and the recommendations of the investigators, Edwards and Northwood, and Langefors and others, particle velocity is more closely associated with damage to structures than either displacement or acceleration. Figure 3.7 shows particle velocity versus frequency on a log-log plot. These have generally been converted to particle velocity from displacement or accelera-

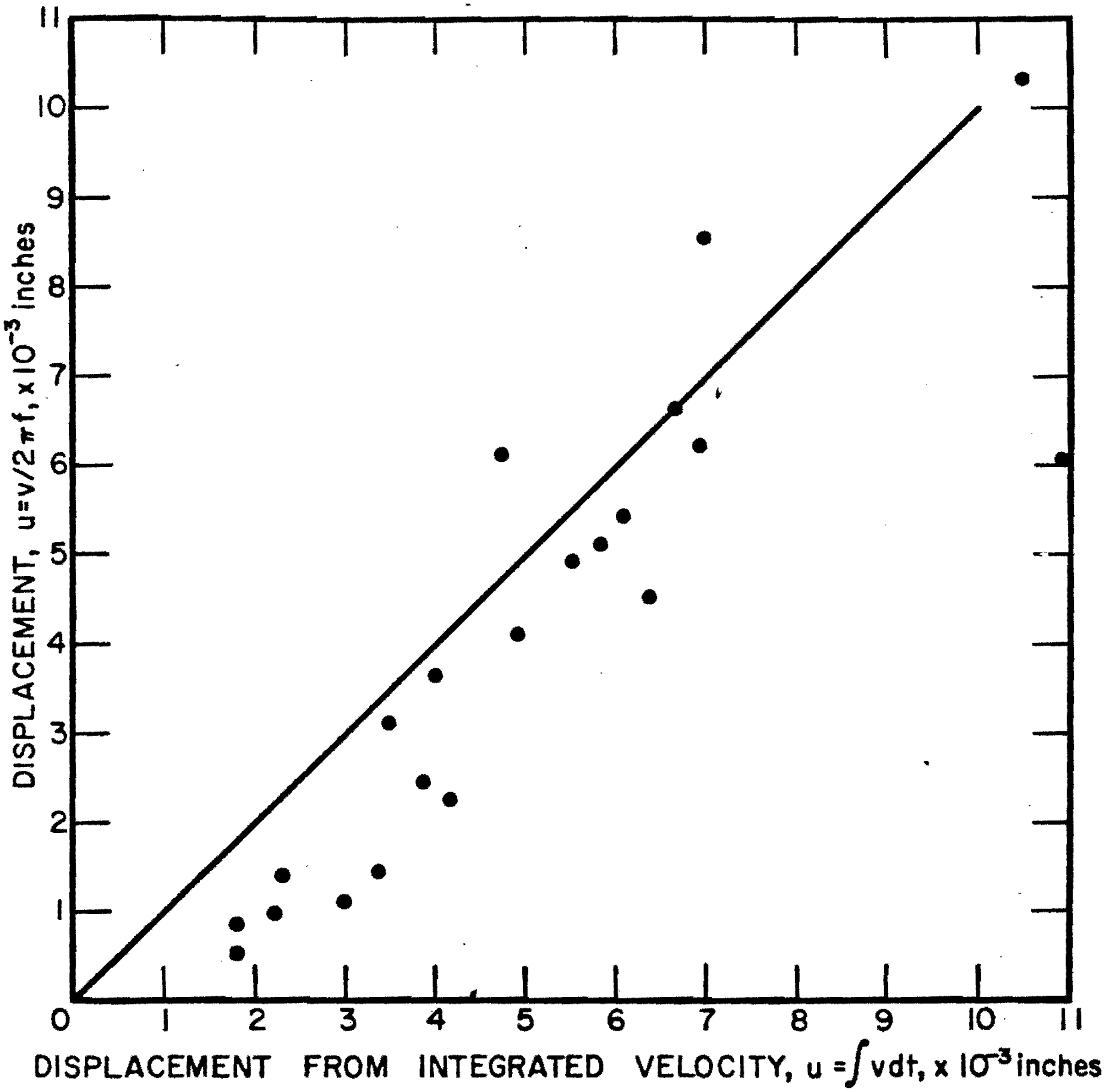

Figure 3.5.—Comparison of displacements from integration and simple harmonic motion calculations.

tion by the Bureau or the original investigators assuming simple harmonic motion. This, of course, builds in a safety factor (see section 3.5). The particle velocity at damage from the recent ASCE-Bureau of Mines test is shown in figure 3.7.

Figure 3.7 shows the major and minor damage data with constant velocity lines of 7.6 in/sec and 5.4 in/sec drawn through their average points. The damage criteria suggested by other investigators are shown also.

The Bureau recommends that only two zones be considered—a safe zone and a damage zone. Based upon the data of figure 3.7, a reasonable separation between the safe and damage zones appears to be a particle velocity of 2.0 in/sec. All of the major damage points and 94 percent of the minor damage points lie above this line. The only data points below the 2.0 in/sec line are from the early Bureau data which have the largest standard deviation.

The recommended safe vibration criterion of 2.0 in/sec particle velocity is a probability type

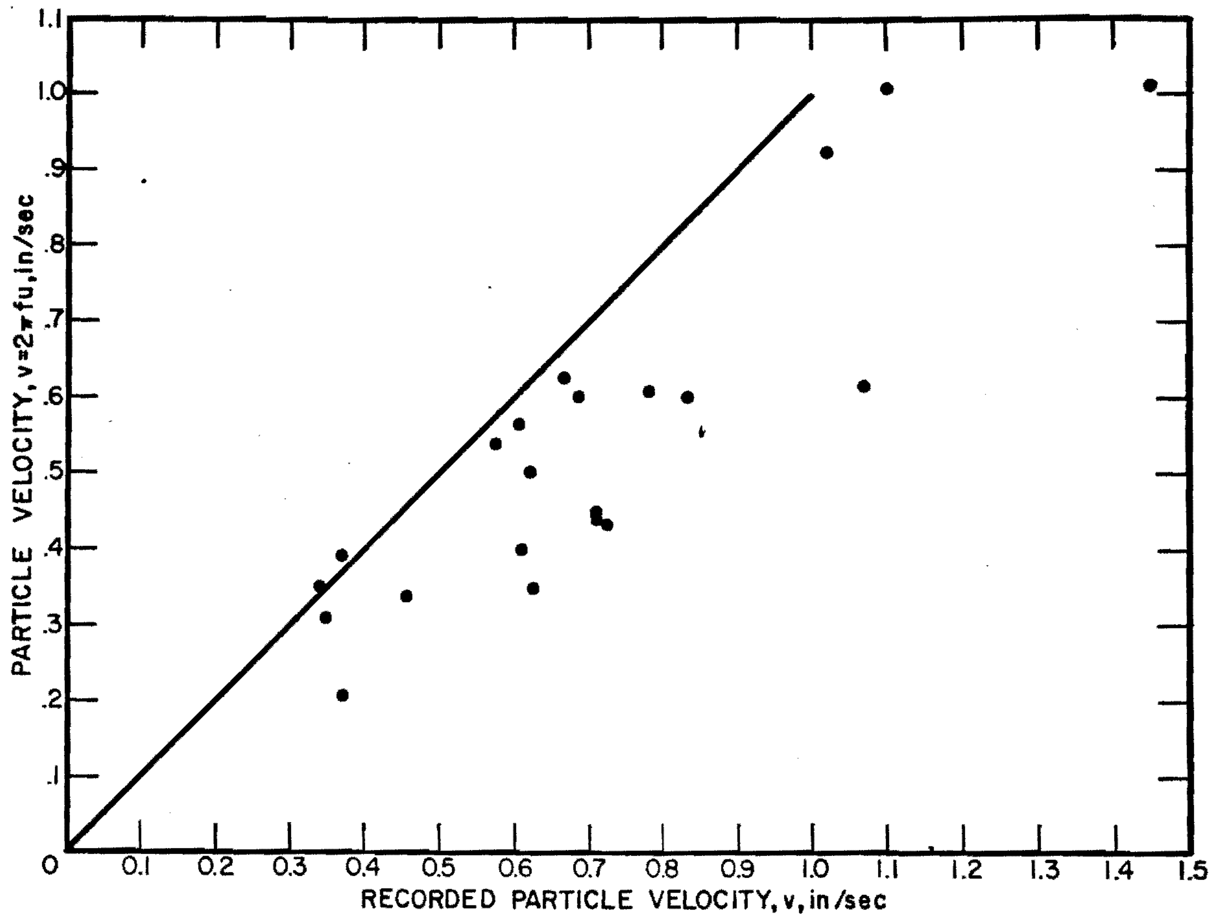

Figure 3.6.—Comparison of particle velocities as recorded and from displacements.

criterion. If the observed particle velocity exceeds 2.0 in/sec in any of the three orthogonal components, there is a reasonable probability that damage will occur to residential structures. The safe vibration criterion is not a value below which damage will not occur and above which damage will occur. Many structures can experience vibration levels greatly in excess of 2.0 in/sec with no observable damage. For example, figure 3.8 presents velocity data from tests in which damage was not observed. However, the probability of damage to a residential structure increases or decreases as the vibration level increases or decreases from 2.0 in/sec.

Having ascertained a safe vibration criterion, the next logical step is to qualify the conditions under which the best assessment of vibration levels can be made. Obviously, particle velocity should be measured directly with instrumentation which responds to particle velocity and with an adequate frequency response. If displacement or acceleration are measured, particle velocity should be calculated only by integration or differentiation, either electronically or mathematically. Calculations which assume simple harmonic motion yield particle velocities which are in general too small. The velocity gages should preferably be mounted on or in the ground rather than in the structure, because most of the data used in establishing the damage criterion were obtained in this manner. Mounting of gages in the ground alleviates the necessity of considering the responses of a large variety of structures. Particle velocity should be observed in three mutually perpendicular directions: a vertical component, a horizontal component radial to the source projected on a horizontal plane, and a horizontal component transverse to the source. The safe vibration criterion is based upon the measurement of individual components, and if the particle velocity of any component exceeds 2.0 in/sec, damage is likely to

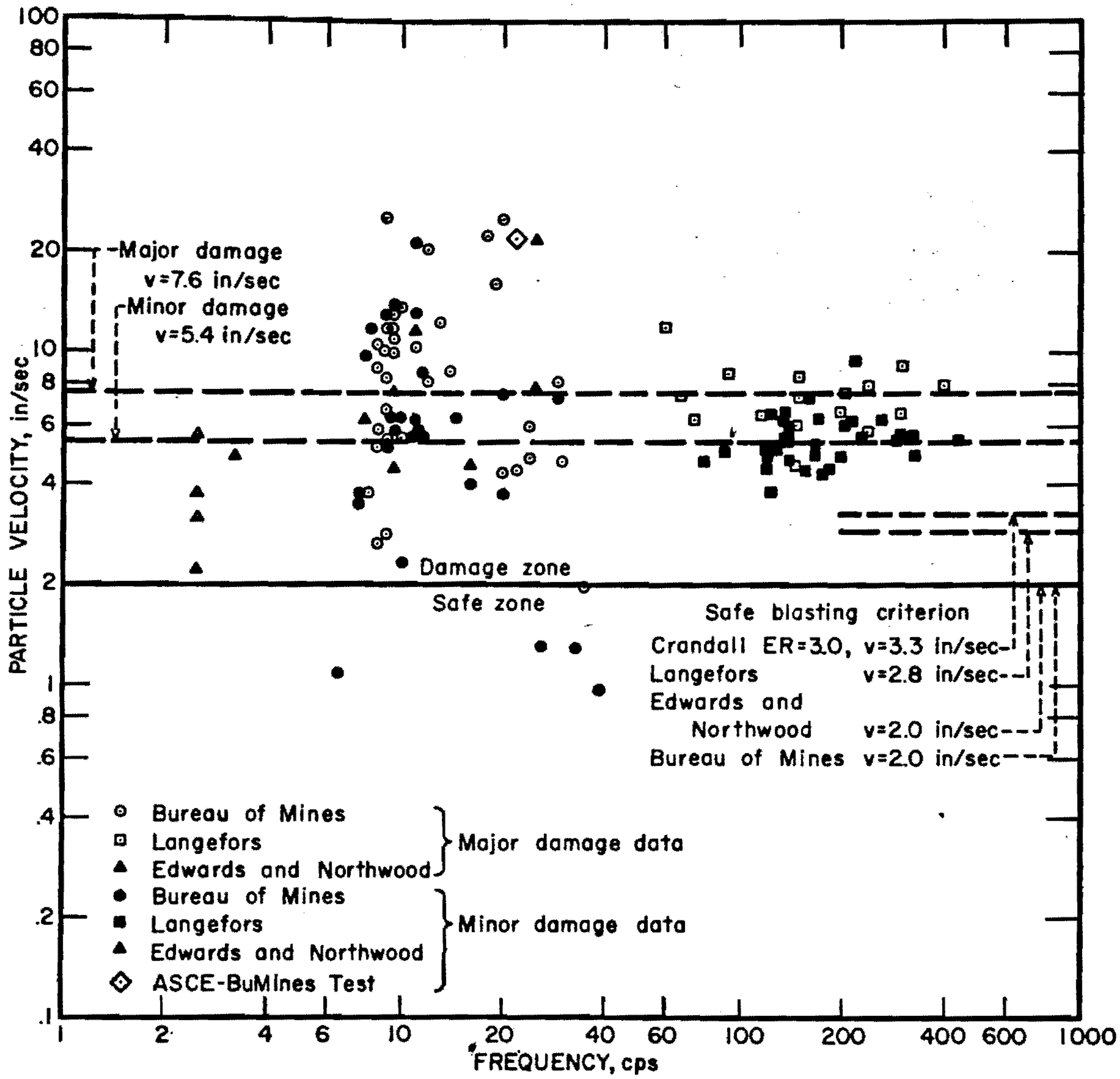

Figure 3.7.—Particle velocity versus frequency with recommended safe blasting criterion.

occur. Since seismic motion is a vector quantity, individual components must be considered.

3.8—PUBLISHED DATA ON AIR VIBRATIONS AND DAMAGE

Windes (*15, 16*) reported on the Bureau of Mines' 1940 study in the early 1940's of the air blast problem associated with quarry and mine blasting. He concluded that window glass failure occurred before any other type of structure failure due to air blast. Explosive charges were detonated in air to induce sufficient air blast overpressures to break window panes. Some panes were broken by an overpressure of 1.0 psi, and all panes failed and plaster walls experienced minor damage at overpressures of 2.0 psi or more. Higher overpressures caused more serious failures, such as masonry cracks. Plaster cracks were generally found to be caused by flexing of wall panels by building vibrations induced by air blast. The condition of the glass in the windows contributed directly to the damage experience. Poorly mounted panes which have been prestressed by improperly inserted glazier's points or other causes, may fail when subjected to over-

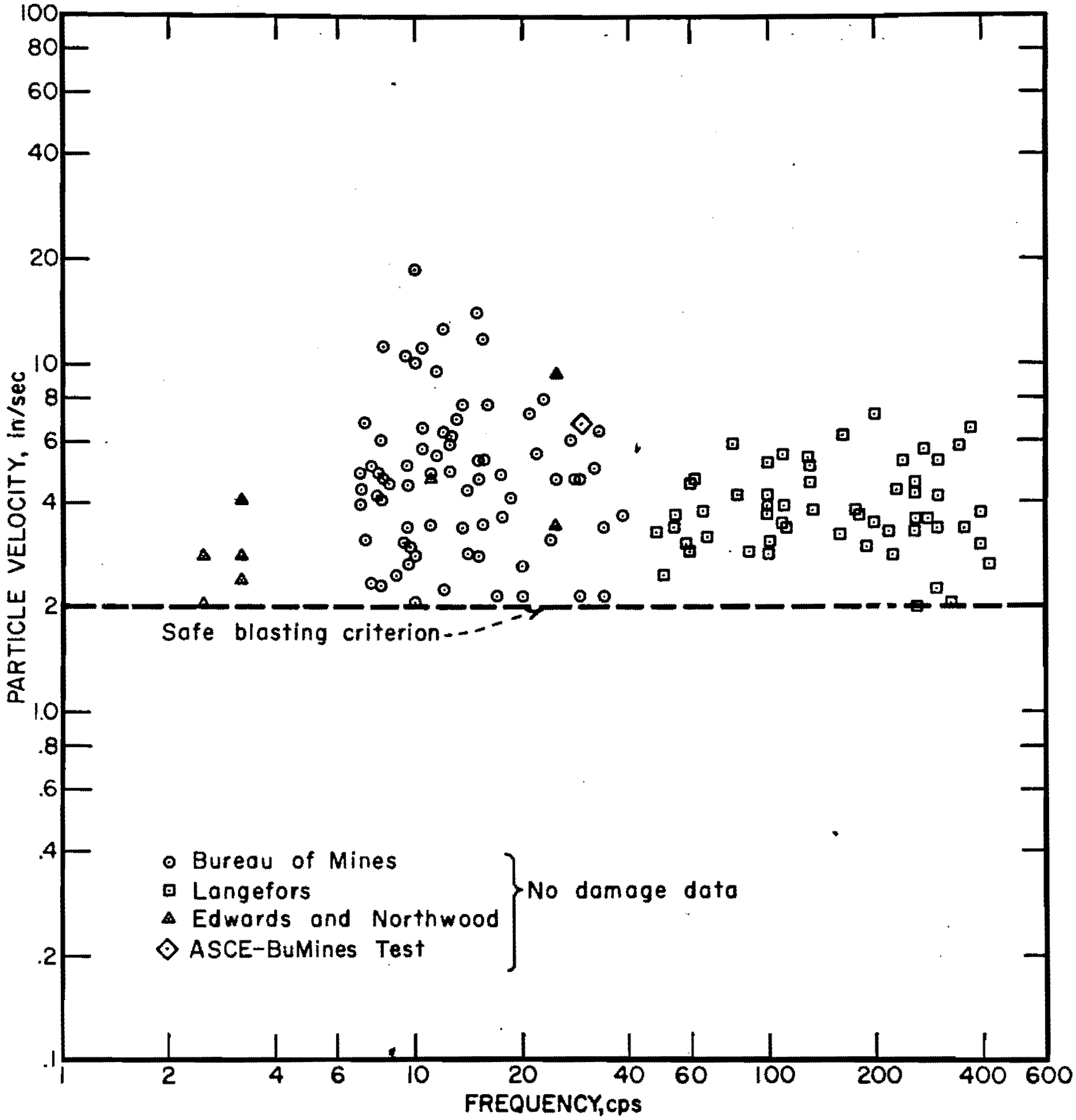

Figure 3.8.—Particle velocity versus frequency for no damage data.

pressures as low as 0.1 psi. Charges of explosives detonated in boreholes at similar explosive-to-window distances as used in the open air blasts did not produce failure of window panes due to air blast overpressure. On the basis of these Bureau studies, Windes concluded that under normal blasting conditions the problem of damage from air blast was insignificant.

The results of an extensive study of the air blast overpressure problem made by the Ballistic Research Laboratories (*9, 10*) were similar to those of Windes. Glass panes forced into frames so as to be under constant strain were found to crack when subjected to overpressures of 0.1 psi. Properly mounted panes were subject to cracking at overpressures of 0.75 psi or greater. Air blast pressures of only 0.03 to 0.05 psi could vibrate loose window sash which might be a source of complaints but would not represent damage.

As a routine procedure, Edwards and Northwood (4) measured air blast pressure during their vibration studies. The measured overpressures ranged from 0.01 to 0.2 psi at locations outside the six structures being blast loaded. These pressures were considerably below the levels expected to cause damage. None of the damage that occurred in any of the six structures was attributed to air blast.

Air blast is not considered to be a significant factor in causing damage to residential structures in most blasting operations. However, air blast and the attendant transmission of noise may be a major factor in nuisance type complaints.

3.9—RECOMMENDED SAFE AIR BLAST PRESSURE LEVELS

The recommended safe air blast pressure level of 0.5 psi is based on a consideration of the results reported in section 3.8. If some panes of glass will fail at overpressures of 0.75 psi and all would be expected to fail at 2.0 psi or more, 0.5 psi provides a reasonable margin of safety. Damage to plaster walls at overpressures greater than 1.0 psi would thereby be precluded. The recommended level would not alleviate the problem of prestressed glass panes failing at 0.1 psi or loose sash vibration. These two conditions would continue to result in complaints. However, most routine blasting operations designed to limit vibrations to less than 2.0 in/sec do not generate air blast overpressures that are significant factors in causing damage to residential structures. The air blast pressures from buried explosive charges and from charges properly stemmed in boreholes are an order of magnitude or more below the pressures required for damage. Sadwin and Duvall (12) pointed out that optimum use of explosives to break rock results in less energy available to generate air blast overpressures.

3.10—HUMAN RESPONSE AND ITS EFFECT ON SAFE VIBRATION LEVELS

Legitimate damage claims result when personal or property damage is caused by seismic or air blast waves from blasts. The advances in blasting technology during the past 25 years, including blasting procedures, damage criteria, knowledge of seismic wave propagation, monitoring instrumentation, and a more knowledgeable blasting profession have minimized claims resulting from real structural damage. More and more blasting operators instrument their own blasts or subscribe to a consulting service to insure vibration levels below those necessary to cause damage. The occasional legitimate damage claim can result from many unknown causes perhaps the best being that any damage criterion is a probability-type criterion.

Vibration levels that are completely safe for structures are annoying and even uncomfortable when viewed subjectively by people. Figure 3.9 has been adapted from Goldman (5) to show the subjective response of the human body to vibratory motion. These limits are based on the results for sinusoidal vibration. Similar results have not been determined for nonsinusoidal vibrations. Predominant frequencies generated by blasting are commonly in the range from 6 to 40 cps. If a building is being vibrated to a particle velocity of 1.0 in/sec, the building is considered safe, but the vibration level as viewed subjectively by people is intolerable. At a particle velocity of 0.2 in/sec, the probability of damage to a building is nil, and yet the vibration level is viewed as quite unpleasant or annoying by some people.

The superposition of the perceptible, unpleasant, and intolerable limits on the case history plot of particle velocity versus percentage of

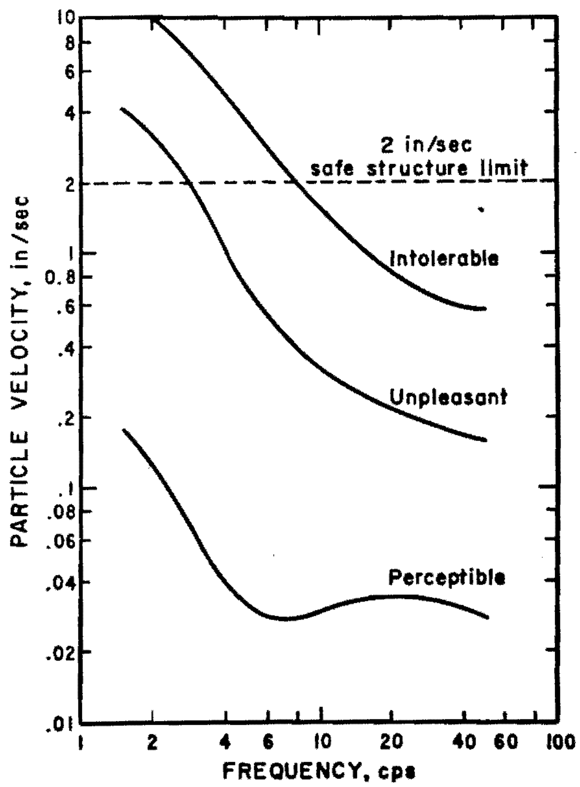

Figure 3.9.—Subjective response of the human body to vibratory motion (after Goldman).

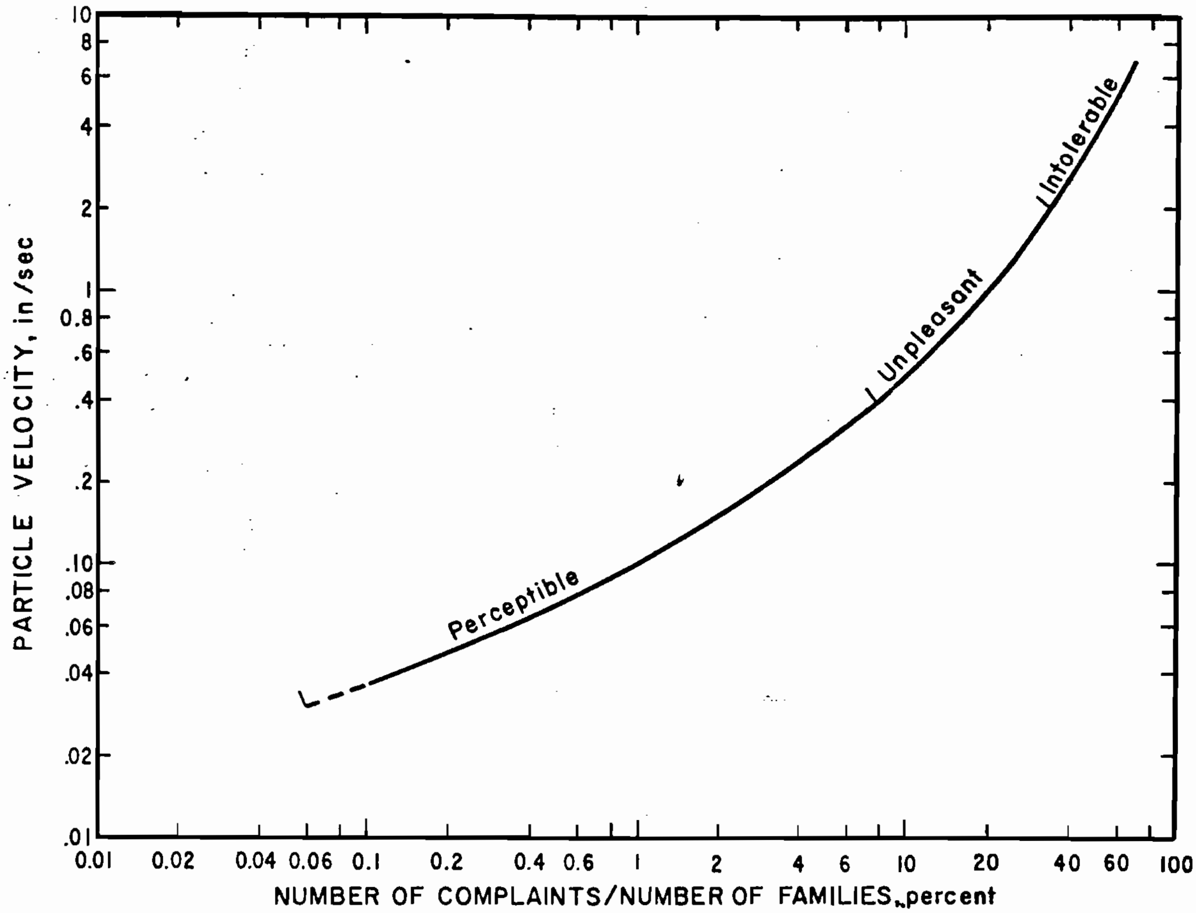

Figure 3.10.—Complaint history, Salmon Nuclear Event, with superposed subjective response.

complaints for the Salmon nuclear event near Hattiesburg, Miss., is shown in figure 3.10 (*11*). More than 35 percent of the families located in the zone where the 2 in/sec was exceeded filed complaints. This is the intolerable subjective response zone and should have been anticipated. In the perceptible zone, less than 8 percent of the families complained. Thus, the Salmon data indicates that a vibration level of 0.4 in/sec should not be exceeded if complaints and claims are to be kept below 8 percent.

A similar relationship exists with the noise associated with air blast pressures. The air blast pressure from most blasts is considerably less than that which causes glass damage. However, the sound level at an overpressure of 0.01 psi is comparable to the maximum sound in a boiler shop or the sound level 4 feet from a large pneumatic riveter (*8*). The sound level at 0.001 psi compares with the sound generated at a distance of 3 feet from a trumpet, auto horn, or an automatic punch press. It is completely understandable that the public reacts to blasting operations. Kringel (*6*) describes a quarry operation where adequate precautions were taken to insure that seismic vibrations and air blast pressures generated were a small fraction of the levels required to cause physical damage. A full-time public relations staff devoted their efforts to acquainting the community with the company's efforts to minimize seismic vibrations, air blast, and noise. The complaints continued. It was concluded from an analysis of the complaints that the problem is one of subjective response. No amount of objective data will convince a person who "feels" strong vibrations that the vibration level as measured was barely perceptible—similarly with noises and air blasts. Personal contact and strong efforts in public relations help alleviate the problem but convince few. An understanding of the overall human response to such stimuli may be achieved some day but will not really solve the problem. The only possible solution is to keep vibration levels and air blast pressures well below the safe vibration criteria and concentrate on noise abatement.

3.11—REFERENCES

1. Crandell, F. J. Ground Vibration Due to Blasting and Its Effect Upon Structures. J. of the Boston Soc. of Civil Engineers, April 1949, pp. 222–245.
2. Duvall, Wilbur I., and D. E. Fogelson. Review of Criteria for Estimating Damage to Residences From Blasting Vibrations. BuMines Rept. of Inv. 5968, 1962, 19 pp.
3. Dvorak, A. Seismic Effects of Blasting on Brick Houses. Prace geofyrikeniha Ustance Ceskoslovenski Akademie Ved. No. 169. Geofysikalni Sbornik, 1962, pp. 189–202.
4. Edwards, A. T., and Northwood, T. D. Experimental Studies of the Effects of Blasting on Structures. The Engineer, v. 210, Sept. 30, 1960, pp. 538–546.
5. Goldman, D. E. A Review of Subjective Responses to Vibrating Motion of the Human Body in the Frequency Range, 1 to 70 cycles per second. Naval Medical Res. Inst. Rept. No. 1, Project NM 004001, Mar. 16, 1948, 17 pp.
6. Kringel, J. R. Control of Air Blast Effect Resulting From Blasting Operations. Mining Congr. J., April 1960, pp. 51–56.
7. Langefors, Ulf, Kihlström, B., and Westerberg, H. Ground Vibrations in Blasting. Water Power, February 1958, pp. 335–338, 390–395, 421–424.
8. Peterson, A. P. G., and E. E. Gross, Jr. Handbook of Noise Measurement. General Radio Co., West Concord, Mass., 5th ed., 1963, p. 4.
9. Perkins, Beauregard, Jr., Paul H. Lorain, and William H. Townsend. Forecasting the Focus of Air Blasts Due to Meteorological Conditions in the Lower Atmosphere. Ballistic Research Laboratories Rept. No. 1118, October 1960, 77 pp.
10. Perkins, Beauregard, Jr., and Willis F. Jackson. Handbook for Prediction of Air Blast Focusing. Ballistic Research Laboratories Rept. No. 1240, February 1964, 100 pp.
11. Power, D. V. A Survey of Complaints of Seismic-Related Damage to Surface Structures Following the Salmon Underground Nuclear Detonation. Bull. of the Seis. Soc. of America, v. 56, No. 6, December 1966, pp. 1413–1428.
12. Sadwin, L. D., and W. I. Duvall. A Comparison of Explosives by Cratering and Other Methods. Trans. of SME of AIME, v. 232, June 1965, pp. 111–115.
13. Thoenen, J. R., and Windes, S. L. Seismic Effects of Quarry Blasting. BuMines Bull. 442, 1942, 83 pp.
14. Wall, J. F., Jr. Seismic-Induced Architectural Damage to Masonry Structures at Mercury, Nevada. Bull. of the Seis. Soc. of America, v. 57, No. 5, October 1967, pp. 991–1007.
15. Windes, S. L. Damage From Air Blast. Progress Report 1. BuMines Rept. of Inv. 3622, 1942, 18 pp.
16. ———. Damage From Air Blast. Progress Report 2. BuMines Rept. of Inv. 3708, 1943, 50 pp.

CHAPTER 4.—GENERATION AND PROPAGATION OF GROUND VIBRATIONS FROM BLASTING

4.1—INTRODUCTION

A major objective of the program was to determine a propagation law for ground-borne surface vibrations. Of primary interest were the relationships among the size of the explosive charge, shot-to-gage distance, and the magnitude of the ground vibration. Other variables considered were explosive type, method of initiation, geology, and directional effects.

The effect of distance and charge weight on the vibration level is basic to all blasting vibration studies. Many types of propagation laws or equations have been proposed. The most widely accepted form is

$$A = kW^bD^n, \quad (4.1)$$

where A is the peak amplitude, W is the charge weight, D is the distance, and k, b, and n are constants associated with a given site or shooting procedure. Both theoretical and empirical methods have been used to estimate values of b and n. Typical values found in the literature for b range from 0.4 to 1.0 and for n from -1 to -2 (*1, 4, 5, 9–12, 14–17*). The quantity, A, may be the peak amplitude of particle displacement, velocity, or acceleration, and k and n will vary correspondingly. For purposes of the present study, particle velocity only was recorded and analyzed, because it correlated most directly with damage (see Chapter 3).

A reasonable aim in any scientific research is to obtain reliable data with a minimum expenditure of experimental effort. This requires that the variables to be studied be controlled in a known manner and that other contributing factors be held constant or randomized. The desired degree of control was not always attained in the study of quarry blasting vibrations. Quarry operators, justifiably, were often reluctant to vary factors, such as method of initiation, hole size, burden, spacing, etc., because such changes could result in additional operating costs. Therefore, it was necessary to visit a large number of quarries and with the close cooperation of the quarry operators select the necessary conditions of explosive placement and initiation, terrain, overburden, etc. Most of the quarries selected were in relatively flat terrain, with more or less uniform overburden extending back from a working face for 1,000 feet or more.

Among the gross factors studied were a comparison of vibration levels from millisecond-delayed blasts and instantaneous blasts, the proper charge weight to be used in scaling data from different blasts, and the scaling factor to be used (*6, 7*). In addition, the effect of the method of blast initiation on vibration amplitudes was investigated, as well as such variables as direction of propagation, overburden thickness, site, and rock type. Most quarries or blasting operations use a particular type or types of explosive that best suit their needs. Explosive type varied within and among quarries and could not be controlled. Therefore, the site effect includes the effect of using different explosives at different sites.

Fourier spectra analysis methods were used on a limited amount of the data where particular results were desired, such as those arrived at in section 3.6. The technique was not used extensively in a routine manner but only as a device to provide specific results.

The basic instrumentation used in these tests (described fully in Chapter 2) consisted of up to 36 particle velocity gages and amplifiers and two direct-writing oscillographs. The gages were generally mounted in or on the overburden, on steel pins driven in the sides of square holes in the soil, or in boxes buried in square holes in the soil. Occasionally the gage boxes were attached directly to the rock surface with cement. The normal gage array consisted of several stations, each at a successively greater shot-to-station distance and each with 3 gages oriented in three mutually perpendicular directions from the shot. At some quarries, extended arrays with only vertically oriented gages were used. At other quarries, the azimuth between arrays or parts of an array was changed either to study directional effects or because of difficulty in maintaining a single azimuth due to terrain or physical obstructions.

Refraction tests were conducted in some of the quarries to determine overburden depths and seismic propagation velocities. Arrival times on the recordings from quarry blasts were also analyzed to determine velocities through the rock beneath the overburden.

A total of 171 blasts were recorded at 26 sites. The charge size ranged from 70 to 180,550 pounds per blast and from 25 to 19,625 pounds per delay. The number of holes per shot ranged from 1 to 490. The rock types included limestone, dolomite, diorite, basalt, sericite schist, trap rock, granite, granite-gneiss, and sandstone.

4.2—MILLISECOND-DELAYED BLASTS VERSUS INSTANTANEOUS BLASTS

In the 1940's and 1950's, millisecond-delay blasting became an accepted technique for reducing vibrations from blasting and as a better method for breaking rock. The main variables associated with a millisecond-delayed blast in a given rock are the delay interval, the number of delay intervals, and the number of holes per delay interval. Although previous work by other investigators had shown that millisecond-delayed blasts produce smaller vibration amplitudes than those produced by instantaneous blasts employing the same total charge weight, the effect of these variables on the vibrations produced by millisecond-delayed blasts was not thoroughly understood.

For the first phase of the field program, the following problems were selected for study: (1) to determine the propagation law for the amplitude of vibrations produced by both instantaneous and millisecond-delayed quarry blasts, (2) to determine if the level of vibration at various distances from the blast area is controlled by either the length of the delay interval or the number of delay periods in a millisecond-delayed quarry blast, and (3) to compare vibration levels from instantaneous quarry blasts with those from millisecond-delayed blasts.

4.2.1—Experimental Procedure

The factorial design and shooting order used to study vibration levels from instantaneous and millisecond-delayed blasts is given in table 4.1. For these 12 tests, only a single row of holes was used. Detonating fuse between holes connected the charges together in series for the instantaneous blasts. Delay intervals were achieved by placing a 9, 17, or two 17 millisecond-delay connectors in series with the detonating fuse between adjacent holes of the round. Only one hole per delay was used.

Table 4.1.—Factorial design and shooting order by test number

No. of holes	Delay interval, msec. 0	9	17	34
3	2	19	3	6
7	8	20	5	7
15	12	21	11	13

The study also included five single-hole and two multiple-row millisecond-delayed blasts. For the two multiple-row blasts, the maximum number of holes per delay was four for one round and six for the other.

An attempt was made to randomize the shooting order and position along the face for these blasts to remove bias due to these variables. The necessity to efficiently mine the face prevented complete randomization. In addition, the tests involving multiple-rows and 9 millisecond-delay intervals were added to the program after the other tests had been completed.

Hole diameter, depth, spacing, burden, and loading procedure were held constant for these tests. Spacing and burden were 15 and 10 feet, respectively. All holes were 6 inches in diameter and 36 feet in depth. Stemming was about 15 feet. A 200-pound charge of explosives in 5-inch diameter sticks was loaded into each hole.

A plan view of the test area at the Weaver Quarry near Alden, Iowa, is shown in Appendix A, figure A-1. The location of each quarry blast is identified by test number, and the area of rock breakage is indicated by broken lines. The instrument arrays were placed along the straight lines shown on the map and are identified by a number signifying the corresponding blast and area. In general, each instrument array was directly behind the blast area and approximately perpendicular to the face. The main exception was the array used for Shot 14. The gaps shown between the blast areas represent the rock quarried when vibration studies were not conducted. The distance to the gage stations along each array was measured from the center of the blast area.

Up to 24 particle velocity versus time records were obtained from each of the 19 quarry blasts. Typical recordings are shown in figures 4.1 through 4.4. The vertical lines represent 10-millisecond intervals. Each record trace is identified as to component of particle velocity and the distance from blast to gage. R, V, and T represent the radial, vertical and transverse components. The center trace of each record is the 100 cps reference timing signal from a standard oscillator.

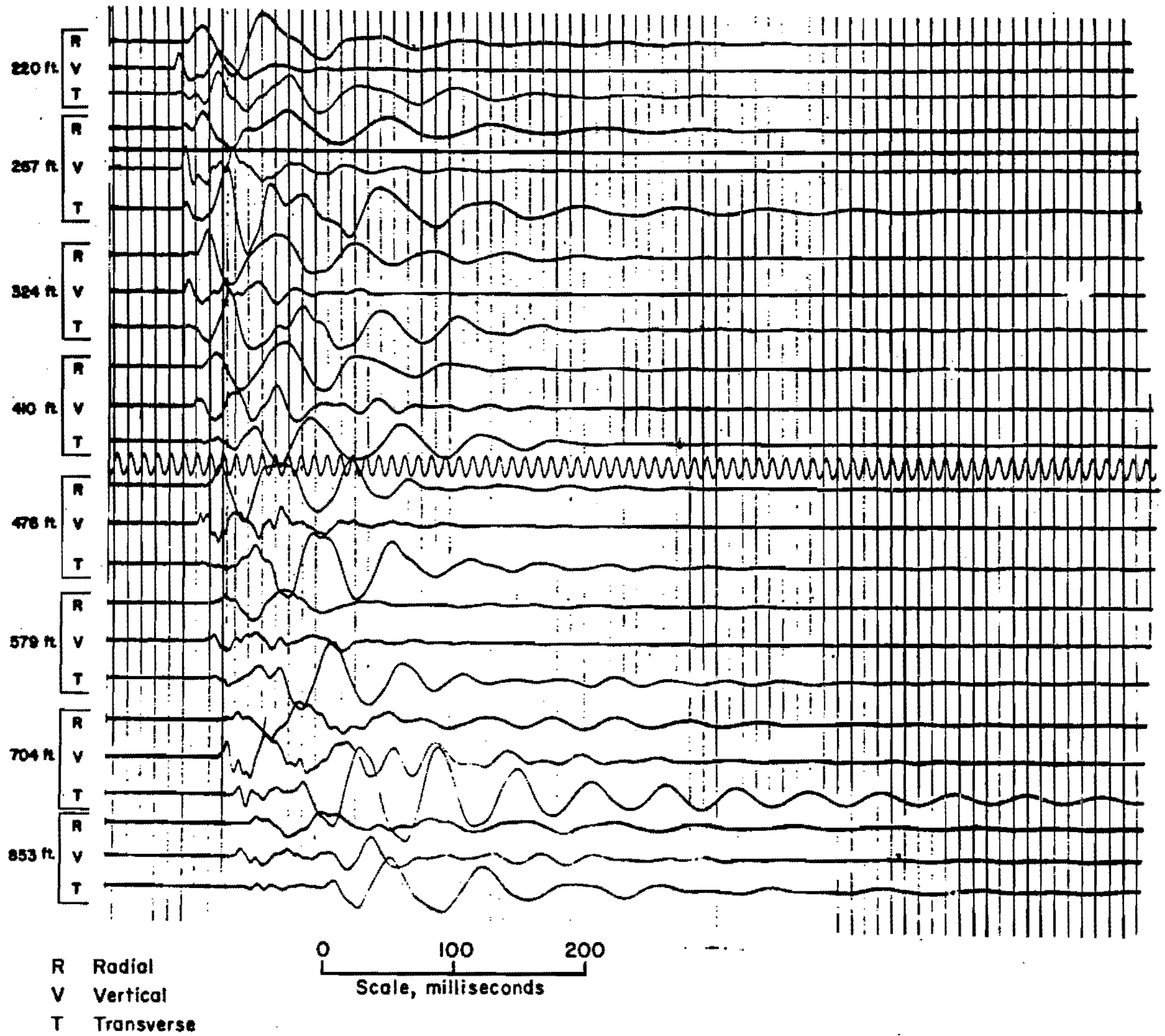

Figure 4.1.—Vibration records for 1-hole blast.

Table 4.2 summarizes the quarry blasts instrumented in this test. For more complete shot information on these and other tests see Appendix B, table B-1. Table C-1 in Appendix C presents the particle velocity and frequency data for the shots in this series.

The time duration of the seismic vibration for the instantaneous blasts averaged 200 milliseconds and for the millisecond-delayed blasts averaged 200 milliseconds plus the product of the length of the delay interval and the number of delays.

The analysis of the data was conducted in a sequential manner: first, to determine propagation laws for data from each blast; second, to determine the effect of charge weight; third, to determine the relation between instantaneous and millisecond-delayed blasts. These three steps are, of course, interdependent. The approach used did not include imposing preconceived ideas based upon existent empirical or theoretical results but was based upon a statistical analysis of the data.

4.2.2—Propagation Law

Plots of peak particle velocity versus distance were made on log-log coordinates. The data, as shown in figures 4.5 to 4.7, are grouped by test, number of holes per blast, and by radial, vertical, and transverse components. The linear grouping

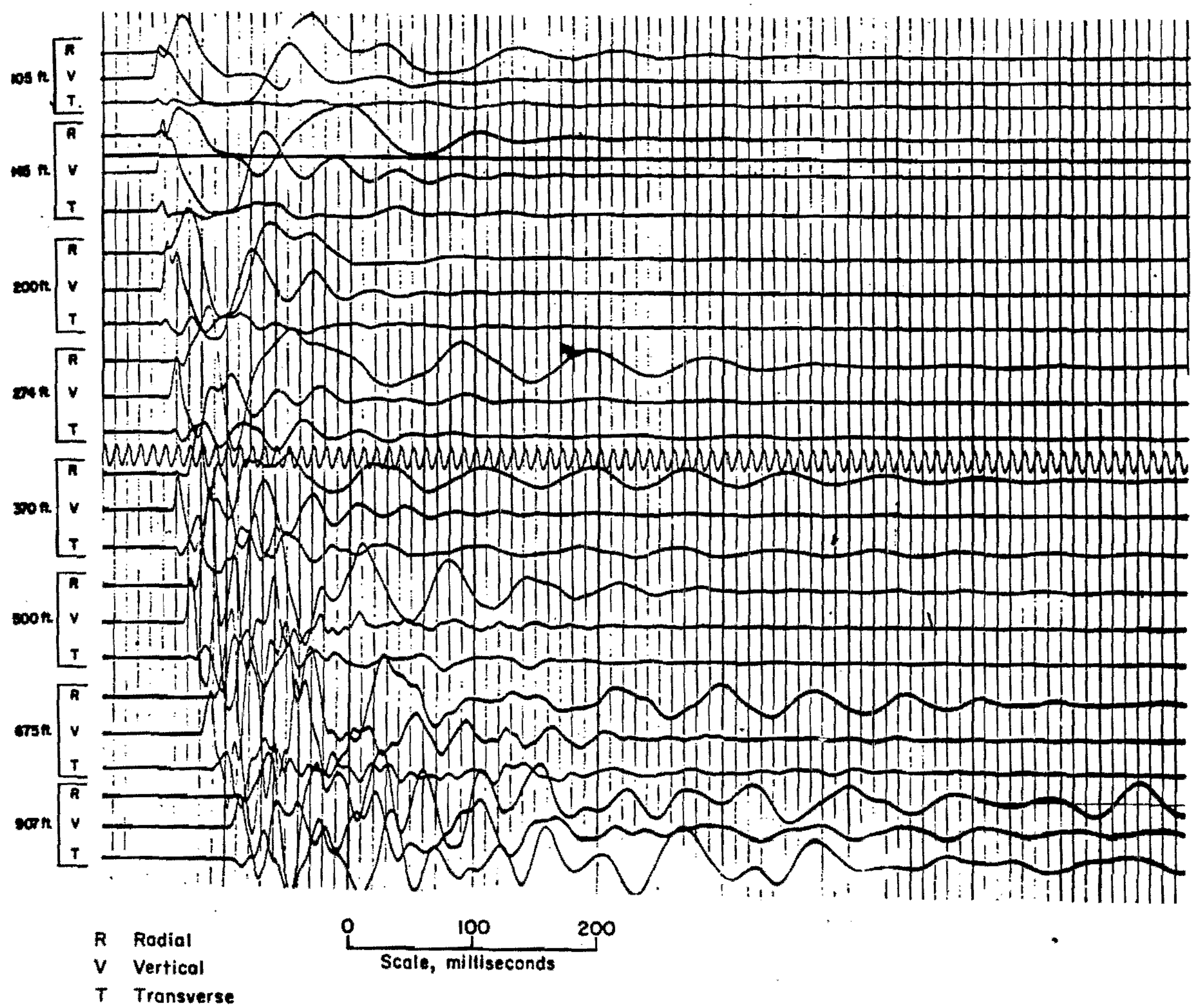

Figure 4.2.—Vibration records for 7-hole instantaneous blast.

of the data permits their representation by an equation of the form:

$$v = kD^{n} \qquad (4.2)$$

where v = peak particle velocity, in/sec;
D = shot-to-gage distance, 100 feet;
k = intercept, velocity at D = unity;
n = exponent or slope.

The values of k and n were determined for each set of data by the method of least squares. Statistical tests showed that a common slope, n, could be used for all data of a given component and that the values of k were significantly different at a confidence level of 95 percent. The average values of n, for each component were significantly different, and a grand common slope for all components could not be used. The average values of n for each component, the standard error of n, the standard deviation about regression, and the average standard error of intercepts are given in table 4.3. The average value of n for each component was used to calculate a new particle velocity intercept for each set of data. The individual values for these intercepts are given in table 4.4 for each component. These intercepts are the values of k from the following equations:

$$v_r = k_r D^{-1.63} \qquad (4.3)$$

$$v_v = k_v D^{-1.74} \qquad (4.4)$$

$$v_t = k_t D^{-1.28} \qquad (4.5)$$

where v is the particle velocity in in/sec, D is the distance from blast to gage expressed in hundreds of feet, and r, v, and t denote the component.

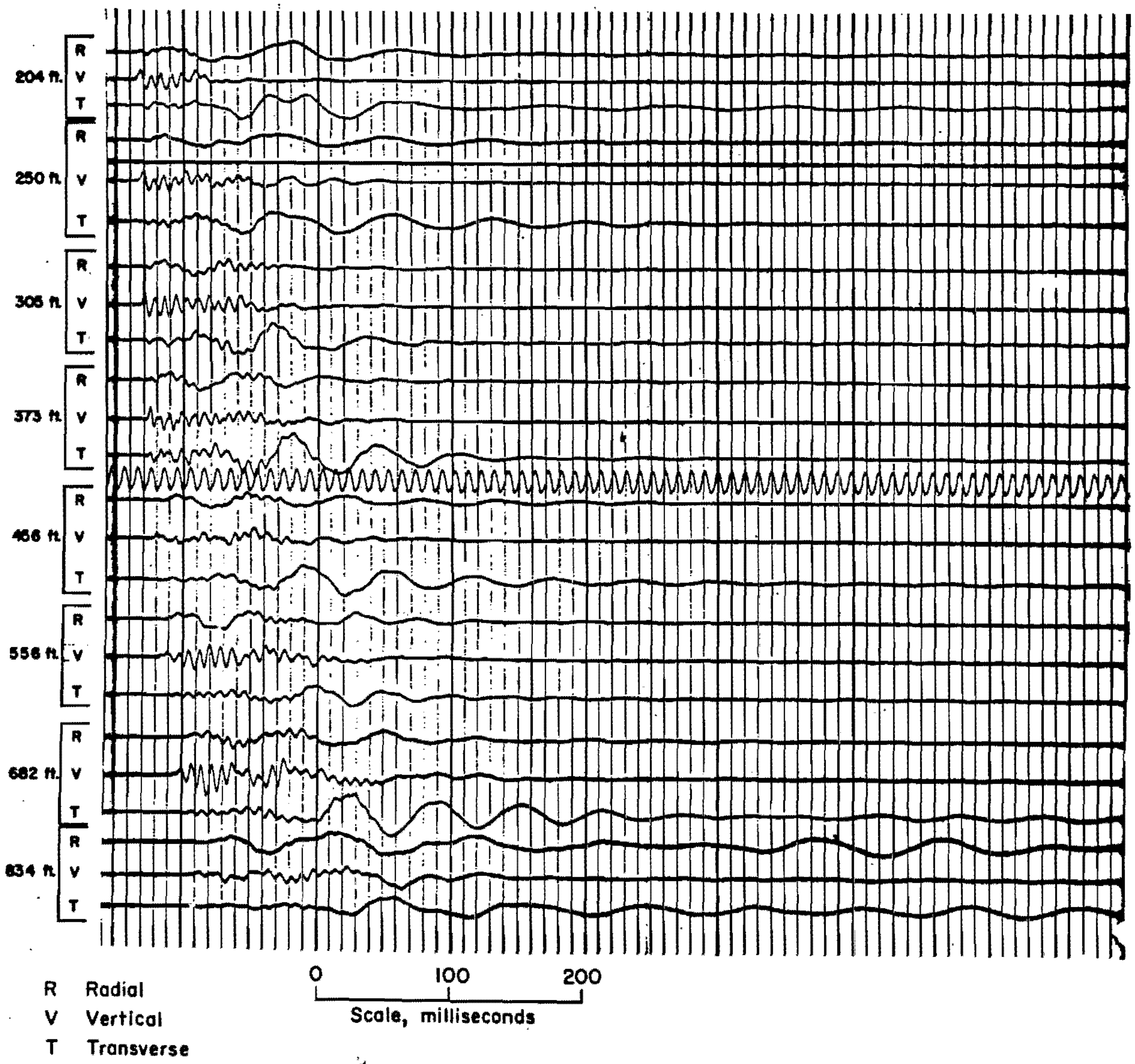

Figure 4.3.—Vibration records for 7-hole, 9-millisecond-delayed blast.

4.2.3—Effect of Charge Weight for Instantaneous Blasts

The data from the instantaneous blasts were studied to determine the effect of charge weight on the level of vibration. The particle velocity intercepts (table 4.4) were plotted as a function of charge weight (figure 4.8). The resultant linear grouping of the data indicated that each group could be represented by an equation of the form:

$$k = KW^b, \tag{4.6}$$

where k = velocity intercept at 100 feet, in/sec;

K = intercept of regression line at W = 1 pound, in/sec;

and W = charge weight, pounds;

b = slope of regression line and exponent of W.

The determination of b and K by the method of least squares results in the following equations:

$$k_r = 0.052\ W^{0.84}, \tag{4.7}$$

$$k_v = 0.071\ W^{0.73}, \tag{4.8}$$

$$k_t = 0.035\ W^{0.67}. \tag{4.9}$$

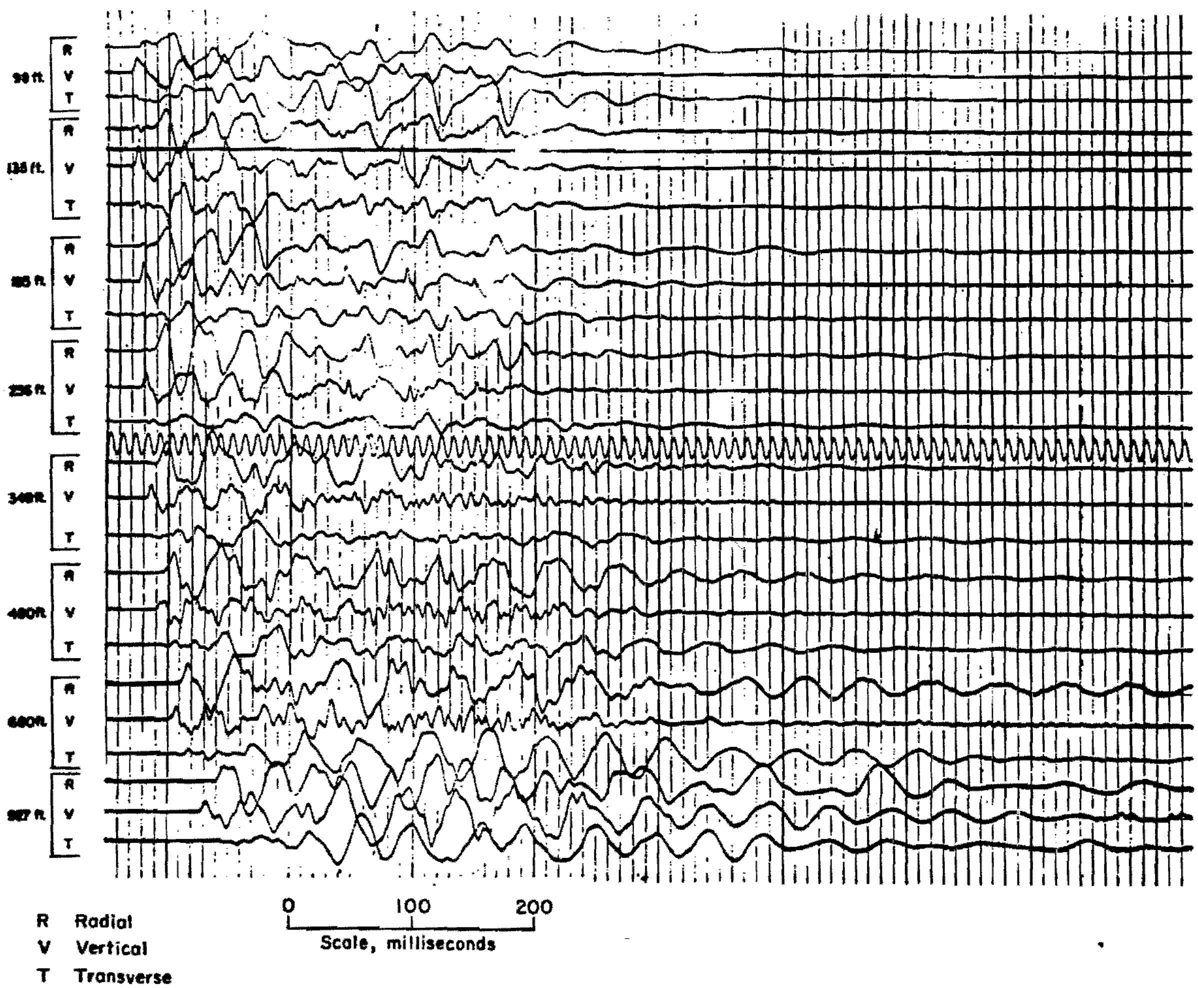

Figure 4.4.—Vibration records for 7-hole, 34-millisecond-delayed blast.

Table 4.2.—Summary of quarry-blasting tests

Test	Number of holes	Holes per delay	Delay, msec	Charge/delay, pounds	Total charge, pounds
2	3	3	0	600	600
3	3	1	17	200	600
4	1	1	0	200	200
5	7	1	17	200	1,400
6	3	1	34	200	600
7	7	1	34	200	1,400
8	7	7	0	1,400	1,400
9	1	1	0	200	200
10	1	1	0	200	200
11	15	1	17	200	3,000
12	15	15	0	3,000	3,000
13	15	1	34	200	3,000
14	1	1	0	100	100
18	1	1	0	200	200
19	3	1	9	200	600
20	7	1	9	200	1,400
21	15	1	9	200	3,000
27	13	4	17	800	2,600
32	21	6	17	1,218	4,263

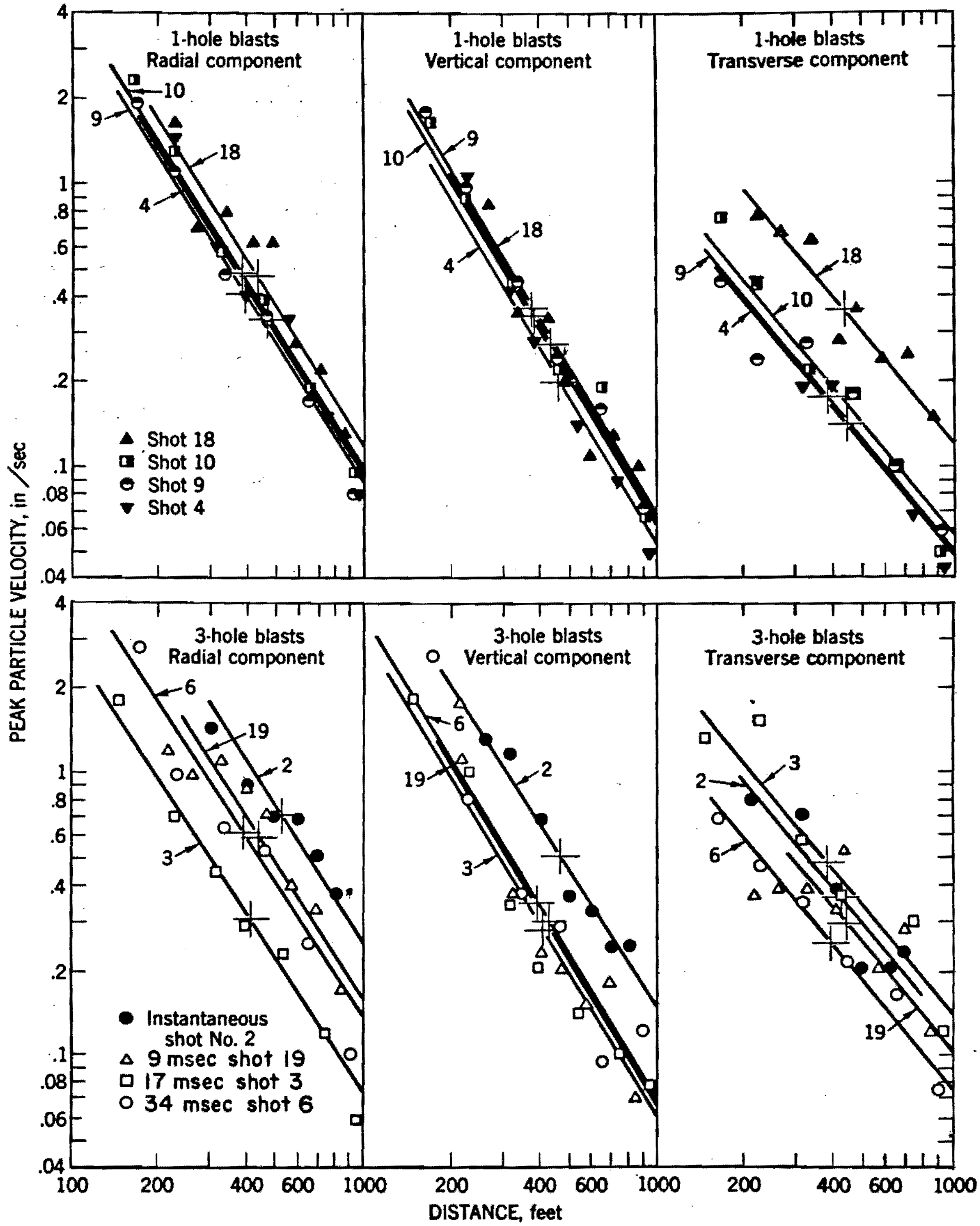

Figure 4.5.—Particle velocity versus distance for 1- and 3-hole blasts.

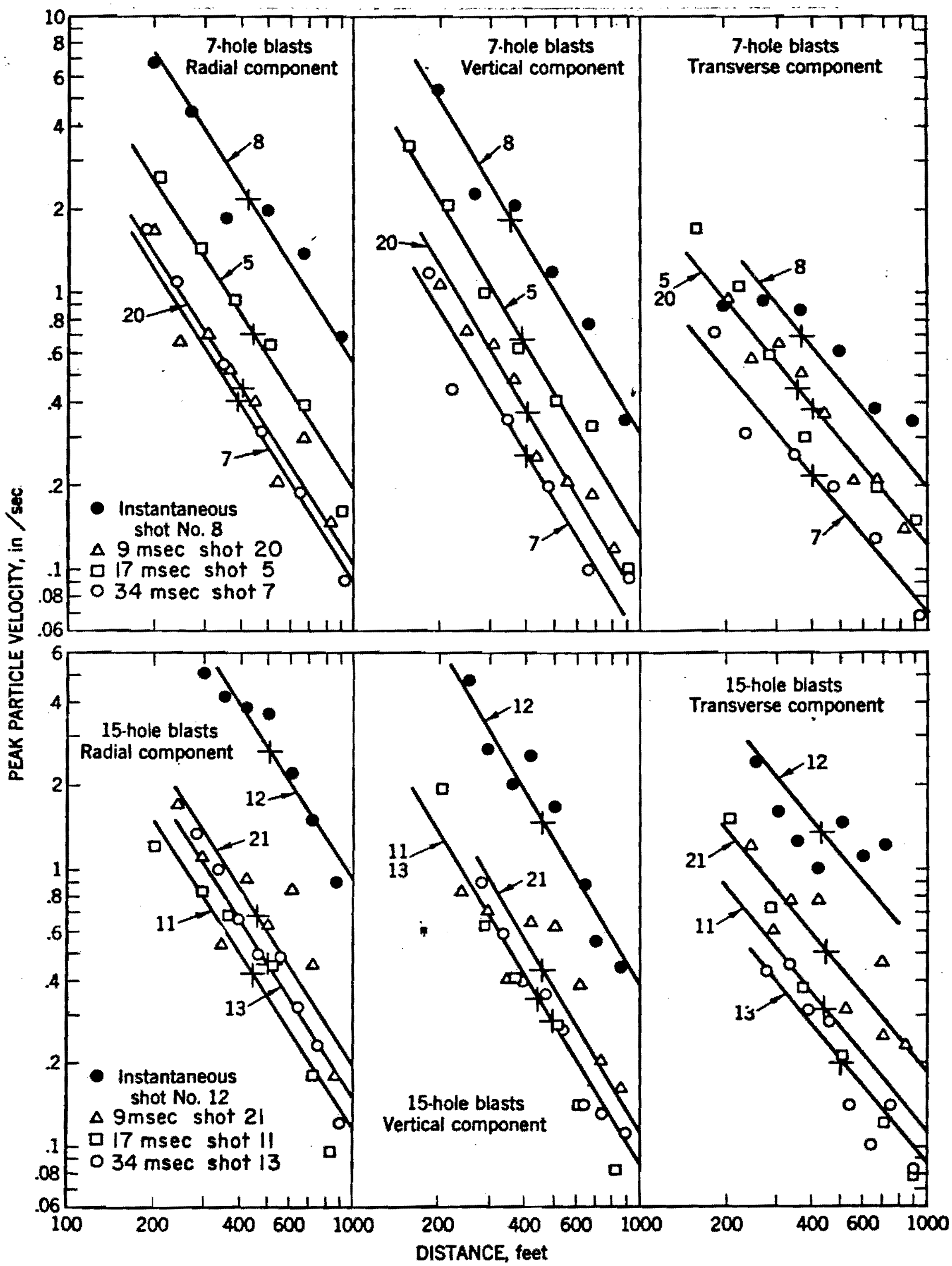

Figure 4.6.—Particle velocity versus distance for 7- and 15-hole blasts.

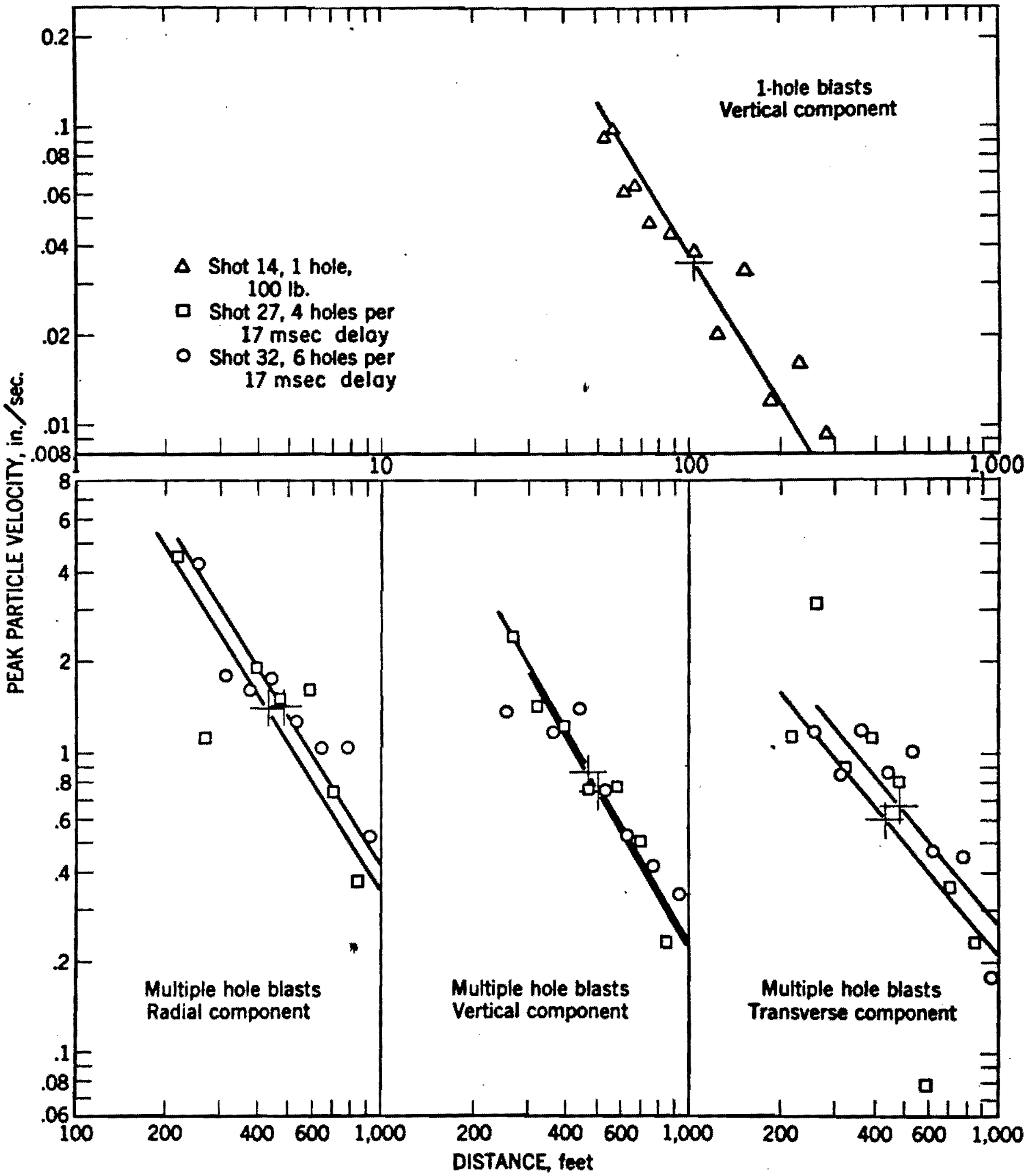

Figure 4.7.—Particle velocity versus distance for a 1-hole and 2-multiple-row blasts.

Table 4.3.—Average n and standard deviations

Component	Average n	Standard deviation about regression, percent	Average standard error of intercepts, percent
Radial	−1.628±0.043	±27	±30
Vertical	−1.741± .049	±32	±27
Transverse	−1.279± .063	±35	±40

The substitution of equations 4.7 to 4.9 into equations 4.3 to 4.5 provides equations difficult to handle, because charge weight and distance would then have different exponents. If charge weight, raised to some power is considered to be a scaling factor, the substitution of equations 4.7, 4.8, and 4.9 into equations 4.3, 4.4, and 4.5 and simplification of terms gives:

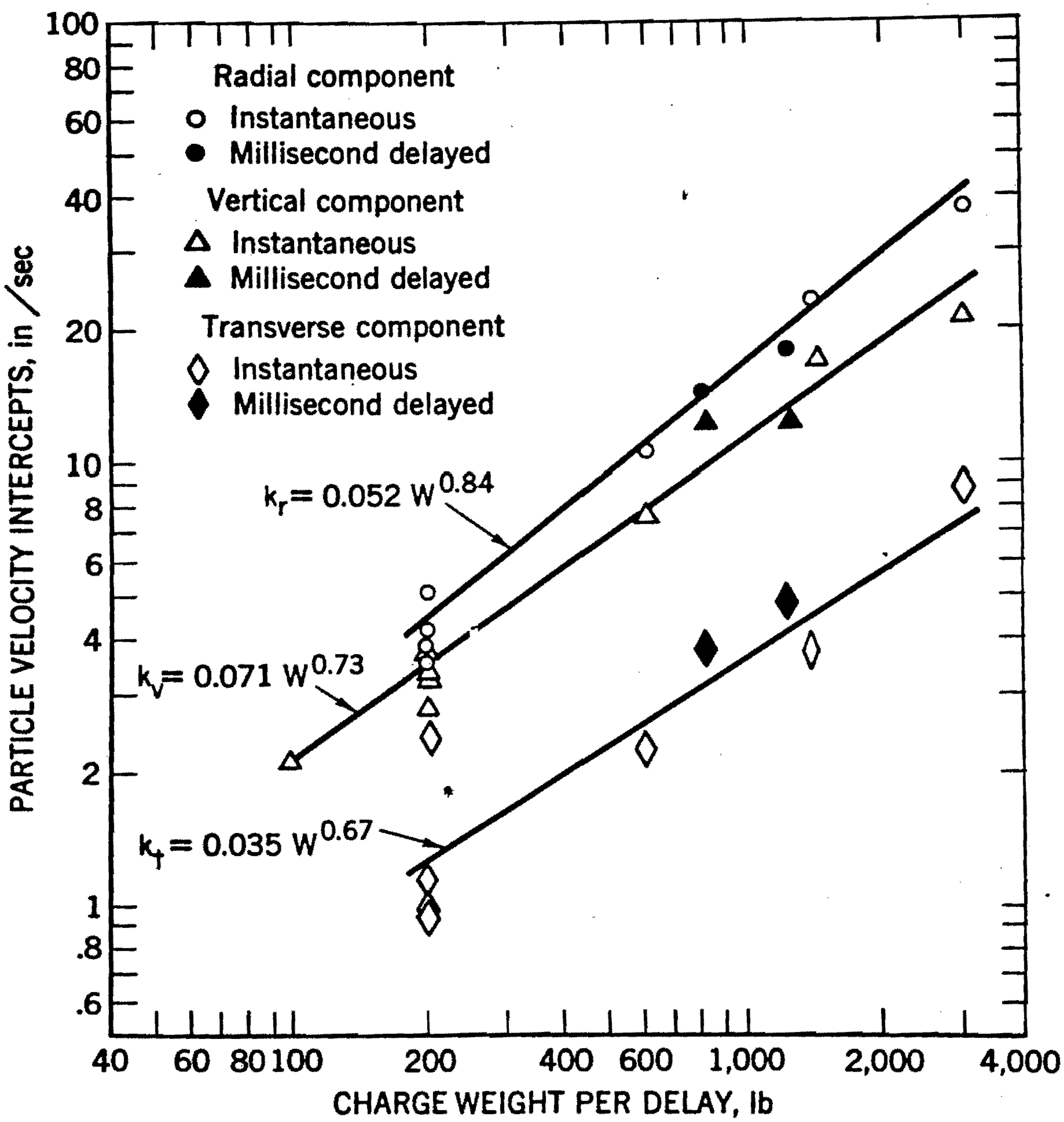

Figure 4.8.—Comparison of effect of charge weight on level of vibration from instantaneous and millisecond-delayed blasts.

Table 4.4—Particle velocity intercepts at 100 feet

Test	Particle velocity intercepts		
	Radial in/sec	Vertical in/sec	Transverse in/sec
14	....	2.15	......
4	4.03	2.88	0.94
9	3.62	3.70	.98
18	5.24	3.48	2.39
10	4.24	3.44	1.02
2	10.8	7.76	2.28
8	23.9	17.9	3.74
12	38.6	22.1	8.99
19	6.66	3.72	1.93
20	4.53	4.35	2.35
21	8.24	6.33	3.60
3	2.99	3.16	2.65
5	8.10	7.04	2.42
11	4.83	4.61	2.14
6	5.81	3.90	1.45
7	4.14	3.06	1.30
13	6.41	4.71	1.61
27	14.4	12.3	3.79
32	18.2	12.7	4.83

$$v_r = 0.052 \left(\frac{D}{W^{0.512}}\right)^{-1.63}, \qquad (4.10)$$

$$v_v = 0.071 \left(\frac{D}{W^{0.421}}\right)^{-1.74}, \qquad (4.11)$$

$$v_t = 0.035 \left(\frac{D}{W^{0.521}}\right)^{-1.28}. \qquad (4.12)$$

Although the exponent of W varies only from 0.421 to 0.521 indicating the square root of W may be the proper scaling factor, there are insufficient data from this one site to statistically support such a conclusion.

4.2.4—Effect of Delay Interval and Number of Holes

The nine quarry blasts employing delays of 9, 17, and 34 milliseconds and three, seven, and 15 holes were used to study the effect of delay interval and number of holes on the vibration level. Inspection of figures 4.5 and 4.6 indicates that the vibration levels from millisecond-delayed blasts are generally lower than those from instantaneous blasts employing the same number of holes. Data from these figures also shows that the relative vibration levels appear to be randomly distributed with respect to delay interval or number of holes. Analyses of variance tests on the particle velocity intercepts (table 4.4) for these blasts showed no significant differences due to delay interval or number of holes. Therefore, it can be concluded that the level of vibrations from millisecond-delay blasts employing only one hole per delay is not controlled significantly either by the delay interval or the number of delay periods.

4.2.5—Comparison of Millisecond-Delayed Blasts with Instantaneous Blasts

The level of vibration from instantaneous blasts depends upon the number of holes in the round or the total charge weight (see equations 4.10 to 4.12). If the level of vibration from millisecond-delayed blasts is independent of the number of delays or the length of delay interval (as shown in section 4.2.4), then the vibration level from these blasts must depend mainly upon the charge size per delay or the number of holes per delay. Therefore, the vibration levels from instantaneous and millisecond-delayed blasts should correspond closely providing the same number of holes are used in the instantaneous blast as are used in each delay.

The results (intercepts, k, and standard deviation, σ) from Shots 4, 9, 10, and 18, one-hole instantaneous blasts are compared with the millisecond-delayed blasts using one hole per delay in table 4.5. Subscript i stands for instantaneous, and subscript d stands for delayed. Millisecond-delayed blasts with one hole per delay produce, on the average, a vibration level 42 percent greater with 2.5 times the data spread than single hole blasts. However, these differences are not statistically significant at the 95 percent confidence level. The trend does show some constructive interference for single hole per delay blasts.

Quarry blasts 27 and 32 were millisecond-delayed blasts with a maximum of four and six holes per delay, respectively. The particle velocity intercepts at 100 feet from these blasts were plotted as a function of charge size per delay on the same graph as the instantaneous blasts (figure 4.8). Examination of these data shows that the vibration levels from millisecond-delayed blasts (multiple hole per delay) are about the same as those from instantaneous blasts. Apparently millisecond-delayed blasts with multiple holes per delay produce a more uniform vibration level than similar blasts with one hole per delay.

Therefore, it can be concluded that no significant error is introduced if comparisons of vibration levels among blasts are made on the basis of equivalent charge weights per delay or total charge for the case of instantaneous blasts. Any scaling or normalizing must be accomplished by using the charge weight per delay because this is the effective charge weight. Furthermore, if the charge weight per delay varies for a given blast due to unequal loading per hole or unequal number of holes per delay, then it is the maxi-

Table 4.5.—Average particle velocity intercepts for single hole and millisecond-delayed blasts

Component	Single hole blasts		Millisecond-delayed blasts		Ratios	
	k_i	σ_i	k_d	σ_d	k_d/k_i	σ_d/σ_i
Radial	4.28	0.688	5.74	1.786	1.34	2.596
Vertical	3.38	.349	4.54	1.356	1.34	3.883
Transverse	1.36	.691	2.16	.709	1.59	1.026
Average	....	....	....	....	1.42	2.502

mum charge weight initiated at any particular delay interval which must be considered.

4.3—W^{α} AS A SCALING FACTOR

Three basic conclusions were made from an analysis of the data from millisecond-delayed and instantaneous blasts. First, the three components of peak particle velocity of ground vibration at a site can be represented by equations of the form:

$$v_i = H_i \left(\frac{D}{W^{\alpha}}\right)^{\beta_i} \qquad (4.13)$$

where

v = particle velocity,
H = particle velocity intercept,
D = shot-to-gage distance,
W = charge weight,
α = exponent,
β = slope or decay exponent,
and i = denotes component, radial, vertical, or transverse.

Second, W is the charge per delay or the total charge for an instantaneous blast, and third, that α may be about 0.5 or that square root scaling exists for these data.

Equation 4.13 for any one component implies that H and β are constants that have to be determined for each quarry site and possibly for each shooting procedure. To determine the applicability of this equation to particle velocity-distance data required a large amount of data from different sites with different propagation parameters, H and β. Statistical methods could then be used to determine the appropriateness of W^{α} as a scaling factor and the value of α.

Data used in this study were from five quarries or construction sites near Alden, Iowa; in Washington, D.C.; near Poughkeepsie, N.Y.; near Flat Rock, Ohio; and near Strasburg, Va. A description of each site is given in Appendix D. Vibrations from 39 blasts were recorded. Among the blasts were 12 instantaneous; 5 single hole per delay, using millisecond-delayed caps; and 22 multiple hole per delay, using millisecond-delay detonating fuse connectors. Charge weights per hole ranged from 7.8 to 1,522 pounds, and charge weights per delay, including the instantaneous blasts, ranged from 25 to 4,620 pounds.

4.3.1—Experimental Procedure

Plan views of the test sites are shown in Appendix A, figures A-1, -7, -10, -11, and -16. As shown, the gage array was oriented towards the blast area and directly behind it where feasible. At the Strasburg site, the data from lines 1 and 2 could not be combined. Therefore, the data from the two lines are treated as if from two separate sites and are denoted as Strasburg-1 and Strasburg-2.

The blasting pattern and method of blast initiation varied considerably from quarry to quarry. Among patterns used were single-hole shots, single-hole per delay shots, multiple-holes per delay shots with all holes in a delay group connected with detonating fuse, and instantaneous multiple-hole shots with all holes connected with detonating fuse. Often each site used more than one of these procedures. Table 4.6 summarizes the pertinent blast data.

For the millisecond-delayed blasts, the delay interval ranged from 5 to 26 milliseconds. Section 4.2.4 shows that the vibration level was independent of delay interval for intervals ranging from 9 to 34 milliseconds. The vibration levels from blasts using 5 millisecond delays did not differ appreciably with those from shots with longer delays and were included in the analysis. As the result of conclusions in section 4.2.5, the maximum charge weight per delay was considered as the charge weight for each shot.

The peak particle velocities, associated frequencies, and shot-to-gage distances are given in Appendix C, tables C-1, -7, -10, -11, and -16.

4.3.2—Data Analysis

Plots of peak particle velocity versus shot-to-gage distance were made for each site, test, and component. Good linear grouping of the data indicated that straight lines could be fitted to the data by a general propagation equation of the form:

Table 4.6. - Quarry blast data by site

Test	Total no. of holes	Hole depth, ft	Face height, ft	Total charge, lb	Max. charge per delay, lb	Charge per hole, lb	No. of delay intervals	Length of delay,[1] msec	Burden, ft	Spacing, ft
					Weaver					
2...	3	36	30	600	600	200	0	0	10	15
4...	1	36	30	200	200	200	0	0	10	-
8...	7	36	30	1,400	1,400	200	0	0	10	15
9...	1	36	30	200	200	200	0	0	10	-
10...	1	36	30	200	200	200	0	0	10	-
12...	15	36	30	3,000	3,000	200	0	0	10	15
18...	1	36	30	200	200	200	0	0	10	-
27...	13	36	30	2,600	800	200	3	17	10	15
32...	21	36	30	4,263	1,218	203	3	17	10	14
					D. C.					
45...	3	20	20	110	37	37	2	25(cap)	4	6
46...	13	20	20	403	31	31	12	25(cap)	4	6.5
50...	9	20	-	70	70	7.8	0	0	-	2.5
51...	13	20	20	403	31	31	12	25(cap)	4	6
52...	13	20	20	325	25	25	12	25(cap)	4	6
54...	13	18	20	308	25	24 avg	12	25(cap)	4	6
					Poughkeepsie					
55...	35	-	28- 54	21,578	920	920	34	17,26	22	20
56...	13	-	83-104	18,471	1,522	1,100-1,522	12	26	22	20
63E..	18	-	67- 73	19,933	1,249	1,039-1,249	17	26	23	20
63SE.	-	-	-	-	-	-	-	-	-	-
64N..	6	-	-	1,200	200	200	5	26	10-15	20
64E..	-	-	-	-	-	-	-	-	-	-
65N..	28	55-60	50- 55	28,810	1,405	700-1,405	27	26	21	20
65E..	-	-	-	-	-	-	-	-	-	-
67...	12	76-82	70- 76	14,576	1,355	1,100-1,355	11	26	22	22
					Flat Rock					
75...	36	24	23	6,430	1,072	180	9	9	12	10
78...	36	56	54	16,520	4,620	459	12	9	14	11
79...	1	56	54	468	468	468	0	0	10	-
					Strasburg-1					
96...	84	20	18	3,350	1,120	40 avg	2	5	8	5
99...	49	20	18	1,950	968	40 avg	1	5	8	5
101...	78	20	18	3,200	1,600	40 avg	1	5	8	5
103...	59	20	18	2,150	589	35 avg	3	5	8	5
104...	60	15-20	15- 20	2,425	1,330	40 avg	1	9	8	6
106...	61	20	18	2,350	1,380	40 avg	1	9	8	5
108...	60	20	18	1,950	1,600	20-35	1	5	10	6
109...	51	20	12- 14	1,700	865	33 avg	1	5	8	5-7
110...	51	20	18	1,750	360	32 avg	4	5	8	6
111...	48	20	18	1,600	367	33 avg	4	5	8	6
					Strasburg-2					
98...	31	20	18	1,250	605	40.3 avg	1	5	8	5
100...	16	22-12	20- 10	475	475	25-35	0	0	8	5
102...	16	10-20	8- 18	450	343	25-35	1	5	8	5
105...	42	4-20	4- 20	1,325	1,325	25-35	0	0	10	5
107...	42	6-20	6- 20	1,250	1,250	25-35	0	0	8	5

[1] The length of the delay is considered to be zero if the shot consisted of a single hole, of one hole per delay, or of multiple holes per delay tied together with detonating fuse.

$$v = K_{ij} D^{\beta_{ij}}, \tag{4.14}$$

where v = peak particle velocity,

D = travel distance,

β_{ij} = exponent of D or the slope of the straight line through the jth set of data at the ith site,

and K_{ij} = velocity intercept at unit travel distance for the jth set of data at the ith site.

The subscript i denotes the site and varies from 1 to 6, whereas the subscript j denotes a test at a specific site and varies from 1 to k_i, where k_i is the total number of tests at a site. Since each test is treated separately at this point, there is no charge weight term needed.

The method of least squares was used to determine the slope, intercept, and standard deviation of the data about the straight line representing the data. Because of the large amount of data, only the least-squared lines are shown in figures 4.9 to 4.11 with the standard deviation shown as a vertical line through the midpoint of the data.

An analysis of variance was performed on the data to determine if sets of data, either by component at each site or among sites, could be pooled. The results showed that significant dif-

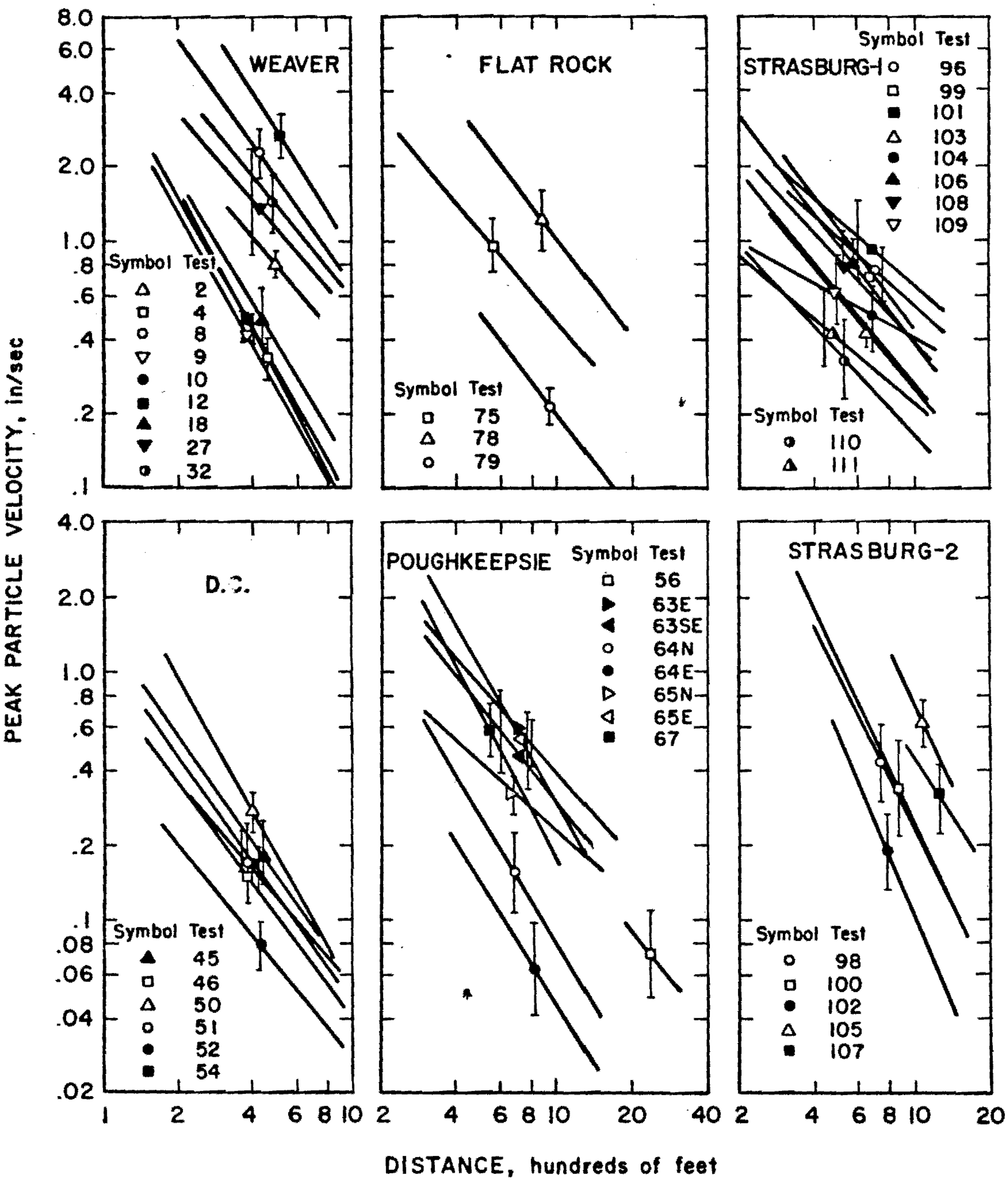

Figure 4.9.—Peak particle velocity versus distance, radial component.

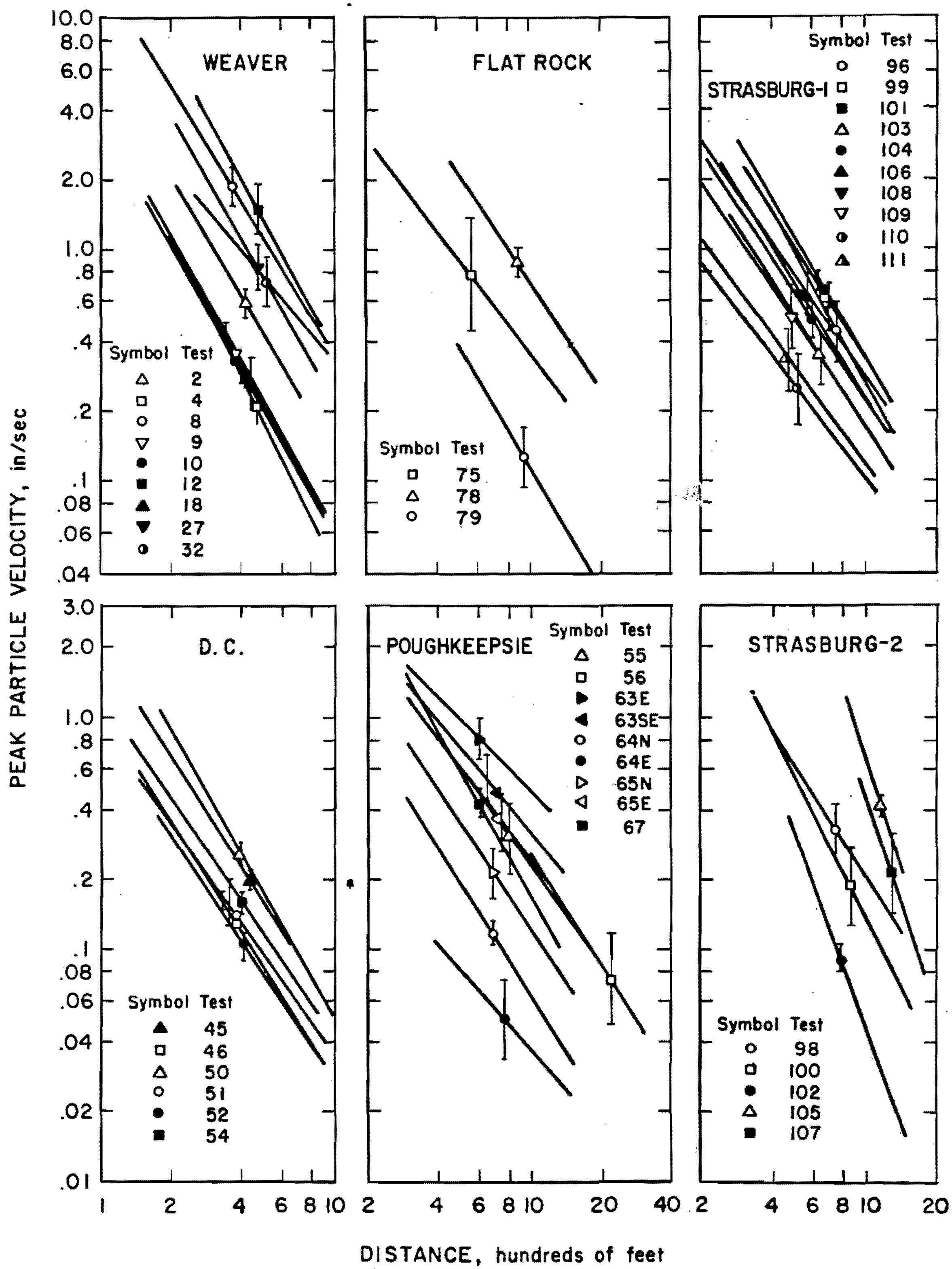

Figure 4.10.—Peak particle velocity versus distance, vertical component.

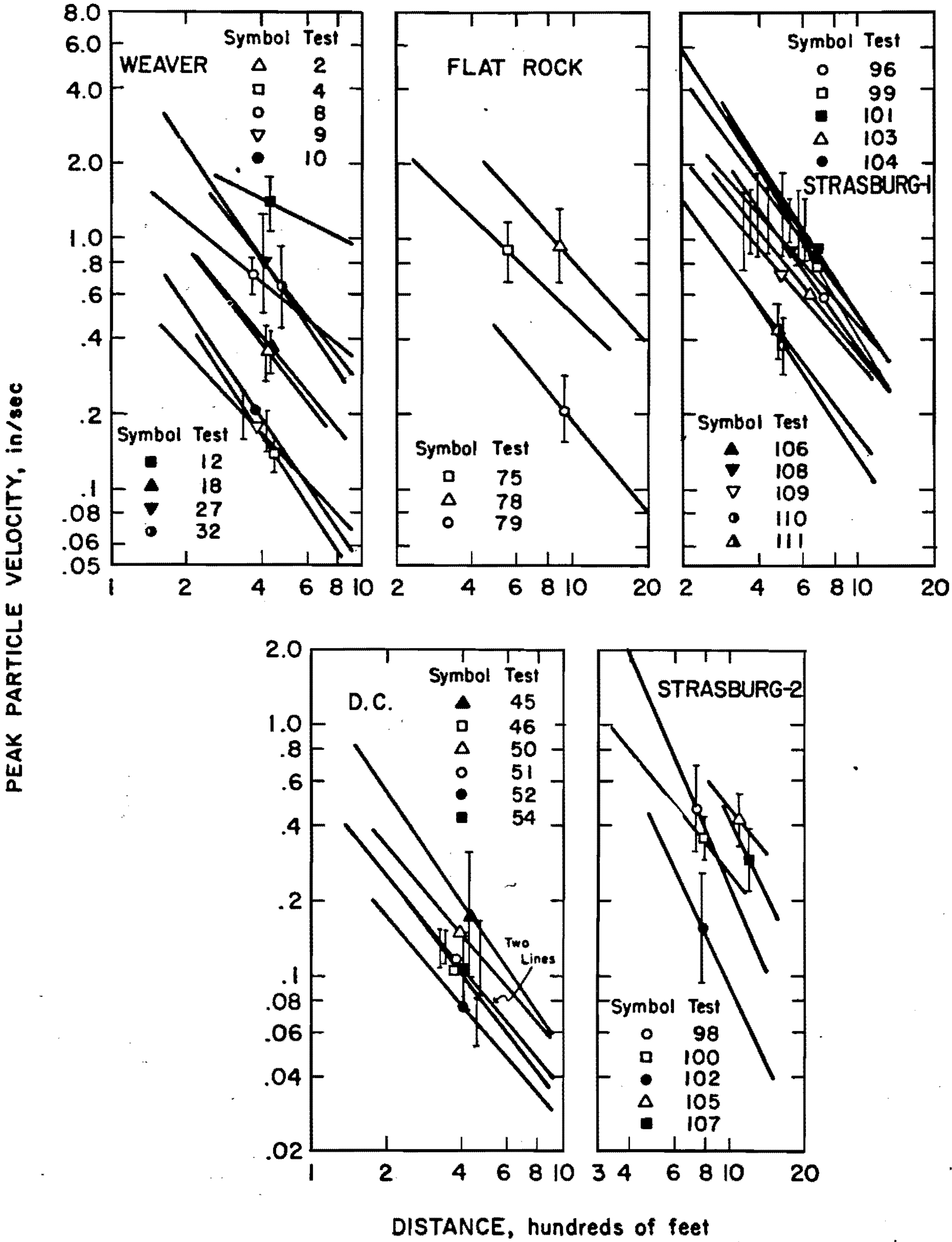

Figure 4.11.—Peak particle velocity versus distance, transverse component.

ferences existed and no pooling could be done. The results also showed that there were no significant differences in the slopes for different tests at each site for each component. Thus an average slope, β_i, was used for each component at each site. These average slopes are given in table 4.7.

Table 4.7—Average slopes, β_i

Site	Component		
	Radial	Vertical	Transverse
Weaver	−1.576	−1.766	−1.189
D.C.	−1.384	−1.548	−1.285
Poughkeepsie	−1.431	−1.475	—
Flat Rock	−1.255	−1.497	−1.083
Strasburg-1	−1.086	−1.548	−1.389
Strasburg-2	−2.148	−2.346	−2.046

An analysis of variance test was performed on data from all sites grouped together by component to determine if significant differences in slope existed because of site effects. There was a significant difference in slope with site for radial and vertical components but not for the transverse component. Examination of the standard deviations on figures 4.9 to 4.11 indicates a greater spread in the data for the transverse component.

No attempt was made to combine these data beyond an average slope, β_i. The intercepts, K_{ij}, for each test were calculated using the average slope, β_i, for each component at each site. Distances were determined in units of 100 feet to reduce the variance in the intercept and to reduce extrapolation. Therefore, the values of K_{ij} represent the particle velocity at 100 feet and are summarized in table 4.8. This table and figures 4.9 to 4.11 show that the level of vibration generally increases as charge weight per delay increases. Equation 4.14 can now be written as

$$v = K_{ij}D^{\beta_i} \qquad (4.15)$$

where D is now in units of 100 feet and β_i is the average slope of the j sets of data at the *ith* site.

Generalizing equation 4.13 gives

$$v = H_i\,(D/W_{ij}^{\alpha})^{\beta_i} \qquad (4.16)$$

where D = distance in units of 100 ft,

W_{ij} = maximum charge weight per delay for each test in units of 100 pounds,

and H_i = velocity intercept at $D/W^{\alpha} = 1$ for all the tests at the *ith* site.

A comparison of equation 4.15 and 4.16 shows that the following relationship must exist:

$$K_{ij} = H_iW_{ij}^{-\alpha\beta_i}. \qquad (4.17)$$

The relationship of equation 4.17 indicates that a log-log plot of the K_{ij} intercept values versus W_{ij}, charge weight per delay, should give a linear grouping of the data by site and component. Plots of these data, K_{ij} versus W_{ij}, from table 4.8, are shown in figures 4.12A, 4.13A, and 4.14A. Linear grouping of the data is obtained, and furthermore, the data from each site group independently indicating that the slope, $\alpha\beta_i$, and the intercept, H_i, are functions of site and component. The values of $\alpha\beta_i$ and H_i as determined by the method of least squares are given in table 4.8.

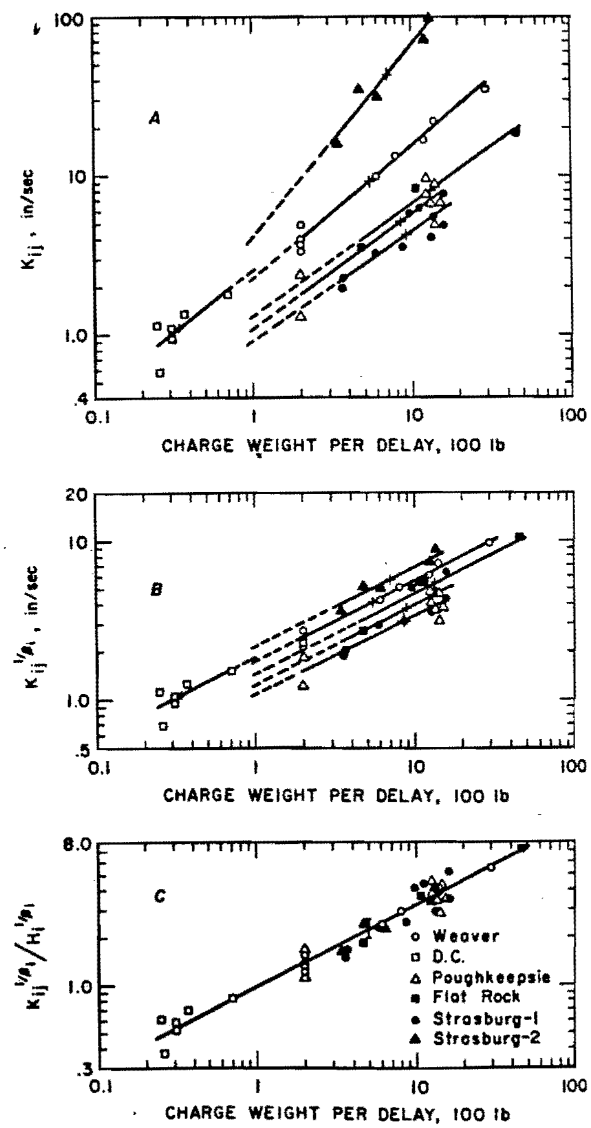

Figure 4.12.—Particle velocity intercepts versus charge weight per delay, radial component.

Table 4.8. - Summary of K_{ij}, $\alpha\beta_i$, and H_i data by quarry

Test	Maximum charge per delay, lb	Radial			Vertical			Transverse		
		K_{ij}, in/sec	$\alpha\beta_i$	H_i	K_{ij}, in/sec	$\alpha\beta_i$	H_i	K_{ij}, in/sec	$\alpha\beta_i$	H_i
					Weaver					
2...	600	9.88	0.830	2.24	7.61	0.753	2.13	1.99	0.710	0.675
4...	200	3.72	-	-	3.12	-	-	.817	-	-
8...	1,400	22.1	-	-	18.4	-	-	3.35	-	-
9...	200	3.34	-	-	3.77	-	-	.874	-	-
10...	200	3.95	-	-	3.51	-	-	.992	-	-
12...	3,000	35.2	-	-	23.3	-	-	7.94	-	-
18...	200	4.88	-	-	3.60	-	-	2.07	-	-
27...	800	13.3	-	-	12.9	-	-	4.27	-	-
32...	1,218	16.9	-	-	13.2	-	-	4.19	-	-
					D. C.					
45...	37	1.38	0.774	2.52	1.92	0.741	2.96	1.16	0.525	1.22
46...	31	.947	-	-	.997	-	-	.603	-	-
50...	70	1.81	-	-	2.17	-	-	.875	-	-
51...	31	1.08	-	-	1.10	-	-	.624	-	-
52...	26	.586	-	-	.897	-	-	.461	-	-
54...	25	1.15	-	-	1.37	-	-	.637	-	-
					Poughkeepsie					
55...	920	-	0.724	1.09	6.59	0.802	0.861	-	-	-
56...	1,522	6.73	-	-	6.94	-	-	-	-	-
63E..	1,249	9.80	-	-	11.4	-	-	-	-	-
63SE.	-	7.64	-	-	8.76	-	-	-	-	-
64N..	200	2.39	-	-	2.00	-	-	-	-	-
64E..	-	1.31	-	-	1.00	-	-	-	-	-
65N..	1,405	5.01	-	-	3.60	-	-	-	-	-
65E..	-	8.99	-	-	6.81	-	-	-	-	-
67...	1,355	6.58	-	-	6.04	-	-	-	-	-
					Flat Rock					
75...	1,072	8.40	0.709	1.32	10.1	0.784	1.25	5.77	0.616	1.04
78...	4,620	18.8	-	-	23.2	-	-	10.1	-	-
79...	468	3.53	-	-	3.58	-	-	2.29	-	-
					Strasburg-1					
96...	1,120	6.37	0.696	0.906	10.4	0.742	1.45	9.37	0.762	1.54
99...	968	5.89	-	-	12.1	-	-	11.2	-	-
101...	1,600	7.58	-	-	12.7	-	-	13.1	-	-
103...	589	3.23	-	-	6.13	-	-	7.90	-	-
104...	1,330	4.06	-	-	8.08	-	-	11.9	-	-
106...	1,380	5.46	-	-	9.48	-	-	12.6	-	-
108...	1,600	4.91	-	-	8.71	-	-	2.23	-	-
109...	865	3.54	-	-	5.89	-	-	1.90	-	-
110...	360	1.99	-	-	3.18	-	-	1.26	-	-
111...	367	2.28	-	-	3.75	-	-	1.35	-	-
					Strasburg-2					
98...	605	31.8	1.21	4.04	36.3	1.49	2.30	29.2	1.05	3.82
100...	475	34.7	-	-	29.4	-	-	24.6	-	-
102...	343	15.7	-	-	11.8	-	-	11.0	-	-
105...	1,325	106	-	-	120	-	-	58.1	-	-
107...	1,250	71.7	-	-	81.9	-	-	48.8	-	-

The value of α can be determined empirically from the data if equation 4.17 is rewritten as:

$$(K_{ij})^{-1/\beta_i} = (H_i)^{-1/\beta_i} W_{ij}^{\alpha}. \qquad (4.18)$$

If W^{α} is a scaling factor, then a plot of $(K_{ij})^{-1/\beta_i}$ versus W_{ij} on log-log coordinates should result in the data grouping about a series of straight lines having a slope of α. If α can be shown to have a single unique value, then these lines would be parallel, but a separate line would exist for each site and component. The average values of β_i for each site and component, from table 4.7, were used to calculate the values of $(K_{ij})^{-1/\beta_i}$. These values are shown plotted as a function of W_{ij} in figures 4.12B, 4.13B, and 4.14B. The values of the slopes, α_i, were determined by the method of least squares and are given in table 4.9. An analysis of variance test performed on these data showed that all the data for each component cannot be pooled as a single set, but that an average α for each component can be used for all sites. These average values of α, one for each component, are given in table 4.9. Statistical t tests showed that there was no significant difference between each of these average slopes and a theoretical value of 0.5. Therefore, using standard statistical procedures and a slope of 0.5, straight lines were fitted to the data given in figures 4.12B, 4.13B, and 4.14B. These straight lines hav-

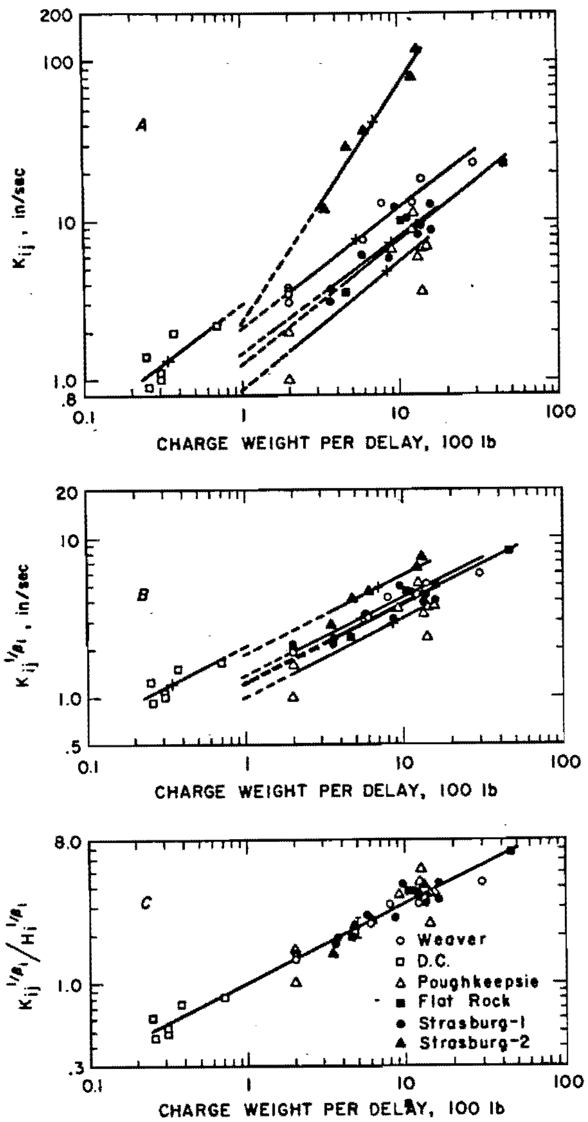

Figure 4.13.—Particle velocity intercepts versus charge weight per delay, vertical component.

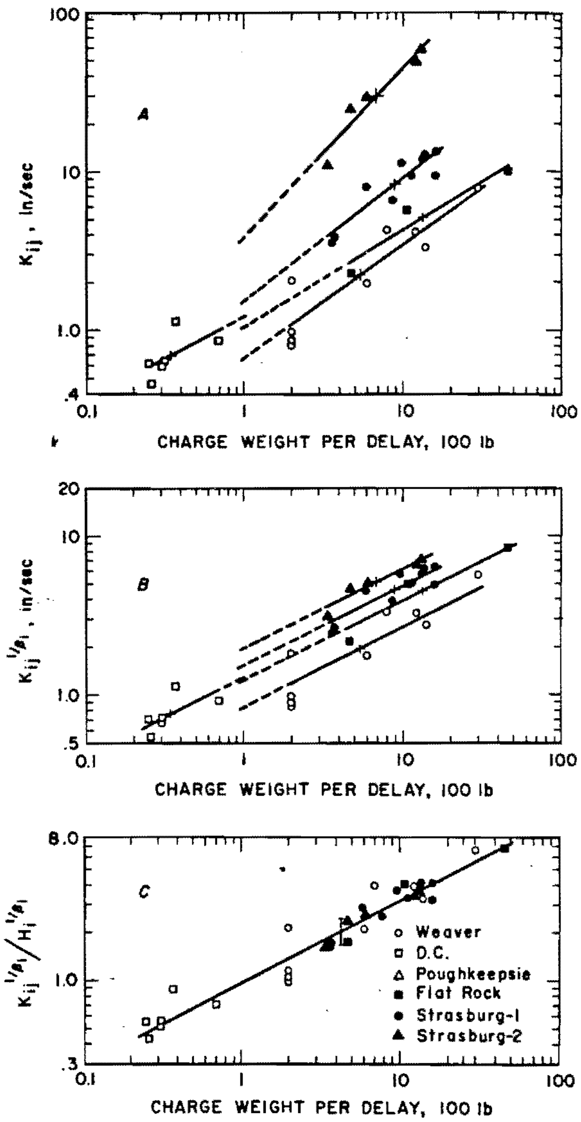

Figure 4.14.—Particle velocity intercepts versus charge weight per delay, transverse component.

ing a slope of 0.5 are parallel, and their separation is a function of test site.

If the site effect can be removed by normalizing the data, then a value of α can be calculated using the data for all sites for each component. Dividing each side of equation 4.18 by $(H_i)^{-1/\beta_i}$ gives:

$$(K_{ij})^{-1/\beta_i}/(H_i)^{-1/\beta_i}=W_{ij}^{\alpha}. \qquad (4.19)$$

The variation in intercepts associated with a site effect no longer exists because of the normalizing procedure as all intercepts now are unity. Figures 4.12C, 4.13C, and 4.14C show log-log plots of the $(K_{ij})^{-1/\beta_i}/(H_i)^{-1/\beta_i}$ values versus W_{ij}, charge weight per delay. These data were treated by component, and the results of analysis of variance tests indicated that one line could be used to represent all the data for one component. The statistically determined slopes and intercepts are given in table 4.10. The slopes in table 4.10 are closer to the theoretical value 0.5 than the average slopes given in table 4.9. A more accurate slope is obtained by using all the data than by grouping the data by site. Additionally, the intercepts (table 4.10) of the straight lines in figures 4.12C, 4.13C, and 4.14C are close to the theoretical value of 1.0 predicted by equation 4.19.

Table 4.9.—Values of α

Site	Component		
	Radial	Vertical	Transverse
Weaver	0.527	0.427	0.598
D.C.	.558	.474	.412
Poughkeepsie	.506	.546	....
Flat Rock	.568	.523	.566
Strasburg-1	.637	.479	.550
Strasburg-2	.567	.637	.516
Average α	.545	.491	.569

Table 4.10.—Slopes and intercepts from combined data

Component	Slope, α	Intercept
Radial	0.513	0.998
Vertical	.497	1.01
Transverse	.516	.976

Statistical analysis of the unscaled particle velocity-distance data as presented in figures 4.9 to 4.11 showed that none of the data could be grouped by site or component. Moreover, the standard deviations of these data about the regression line, assuming they could be grouped by site, varied from 42 to 136 percent. If these data are scaled by $W^{1/2}$ which is the square root of the charge per delay and similar analyses are performed, a significant reduction in the spread of the data is achieved. The same basic data plotted in figures 4.9 to 4.11 as particle velocity, v, versus distance, D, have been replotted in figures 4.15, to 4.17 as particle velocity, v, versus scaled distance, $D/W^{1/2}$. Comparing these figures shows that the total spread in the data has been reduced considerably. Analysis of variance tests after scaling shows that of the 17 possible groupings of data by site and component, no significant differences existed in eight of the groups. The standard deviations now varied from 28 to 53 percent, a significant reduction in the spread of the data. The fact that one line cannot be used to represent all the data from one component is probably a result of such variables as burden, spacing, charge geometry, and soil and rock properties.

The peak particle velocity of each component of ground motion can be related to distance and charge weight per delay interval by an equation of the form:

$$v = H_i \left(\frac{D}{W^{1/2}}\right)^{\beta_i}. \qquad (4.20)$$

Thus, when particle velocity is plotted on log-log coordinates as a function of scaled distance, $D/W^{1/2}$, straight lines with a slope of β_i can be placed through the data from each site and component.

The method of scaling distance by the square root of the charge weight per delay as determined empirically is a satisfactory procedure for removing the effect of charge weight on the amplitude of peak particle velocity. Other investigators have suggested that cube root scaling be used, because it can be supported by dimensional analysis. Cube root scaling can be derived from dimensional analysis if a spherical charge is assumed or if a cylindrical charge is assumed whose height changes in a specified manner with a change in radius. Taking the case of a sphere, a change in radius results in a volume increase proportional to the change in radius cubed. Weight is usually substituted for volume. The relationships result in cube root scaling. Blasting, as generally conducted, does not provide a scaled experiment. Charges are usually cylindrical. The height of the face or depth of lift are usually fixed. Therefore, the charge length is constant. Charge size is varied by changing hole diameter or the number of holes. The fixed length of the charge presents problems in dimensional analysis and prevents a complete solution. However, a change in radius, while holding the length constant results in a volume increase proportional to the radius squared. This indicates that scaling should be done by the square root of the volume or weight as customarily used. It is the geometry involved, cylindrical charges, and the manner in which charge size is changed by changing the diameter or number of holes which results in square root scaling being more applicable than cube root scaling to most blasting operations. The Bureau data, if analyzed using cube root scaling, does not show a reduction in the spread of the data which would occur if cube root scaling were more appropriate. In summary, the empirical results and a consideration of the geometry, including the procedure used to change charge size, and dimensional analysis indicate that data of the type from most blasting should be scaled by the square root of the charge weight per delay.

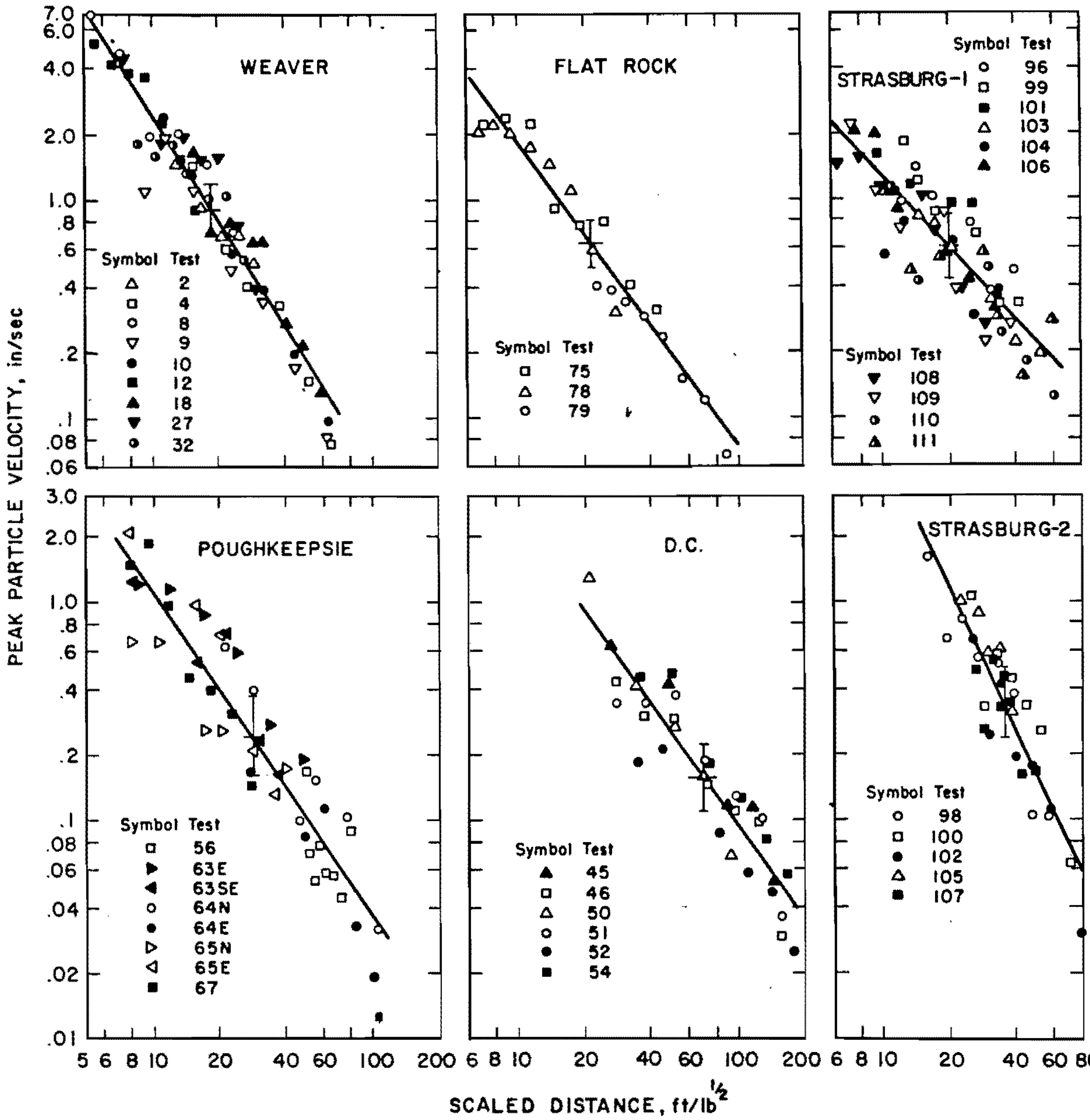

Figure 4.15.—Peak particle velocity versus scaled distance, radial component.

4.4—EFFECT OF METHOD OF INITIATION

A previous Bureau report (*8*) discussed the effect on particle velocity amplitude of delay shooting initiated by three methods. Method 1 consisted of connecting all holes in one delay period in series with Primacord. The groups of holes for each delay period were connected in series with Primacord delay connectors. Method 2 consisted of holes in a row connected in series with Primacord. Rows were connected in series with Primacord delay connectors with initiation originating at the center row. The difference between methods 1 and 2 was that in method 2 pairs of rows were parallel connected with Primacord delay connectors. Method 3 consisted of priming the charge in each hole with an electric millisecond-delay cap. Figure 4.18 illustrates the three methods of initiation.

It was concluded from the analysis of these data that method 1 produced a higher and more

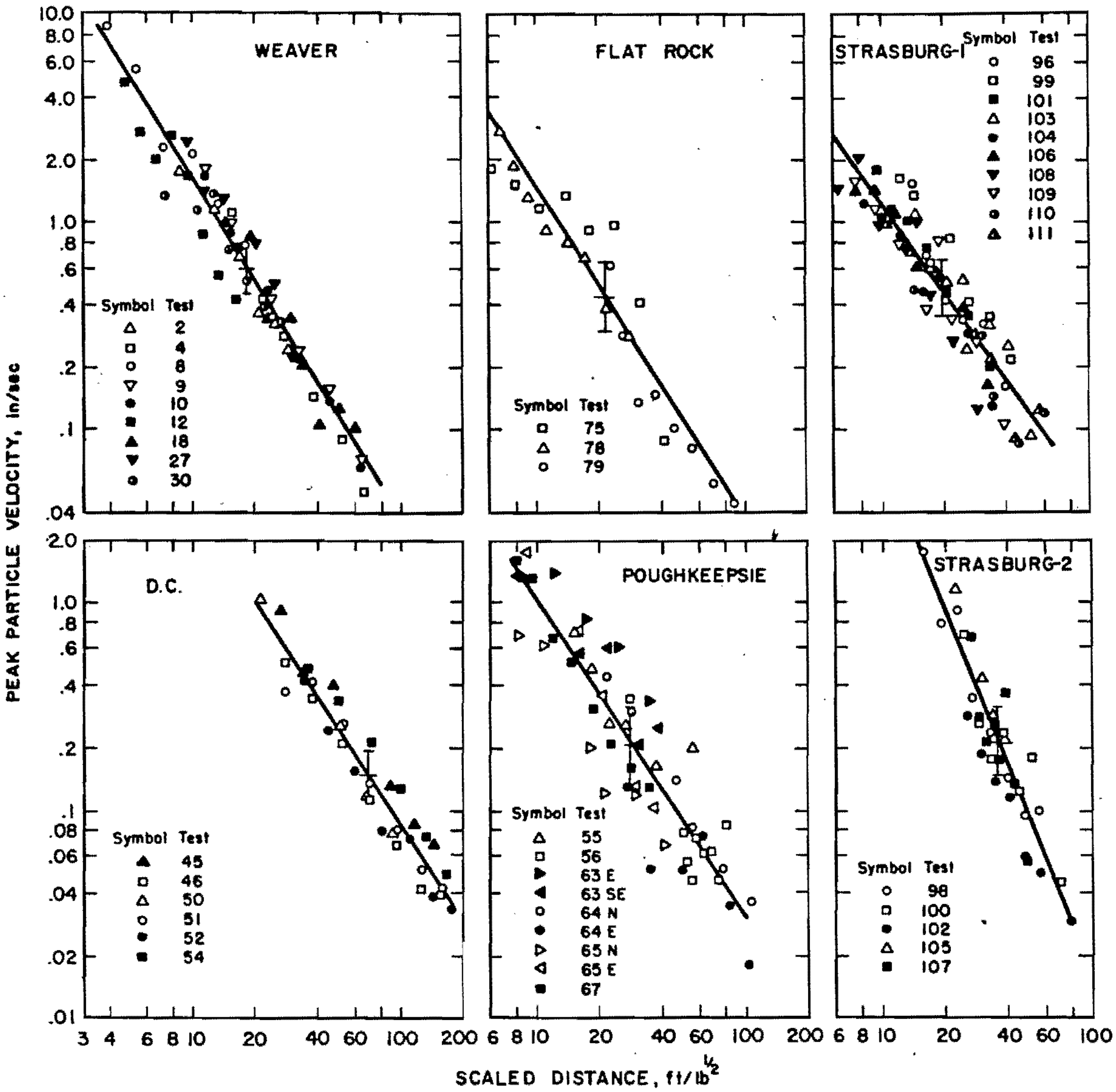

Figure 4.16.—Peak particle velocity versus scaled distance, vertical component.

consistent vibration level at a given scaled distance than either method 2 or 3. The burden and spacing in these tests were generally less than 10 feet. The high detonation rate of Primacord permitted the vibrations radiating from each hole in a row in methods 1 and 2 to add together at a distance from the blast. The vibrations apparently resulted from the simultaneous detonation of the total charge for all the holes of the row. The scatter in the firing time of Primacord connectors or electric delay caps used to connect rows is greater than the detonation time of the Primacord connecting holes in a row. For initiation methods 2 and 3, the scatter in delay interval connectors did not appear to result in appreciable addition of vibrations radiating from each hole. The vibration levels from methods 2 and 3 were approximately the same.

As an adjunct to these results, data were obtained to directly compare the vibration levels from instantaneous blasts, Primacord connector delayed blasts, and/or electric cap delayed blasts in selected quarries. Data were obtained from five quarries: Weaver, Flat Rock, Bloomville,

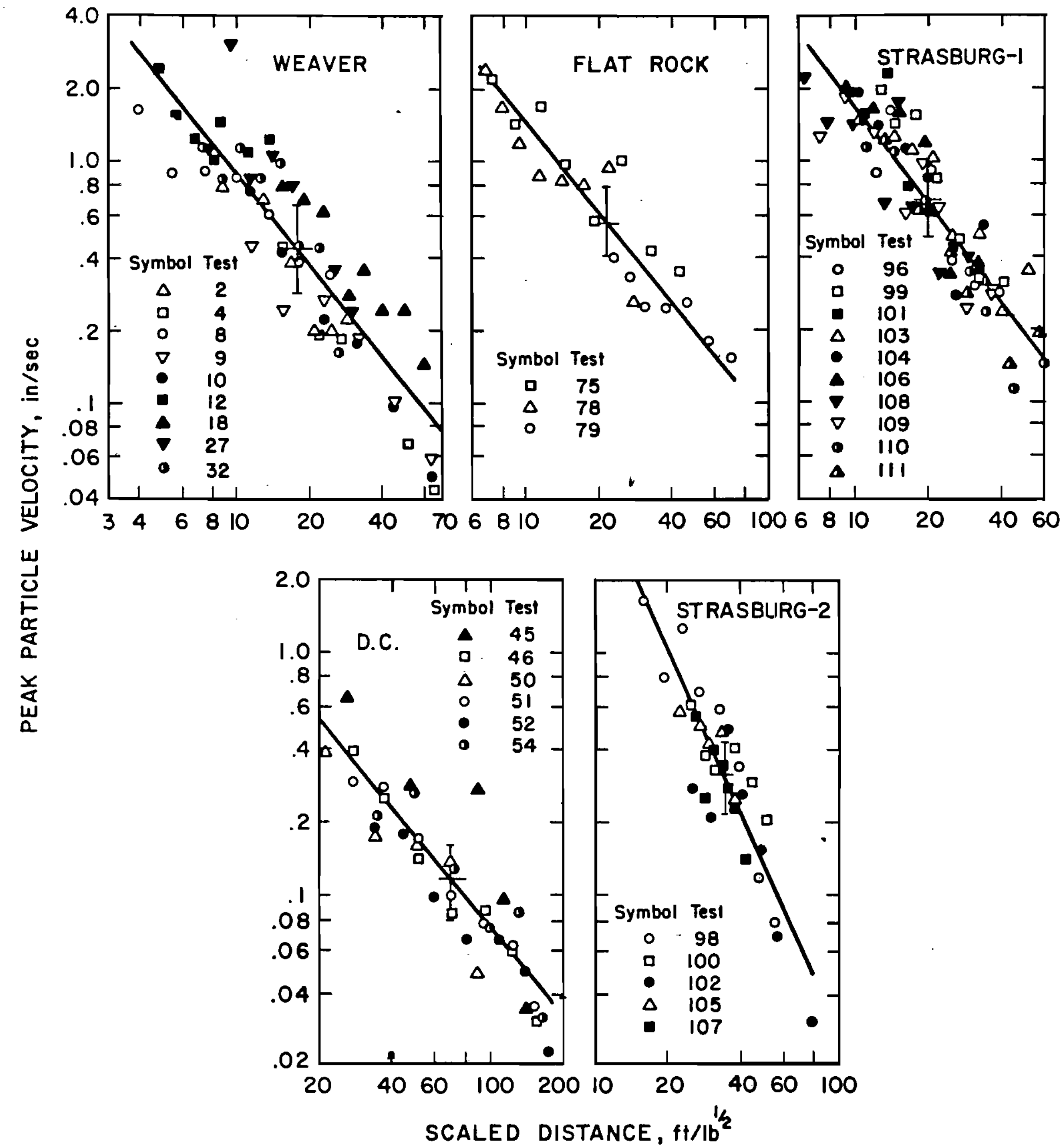

Figure 4.17.—Peak particle velocity versus scaled distance, transverse component.

Shawnee, and Jack. A description of each site is given in Appendix D. Data from 32 blasts are included. The number of delays varied from 0 to 14, and charge weight per delay ranged from 80 to 4,620 pounds.

4.4.1—Experimental Procedure

Plan views of the test sites are shown in Appendix A, figures A-1, -5, -7, -9, and -21. Additional vibration data were recorded in these quarries, but only those data directly applicable to this study were included. Only data recorded over a similar or parallel propagation path were used to insure exclusion of directional effects. Data are not compared among quarries, only within quarries, so that geologic effects could be

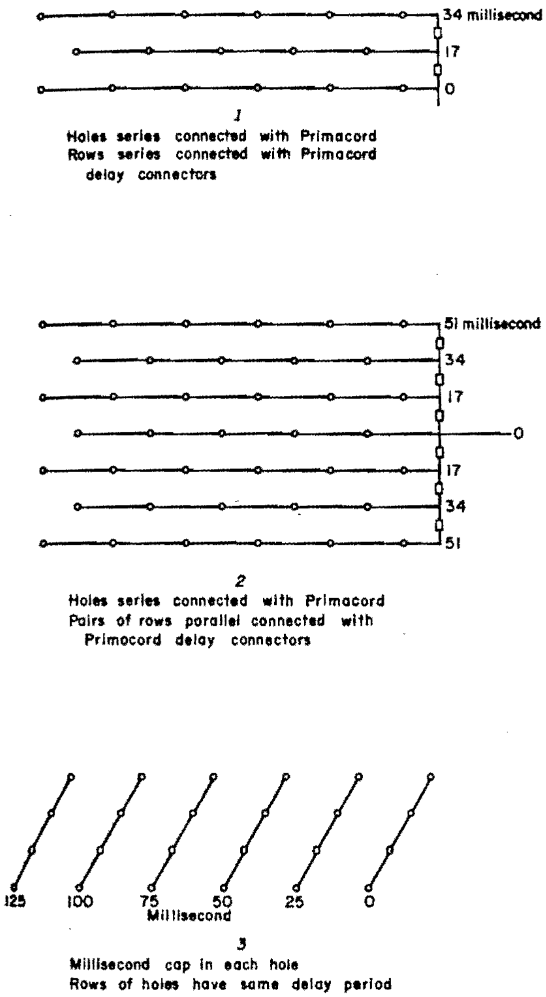

Figure 4.18.—Three methods of initiating blasts.

ignored. The Weaver quarry offered a comparison among instantaneous, Primacord delay, and electric cap delay initiated blasts. At the other quarries, Primacord or electric cap delay initiated blasts are compared with instantaneous blasts. Table 4.11 summarizes the blast data. The square root of the maximum charge weight per delay was used to scale the data. The peak particle velocities, associated frequencies, and shot-to-gage distances are given in Appendix C, tables C-1, -5, -7, -9, and -21.

4.4.2—Data Analysis

Plots of peak particle velocity versus scaled shot-to-gage distance were made for each shot. Straight lines were fitted to the data using a propagation equation of the form:

$$v = H\,(D/W^{1/2})^{\beta}. \qquad (4.21)$$

Analysis of variance indicated that the data from the several shots at a given quarry could not be grouped, but an average slope β_r, β_v, or β_t was acceptable for each component (radial, vertical, or transverse) at each quarry. These average slopes are given in table 4.11. The appropriate average slope was then used to calculate the value of v at a scaled distance of 10.0 for each component, for each blast at a given quarry. This results in a value, H_{10r}, H_{10v}, or H_{10t}, within the range of the observed field data, while H would have been an extrapolated value. These values are tabulated in table 4.11.

Inspection of these H_{10i} values indicated that vibration levels from Primacord delayed blasts were generally higher than the levels from instantaneous blasts, while the vibration levels from electric cap delayed blasts were generally less than the levels from instantaneous blasts. Therefore, the vibration levels from Primacord delayed blasts were higher than those from electric cap delayed blasts. Apparently the inherent scatter in time of Primacord delay connectors was less than the inherent scatter in the time delay of electric delay caps. Primacord delay connectors appear to result in constructive interference or addition of the seismic waves, and electric caps with greater scatter result in destructive interference or a decrease in vibration levels. The data from the Weaver quarry where all three methods were observed appears to bear out this conclusion.

The results were not obtained from a rigorous analysis but do indicate a trend whereby some reduction in vibration level can be attained if necessary. There are unexplained differences, such as the high level from test 18 at Weaver or test 36 from Bloomville. These may reflect the normal variation to be expected in such data. The trend is believed to be both valid and significant.

4.5—EFFECT OF GEOLOGY, INCLUDING DIRECTION OF PROPAGATION AND OVERBURDEN

The data presented in section 4.3 is indicative of geologic effects which give rise to differences in propagation which are apparently due to direction of propagation. If a site is horizontally stratified or of massive rock with horizontal isotropy and uniform overburden, little difference in wave propagation would be expected with direction. Conversely, if there is structural dip, geologic complexity, anisotropy, or any type

Table 4.11. - Summary - method of initiation tests by quarry

Test	No. of holes	No. of delays	Type of delay[1]	Delay interval, msec	Max.chg/ delay, lb	Total charge, lb	Particle velocity intercepts, in/sec			Average slopes
							H_{10r}	H_{10v}	H_{10t}	
Weaver										
15...	291	6	EDC	25	1,100	6,400	--	0.733	--	—
16...	147	6	EDC	25	484	3,234	--	1.75	--	—
17...	60	6	EDC	25	420	1,680	--	.463	--	—
19...	3	2	PDC	9	200	600	3.97	1.86	0.961	—
20...	7	6	PDC	9	200	1,400	2.66	2.18	1.45	—
5...	7	6	PDC	17	200	1,400	4.85	3.53	1.52	—
11...	15	14	PDC	17	200	3,000	2.92	2.27	1.31	—
6...	3	2	PDC	34	200	600	3.00	2.05	.914	$\bar{\beta}_r$ = -1.66
7...	7	6	PDC	34	200	1,400	2.48	1.57	.819	$\bar{\beta}_v$ = -1.66
13...	15	14	PDC	34	200	3,000	2.78	2.32	.990	$\bar{\beta}_t$ = -1.24
27...	13	3	PDC	17	800	2,600	3.63	1.92	1.09	—
9...	1	0	INST	0	200	200	2.10	1.86	.613	—
10...	1	0	INST	0	200	200	2.48	1.75	.698	—
18...	1	0	INST	0	200	200	3.13	1.73	1.46	—
2...	3	0	INST	0	600	600	2.56	1.46	.712	—
8...	7	0	INST	0	1,400	1,400	2.83	1.70	.698	—
12...	15	0	INST	0	3,000	3,000	2.41	1.16	1.04	—
Flat Rock										
75...	36	9	PDC	9	1,072	6,430	1.97	1.67	1.52	$\bar{\beta}_r$ = -1.32
78...	36	12	PDC	9	4,620	16,520	1.72	1.28	1.23	$\bar{\beta}_v$ = -1.45
79...	1	0	INST	0	468	468	1.48	1.05	.861	$\bar{\beta}_t$ = - .99
Bloomville										
36...	12	2	EDC	25	840	1,680	2.77	1.48	1.02	$\bar{\beta}_r$ = -1.17
76...	31	2	EDC	25	1,218	2,519	2.04	1.26	.741	$\bar{\beta}_v$ = -1.46
77...	1	0	INST	0	80	80	2.71	2.01	1.19	$\bar{\beta}_t$ = -1.29
Shawnee										
81...	12	3	EDC	25	612	1,224	.998	.719	.463	$\bar{\beta}_r$ = -1.37
82...	13	3	EDC	25	660	1,636	1.15	.684	.607	$\bar{\beta}_v$ = -1.65
83...	1	0	INST	0	132	132	1.67	1.51	1.40	$\bar{\beta}_t$ = -1.40
Jack										
165...	122	7	EDC	25	3,003	16,650	.970	.923	.835	$\bar{\beta}_r$ = -1.34
166...	125	7	EDC	25	2,565	16,950	.923	.811	.771	$\bar{\beta}_v$ = -1.17
167...	128	7	EDC	25	3,124	18,200	1.36	1.17	1.00	$\bar{\beta}_t$ = -1.14
168...	1	0	INST	0	150	150	1.52	1.75	.861	

[1] EDC = Electric delay cap, PDC = Primacord delay connector, INST = Instantaneous.

of lineation, such as gneissic, schistose, or joint system, propagation may differ with direction. In several quarries, gage lines were laid out to study this effect.

Investigations were similarly conducted in the same rock type over a large region to determine if amplitudes and attenuation rates were comparable. Investigations were conducted in several rock types to determine what correlations, if any, exist among rock types. Appendix D describes briefly the geology at each site.

An earlier Bureau bulletin (*16*) indicated that thickness of overburden had a direct effect on the amplitude and frequency of displacement recordings. For equal explosive charges and distances, gages on rock outcrops gave lower amplitudes and higher frequencies than gages on overburden. Because overburden thickness varies from quarry to quarry and within some quarries, brief, simple tests were conducted to determine whether or not similar effects were present in particle velocity recordings.

In this section, no attempt has been made to present a rigorous analysis of the data. For example, no correlation has been attempted between rock properties and amplitude of vibrations. The results presented are intended to illustrate in a gross manner what correlations, or lack thereof, and what range of vibrations should and can be expected under certain conditions and to summarize the propagation characteristics of the quarries visited.

4.5.1—Geology and Direction

As stated previously, little difference in propagation characteristics due to direction should be expected for those quarries with simple geology whether bedded or massive. At the Jack quarry (geology as noted in Appendix D), two instrumentation arrays, as shown in figure 4.19,

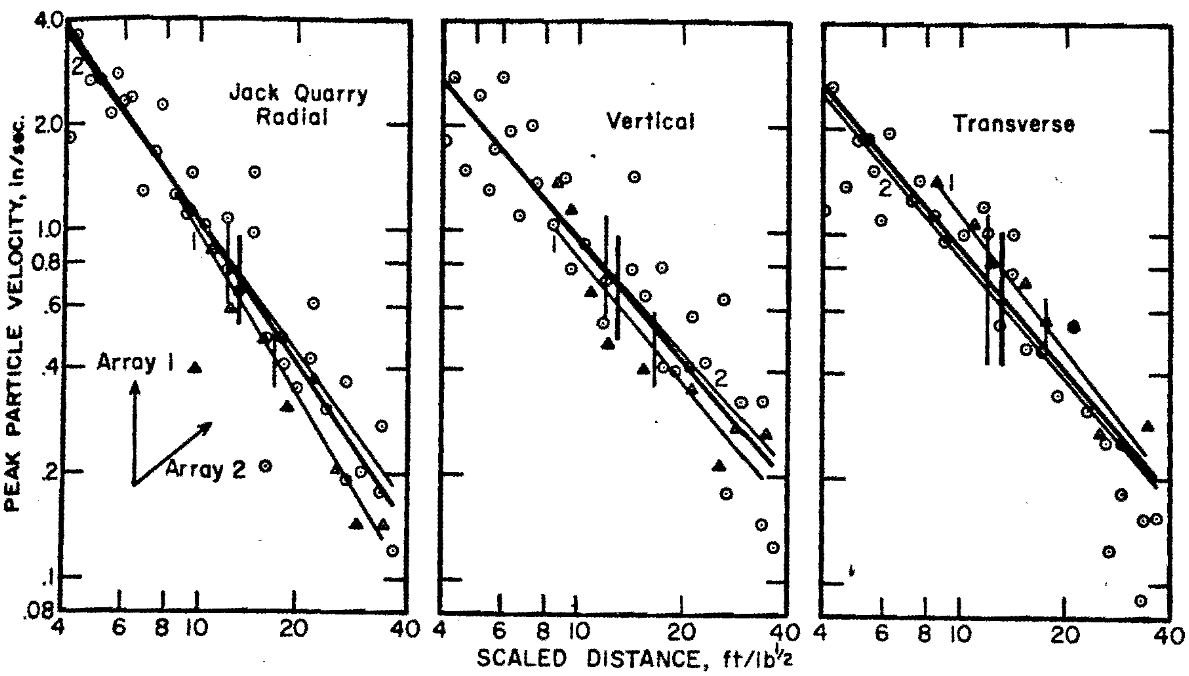

Figure 4.19.—Effect of direction, Jack Quarry, peak particle velocity versus scaled distance.

were located 50° apart. In the inset, vertically up is north. Regression lines through the data for arrays 1 and 2 are shown. The heavy line indicates a pooled regression line representing all the data. The vertical lines represent the standard deviation of the data about the line. The variation in amplitude and attenuation (slope) between arrays 1 and 2 is small and can be ignored. Similar results would be expected in the data from the limestone and dolomite quarries in Iowa and Ohio. At Bellevue and at Ferguson, no appreciable difference in the data from gage arrays in two or more orientations was noted.

At Culpeper and at Webster City, there was a distinct difference in amplitude but not in attenuation with direction. The data from Culpeper are shown in figure 4.20. Although the geology is less complex at Webster City, data obtained in two directions there resemble those at Culpeper.

Data from the Strasburg and Centreville quarries displayed the most variation with direction. Strasburg data, treated separately in section 4.3, represent differences which are probably attributable to orientation with respect to strike and dip of dipping beds. In a diabase at Centreville, variation in the radial component (figure 4.21) was as great as at Strasburg. Less variation was noted in the vertical and transverse components in the diabase. Directional effects in a diabase mass are probably due to anisotropy and/or jointing. In the diabase at the Manassas and West Nyack quarries, data from three directions show little variation. Therefore, variation with direction is not necessarily expected in diabase quarries. However, a fourth line at West Nyack, intermediate in direction with the other three lines, was of considerably lower amplitude, possibly being separated from the blast by major faulting or joints.

Variation with direction due to geology may be large or small. Such variation is not predictable; West Nyack, with little, and Centreville, with large variations, are both diabases. Ferguson, in a flat-lying limestone showed relatively large variation. The primary conclusion that can be drawn is that generalizations cannot be made with reference to the effect of geology in the grossest sense on propagation variations with direction either within or among quarries.

4.5.2—Effect of Rock Type on Vibration Levels

Investigations were conducted in the following rock types: limestone, dolomite, diabase, granite-type, sandstone, and a quartz-sericite schist. Data from similar rock types have been combined. The limestones and dolomites have been grouped together. The granite-type rocks included

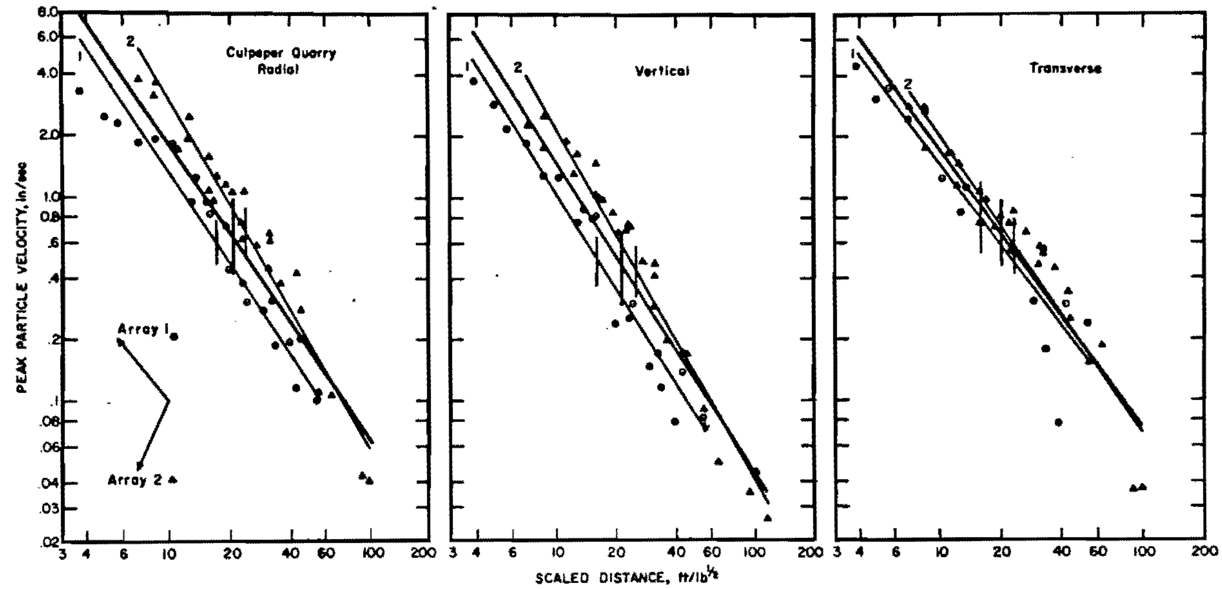

Figure 4.20.—Effect of direction, Culpeper Quarry, peak particle velocity versus scaled distance.

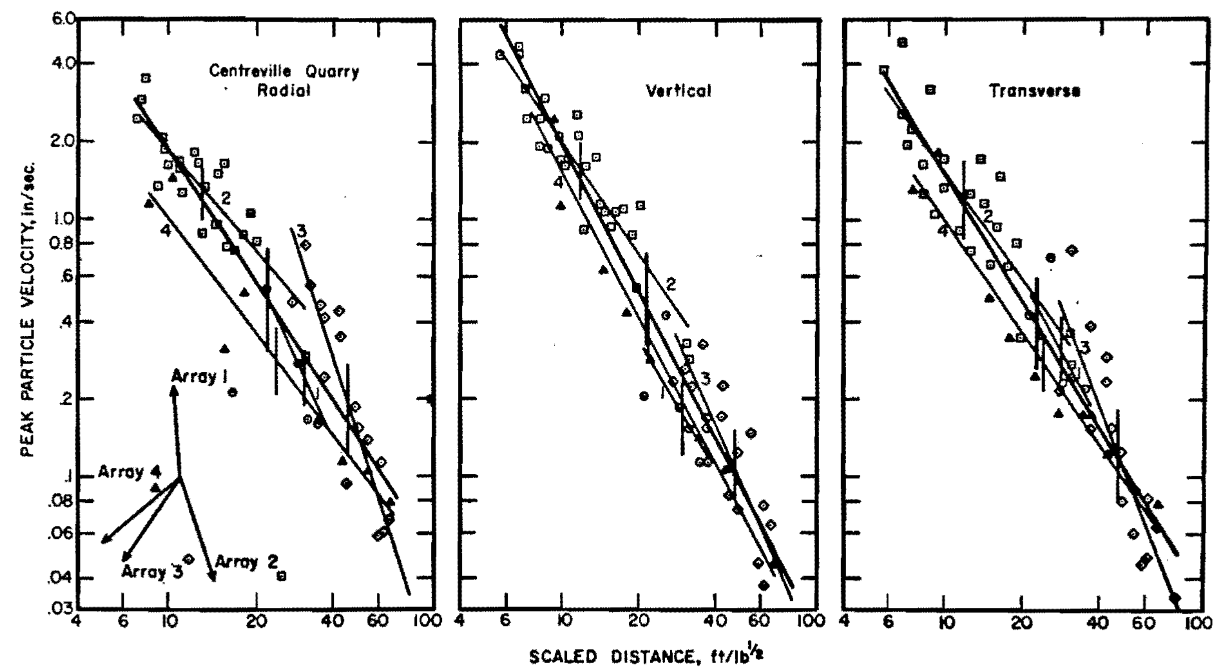

Figure 4.21.—Effect of direction, Centreville Quarry, peak particle velocity versus scaled distance.

granite-gneisses, a granite-diorite, and a gneissic diorite. The data from the quartz-sericite schist were grouped with the data from the granite-type rocks.

The data from tests in 12 limestone or dolomite quarries are shown combined in figure 4.22. The data collectively show a scatter of almost a factor of 3. In figures 4.22 to 4.25 the dashed lines represent the envelope of data points from all quarries instrumented. Both lowest and highest amplitudes were observed in limestone and dolomites.

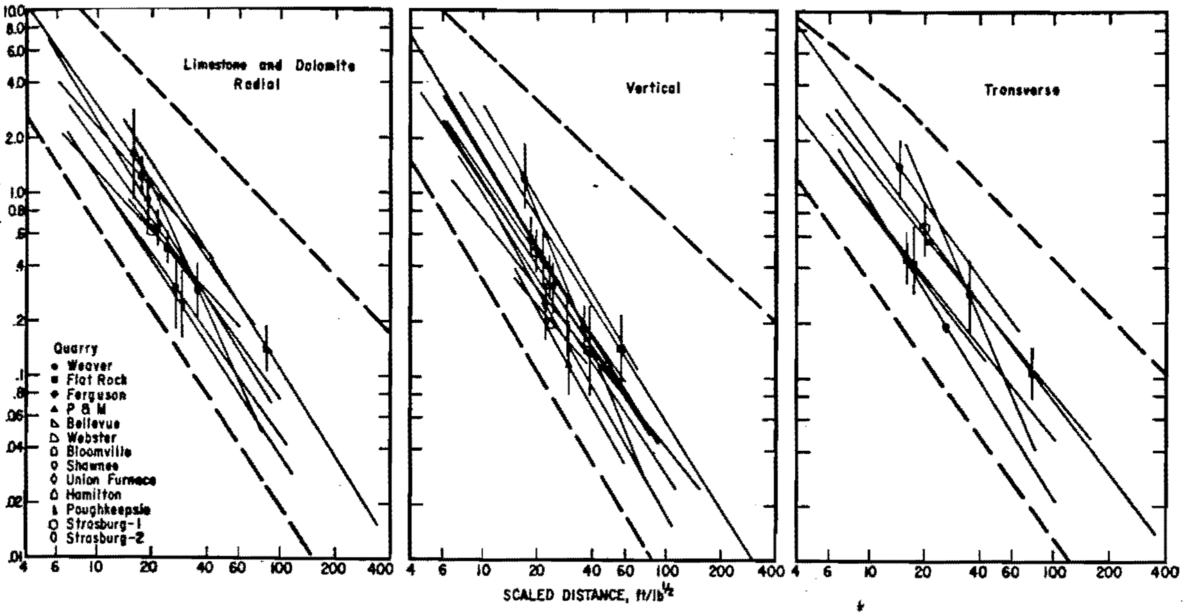

Figure 4.22.—Combined data, limestone and dolomite quarries, peak particle velocity versus scaled distance.

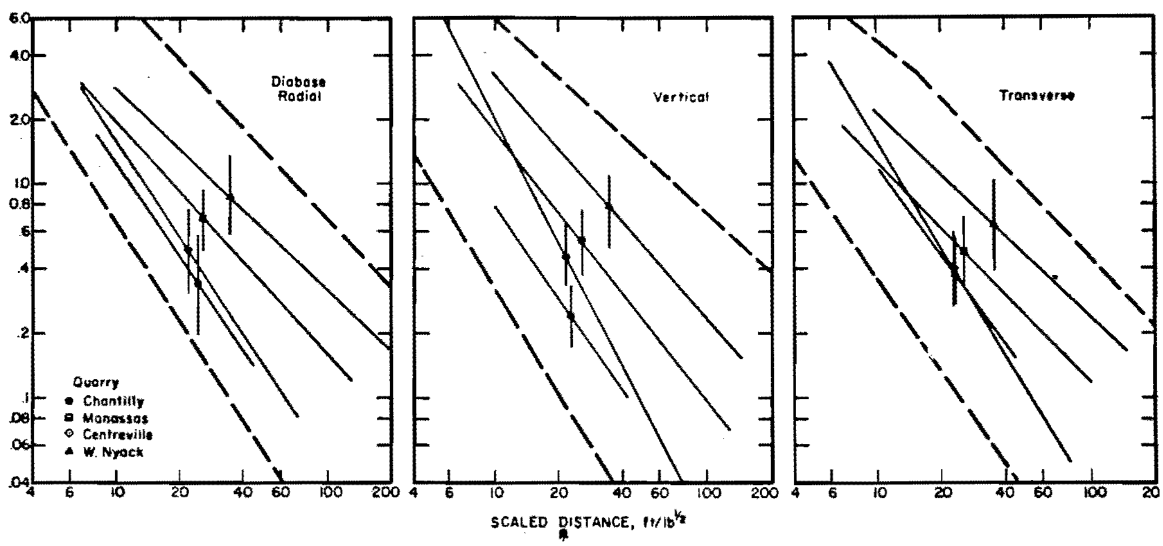

Figure 4.23.—Combined data, diabase quarries, peak particle velocity versus scaled distance.

Figure 4.23 gives the data from 4 quarries in diabase where there was a greater variation in slope than for the limestones, but this greater variation may be fortuitous due to the limited number of quarries investigated in diabase. It should be noted that the diabase data span the limits of all rock types.

The data from the granite-type rocks are combined in figure 4.24. From quarry to quarry, these data show less spread than the other rock types. These data are also of lower amplitude than the composite of all rock types shown with dashed lines.

Figure 4.25 shows the data from sandstone at the Culpeper quarry. Data from one quarry are not representative of the range from a rock type. It can only be stated that again the data fall within the dashed lines representing all rock types.

Two facts need stressing. First, the data from

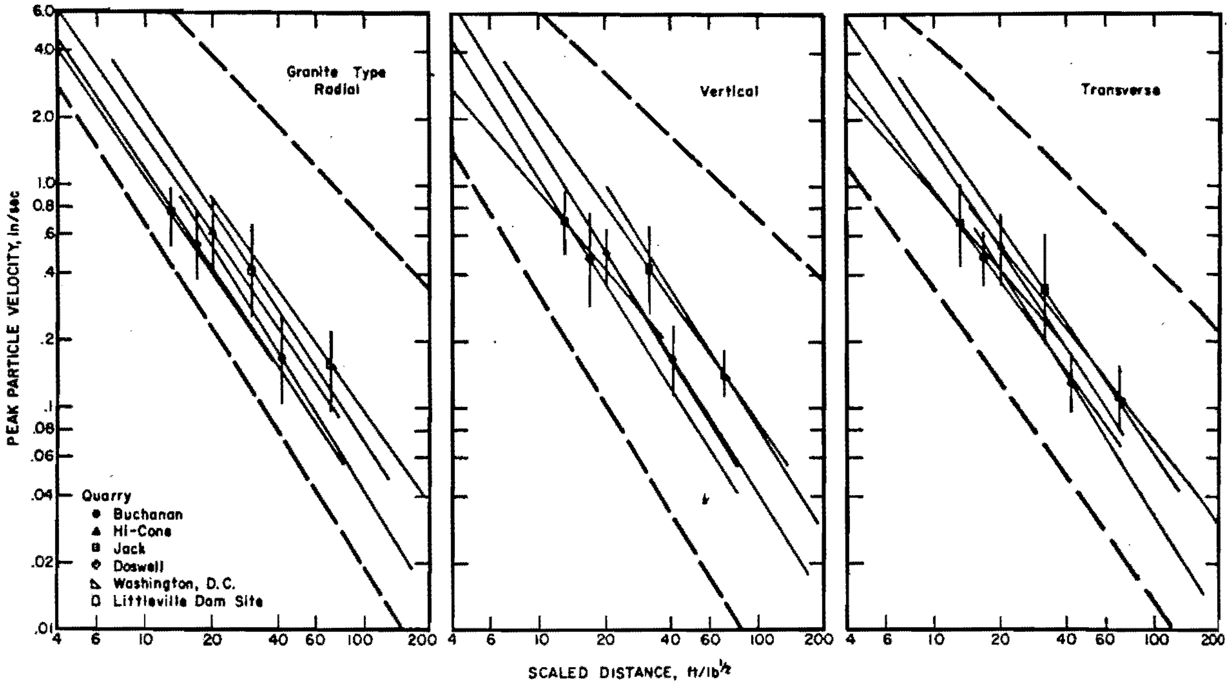

Figure 4.24—Combined data, granite-type quarries, peak particle velocity versus scaled distance.

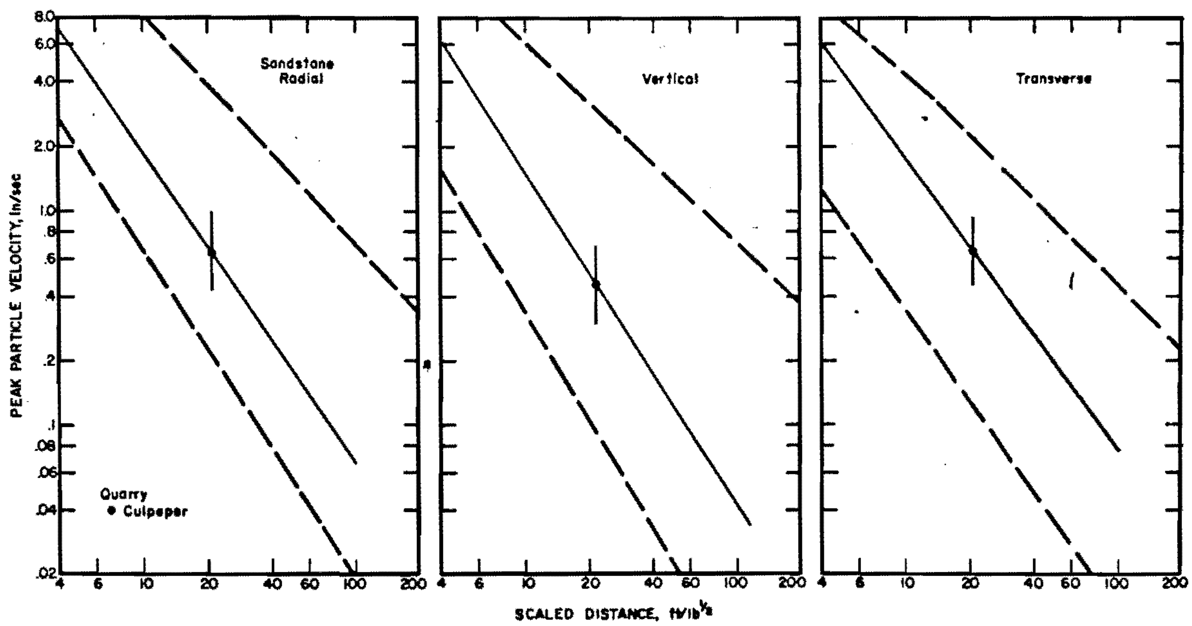

Figure 4.25.—Sandstone quarry data, peak particle velocity versus scaled distance.

each quarry for each component has been represented by a single line, with the exception of Strasburg. This may or may not be the best method (see figures 4.19 to 4.21). However, using statistical methods, 67 percent of the data will lie within plus or minus 1 standard deviation (vertical lines) of the regression line; 95 percent will fall within plus or minus 2 standard deviations. On this basis, the presentation of the data is believed valid. Second, the composite lines for all rock types as shown by the dashed lines in figures 4.22 to 4.25 represent more than 99 percent of the data obtained. This does not mean that all data from all quarries would fall between these lines, but most data would be expected to lie within these limits.

4.5.3—Overburden

Several tests were conducted to determine the effect of overburden on particle velocity amplitude. The results in all cases showed no effect on amplitude. Figure 4.26 is typical of the results. The filled-in symbols represent gage stations on bedrock or with less overburden. The open symbols represent gage stations on overburden. At the Webster City quarry, stations 5 and 6 were placed at the bottom of a valley and had 34 feet less overburden. At the Bellevue quarry, stations 1, 2, and 3 were on bedrock, and the balance of the stations were on 10 feet of overburden. In both cases, regression lines were fitted to the data omitting the stations with less or no overburden. It is concluded for the tests shown that no amplification of particle velocity amplitude occurs due to presence or absence of overburden.

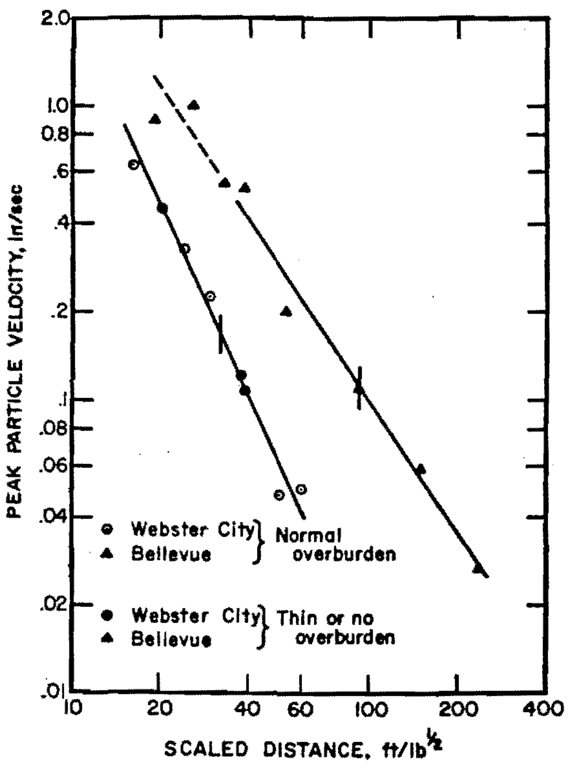

Figure 4.26.—Effect of overburden, peak particle velocity versus scaled distance.

However, other effects are observed. The initial particle velocity pulse arrives proportionately earlier at stations on little or no bedrock by an amount attributable to the missing overburden. The frequency of vibration with less overburden is two or three times that recorded on thicker overburden. Displacements obtained by integration of particle velocity are one-half to one-third the level expected if the overburden thickness had been uniform. These results are in general agreement with the conclusions of Thoenen and Windes (*16*). Displacements are higher and frequencies are lower on thick overburden. These changes are such that the resulting particle velocity is not appreciably affected.

4.6—APPLICATION OF FOURIER ANALYSIS TECHNIQUES TO VIBRATION DATA

The development and utilization of high-speed electronic digital computers has brought about the widespread application of Fourier techniques to all types of seismic data. The Fourier integral representation of a function, f (t), may be simply given by:

$$f(t) \rightleftarrows F(\omega) \qquad (4.22)$$

where f (t) is the function in the time domain, and F (ω) is the transform of f (t) and represents the function in the frequency domain. The process is reversible, so that if either f (t) or F (ω) is known, the other function may be determined (*2, 3*).

The authors feel that there is a hidden fallacy in the use of Fourier techniques; that is, if the end product of the process is to determine the frequency content of the signal, nothing is gained. Familiarity with seismic-type records and their transforms leads one to conclude that there is little if anything (perhaps phase information) contained in the transform that cannot be discerned from the original records. However, if the purpose is to determine ground response spectra, to filter, to determine energies, to integrate or differentiate, or to study absorption or many other phenomena, then Fourier analysis provides a strong and useful tool.

The primary use of Fourier techniques was to determine displacements and accelerations from particle velocity records and to examine the relationship of instantaneous and delayed-type blasts. While the details of the mathematics are available (*2, 3*) and are not presented here, the general procedures are described.

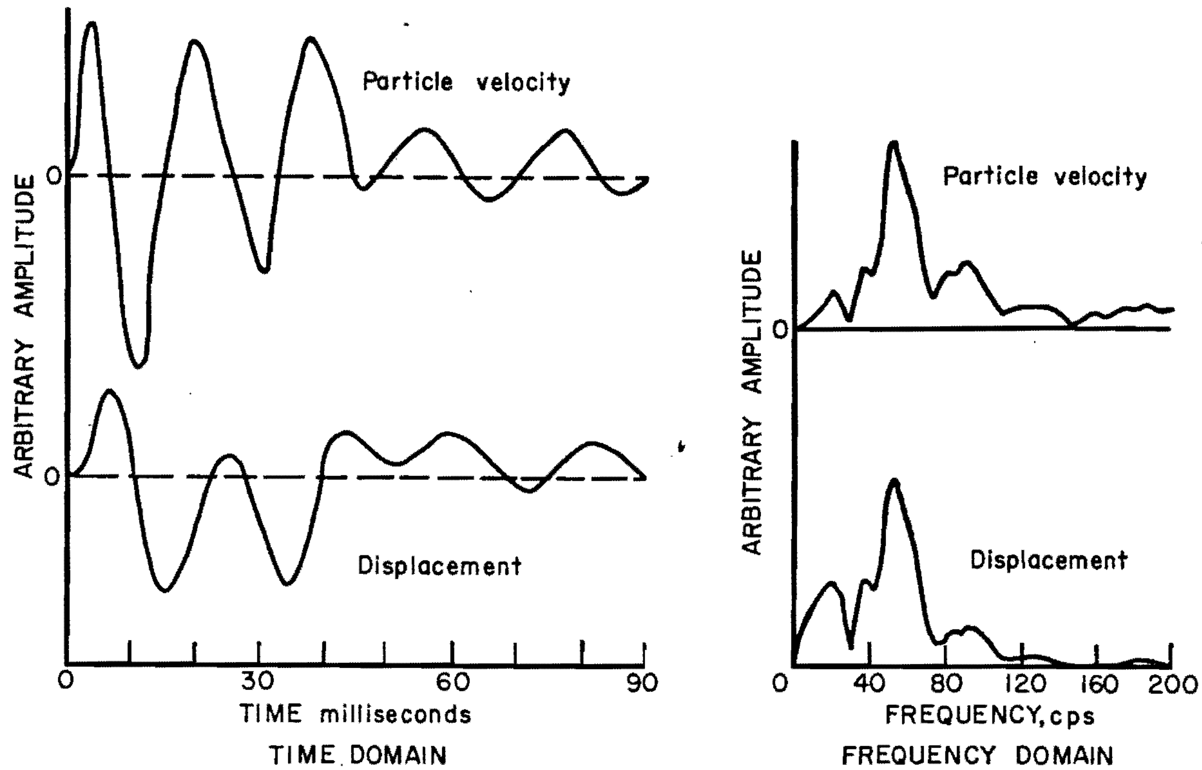

Figure 4.27.—Comparison of particle velocity and displacement in the time and frequency domains.

4.6.1—Displacement and Acceleration from Particle Velocities

Many analyses, including integration and differentiation, are performed more easily in the frequency domain than on the original time series data. The bulk of the data recorded in the field program were particle velocity-time records. Using standard procedures, the particle velocity records were converted to digital form with one three-digit number representing each sample at approximately 1 millisecond intervals. These data with a computer program were input to a computer. The coefficients, phase, and amplitude were calculated for selected frequencies. This output is the amplitude spectrum or transform of the original time function. By taking the inverse transform of the spectrum, we synthesize or regenerate the original time function.

If the velocity spectrum obtained from the velocity record is integrated or differentiated, the resultant is the displacement or acceleration spectrum, respectively. Base line shifts or digitizing errors may be corrected more easily and more adequately in the frequency domain than in the time domain. If after application of appropriate corrections, the inverse transform of the displacement or acceleration spectrum is taken, the result is the synthesized displacement- or acceleration-time record. Figure 4.27 shows tracings of a typical particle velocity-time record, the velocity spectrum, the displacement spectrum integrated from the velocity spectrum, and the displacement-time record synthesized from the displacement spectrum. This procedure was used in section 3.6 to evaluate the reliability of calculating particle velocity from displacement or acceleration.

4.6.2—Comparison of Instantaneous and Delay-Type Blasting Through Fourier Techniques

During the study of millisecond-delayed blasts, it was noted that the effect of delays was not only present in the amplitude but also in the wave shape. Figures 4.1 and 4.2 from one- and seven-hole instantaneous blasts, respectively, are generally smooth low-frequency records. Figure 4.3 is from a seven-hole blast with a 9-millisecond delay between holes. The traces in this figure show a high frequency wave train of about 8 to 9-millisecond period. This is most noticeable on

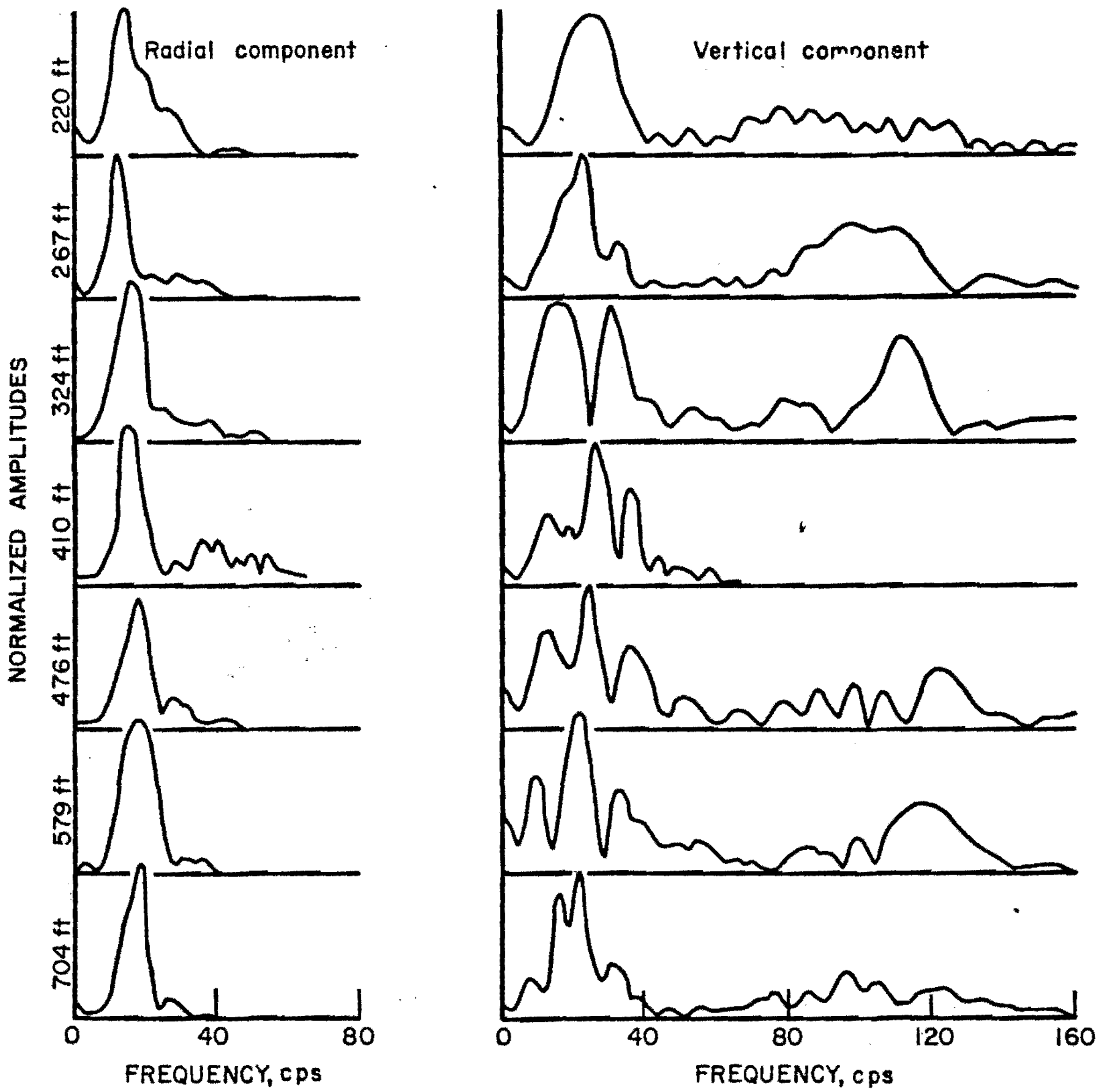

Figure 4.28.—Spectral amplitudes, radial and vertical components, from a 3-hole, 9-millisecond-delayed blast.

the vertical components. Figure 4.4 shows a similar phenomenon from a 7-hole, 34-millisecond delayed blast. A longer duration as expected is apparent from the longer delayed blast.

The higher frequencies generated by the delayed blast are a function of the interval delay time. If a number of identical amplitude-time signals, each delayed from the previous by a delay time, are summed, it can be shown mathematically that a periodicity comparable to the delay time results (*13*). Figure 4.28 shows the spectra for radial and vertical components at various distances from a 3-hole, 9-millisecond delay blast. The spectral amplitudes have been normalized to about 1.0 at the peak frequency. In these and ensuing plots, the spectra have been truncated at a point where all higher frequencies have amplitudes less than 5 percent of the peak amplitude. The spectra from an instantaneous shot are not shown, since the radial, vertical, and transverse spectra would all resemble the radial spectra of figure 4.28. Similarly, transverse spectra

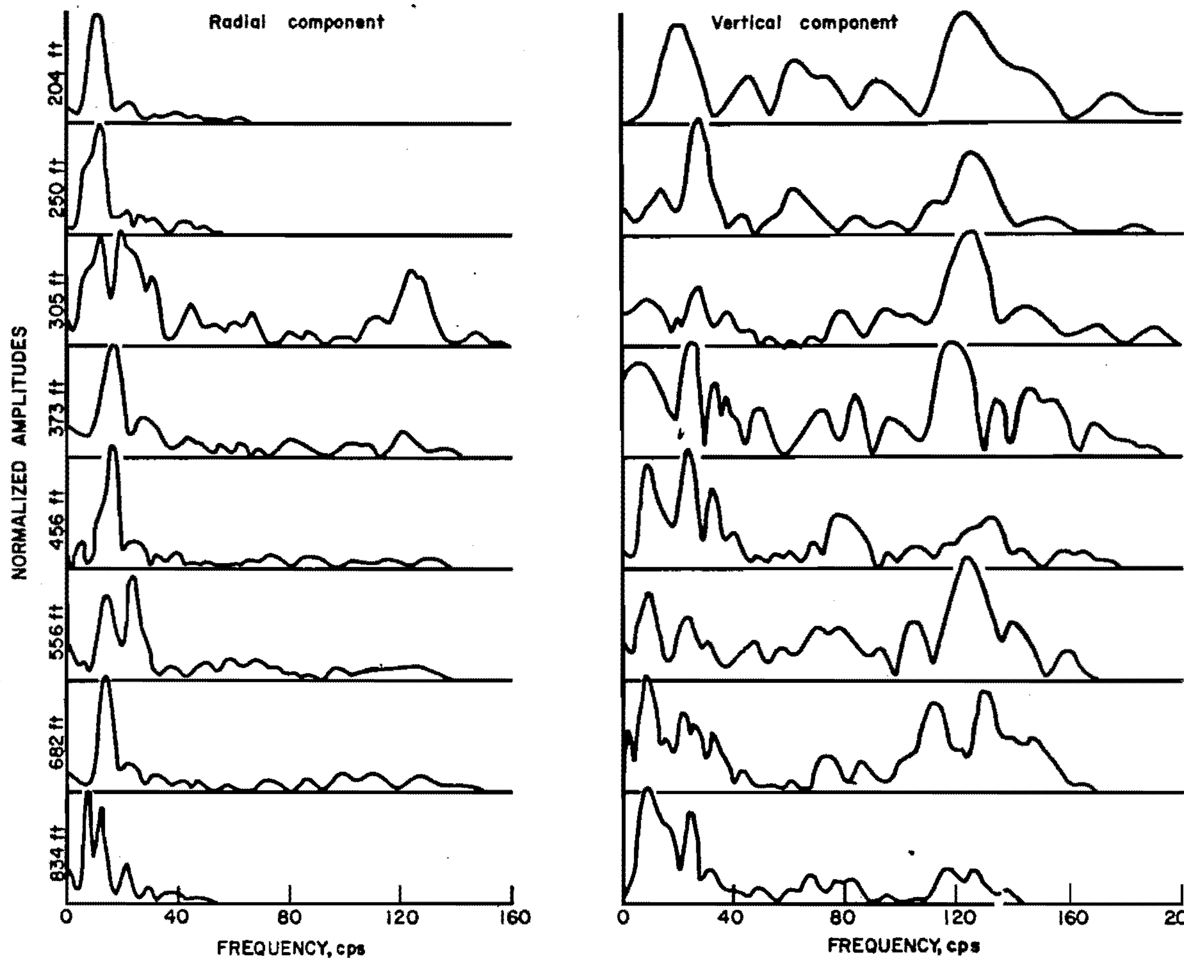

Figure 4.29.—Spectral amplitudes, radial and vertical components, from a 7-hole, 9-millisecond-delayed blast.

are not given in figure 4.28, because they would resemble the radial spectra. In figure 4.28, there is little evidence of the delay interval on the radial spectra, while there is a general increase in amplitude on the vertical spectra in the 100–120 Hz range as expected from 9-millisecond delays. The radial and vertical spectra from a 7-hole 9-millisecond delay blast are shown in figure 4.29. As the number of delays increases, there should be a proportionately greater amplitude in the spectra for the frequency related to the delay interval. This is shown in figure 4.29 as the radial spectra has some high frequency content, and the vertical spectra contains much high frequency energy. Figure 4.3 which is the velocity-time record for the same blast shows the same frequency content.

By integrating the velocity spectra and synthesizing, the displacement-time record may be obtained for each velocity-time record. If the displacement at common successive times is plotted by pairs (radial-vertical, vertical-transverse, or radial-transverse), the trajectory of the particle is mapped out in a plane. Figure 4.30 shows the R-V and R-T particle motion trajectories for one station from an instantaneous blast. The arrows denote a 10-millisecond sampling interval. For an instantaneous blast, these curves are generally smooth. Figure 4.31 shows R-V particle motion trajectories for a 3-hole, 9-millisecond blast and a 7-hole, 9-millisecond blast. Although it is difficult to pick the instant of arrival of the energy from successive holes, the trajectory becomes more erratic as the number of delays increases.

The apparent lack of high-frequency signal in the spectra and the velocity-time records for radial and transverse motion (as compared to

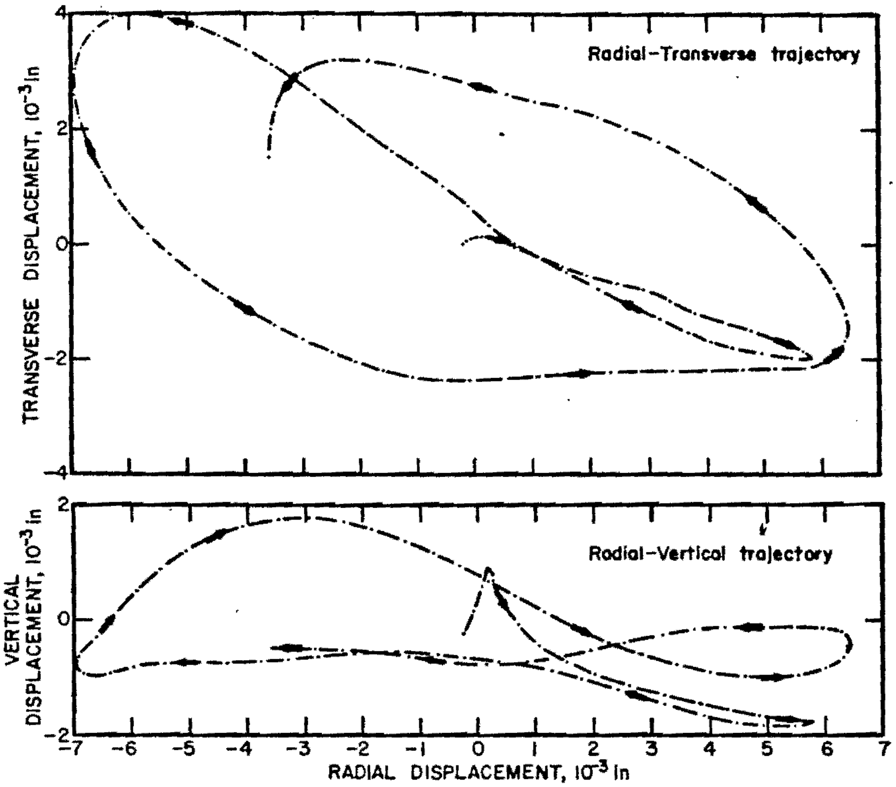

Figure 4.30.—Particle motion trajectories, 300 feet from an instantaneous blast.

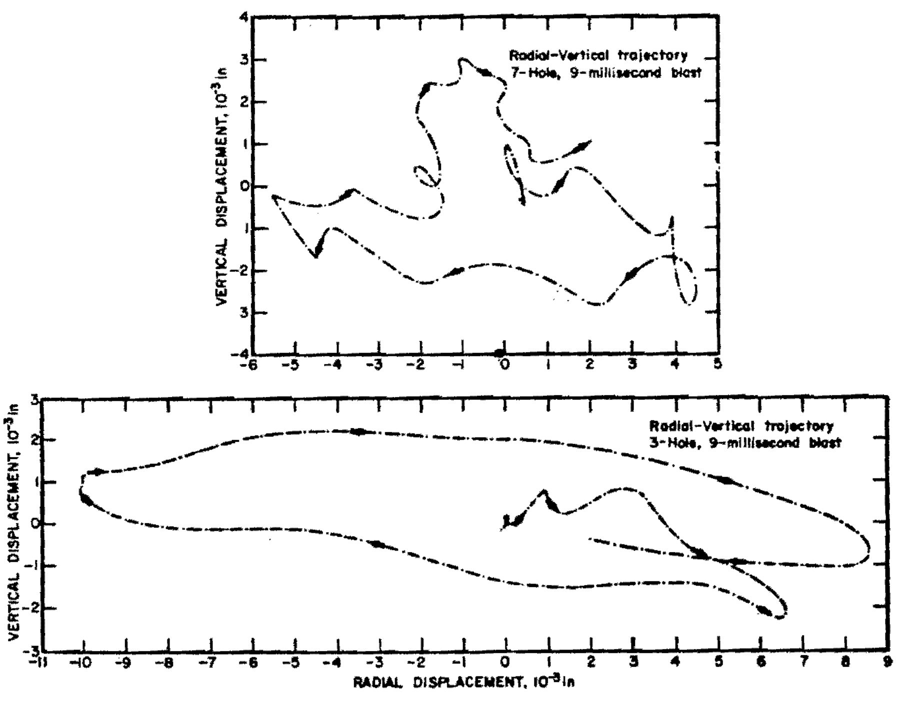

Figure 4.31.—Radial-Vertical particle motion trajectories, 300 feet from 3-hole, and 7-hole, 9-millisecond-delayed blasts.

vertical motion) may be a consequence of the free half-space in the vertical direction. The earth is more free to vibrate in the vertical direction and may carry higher frequency vibrations. However, the presence of higher frequencies should cause greater attenuation with distance for the vertical component. This was true for almost every quarry blast recorded.

A similar and perhaps corresponding phenomenon was apparent in the velocity-time records (figures 4.1 to 4.4). The radial and transverse component traces tend to oscillate for a much longer time than the vertical traces. This may be the consequence of some type of trapped wave in the horizontal plane or the result of the generation of Love waves at the surface. These lower frequency oscillations often being sustained tend to mask higher frequency energies on the radial and transverse components in both the time and frequency domains.

4.7—REFERENCES

1. Adams, W. M., R. G. Preston, P. L. Flanders, D. C. Sachs, and W. R. Perrett. Summary Report of Strong Motion Measurements, Underground Detonations. J. Geophys. Res., v. 66, No. 3, March 1961, pp. 903–942.
2. Blackman, R. B., and J. W. Tukey. The Measurement of Power Spectra. Dover Publications, New York, 1958, 190 pp.
3. Bracewell, R. The Fourier Transform and Its Applications. McGraw-Hill, Inc., New York, 1965, 381 pp.
4. Carder, D. S., and W. K. Cloud. Surface Motion From Large Underground Explosions, J. Geophys. Res., v. 64, No. 10, October 1959, pp. 1471–1487.
5. Crandell, F. J. Transmission Coefficient for Ground Vibrations Due to Blasting. J. Boston Soc. Civil Eng., v. 47, No. 2, April 1960, pp. 152–168.
6. Devine, J. F., R. H. Beck, A. V. C. Meyer, and W. I. Duvall. Effect of Charge Weight on Vibration Levels From Quarry Blasting. BuMines Rept. of Inv. 6774, 1966, 37 pp.
7. Duvall, W. I., C. F. Johnson, A. V. C. Meyer, and J. F. Devine. Vibrations From Instantaneous and Millisecond-Delayed Quarry Blasts. BuMines Rept. of Inv. 6151, 1963, 34 pp.
8. Duvall, W. I., J. F. Devine, C. F. Johnson, and A. V. C. Meyer. Vibrations From Blasting at Iowa Limestone Quarries. BuMines Rept. of Inv. 6270, 1963, 28 pp.
9. Habberjam, G. M., and J. T. Whetton. On the Relationship Between Seismic Amplitude and Charge of Explosive Fired in Routine Blasting Operations. Geophysics, v. 17, No. 1, January 1952, pp. 116–128.
10. Hudson, D. E., J. L. Alford, and W. D. Iwan. Ground Accelerations Caused by Large Quarry Blasts. Bull. of the Seis. Soc. of America, v. 51, No. 2, April 1961, pp. 191–202.
11. Ito, Ichiro. On the Relationship Between Seismic Ground Amplitude and the Quantity of Explosives in Blasting. Reprint from Memoirs of the Faculty of Eng., Kyoto Univ., v. 15, No. 11, April 1953, pp. 579–587.
12. Morris, G. The Reduction of Ground Vibrations From Blasting Operations. Engineering, Apr. 21, 1950, pp. 430–433.
13. Pollack, H. N. Effect of Delay Time and Number of Delays on the Spectra of Ripple-Fired Shots. Earthquake Notes, v. 34, No. 1, March 1963, pp. 1–12.
14. Ricker, N. The Form and Nature of Seismic Waves and the Structure of Seismograms. Geophysics, v. 5, No. 4, October 1940, pp. 348–366.
15. Teichmann, G. A., and R. Westwater. Blasting and Associated Vibrations. Engineering, Apr. 12, 1957, pp. 460–465.
16. Thoenen, J. R., and S. L. Windes. Seismic Effects of Quarry Blasting. BuMines Bull. 442, 1942, 83 pp.
17. Willis, D. E., and J. T. Wilson. Maximum Vertical Ground Displacement of Seismic Waves Generated by Explosive Blasts. Bull. of the Seis. Soc. of America, v. 50, No. 3, July 1960, pp. 455–459.

CHAPTER 5.—GENERATION AND PROPAGATION OF AIR VIBRATIONS FROM BLASTING

5.1—INTRODUCTION

Noise is an undesirable by-product of blasting. Air vibrations are generated by the blast and are propagated outward through the air under the influence of the existing topographic and atmospheric conditions. Three mechanisms are usually responsible for the generation of air blast vibrations: The venting of gasses to the atmosphere from blown-out unconfined explosive charges, release of gasses to the atmosphere from exposed detonating fuse, and ground motions resulting from the blast. The detonation of unconfined explosives results in the rapid release of all the gasses, heat, and light generated to be dissipated in the atmosphere. The expanding gasses do little useful work in this type of blast, and large amplitude shock waves are generated in the air. Unstemmed explosive charges in open boreholes still allows venting of the gasses to the atmosphere. However, the partial confinement allows some useful work to be done and results in some reduction of the amplitude of the air blast. Further confinement of the blast in the boreholes by the addition of stemming reduces the air blast by allowing a more gradual release of the gasses by pushing out the stemming and through the broken burden. The air vibrations generated by ground motion resulting from the blast are small. The surface acts as a piston moving the air above the point of detonation. Thus, the quantity of air displaced by the ground motion is small compared to the volume of gas released during a blast. Because the greatest amount of noise is generated by venting gasses, the use of stemmed charges with buried detonating fuse is a logical procedure to follow to reduce blast noise. A concise presentation of the theory of generation and propagation of shock waves in air can be found in standard text and reference books (*3*).

Early studies by the Bureau of Mines (*7, 8*) established that pressure attenuation with distance greater than the inverse square might be observed from blasts set off in the air and that doubling the weight of the charge increased the maximum pressure by about 50 percent.

Other investigators have studied the decay of amplitude of air waves with distance and the depth of burial of charges as a factor in the reduction of air vibrations from blasting. The Ballistic Research Laboratories at Aberdeen Proving Ground, Maryland, have published information concerning the decay of amplitude of blast-generated air waves with distance, the effects of depth of burial of the charges, and the prediction of focusing of blast waves due to meteorological effects (*4–6*). Under certain conditions local regions of high overpressure can develop as a result of changes in the propagation velocity of blast waves. The propagation velocity may increase with altitude due to the existence of temperature inversion or increased wind velocity at higher altitude, causing the blast waves to be refracted downward to focal areas some distance from the blast.

Grant and others (*2*) investigated blast wave generation and propagation for a noise abatement program and established that wind velocity and direction, barometric pressure, and atmospheric temperature had the most profound effect on the propagation of blast waves.

Previous air blast studies dealt with point source generation and ammunition disposal and did not include data from mining rounds designed to break and move rock. Consequently, Bureau of Mines personnel made additional observations of air blast overpressures from mining rounds at eight different crushed stone quarries. The blasts were recorded without regard to season, weather, atmospheric temperature conditions, or wind in order to cover the range of conditions under which these blasts are normally detonated. These overpressure data are presented for comparison with the published curves and observed data from other investigators.

5.2—PREVIOUSLY PUBLISHED DATA

A program of research of air blast damage was started by the Bureau of Mines in the early 1940's. These early studies were concerned with the decay of amplitude of air blast with distance and damage to structures from air blast (*7, 8*).

The decay of amplitude of air blast with distance was studied by detonating explosive charges in air and measuring the increase in air pressure due to the passage of the blast wave at various distances from the point of detonation. The explosive charges were detonated far enough above the ground to minimize the effects of ground reflection on the pressure envelope. The distances and the charge sizes were varied in a controlled test program. The damaging effects of air blast were studied by placing a frame of mounted glass window panes in the vicinity of the blasts detonated in the air. Thus, the distances from the charge to the frame were varied, as well as the charge weight. The weight of the charge detonated in the air varied between 0.5 and 1,800 pounds, and the shot-to-gage distances varied from 10 to 17,100 feet. The distance from the window frame positions to the charges was varied to determine how far from various size blasts damage occurred.

Figure 5.1 is a combined data plot of overpressure versus scaled distance, where scaled distance is defined here as distance in feet divided by the cube root of the charge weight in pounds. The air blast data from 60 tests conducted by Windes (*7, 8*) are represented by 16 data points. The scaled distance representative of these data range from about 12.5 to 3,400 ft/lb$^{1/3}$. Average overpressure values for these tests range from 0.006 psi to 3.4 psi. No detailed meteorological data were recorded during these tests. Thus, no corrections can be made for the effects of atmospheric conditions.

The author did not deduce a propagation law from these data, but noted only that, in general, pressure attenuation with distance was greater than the inverse square and that doubling the charge weight increased the overpressure by about 50 percent.

It was noted that the main air blast wave consisted of a positive pressure pulse of a few milliseconds duration which rose quickly to its maximum value and dropped off more slowly. The positive phase is followed by a negative phase of longer duration but less pressure change. The failure of window glass due to air blast can, in most instances, be distinguished from breakage due to missiles. Fragmentation due to air blast in most instances will be outward from the building with some pieces left in the frame. However, this will not be true if the glass is close to the blast source. Thus, at a distance from the blast the projection and penetration of glass fragments is of no great importance. It was found that window glass failure from air blast did not occur when the blasts were confined in wells or drill holes in blocks of rock. In general, this study concluded that damage from air blast from actual quarry blasts was insignificant.

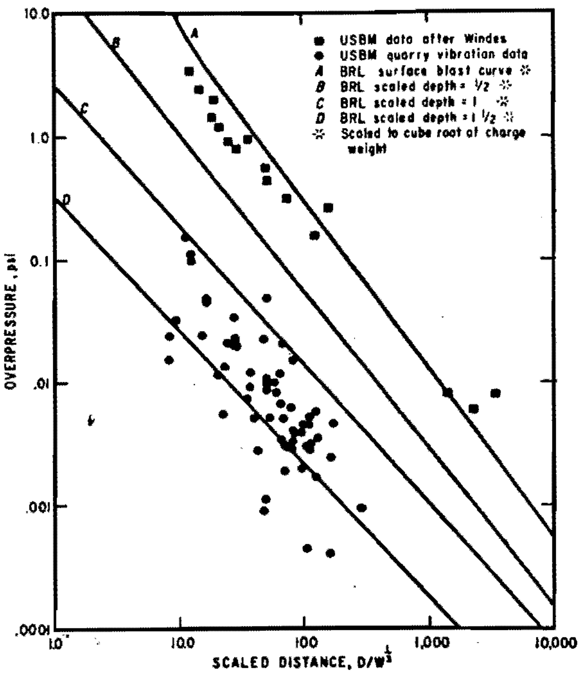

Figure 5.1.—Combined data plot, overpressure versus scaled distance.

The decay of amplitude of air blast with distance was measured by the Ballistic Research Laboratories (BRL), and these results were compared to theoretical values for a large number of tests conducted over a period of years. These studies led to observations of damage generated by air blast (*4–6*). During the course of BRL's investigation, meteorological data were collected concerning temperature as a function of altitude and wind direction and velocity both at the surface and aloft. The velocity of sound increases 2 feet per second for each 1 degree centigrade temperature increase and is increased in the downwind direction. Thus, in the case of a temperature inversion or an increase of wind velocity with altitude, the blast waves are refracted downward and may converge at some focal point at a large distance from the blast. Increases of blast overpressure in such cases can be as much as a hundredfold.

The decay of amplitude with distance was determined from a large number of tests that included data from very large blasts. The solid sloping lines on figure 5.1 show the decay of amplitude with distance for surface blasts and

Table 5.1. - Charge and overpressure data for W. E. Graham and Sons, Manassas Quarry, Manassas, Va.

Test	Max.chg./delay, lb	Chg./hole, lb	Hole diameter, in	Stemming, ft	Scaled burden, ft/lb$^{1/3}$	Scaled distance, ft/lb$^{1/3}$	Over-pressure, psi
120...	1200	164.0	4.5	6.0	1.64	23.4 67.1	0.0135 .00353
125...	150	9.5	2.5	3.0	--	37.6 128.	0.0120 .00170
126...	933	186.5	4.5	8.0	1.23	20.5 70.3 70.3	0.0117 .00198 .00194

Table 5.2. - Charge and overpressure data for Culpeper Crushed Stone Company Quarry, Culpeper, Va.

Test	Max.chg./delay, lb	Chg./hole, lb	Hole diameter, in	Stemming, ft	Scaled burden, ft/lb$^{1/3}$	Scaled distance, ft/lb$^{1/3}$	Over-pressure, psi
127...	961	74.0	2.75	5.0	1.19	15.5	0.0244
129...	1206	75.4	2.75	5.0	1.18	12.7 50.8 64.7	0.111 .0498 .0119
130...	624	69.3	2.75	4.0	1.46	299.	0.000950
132...	712	71.3	2.75	2.5	1.45	16.7 50.1	0.0443 .00885
133...	686	68.6	2.75	3.0	1.47	16.4 50.9 163.	0.0483 .00998 .00243
135...	630	70.8	3.0	3.0	1.69	11.6 176.	0.154 .00477

Table 5.3. - Charge and overpressure data for Chantilly Crushed Stone Company Quarry, Chantilly, Va.

Test	Max.chg./delay, lb	Chg./hole, lb	Hole diameter, in	Stemming, ft	Scaled burden, ft/lb$^{1/3}$	Scaled distance, ft/lb$^{1/3}$	Over-pressure, psi
136...	1641	149.2	3.5	5.0	1.54	22.7 50.0	0.00560 .00112

Table 5.4. - Charge and overpressure data for New York Trap Rock Corporation Quarry, West Nyack, N.Y.

Test	Max.chg./delay, lb	Chg./hole, lb	Hole diameter, in	Stemming, ft	Scaled burden, ft/lb$^{1/3}$	Scaled distance, ft/lb$^{1/3}$	Over-pressure, psi
139...	335	335	6.5	16.0	2.45	82.8 98.6	0.0150 .00390
140...	400	400	6.5	16.5	2.17	101. 115.	0.00460 .00530
141...	303	303	6.5	16.0	2.23	86.9 105.	0.00392 .00313
142...	325	325	5.5	19.0	2.18	82.3 131.	0.00415 .00349

Table 5.5. - Charge and overpressure data for Superior Stone Company, Buchanan Quarry, Greensboro, N.C.

Test	Max.chg./delay, lb	Chg./hole, lb	Hole diameter, in	Stemming, ft	Scaled burden, ft/lb$^{1/3}$	Scaled distance, ft/lb$^{1/3}$	Over-pressure, psi
159...	658	73.0	3.5	8.0	1.68	129.0	0.00582

Table 5.6. - Charge and overpressure data for Superior Stone Company, Hi-Cone Quarry, Greensboro, N.C.

Test	Max.chg./delay, lb	Chg./hole, lb	Hole diameter, in	Stemming, ft	Scaled burden, ft/lb$^{1/3}$	Scaled distance, ft/lb$^{1/3}$	Over-pressure, psi
160...	690	115.0	2.75	6.0	1.03	12.5 12.5 81.3	0.136 .0998 .00630
161...	644	105.0	2.75	6.0	1.06	28.4 28.4 99.4	0.0234 .0203 .00198
162...	857	172.0	3.5	6.0	1.26	9.37 74.0	0.0321 .00298
163...	816	136.0	2.5	6.0	1.17	8.24 8.24 43.7	0.0240 .0155 .0287

Table 5.7. - Charge and overpressure data for Southern Materials Corporation, Jack Stone Quarry, Peterburg, Va.

Test	Max. chg./delay, lb	Chg./hole, lb	Hole diameter, in	Stemming, ft	Scaled burden, ft/lb$^{1/3}$	Scaled distance, ft/lb$^{1/3}$	Over-pressure, psi
164...	2965	700.0	6.0	12.0	1.58	24.3 35.9 58.4	0.0210 .00754 .0107
165...	3003	136.0	3.5	7.0	1.56	27.7	0.0204
166...	2565	111.5	3.5	7.0	1.66	48.0 69.4	0.0230 .0208
167...	3124	142.0	3.5	7.0	1.53	27.4 36.3 69.5	0.0336 .00938 .00512
168...	150	150.0	3.5	6.0	1.88	48.9 109. 161.	0.000910 .000450 .000410

Table 5.8. - Charge and overpressure data for Rockville Crushed Stone, Inc., Quarry, Rockville, Md.

Test	Max.chg./delay, lb	Chg./hole, lb	Hole diameter, in	Stemming, ft	Scaled burden, ft/lb$^{1/3}$	Scaled distance, ft/lb$^{1/3}$	Over-pressure, psi
169...	763	63.6	5.0	8.0	3.76	40.5 54.2 71.7 71.7 105. 114.	0.00514 .00516 .00297 .00300 .00303 .00317
170...	1152	64.0	5.0	8.0	3.75	61.1 70.4 83.0 83.0 111. 113.	0.00835 .00520 .00340 .00294 .00452 .00286

for scaled depths of burial of $\frac{1}{2}$, 1, and $1\frac{1}{2}$ lb/ft$^{1/3}$, respectively. Both the depth of burial and the distance have been scaled to the cube root of the charge weight. The overpressures are based upon standard sea level conditions and can be corrected for barometric pressure by a multiplier that is the ratio of the pressures.

Studies of air blast in relation to noise abatement were conducted by Grant, Murphy, and Bowser (*2*). The objective of the study was to determine the effect of weather variables on the propagation of sound through the atmosphere. The significant variables in the order of their importance were wind velocity and direction, barometric pressure, and temperature, respectively. The sound intensity and duration were found to be enhanced in the downwind direction. High barometric pressure and temperature were found to relate to low intensity and duration. The duration of the sound was found to increase with increasing distance from the source under all conditions.

5.3—BUREAU OF MINES DATA

One of the objectives of the quarry vibration study by the Bureau of Mines was to measure the amplitude of air-blast overpressures resulting from detonation of mining rounds in operating quarries. Accordingly, measurements were made of the air blast amplitudes from 26 mining blasts detonated in eight crushed stone quarries. The data were collected during the routine mining operations without regard to atmospheric conditions, time of day, rock type, or explosives used. The burden and spacing were controlled by the operators to achieve desired rock breakage, and the blasts were stemmed in accordance with the blasting procedure practiced at each quarry. Thus, the data obtained are representative of actual operating conditions.

The use of cube root scaling implies spherical propagation from a point source. The configuration of a normal mining round does not conform to a point source model, and burial of the charges in long boreholes behind a shallow burden precludes either true spherical or hemispherical propagation in the air over distances of a few thousands of feet. However, it has been common practice to scale air blast data to the cube root of the charge weight. Therefore, the Bureau of Mines air blast data (shot-to-gage distances) have been scaled to the cube root of the maximum charge weight per delay. These data are presented in tables 5.1 through 5.8 and are shown in figure 5.1 by 66 data points on the overpressure versus scaled distance plot.

The confinement of an adequately stemmed charge in a borehole in a mining round is the distance from the borehole to the free face, which is the burden. Therefore, the burden scaled to the cube root of the charge weight per hole would be expected to correspond to the scaled depth of burial of the charge as determined by the Ballistic Research Laboratories (*5, 6*).

A careful study of the Bureau of Mines air blast data was made, and it was determined that adequate stemming might be achieved by maintaining a ratio of stemming height in feet to hole diameter in inches of 2.6 ft/in or greater. Under this condition, the burden, scaled to the cube root of the charge weight per hole, will compare favorably with the scaled depth of burial of the charge as used by the Ballistic Research Laboratories (*5, 6*). Also, the value of 2.6 ft/in for the stemming height to hole diameter ratio agrees with published data of Ash (*1*).

It is interesting to note that only one point from the quarry blast data on figure 5.1 lies above a scaled depth of 1. The maximum overpressures measured did not exceed 0.16 psi, and most of the overpressures are at least an order of magnitude lower. Thus, it is reasonable to assume that a properly stemmed mining round designed to break and move rock efficiently will not generate air blast overpressures of a damaging level under average operating conditions.

5.4—REFERENCES

1. Ash, Richard L. The Mechanics of Rock Breakage. Pit and Quarry, v. 56, No. 3, September 1963, pp. 118–123.
2. Grant, R. L., J. N. Murphy, and M. L. Bowser. Effect of Weather on Sound Transmission From Explosive Shots. U. S. BuMines Rept. of Inv. 6921, 1967, 13 pp.
3. Kenney, Gilbert F. Explosive Shocks in Air. The McMillan Company, New York, 1962, 198 pp.
4. Kingery, C. N., and B. F. Pannill. Peak Overpressure Versus Scaled Distance for TNT Surface Bursts (Hemispherical Charges). Ballistic Research Laboratories Rept. No. 1518, April 1964, 22 pp.
5. Perkins, Beauregard, Jr., Paul H. Lorrain, and William H. Townsend. Forecasting the Focus of Air Blasts Due to Meteorological Conditions in the Lower Atmosphere. Ballistic Research Laboratories Rept. No. 1118, October 1960, 77 pp.
6. Perkins, Beauregard, Jr., and Willis F. Jackson. Handbook for Prediction of Air Blast Focusing. Ballistic Research Laboratories Rept. No. 1240, February 1964, 100 pp.
7. Windes, S. L. Damage From Air Blast. Progress Report 1. BuMines Rept. of Inv. 3622, February 1942, 18 pp.
8. ______. Damage From Air Blast. Progress Report 2. BuMines Rept. of Inv. 3708, June 1943, 50 pp.

CHAPTER 6.—ESTIMATING SAFE AIR AND GROUND VIBRATION LEVELS FOR BLASTING

6.1—INTRODUCTION

Blasting operators are often faced with the necessity of limiting vibration levels to minimize or eliminate the possibility of damage to nearby residential structures or to reduce complaints from neighbors. As discussed in Chapter 3, the Bureau recommends a safe blasting limit of 2.0 in/sec peak particle velocity that should not be exceeded if damage is to be precluded. If complaints are a major problem, the operator may wish to further limit the particle velocity level to reduce the number of complaints which he feels are attributable to vibration level. Again, as discussed in Chapter 3, from the case history of the Salmon event, a particle velocity limit of 0.4 in/sec could be established by the operator if complaints are to be kept below 8 percent of the potential number of complainants. In a densely populated area, or where the history of complaints has been a serious problem, an operator may find it desirable to still further limit the vibration level to minimize complaints. It should be clearly understood that the authors are not advocating a limit below the 2.0 in/sec criterion which will preclude damage but are suggesting that an operator may, by choice, find it desirable to impose a more restrictive limit to minimize complaints.

The two variables which appear to affect vibration level the most at a given distance are the charge weight per delay and, to a lesser extent, the method of initiation. The same total charge weight which would result in damage can often be shot in a series of delays with no damage. Electric delay caps can often be used with a net decrease in vibration level as opposed to the levels from Primacord delay connectors or instantaneous blasts. The operator has a design problem to obtain the proper procedure for best breakage, proper throw from the working face, the best economy, and other considerations. Conversion to delay shooting, increasing the number of delays, or electric delay caps may not provide the best solution or even any solution to many blasting problems. However, where the vibration problem is urgent, changes in the two variables cited will provide the greatest change in vibration level at a given distance.

There are two approaches to the problem of how to estimate charge size so that safe vibration level limits will not be exceeded at a given distance. The first and best is to use instrumentation on blasts to determine within a quarry what the specific constants are in equation 4.21 for the actual blasting conditions. The second approach is to use general data taken under varying conditions (such as the data in figures 4.22 through 4.25) to determine empirical rules of thumb which must inherently have larger safety factors than those where a specific quarry monitors its own blasts.

Although air blast is rarely a problem in normal blasting operations, a discussion of estimating procedures for the control of overpressures is included in section 6.5. As pointed out in section 5.3, this report continues the general practice of scaling air blast data to the cube root of the charge weight per delay.

6.2—ESTIMATING VIBRATION LIMITS WITH INSTRUMENTATION

Obviously, the best way to control vibration levels is to determine and know these levels. Many blasting operations record the particle velocity from each blast on a routine basis either with owned or leased equipment or through consultant services. Data from one station may be used to accumulate sufficient data to make plots similar to those shown in figures 4.15 through 4.17. This can be done in either of two ways: by recording at a fixed gage location from several shots at different scaled distances; or by locating the gage station at successively further scaled distances from successive shots at the working face. The second method is recommended, because it only requires a gage station at preselected scaled distances from several routine blasts.

As an illustration, one data point was selected from each of the tests at the Weaver quarry shown in figure 4.15. Eight data points were chosen at random but at various scaled distances. A ninth point, from Weaver test 9, was chosen to provide the largest scatter possible within the data of figure 4.15. These nine data points, shown in figure 6.1, represent a single data point from each of nine blasts and illustrate the use of a single gage station for several blasts at a quarry. The single point selected to have the largest deviation is shown with a different symbol. Three regression lines have been placed through the data. Line A represents all the data from the Weaver quarry in figure 4.15. Line B represents the 8 data points selected at random but at various scaled distances. Line C represents those 8 data points plus the data point from figure 4.15 with the most deviation. It is obvious that these 8 or 9 points are representative of the approximately 60 points used in figure 4.15. From these data, shown in figure 6.1, an operator might select a scaled distance of 15.0 to insure that 2.0 in/sec peak particle velocity is not exceeded at a particular distance or a scaled distance of 20.0 to be more conservative. While the illustration is only for the radial component data from Weaver, similar results could have been obtained for the vertical and transverse component data.

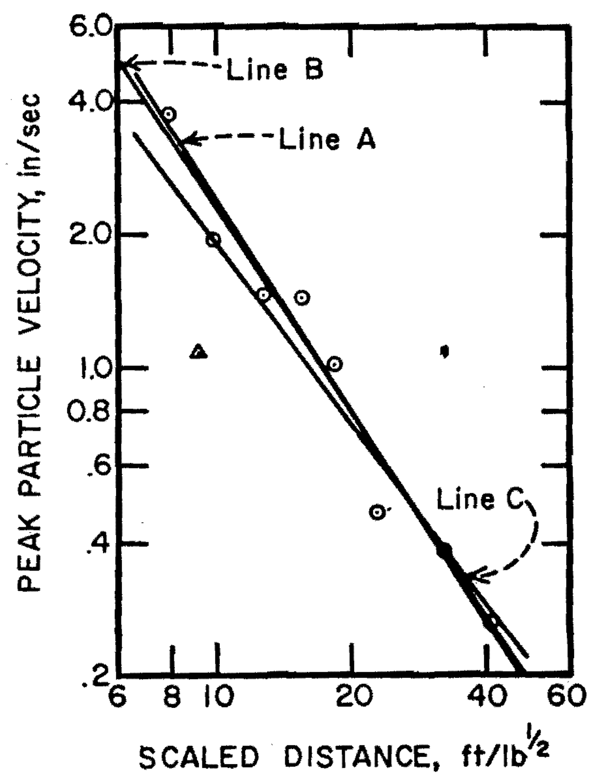

Figure 6.1.—Comparison of particle velocity data from different shots within a quarry.

A single three-component gage station would be the minimum used in determining propagation data for a blasting operation. Data should be taken in more than one direction to insure that directional effects, such as those discussed in section 4.5 are determined if present. Establishment of a propagation law, such as shown in figure 6.1 removes all questions and permits design of blasts and maintenance of controls on blasting limits which will preclude exceeding safe blasting criteria.

6.3—ESTIMATING VIBRATION LIMITS WITHOUT INSTRUMENTATION

For many quarries or blasting operations, it is not possible to obtain data as suggested in section 6.2. In such cases, it is advisable to use empirical data derived from investigations in various quarries. Figure 6.2 represents the combined particle velocity versus scaled distance data from Bureau tests in many quarries. The heavy line is the upper limit envelope of all the data points collected. If it is assumed that these data represent a sufficiently random sample of all possible blasting sites, then these data can be used to estimate a safe scaled distance for any blasting site. At a scaled distance of 50 ft/lb$^{1/2}$ the probability is small of finding a site that produces a vibration level that exceeds the safe blasting limit of 2.0 in/sec. Therefore, it is concluded that a scaled distance of 50 ft/lb$^{1/2}$ can be used as a control limit with a reasonable margin of safety where instrumentation is not used or is not available. For cases where a scaled distance of 50 ft/lb$^{1/2}$ appears to be too restrictive, a controlled experiment with instrumentation should be conducted to determine what scaled distances can be used to insure that vibration levels do not exceed 2.0 in/sec particle velocity.

6.4—USE OF SCALED DISTANCE AS A BLASTING CONTROL

The significance of scaled distance and its proper use has raised many questions and is often misunderstood. As discussed in section 4.3, the peak particle velocity of each component of ground motion can be expressed as a function of distance from the blast and the maximum charge weight per delay by the equation:

$$v = H\left(\frac{D}{W^{1/2}}\right)^{\beta} \qquad (6.1)$$

where v = particle velocity,
H = intercept at $D/W^{1/2} = 1.0$,
D = distance,

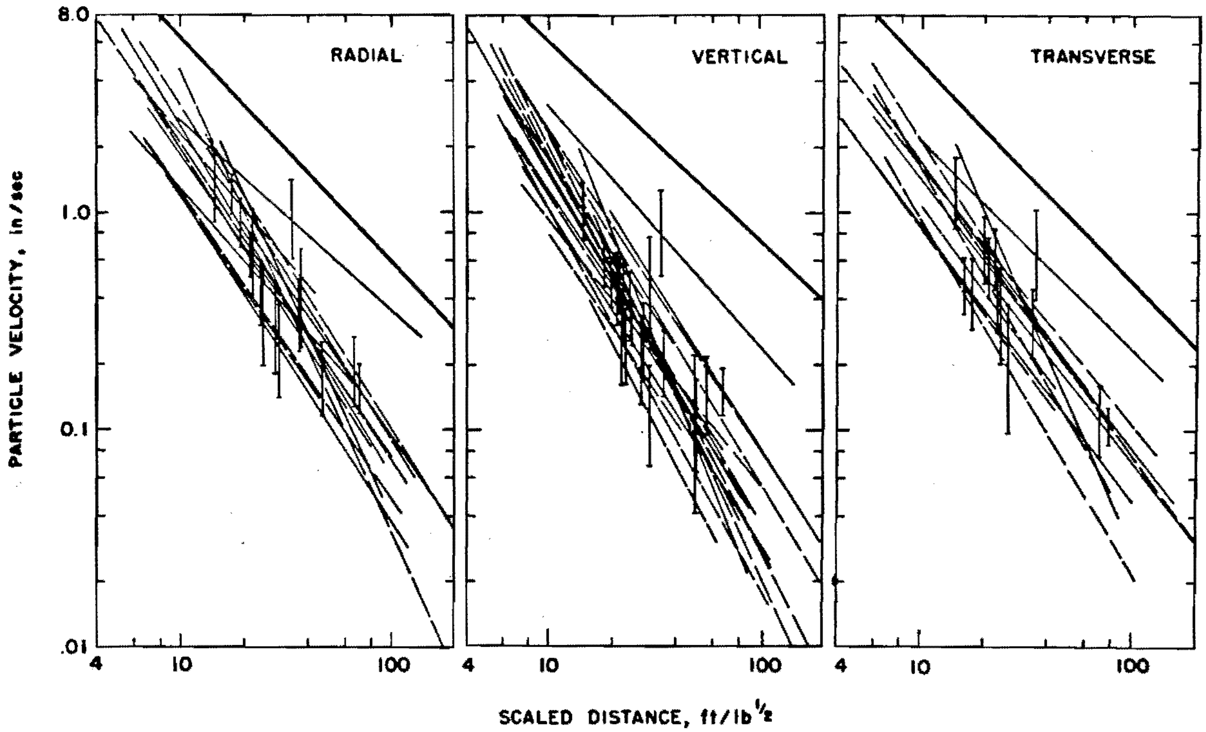

Figure 6.2.—Combined velocity data from all quarries in Bureau of Mines studies.

W = maximum charge weight per delay,
D/W½ = scaled distance,
and β = regression exponent or slope.

The values of both H and β will vary with site and component.

After plotting values of peak particle velocity versus scaled distance, D/W½ on log-log coordinate paper from instrumented shots (as shown in figure 6.1), the scaled distance at which 2.0 in/sec particle velocity is not exceeded, can readily be picked from the graph. For illustrative purposes, a scaled distance of 20 ft/lb½ has been chosen. Similarly, in the absence of data from instrumented blasts, the data of figure 6.2 can be used empirically. A scaled distance of 50 ft/lb½ has been chosen from these data and is recommended for use where instrumentation has not been used. This will insure that vibration levels will not exceed 2.0 in/sec particle velocity. Two examples have thus been set up: one, where instrumented data has been available and a second, where no data was available. The two hypothesized scaled distances for the two situations are 20 and 50 ft/lb½, respectively.

Normally, the distance from the blast to a potential damage point will be fixed. The charge per delay must then be varied to provide the proper scaled distance limit. Since D/W½ is the scaled distance, one may determine the proper charge weight per delay from the equation:

$$W = D^2/(S.D.)^2. \qquad (6.2)$$

The quantity, S.D., in equation 6.2 is the selected scaled distance to preclude damage. For the examples, S.D. has the value of 20 ft/lb½ and 50 ft/lb½. Assuming the potential damage point is 500 feet from the blast and solving equation 6.2 for the charge weight per delay, 625 and 100 pounds of explosives could be detonated per delay without exceeding the safe vibration criterion if the control limit was a scaled distance of 20 ft/lb½ or 50 ft/lb½, respectively. If the distance to the potential damage point is 1,000 feet, the maximum charge per delay that could be detonated safely would be 2,500 or 400 pounds for scaled distances of 20 or 50 ft/lb½, respectively.

Figure 6.3 is useful to quickly determine the maximum charge per delay for scaled distances of 20 or 50 ft/lb½. The line for a scaled distance of 50 ft/lb½ can be used where no data are available. The line for a scaled distance of 20 ft/lb½ is used only to illustrate what might be done if previous shots had been instrumented and data plotted as shown in figure 6.1. Two of the four previous numerical examples are shown on

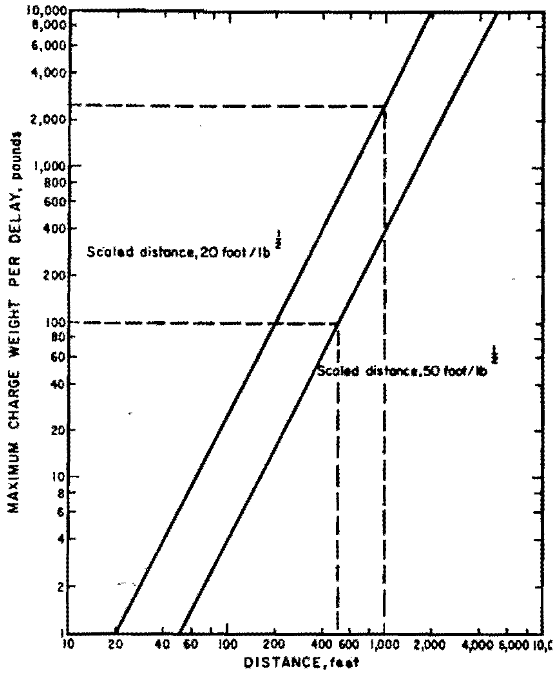

Figure 6.3.—Nomogram for estimating safe charge and distance limits for scaled distances of 20 and 50 ft/lb$^{1/2}$.

figure 6.3 through the use of dashed lines. At a distance of 1,000 feet, a vertical line is constructed to intersect the scaled distance equal to 20 ft/lb$^{1/2}$ line. A horizontal line is drawn through the intersection to the charge weight axis indicating a permissible charge weight per delay of 2,500 pounds. As an additional exercise, if the distance is 500 feet and a limiting scaled distance of 50 ft/lb$^{1/2}$ is used, a vertical line is drawn at 500 feet to intersect the scaled distance equal to 50 ft/lb$^{1/2}$ line. A horizontal line is drawn through the intersection indicating that 100 pounds of explosives could be used per delay. These results determined graphically are, as expected, identical with those obtained numerically. After construction, such a nomograph, permits the determination of the permissible charge weight using only a straight edge. If data are available from instrumented shots, and a more appropriate scaled distance is selected, a new nomograph can be constructed using equation 6.2.

6.5—ESTIMATING AIR BLAST LIMITS

The control of blasting procedures to maintain vibration levels below the safe blasting limits of 2.0 in/sec particle velocity generally results in air blast overpressures being much less than required to produce damage from air blast to residential structures. Curve C of figure 5.1 can be used to predict overpressures empirically. This curve represents an equation of the type:

$$P = K\left(\frac{D}{W^{1/3}}\right)^{\beta} \qquad (6.2)$$

where P = peak overpressure,
K = intercept at $D/W^{1/3} = 1.0$,
D = distance,
W = maximum charge weight per delay,
$D/W^{1/3}$ = scaled distance for air blast considerations,
and β = slope.

Using similar logic and a numerical example from section 6.4 and curve C as an appropriate estimating curve, overpressures may be estimated. Assuming the potential damage point is 500 feet from the blast, we had previously determined that 625 and 100 pounds of explosives could be detonated at scaled distances ($D/W^{1/2}$) of 20 ft/lb$^{1/2}$ and 50 ft/lb$^{1/2}$, the hypothetical limits to limit particle velocity to 2.0 in/sec. Using 500 feet and 625 and 100 pounds for predicting overpressure, these values represent scaled distances ($D/W^{1/3}$) of 58.3 and 108 ft/lb$^{1/3}$, respectively. From curve C, figure 5.1, the overpressures are 0.027 and 0.0135 psi for these conditions. These values are considerably below the 0.5 psi recommended safe air blast limit. Using an alternate approach, 0.5 psi from curve C occurs at a scaled distance ($D/W^{1/3}$) of 4.4 ft/lb$^{1/3}$. This represents an explosive charge of 734 tons at 500 feet compared to the 625 or 100 pounds permissible under the safe vibration limit. This comparison illustrates the estimation of charge size for safe air blast limits and also that under normal blasting conditions air blast is not a significant problem in causing damage. Except in very extreme cases where it is necessary to detonate relatively unconfined charges, the control of blasting procedures to limit vibration levels below 2.0 in/sec automatically limits overpressures to safe levels.

CHAPTER 7.—SUMMARY AND CONCLUSIONS

7.1—SUMMARY

This study is based on the 10-year Bureau program to reexamine the problem of vibrations from blasting. Included in the program were an extensive field study of ground vibrations from blasting; an evaluation of instrumentation to measure vibrations; establishment of damage criteria for residential structures; a consideration of human response; a determination of parameters of blasting which grossly affected vibrations; and empirical safe blasting limits which could be used with or without instrumentation for the design of safe blasts.

In all sections of this report, the authors have drawn heavily on the published work of others. This is particularly true in Chapters 3 and 5. In addition to the many publications referenced, all known, available, and pertinent articles published through August 1969 were critically reviewed. Obviously, many articles have been left out of the discussion either because of duplication or because they did not present significant contributions to other discussed data.

The Bureau study included data from 171 blasts at 26 sites. The sites included many rock types, such as limestone and dolomite, granite-type, diabase, schist, and sandstone and covered simple and complex geology with and without overburden.

The tests covered the detonation of explosive charges ranging from 25 to 19,625 pounds per delay at scaled distances ranging from 3.39 to 369 ft/lb$^{1/2}$. Recorded amplitudes of particle velocity ranged from 0.000808 to 20.9 in/sec. Frequencies of the seismic waves at peak amplitudes ranged from 7 to 200 cycles per second.

7.2—CONCLUSIONS

Damage to residential structures from ground-borne vibrations from blasting correlates more closely with particle velocity than with acceleration or displacement. The safe blasting limit of 2.0 in/sec peak particle velocity as measured from any of three mutually perpendicular directions in the ground adjacent to a structure should not be exceeded if the probability of damage to the structure is to be small (probably less than 5 percent). Complaints can be further reduced if a lower vibration limit is imposed. As an example, a peak velocity level of 0.4 in/sec should be imposed if complaints and claims are to be kept below 8 percent of the potential number of complainants. In the absence of instrumentation, a scaled distance of 50 ft/lb$^{1/2}$ may be used as a safe blasting limit for vibrations.

Air blast does not contribute to the damage problem in most blasting operations. A safe blasting limit of 0.5 psi air blast overpressure is recommended. Except in extreme cases (lack of standard stemming procedures), the control of blasting procedures to limit ground vibration levels below 2.0 in/sec automatically limits overpressures to safe levels.

Human response levels to ground vibrations, air blast, and noise are considerably below those levels necessary to induce damage to residential structures. The human response level is a major factor contributing to complaints. The ground and air vibrations observed in this study at reasonable distances from routine blasts are significantly lower than the vibrations necessary to damage residential structures. However, many of the observed vibration levels were at values that would cause people discomfort and, therefore, result in their filing complaints.

Millisecond-delay blasting can be used to decrease the vibration level from blasting, because it is the maximum charge weight per delay interval rather than the total charge which determines the resultant amplitude. To relate the ground vibration effects of different blasts, peak amplitudes at common scaled distances should be compared. The distance is scaled by dividing it by the square root of the charge weight per delay interval. Blasts initiated with electric millisecond-delay caps generally produce a lower vibration level than blasts initiated with Primacord delay connectors.

Geology and/or direction can have a major effect on both amplitude level and decay of amplitude with distance. If a site is instrumented to provide blasting limits, these effects should be examined, particularly in directions where structures might be subjected to damage. In an overall sense, from quarry to quarry, effects of geology including rock type, could not be determined from the data. Amplitudes at comparable scaled distances were similar irrespective of rock type. The presence or absence of overburden does not give rise to differences in particle velocity amplitude but does alter the wave frequency giving rise to changes in displacement and acceleration amplitudes.

ACKNOWLEDGMENTS

The authors wish to express their appreciation to the original sponsors whose interest and financial assistance supported the program: the National Crushed Stone Association, the National Board of Fire Underwriters, the National Association of Mutual Casualty Companies, and the Association of Casualty and Surety Companies. This investigation could not have been conducted without the cooperation of the management and personnel of many quarry companies. Most of these companies have been acknowledged in previous reports covering the various phases of the program. The authors again thank these operators and the quarry industry for their cooperation and assistance. Support from individuals and companies in all phases of the blasting industry was generously given. These included: vibration consultants, equipment manufacturers, other government agencies, explosive companies, and construction companies. The authors wish to again thank these individuals and groups for their support. The authors also wish to thank a large number of Bureau employees, past and present, who assisted in the field and laboratory phases of this project.

EXPLANATION OF APPENDICES

The appendices present the pertinent data concerning the field studies. Appendix A presents plan views of the various sites. Appendix B gives the shot and loading data for the ground vibration tests. Appendix C gives the particle velocity and frequency data. Appendix D gives a brief geologic site description. The order of sites is uniform throughout the appendices. For example, the Chantilly quarry is represented as figure A-17, tables B- and C-17, or site 17.

Two sites have been treated slightly different because of the limited data obtained there. Only pressure measurements were obtained at the Rockville quarry. A plan view of the tests is given in figure A-25, and the pertinent blast and loading data are given in table 5.8. The Rockville quarry does not appear elsewhere in the appendices. Site 26, the location of the Bureau—ASCE damage study tests, does not appear in the appendices. These two sites do not represent the same type tests as sites 1 through 24 and have therefore been excluded from the appendices.

Appendix A.—Plan Views of Test Sites

The gage station arrays and blast areas, mapped by a stadia survey at each site, are shown in figures A-1 through -25. The location of each blast is identified by test number. The gage station locations are shown by a series of circles along a line and are indicated as station 1, 2, 3, etc. At the Weaver quarry where gage arrays were numerous and close together, only a line is shown to represent the gage stations along the line. Gage arrays are identified with blasts by the corresponding test number as necessary to indicate which blast was recorded along which gage line. Gaps between blast areas on the maps represent rock quarried during periods when vibration studies were not conducted.

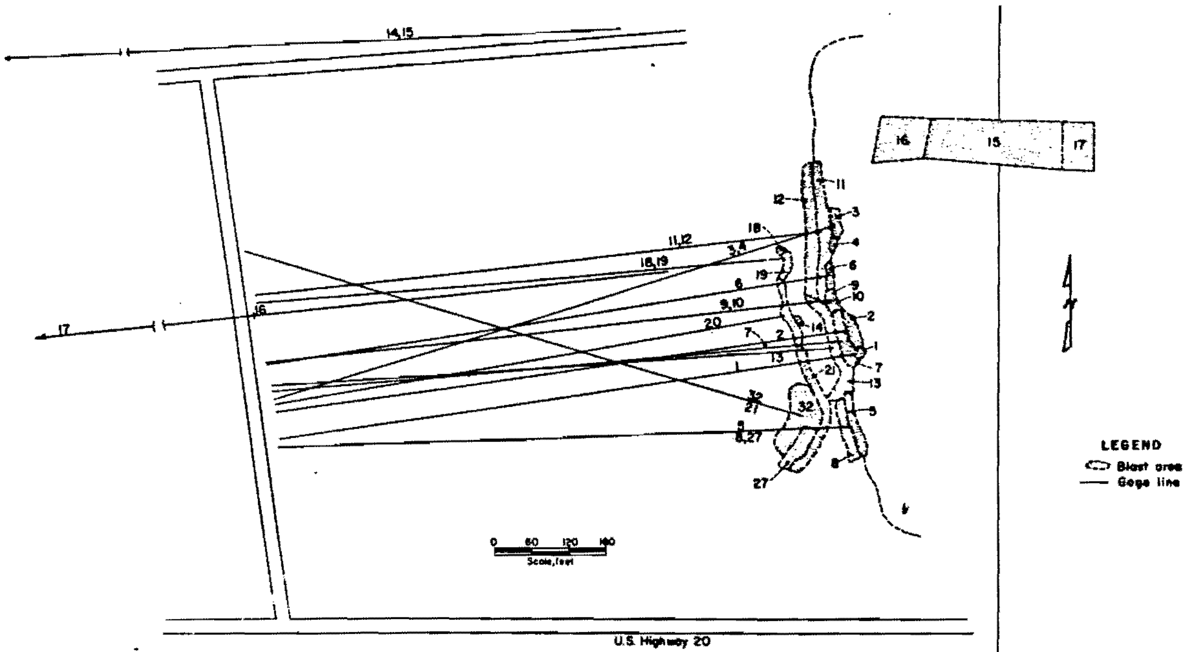

Figure A-1.–Weaver Quarry.

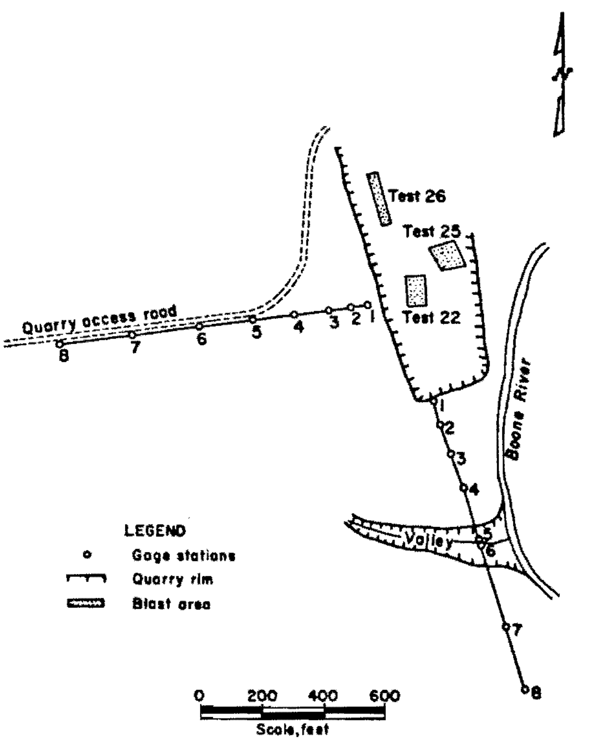

Figure A-2.–Webster City Quarry.

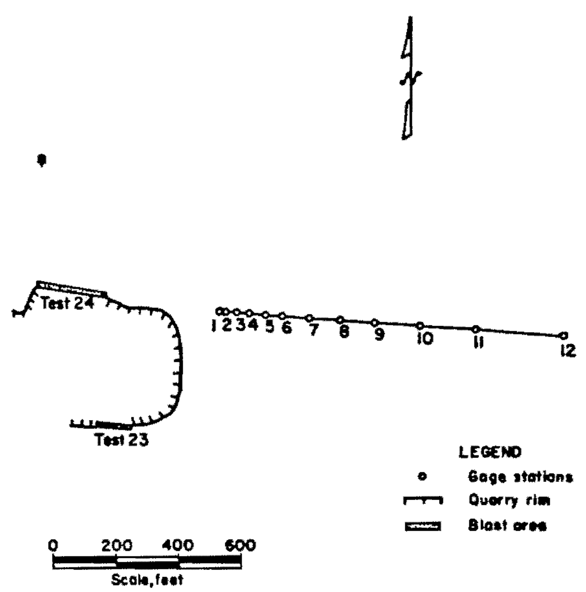

Figure A-3.–P & M Quarry.

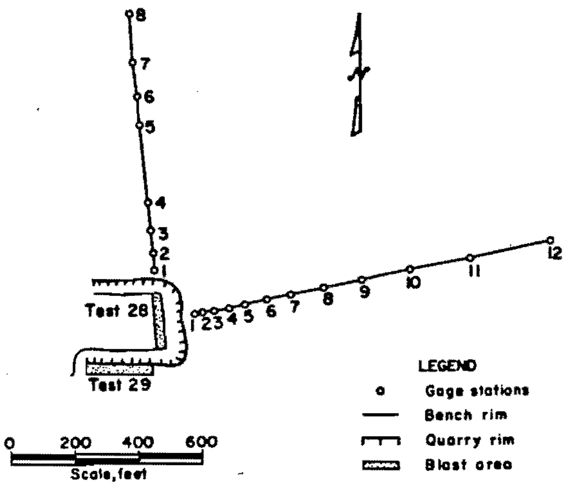

Figure A-4.—Ferguson Quarry.

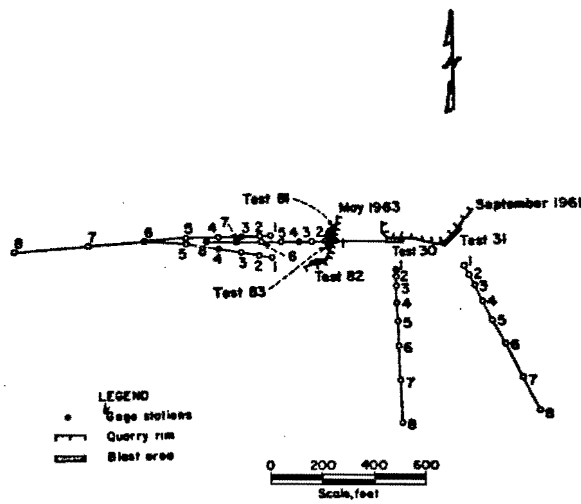

Figure A-5.—Shawnee Quarry.

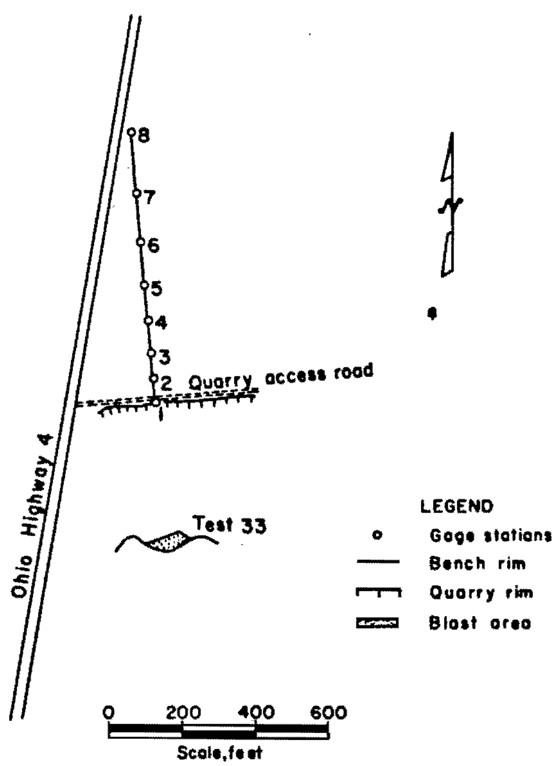

Figure A-6.—Hamilton Quarry.

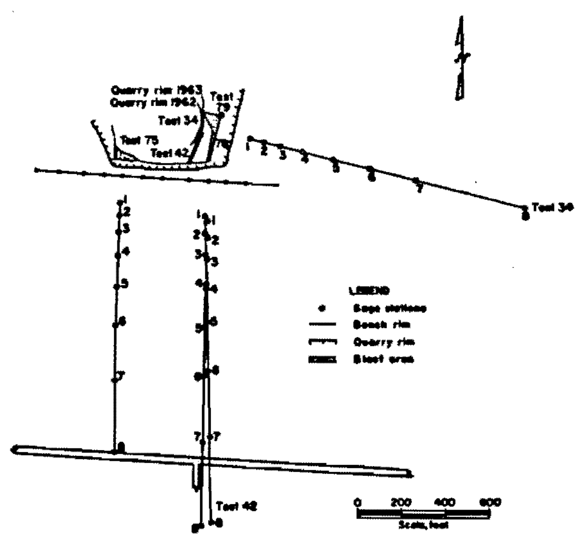

Figure A-7.—Flat Rock Quarry.

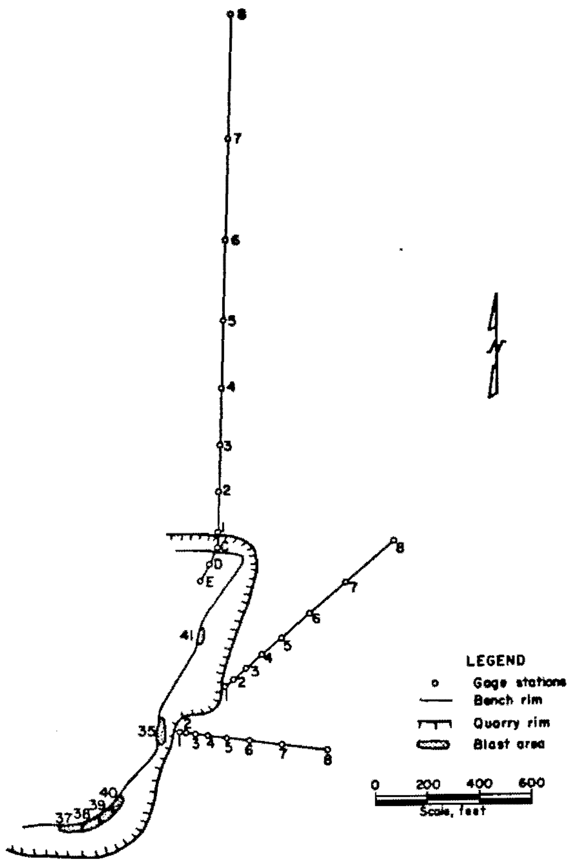

Figure A-8.—Bellevue Quarry.

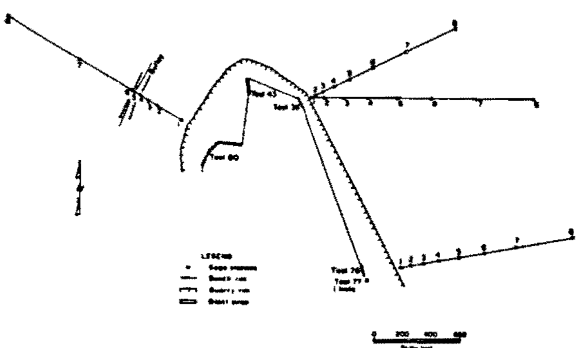

Figure A-9.—Bloomville Quarry.

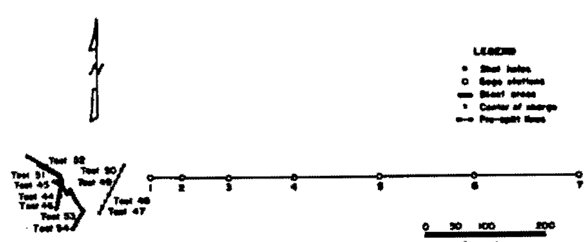

Figure A-10.—Washington, D.C. Site.

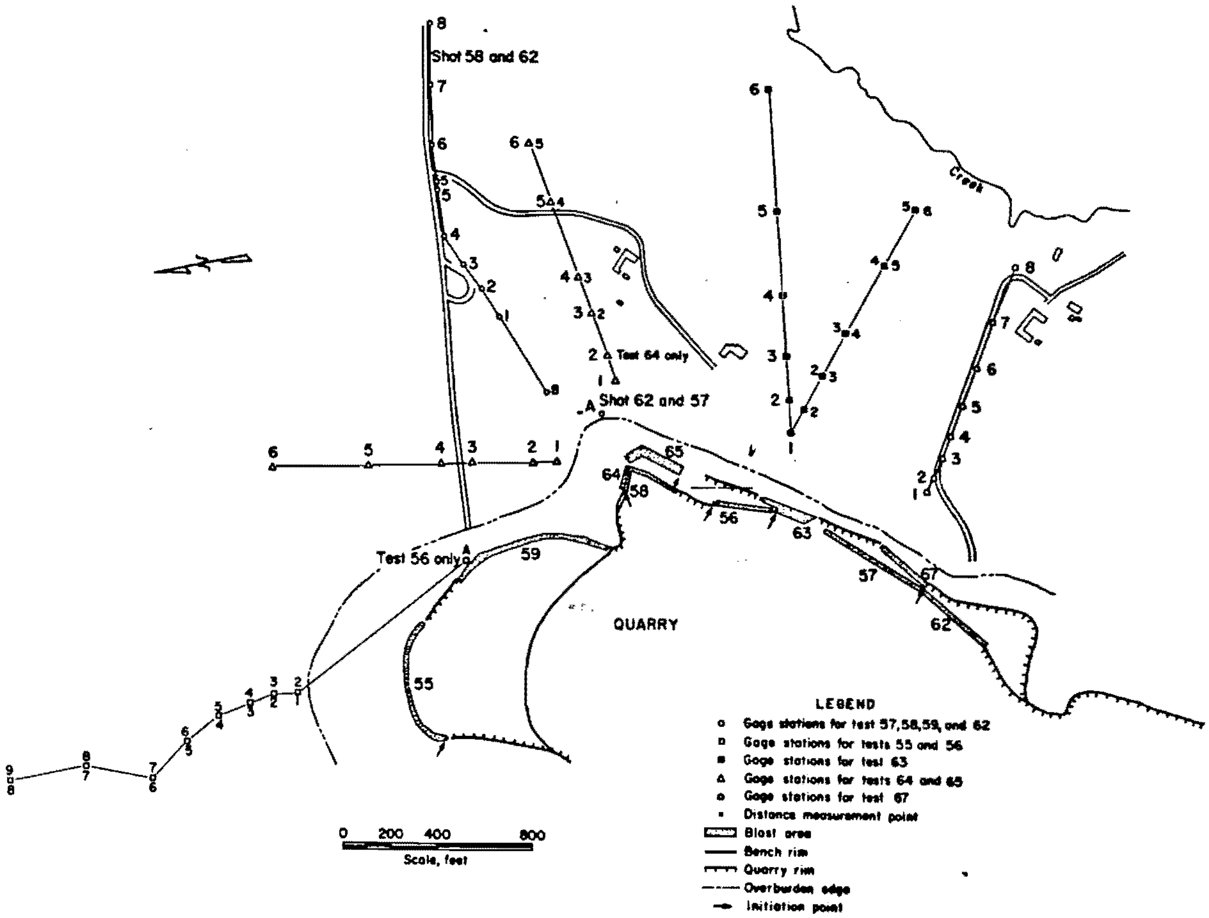

Figure A-11.–Poughkeepsie Quarry.

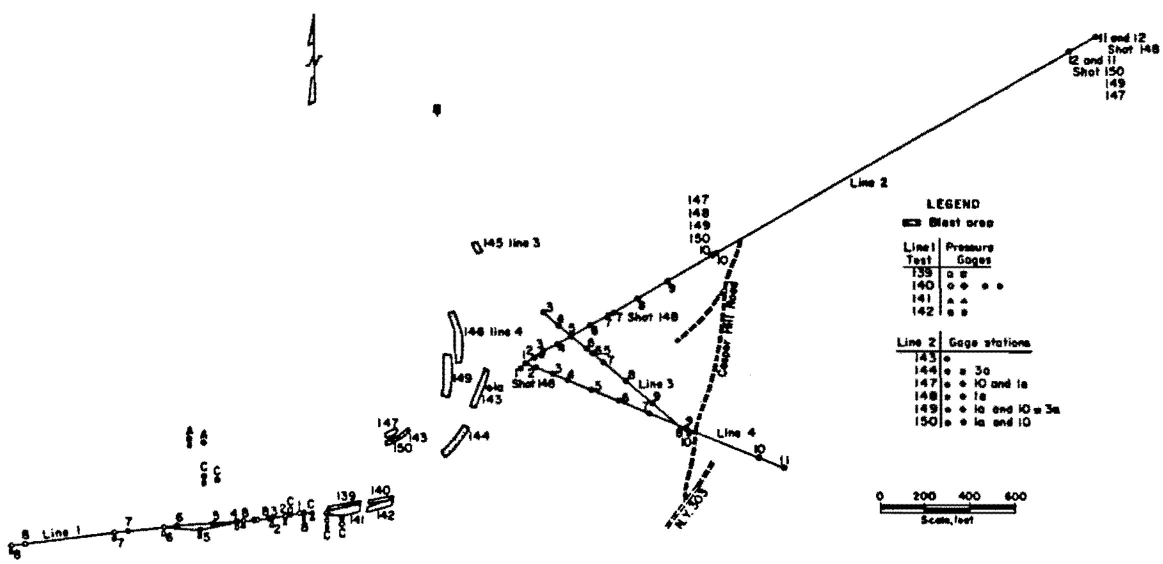

Figure A-12.–West Nyack Quarry.

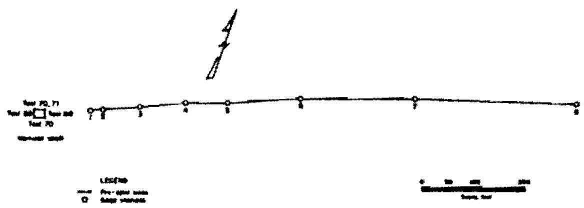

Figure A-13.–Littleville Dam Site.

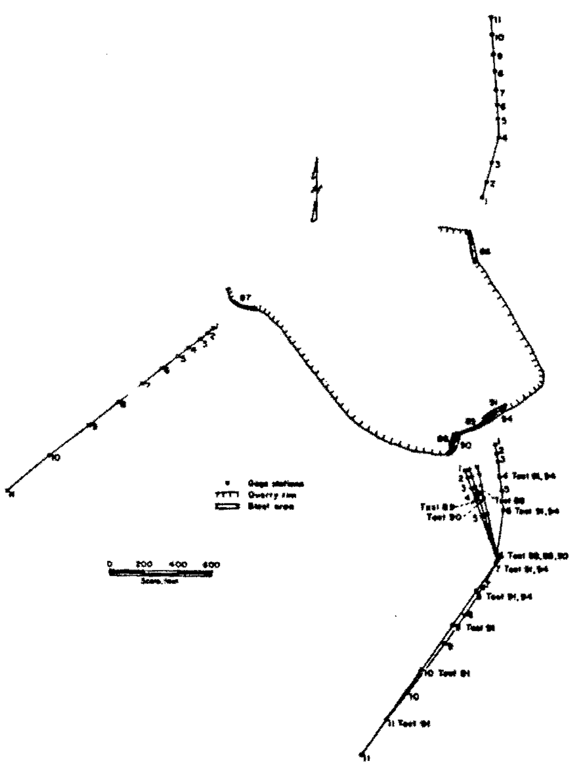

Figure A-14.–Centreville Quarry.

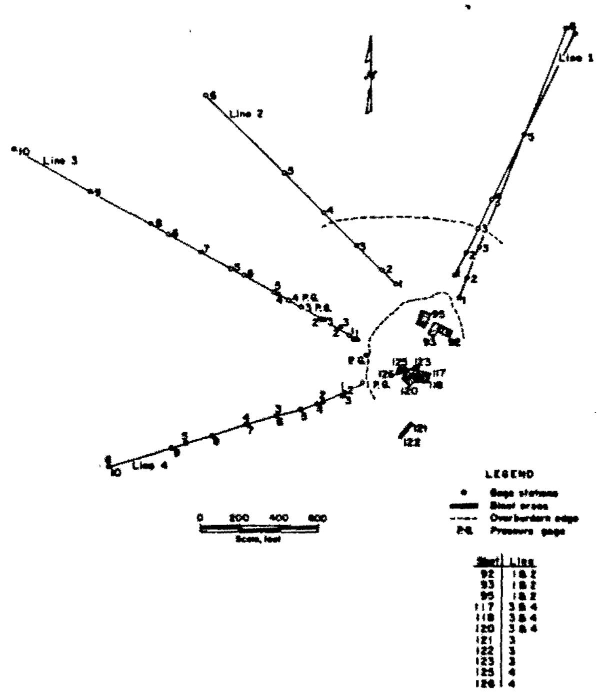

Figure A-15.–Manassas Quarry.

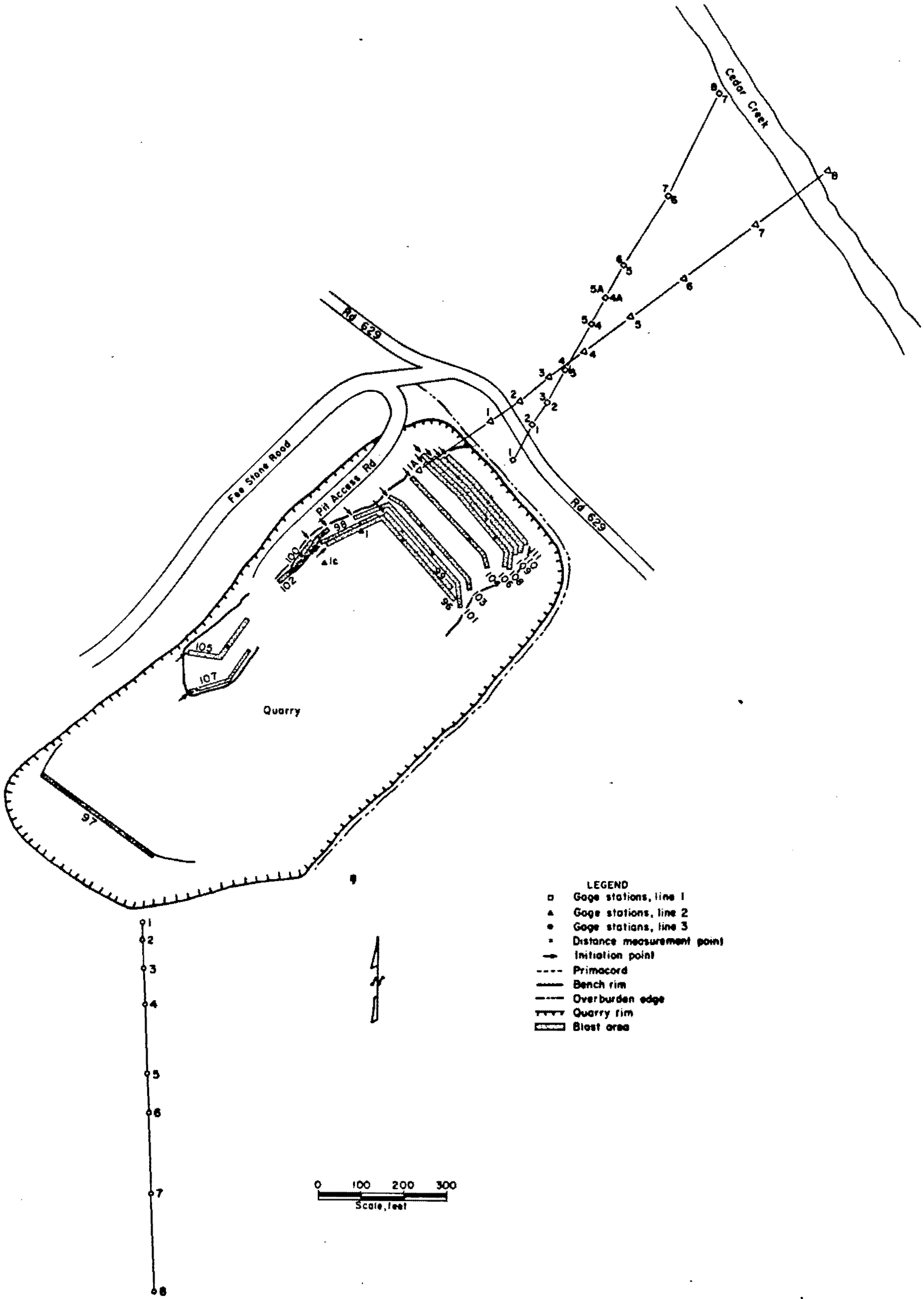

Figure A–16.–Strasburg Quarry.

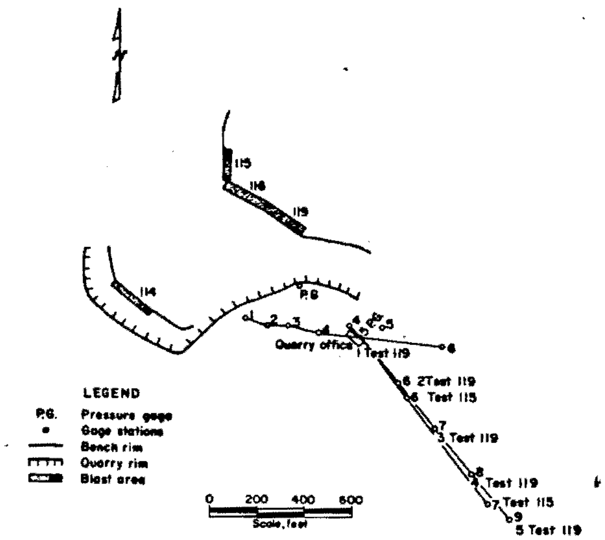

Figure A-17.—Chantilly Quarry.

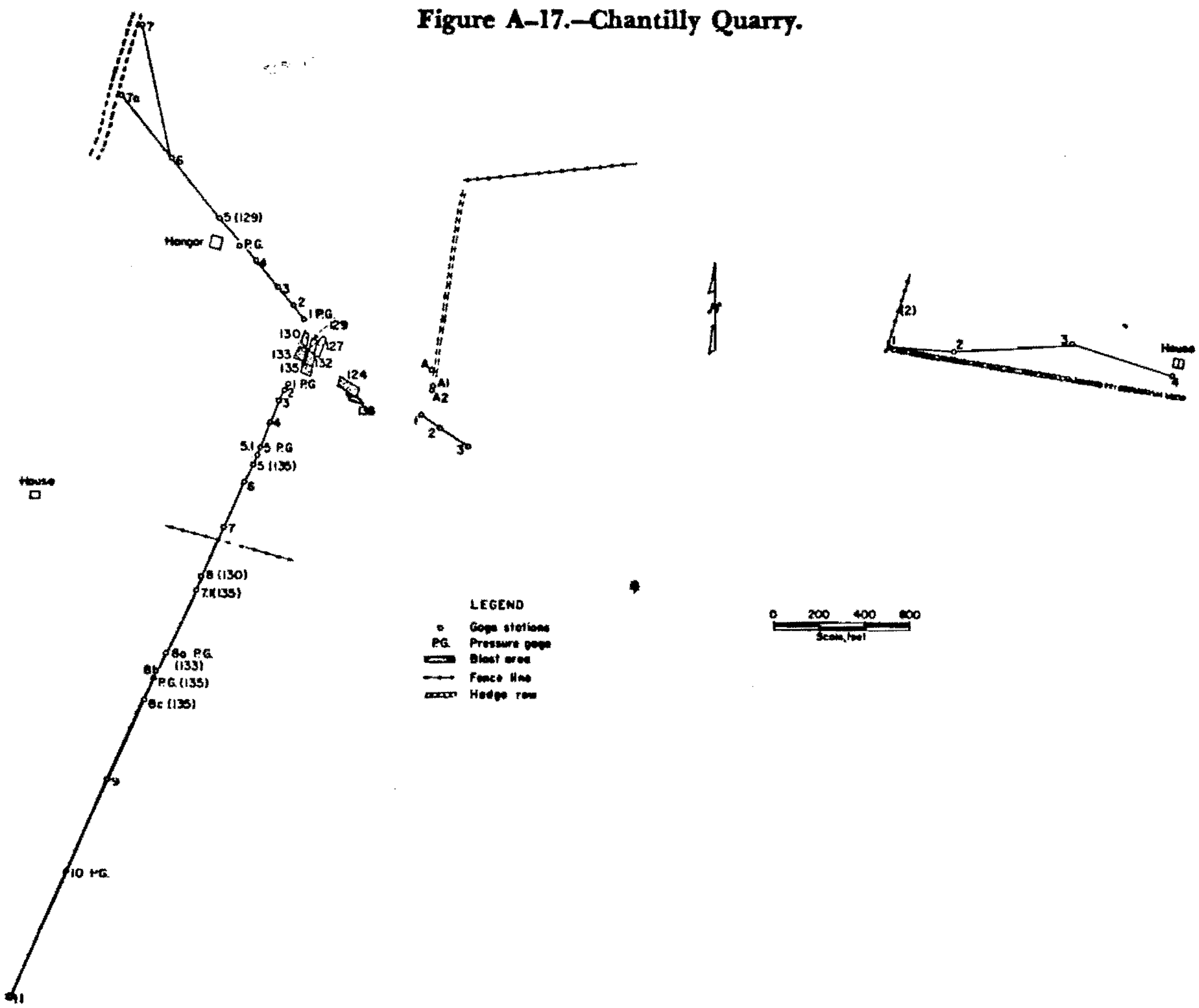

Figure A-18.—Culpeper Quarry.

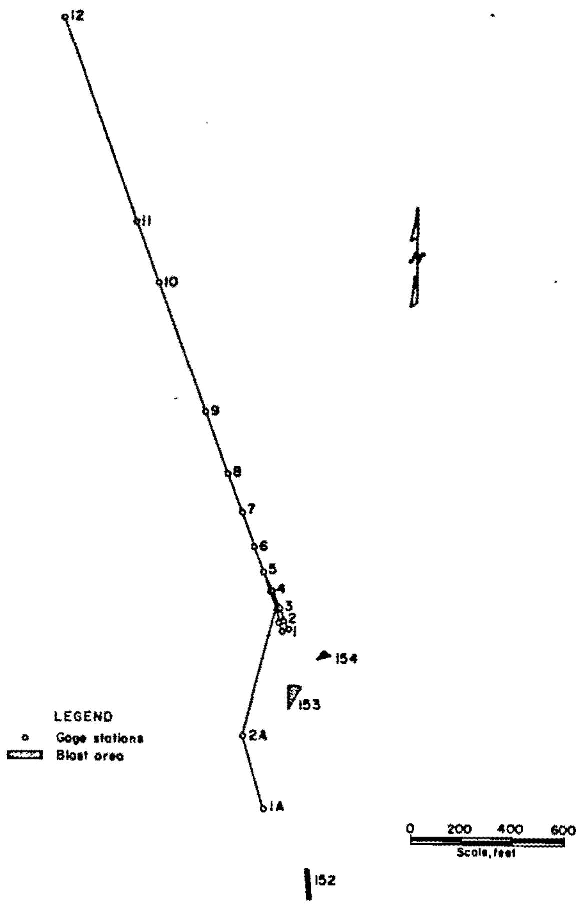

Figure A-19.—Doswell Quarry.

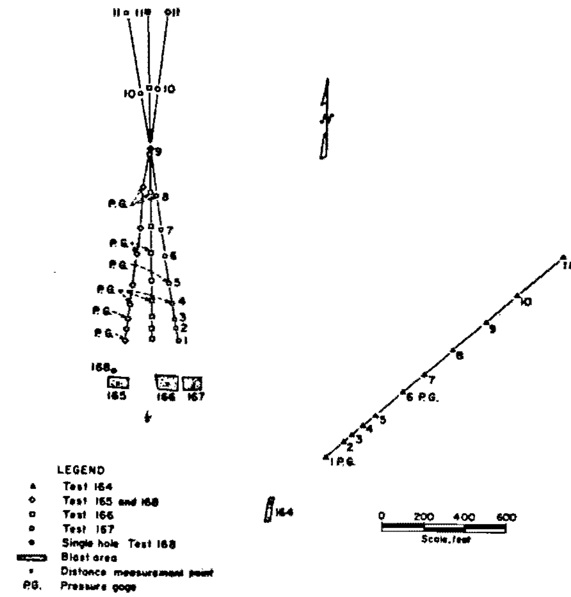

Figure A-21.—Jack Quarry.

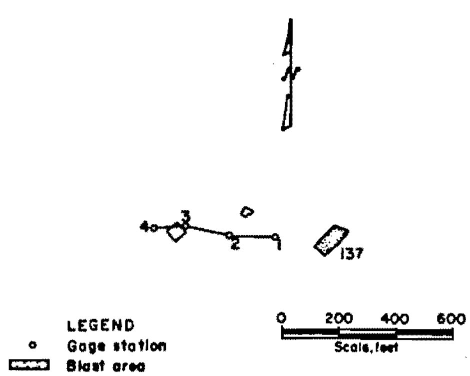

Figure A-20.—Riverton Quarry.

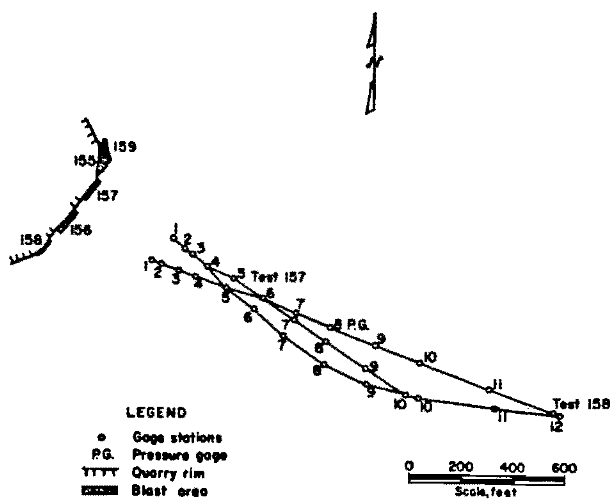

Figure A-22.—Buchanan Quarry.

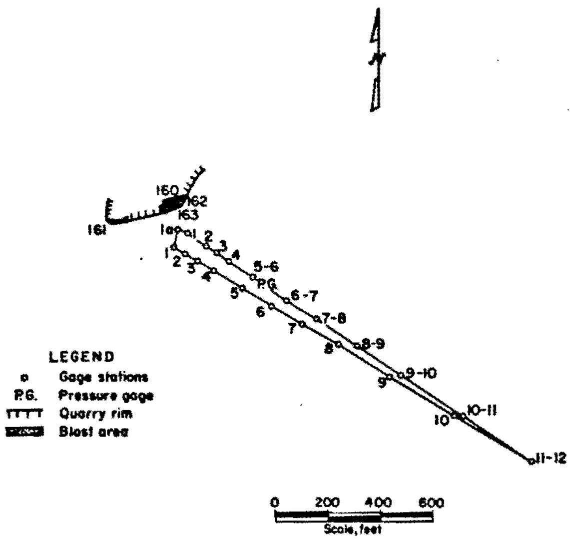

Figure A-23.—Hi-Cone Quarry.

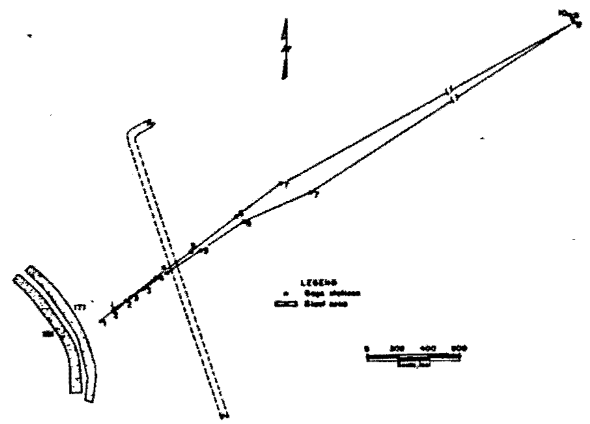

Figure A-24.—Union Furnace Quarry.

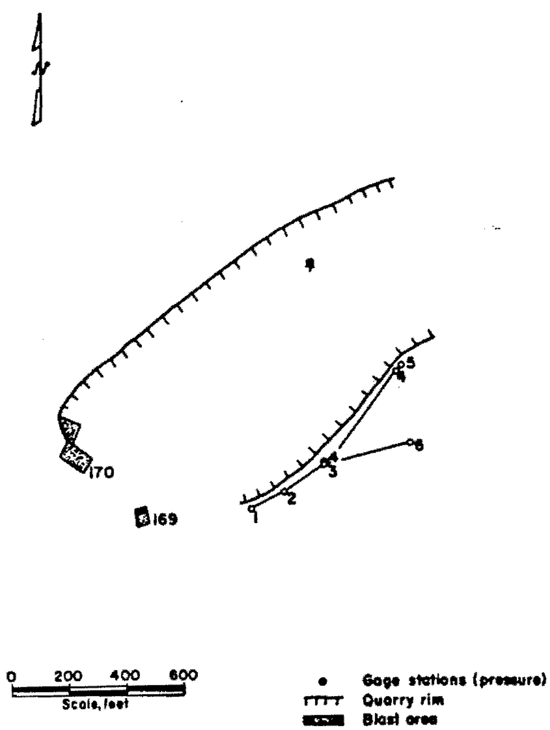

Figure A-25.—Rockville Quarry.

Appendix B.—Shot and Loading Data

A summary of the shot and loading data is given by site in Appendix B. Included are the number of holes, dimensions of holes and blast pattern, and the loading information including charge per hole and delay, type of initiation and delay interval.

Table B-1. - Weaver Quarry, Alden, Iowa

Test	Total No. of holes	Hole size, in	Hole depth, ft	Face height, ft	Stemming, ft	Burden, ft	Spacing, ft	Charge per hole, lb	No. of delay intervals	Max. charge per delay, lb	Length delay, msec	Type of initiation
2...	3	6	36	30	15	10	15	200	0	600	0	Primacord
3...	3	6	36	30	15	10	15	200	2	200	17	Do.
4...	1	6	36	30	15	10	0	200	0	200	0	Do.
5...	7	6	36	30	15	10	15	200	6	200	17	Do.
6...	3	6	36	30	15	10	15	200	2	200	34	Do.
7...	7	6	36	30	15	10	15	200	6	200	34	Do.
8...	7	6	36	30	15	10	15	200	0	1,400	0	Do.
9...	1	6	36	30	15	10	0	200	0	200	0	Do.
10...	1	6	36	30	15	10	0	200	0	200	0	Do.
11...	15	6	36	30	15	10	15	200	14	200	17	Do.
12...	15	6	36	30	15	10	15	200	0	3,000	0	Do.
13...	15	6	36	30	15	10	15	200	14	3,000	34	Do.
14...	1	6	10	30	14-16	10	0	100	0	100	0	Do.
15...	291	3	10	9	2	6	12	22	Toe shot	1,100	25	Cap
16...	147	3	10	9	2	5	10	22	Toe shot	484	25	Do.
17...	60	3	14	12	2	5	10	28	Toe shot	420	25	Do.
18...	1	6	36	30	16	10	0	200	0	200	0	Primacord
19...	3	6	36	30	16	10	15	200	2	200	9	Do.
20...	7	6	36	30	16	10	15	200	6	200	9	Do.
21...	15	6	36	30	16	10	15	200	14	200	9	Do.
27...	13	6	36	30	16	10	15	200	3	800	17	Do.
32...	21	6	36	30	16	10	14	203	3	1,218	17	Do.

Table B-2. - Moberly Quarry, Webster City, Iowa

Test	Total No. of holes	Hole size, in	Hole depth, ft	Face height, ft	Stemming, ft	Burden, ft	Spacing, ft	Charge per hole, lb	No. of delay intervals	Max. charge per delay, lb	Length delay, msec	Type of initiation
22...	490	3	12	9	2	5	9	25	3	1,100	17	Primacord
25...	160	3	12	9	2	5	9	25	4	400	17	Do.
26...	75	3	14	10	2	5	9	30	18	120	17	Do.

Table B-3. - P & M Quarry, Bradgate, Iowa

Test	Total No. of holes	Hole size, in	Hole depth, ft	Face height, ft	Stemming, ft	Burden, ft	Spacing, ft	Charge per hole, lb	No. of delay intervals	Max. charge per delay, lb	Length delay, msec	Type of initiation
23...	28	3	28	24	4	8	8	40	1	560	50	Cap
24...	78	3	20	18	4	8	9	25	2	625	50	Do.

Table B-4. - American Marietta Quarry, Ferguson, Iowa

Test	Total No. of holes	Hole size, in	Hole depth, ft	Face height, ft	Stemming, ft	Burden, ft	Spacing, ft	Charge per hole, lb	No. of delay intervals	Max. charge per delay, lb	Length delay, msec	Type of initiation
28...	44	3	17	18	3	7.5	15	50	3	700	25	Cap
29...	55	3	12	11	3-7.5	7.5	15	15	3	270	25	Do.

TABLE B-5. - Marble Cliff Quarries, Shawnee, Ohio

Test	Total No. of holes	Hole size, in	Hole depth, ft	Face height, ft	Stemming, ft	Burden, ft	Spacing, ft	Charge per hole, lb	No. of delay intervals	Max. charge per delay, lb	Length delay, msec	Type of initiation
30...	11	6	26	25	10-12	10	12	112	4	448	25	Cap
31...	11	6	26	25	10-12	10	12	125	3	500	25	Do.
81...	12	5.875	25	25	10-11	10	10	102	3	612	25	Do.
82...	13	5.875	30	30	12	10	10	132	3	660	25	Do.
83...	1	5.875	31	30	11	10	0	132	0	132	0	Do.

Table B-6. - Hamilton Quarry, Marion, Ohio

Test	Total No. of holes	Hole size, in	Hole depth, ft	Face height, ft	Stemming, ft	Burden, ft	Spacing, ft	Charge per hole, lb	No. of delay intervals	Max.charge per delay, lb	Length delay, msec	Type of initiation
33...	126	2.5	20	20	5-6	5	7	35	7	910	25	Cap

Table B-7. - Flat Rock Quarry, Flat Rock, Ohio

Test	Total No. of holes	Hole size, in	Hole depth, ft	Face height, ft	Stemming, ft	Burden, ft	Spacing, ft	Charge per hole, lb	No. of delay intervals	Max.charge per delay, lb	Length delay, msec	Type of initiation
34...	12	6	56-58	53-55	--	11	14	450	8	888	17	Primacord
42...	37	6	52	51	9	12	16	392	7	2,744	17	Do.
75...	36	6.25	24	23	6	12	10	182	9	1,072	9	Do.
78...	36	6.25	56	54	7	14	11	459	12	4,620	9	Do.
79...	1	6.25	56	54	4	10	0	468	0	468	0	Cap

Table B-8. - France Stone Company Quarry, Bellevue, Ohio

Test	Total No. of holes	Hole size, in	Hole depth, ft	Face height, ft	Stemming, ft	Burden, ft	Spacing, ft	Charge per hole, lb	No. of delay intervals	Max.charge per delay, lb	Length delay, msec	Type of initiation
35...	12	4	15	14	--	10	11	42	5	84	25	Cap
37...	7	5.625	18	18	--	12	10	73.5	6	73.5	25	Do.
38...	7	5.625	18	18	--	12	10	73.5	6	73.5	25	Do.
39...	7	5.625	18	18	--	12	10	78.5	6	78.5	25	Do.
40...	7	5.625	18	18	--	12	10	78.5	6	78.5	25	Do.
41...	12	5.625	18	18	--	12	10	51	5	102	25	Do.

Table B-9. - France Stone Company Quarry, Bloomville, Ohio

Test	Total No. of holes	Hole size, in	Hole depth, ft	Face height, ft	Stemming, ft	Burden, ft	Spacing, ft	Charge per hole, lb	No. of delay intervals	Max.charge per delay, lb	Length delay, msec	Type of initiation
36...	12	6	32	32	--	9	14	140	2	840	25	Cap
43...	41	4.75	18	18	--	10	11	77	2	1,540	25	Do.
76...	31	4.75	18	17	6.5	10	11	81.2	2	1,218	25	Do.
77...	1	4.75	18	17	6.5	11	0	80	0	80	0	Do.
80...	69	4.75	18	18	6.5-7.0	10	11	79.8	3	2,714	25	Do.

Table B-10. - Theodore Roosevelt Bridge Construction Site, Washington, D.C.

Test	Total No. of holes	Hole size, in	Hole depth, ft	Face height, ft	Stemming, ft	Burden, ft	Spacing, ft	Charge per hole, lb	No. of delay intervals	Max.charge per delay, lb	Length delay, msec	Type of initiation
44...	13	2.625	20	16	--	4	4	10	6	31	25	Cap
45...	3	2.625	20	16	--	4	6	37	2	37	25	Do.
46...	13	2.625	20	16	--	4	6.5	31	12	31	25	Do.
47...	9	2.625	20	No face	None	0	2.5	7.75	0	70	25	Do.
48...	9	2.625	20	No face	None	0	2.5	8	0	72	25	Do.
49...	9	2.625	20	No face	None	0	2.5	8	0	72	25	Do.
50...	9	2.625	20	No face	None	0	2.5	7.8	0	70	0	Primacord
51...	13	2.625	20	20	--	4	6	31	12	31	25	Cap
52...	13	2.625	20	20	--	4	6	26	12	26	25	Do.
53...	13	2.625	20	20	--	4	6	21	8	42	25	Do.
54...	13	2.625	18	18	--	4	6	25	12	25	25	Do.

Table B-11. - New York Trap Rock Corporation, Clinton Point Quarry, Poughkeepsie, N.Y.

Test	Total No. of holes	Hole size, in	Hole depth, ft	Face height, ft	Stemming, ft	Burden, ft	Spacing, ft	Charge per hole, lb	No. of delay intervals	Max.charge per delay, lb	Length delay, msec	Type of initiation
55...	35	9	30-56	28-54	19-23	22	20	920	34	920	17-26	Primacord
56...	13	9	85-106	83-104	20-22	22	20	1,100-1,500	12	1,522	26	Do.
57...	28	9	85	80-85	20	17	23	1,570	27	1,570	17-26	Do.
58...	30	9	55-72	53-70	20	20	16-20	1,116	29	1,116	17	Do.
59...	48	9	17-44	15-42	12-21	20	9-21	700	47	700	17	Do.
62...	20	9	61-89	59-91	12-23	23	25	1,620	19	1,620	26	Do.
63...	18	9	69-75	67-73	--	23	20	1,050-1,249	17	1,249	26	Do.
64...	6	9	--	--	--	10-15	20	200	5	200	26	Do.
65...	28	9	55-60	53-58	--	21	20	700-1,400	27	1,405	26	Do.
67...	12	9	76-82	70-76	--	22	22	1,150-1,350	11	1,355	26	Do.
												Do.

Table B-12. - New York Trap Rock Corporation Quarry, West Nyack, N.Y.

Test	Total No. of holes	Hole size, in	Hole depth, ft	Face height, ft	Stemming, ft	Burden, ft	Spacing, ft	Charge per hole, lb	No. of delay intervals	Max.charge per delay, lb	Length delay, msec	Type of initiation
60...	10	6.5	63-68	69-74	22-29	20	15	558	9	558	26	Primacord
139...	23	6.5	46	39	16-18	16-19	15	335	22	335	17-25	Primacord - Cap
140...	19	6.5	52-54	47	16.5-18	16-18	15-18	360	18	400	17-25	Do.
141...	31	6.5	29-51	22-44	16-18	15-16	16-18	92-300	30	303	17-25	Do.
142...	16	5.5	48-50	41-43	19-22	15-16	16-18	300-325	15	325	17-25	Do.
143...	23	6.5	45	38	15-19	15	16-18	308	22	308	25	Do.
144...	22	6.5	46	40	17-18	16-19	15	303-393	21	393	25	Do.
145...	8	6.5	51	45	19	15-18	16	303-353	7	353	25	Cap
146...	15	6.5	50	43	17.5	18	16	328-350	14	350	25	Primacord - Cap
147...	100	--	Toe shot	--	--	--	--	1.2	0	120	0	Cap
148...	27	6.5	52	45	18	15	16	303-358.5	25	606	9-25	Primacord - Cap
149...	35	--	Toe shot	--	--	--	--	2.72	0	95	0	Cap
150...	60	--	Toe shot	--	--	--	--	.6	0	100	0	Do.

Table B-13. - Littleville Dam Construction Site, Huntington, Mass.

Test	Total No. of holes	Hole size, in	Hole depth, ft	Face height, ft	Stemming, ft	Burden, ft	Spacing, ft	Charge per hole, lb	No. of delay intervals	Max.charge per delay, lb	Length delay, msec	Type of initiation
68...	10	2	50	0	0	0	21.4	9.79	0	97.9	0	Primacord
69...	10	2	50-52	0	0	0	21.4	10.8	0	108	0	Do.
70...	21	2	50	0	0	0	22.8	9.79	0	206	0	Do.
71...	14	2	50	0	0	0	20.3	5.4	0	75	0	Do.
72...	52	2	10	0	0	0	Irregular	10	5	130	600-800	Do.
73...	43	2	10	0	0	0	Irregular	11	6	66	600-800	Do.
74...	49	2	10	0	0	0	Irregular	11	6	100	600-800	Do.

Table B-14. - Fairfax Quarries, Inc., Quarry, Centreville, Va.

Test	Total No. of holes	Hole size, in	Hole depth, ft	Face height, ft	Stemming, ft	Burden, ft	Spacing, ft	Charge per hole, lb	No. of delay intervals	Max.charge per delay, lb	Length delay, msec	Type of initiation
86...	50	3.5	56	50	16	8	10	173	10	1,384	25	Cap
87...	45	3.5	36	30	12	8	10	100.5	10	703.5	25	Do.
88...	28	3.5	46-50	42-46	12	8	10	110-160	10	605	25	Do.
89...	45	3.5	50-56	46-52	12	8	10	160-185	10	1,220	25	Do.
90...	30	3.5	46-50	42-46	10	8	10	155	10	620	25	Do.
91...	42	3.5	56	50	12	8	8	173.8	9	869	25	Do.
94...	24	4.5	56	50	12	10	11	280	9	1,120	25	Do.

Table B-15. - W. E. Graham & Sons, Manassas Quarry, Manassas, Va.

Test No.	Total No. of holes	Hole size, in	Hole depth, ft	Face height, ft	Stemming, ft	Burden, ft	Spacing, ft	Charge per hole, lb	No. of delay intervals	Max. charge per delay, lb	Length delay, msec	Type of initiation
92...	40	3.5	30	30	6	8	10	70	5	700	25-500	Cap
93...	35	3.5	30	30	6	9	11	68.6	5	480	25-500	Do.
95...	48	3.5	30	28	5	9	11	86.5	7	693	25-500	Do.
117...	24	4.5	40	22	8.5	10	12	185	5	1,110	25-170	Do.
118...	38	3.5-4.5	45	40-46	3.5-9.5	9-10	11-12	150	6	1,500	25-205	Do.
120...	46	3.5-4.5	45	45	6-8	9-10	11-12	164	8	1,200	25-280	Do.
121...	36	2.5	16	Ditch shot	8	3.5	4	15	10	60	25-5,300	Do.
122...	12	2.5	16	Ditch shot	8	3.5	4	16.7	4	66.8	800-4,500	Do.
123...	20	3.5	44	45	12	10	14	220	7	1,100	25-500	Do.
124...	61	2.75	45	45	5	7	5	84.9	7	905	8-150	Do.
125...	16	2.5	42-50	45	3	0	2	9.5	0	150	0	Do.
126...	26	3.5-4.5	40-48	37	8-10	7-10	9-12	186.5	7	933	25-240	Do.

Table B-16. - Chemstone Corporation Quarry, Strasburg, Va.

Test No.	Total No. of holes	Hole size, in	Hole depth, ft	Face height, ft	Stemming, ft	Burden, ft	Spacing, ft	Charge per hole, lb	No. of delay intervals	Max. charge per delay, lb	Length delay, msec	Type of initiation
96...	84	2.5	20	18	8-10	8	5	40	2	1,160	5	Primacord
97...	63	3.5	20	18	8-10	8	5	30.2	2	633	5	Do.
98...	31	3.5	20	18	8-9	8	5	40.3	1	645	5	Do.
99...	49	3.5	20	18	10	8	5	39-44	1	982	5	Do.
100...	16	3.5	12-22	10-20	8	8	5	30	0	475	0	Do.
101...	78	3.5	20	18	10	8	5	41	1	1,600	5	Do.
102...	16	3.5	10-20	8-18	8-10	8	5	28	1	343	5	Do.
103...	59	3.5	20	18	8	8	5	36	3	589	5	Do.
104...	60	3.5	15-20	15-20	9	8	6	40	1	1,330	9	Do.
105...	42	3.5	4-20	4-20	3-6	10	5	25-35	0	1,325	0	Do.
106...	61	3.5	20	18	0-4	8	5	35-45	1	1,380	9	Do.
107...	42	3.5	6-20	8-18	0-4	8	5	30	0	1,250	0	Do.
108...	60	3.5	20	18	12-16	10	6	33	1	1,600	5	Do.
109...	51	3.5	20	12-14	16	5	7	33	1	865	5	Do.
110...	51	3.5	20	18	8-10	8	6	32.4	4	360	5	Do.
111...	48	3.5	20	18	8-10	8	6	33.3	4	367	5	Do.

Table B-17. - Chantilly Crushed Stone Company Quarry, Chantilly, Va.

Test No.	Total No. of holes	Hole size, in	Hole depth, ft	Face height, ft	Stemming, ft	Burden, ft	Spacing, ft	Charge per hole, lb	No. of delay intervals	Max. charge per delay, lb	Length delay, msec	Type of initiation
114...	56	3.5	36	34	7-10	8	13	116	7	2,090	25-240	Cap
115...	42	3.5	48	46	6	8	13	157	8	1,570	25-240	Do.
116...	87	3.5	44-48	42-45	7	8	13	151	5	2,260	25-170	Do.
119...	66	3.5	46	44	6.5	8	13	166.5	8	1,665	25-275	Do.

Table B-18. - Culpeper Crushed Stone Company Quarry, Culpeper, Va.

Test No.	Total No. of holes	Hole size, in	Hole depth, ft	Face height, ft	Stemming, ft	Burden, ft	Spacing, ft	Charge per hole, lb	No. of delay intervals	Max. charge per delay, lb	Length delay, msec	Type of initiation
124...	61	2.75	45	45	5	7	5	84.9	7	905	8-150	Cap
127...	67	2.75	30-32	30-32	5	5	9	74	6	961	8-150	Do.
129...	77	2.75	30-32	30-32	5	5	8	75.4	5	1,206	8-125	Do.
130...	57	2.75	33	33	4	6	9	69.3	8	624	8-175	Do.
132...	58	2.75	30-32	30-32	2.5	6	8	71.3	8	712	25-200	Do.
133...	70	2.75	30-32	30-32	3-4	6	8	68.6	10	686	25-300	Do.
135...	87	3	10-32	30-32	3-6	7	9	10.5-70.8	9	630	8-250	Do.
138...	59	2.75	45	45	3	6	9	93.7	6	937	8-150	Do.

Table B-19. - General Crushed Stone Company Quarry, Doswell, Va.

Test	Total No. of holes	Hole size, in	Hole depth, ft	Face height, ft	Stemming, ft	Burden, ft	Spacing, ft	Charge per hole, lb	No. of delay intervals	Max.charge per delay, lb	Length delay, msec	Type of initiation
152...	18	6	53	50	10	13	16	439-564	6	2,081	25-205	Cap
153...	20	6	45	42	11	13	16	354-504	6	1,616	25-205	Do.
154...	14	6	54	51	11-18	13	16	504-624	5	1,837	25-170	Do.

Table B-20. - Riverton Lime & Stone Company Quarry, Riverton, Va.

Test	Total No. of holes	Hole size, in	Hole depth, ft	Face height, ft	Stemming, ft	Burden, ft	Spacing, ft	Charge per hole, lb	No. of delay intervals	Max.charge per delay, lb	Length delay, msec	Type of initiation
137...	88	3.5	18	Bottom Shot	8	9	9	25.6	4	666	25	Cap

Table B-21. - Southern Materials Corporation, Jack Stone Quarry, Petersburg, Va.

Test	Total No. of holes	Hole size, in	Hole depth, ft	Face height, ft	Stemming, ft	Burden, ft	Spacing, ft	Charge per hole, lb	No. of delay intervals	Max.charge per delay, lb	Length delay, msec	Type of initiation
164...	26	6	80	80	12	14	16	700	9	2,965	25	Cap
165...	122	3.5	45	42	7	8	8	136	7	3,003	25	Do.
166...	152	3.5	44	40	7	8	8	111.5	7	2,565	25	Do.
167...	128	3.5	45	42	7	8	8	142	7	3,124	25	Do.
168...	1	3.5	45	50	6	10	0	150	0	150	0	Do.

Table B-22. - Superior Stone Company, Buchanan Quarry, Greensboro, N.C.

Test	Total No. of holes	Hole size, in	Hole depth, ft	Face height, ft	Stemming, ft	Burden, ft	Spacing, ft	Charge per hole, lb	No. of delay intervals	Max.charge per delay, lb	Length delay, msec	Type of initiation
155...	49	3.5	30	27	8-10	7	7	60-68	8	520	17	Cap
156...	44	3.5	30	27	8	7	7	80	9	565	17	Do.
157...	34	3.5	30	33	10	7	7	85	6	510	17	Do.
158...	11	3.5	30	27	8-10	7	7	86	5	173	17	Do.
159...	54	3.5	33	30	8-10	7	7	73	7	658	17	Do.

Table B-23. - Superior Stone Company, Hi-Cone Quarry, Greensboro, N.C.

Test	Total No. of holes	Hole size, in	Hole depth, ft	Face height, ft	Stemming, ft	Burden, ft	Spacing, ft	Charge per hole, lb	No. of delay intervals	Max.charge per delay, lb	Length delay, msec	Type of initiation
160...	42	2.75	55	59	6	5	5	115	7	690	25	Cap
161...	45	2.75	55	59	6	5	5	105	7	644	25	Do.
162...	33	3.5	55	59	6	7	7	172	7	857	25	Do.
163...	43	2.5	58-63	60	6	6	6	136	7	816	25	Do.

Table B-24. - Warner Company Quarry, Union Furnace, Pa.

Test	Total No. of holes	Hole size, in	Hole depth, ft	Face height, ft	Stemming, ft	Burden, ft	Spacing, ft	Charge per hole, lb	No. of delay intervals	Max.charge per delay, lb	Length delay, msec	Type of initiation
151...	39	7.375	200-215	185-200	12	30	24	3,910	26	7,820	17	Cap
171...	46	7.375	200-215	185-200	12	30	23	3,925	22	19,625	17	Do.

Appendix C.—Particle Velocity and Frequency Data

A summary of the peak particle velocity and associated frequency data is given by component and site in Appendix C. The peak particle velocity given is the maximum value recorded, regardless of where it occurred during the recording. The frequency given is the frequency associated with the peak particle velocity. When the peak particle velocity is associated with two frequencies, one superimposed on the other, both frequencies are listed in the tables, with the predominant frequency appearing first. The scaled distance is given for each gage station for each test. This is the distance from blast-to-gage divided by the square root of the maximum charge weight per delay or the total charge weight for instantaneous blasts. The shot-to-gage distances, from which the scaled distance was calculated, were determined by measuring the distance from each gage to the center of the blast holes having the maximum charge weight per delay.

Table C-1. - Weaver Quarry, Alden, Iowa

Test	Scaled distance, ft/lb$^{1/2}$	Radial		Vertical		Transverse	
		Particle velocity, in/sec	Frequency, cps	Particle velocity, in/sec	Frequency, cps	Particle velocity, in/sec	Frequency, cps
2...	8.70	-	-	1.74	50	0.789	50
	12.8	1.47	25	1.17	25	.699	50
	16.9	.923	20	.680	40	.384	30
	20.9	.680	16	.363	100	.199	25
	25.0	.694	20	.324	40	.201	20
	29.1	.511	30	.241	50	.228	16
3...	10.6	1.77	40	1.76	40	1.25	100+200
	16.3	.721	45	1.06	35	1.51	35
	22.6	.455	50	.338	100	.575	15
	28.3	.290	50	.201	100	.361	16
	38.9	.236	40	.140	200	-	-
	53.0	.122	18	.0966	80	.232	24
	67.2	.0607	50	.0773	26	.119	17
4...	15.6	1.45	24	1.08	167	.456	36
	21.9	.597	26	.418	80	.192	42
	27.5	.403	29	.280	200	.185	14
	38.0	.325	21	.144	125	-	-
	52.2	.150	21	.0898	25	.0680	71
	65.9	.0792	56	.0502	66	.0440	20
5...	11.3	-	-	3.42	28	1.70	50
	15.2	2.63	25	2.12	33	1.03	42
	20.4	1.45	27	1.02	30	.606	31
	27.2	.951	33	.644	30	.303	25
	36.4	.637	31	.407	31	-	-
	48.8	.397	22	.328	48	.197	38
	65.2	.164	22	.105	48	.147	23
6...	12.5	2.76	40	2.54	82	.683	38
	16.2	1.03	26	.807	100	.458	39
	24.1	.632	28	.375	100	.340	19
	33.4	.529	17	.289	125	.209	19
	46.3	.249	25	.0959	19	.164	18
	64.3	.107	29	.122	22	.0755	19
7...	13.1	1.74	27	1.24	18	.716	33
	16.7	1.16	28	.467	26	.313	33
	24.7	.566	18	.363	28	.269	20
	33.9	.318	18	.196	50	.197	22
	46.7	.192	20	.106	42	.134	23
	65.5	.0899	23	.0920	23	.0680	23
8...	3.88	-	-	8.76	15	1.65	25
	5.35	6.92	15	5.45	14	.900	50
	7.32	4.65	14	2.27	50	.932	20
	9.89	1.94	50	2.11	50	.859	30
	13.4	2.00	50	1.20	50	.614	50
	18.0	1.45	50	.780	30	.381	50
	24.2	.694	28	.350	20	.344	18
9...	11.5	1.88	37	1.79	71	.450	17
	15.6	1.10	31	.977	83	.245	83
	22.8	.475	42	.448	71	.269	71
	32.2	.340	30	.238	125	.182	20
	45.5	.169	36	.157	125	.103	20
	63.9	.0811	23	.0710	83	.0589	31
10...	11.5	2.34	50	1.64	71	.757	50
	15.6	1.30	38	.892	111	.450	36
	22.8	.567	31	.448	71	.223	56
	32.2	.386	30	.219	31	.182	26
	45.5	.195	45	.137	105	.101	22
	63.9	.0957	21	.0676	83	.0500	25
11...	14.7	1.17	100	1.86	62	1.54	52
	21.1	.833	29	.623	71	.723	29
	26.7	.693	15+54	.398	140	.372	38
	37.3	.448	71	.269	200	.238	100
	51.5	.179	50	.138	44	.117	13+167
	65.6	.0939	114+16	.0807	100	.0793	50
12...	4.75	-	-	4.72	25	2.41	25
	5.59	5.10	16	2.73	25	1.57	20
	6.65	4.15	12	2.00	25	1.24	25
	7.96	3.77	20	2.64	25	1.01	30
	9.46	3.64	20	1.65	29	1.47	25
	11.3	2.19	22	.866	25	1.09	22
	13.4	1.49	20	.548	20	1.25	25
	16.2	.903	15	.420	30	-	-
13...	20.2	1.35	24	.884	24	.424	35
	23.8	.963	26	.586	28	.448	24
	28.0	.663	24	.397	35	.310	24
	33.0	.486	23	.354	60	.280	20
	38.9	.475	22	.260	62	.145	21
	45.8	.314	22	.137	23	.100	22
	54.0	.236	24	.131	23	.134	22
	64.3	.125	24	.108	24	.0838	26
14...	54.0	-	-	0.0940	62	-	-
	57.0	-	-	.100	30	-	-
	61.5	-	-	.0620	50	-	-
	68.0	-	-	.0640	50	-	-
	76.5	-	-	.0490	71	-	-
	88.8	-	-	.0430	62	-	-
	105	-	-	.0370	20	-	-
	126	-	-	.0200	39	-	-
	153	-	-	.0340	17	-	-
	187	-	-	.0120	17	-	-
	230	-	-	.0160	18	-	-
	291	-	-	.00944	17	-	-
15...	18.9	-	-	.287	63	-	-
	20.7	-	-	.183	22	-	-
	22.9	-	-	.0980	29	-	-
	25.6	-	-	.148	36	-	-
	29.0	-	-	.0798	25	-	-
	33.2	-	-	.142	33	-	-
	38.7	-	-	.120	17	-	-
	45.5	-	-	.0480	36	-	-
	54.0	-	-	.0896	28	-	-
	64.4	-	-	.0400	26	-	-
	77.6	-	-	.0500	17	-	-
	96.6	-	-	.0280	13	-	-
16...	21.0	-	-	.350	22	-	-
	23.0	-	-	.500	23	-	-
	25.5	-	-	.275	23	-	-
	28.4	-	-	.396	33	-	-
	32.0	-	-	.254	30	-	-
	36.8	-	-	.140	50	-	-
	42.0	-	-	.132	30	-	-
	49.0	-	-	.120	21	-	-
	89.5	-	-	.0470	18	-	-
	94.3	-	-	.0530	19	-	-
	99.5	-	-	.0370	15	-	-
17...	34.4	-	-	.0760	50	-	-
	36.6	-	-	.0470	18	-	-
	39.9	-	-	.0280	36	-	-
	43.5	-	-	.0380	31	-	-
	46.7	-	-	.0420	31	-	-
	51.7	-	-	.0180	18	-	-
	57.8	-	-	.0340	20	-	-
	65.0	-	-	.0350	21	-	-
18...	15.6	1.66	19	.998	25	0.778	32
	18.9	.713	21	.850	56	.696	28
	22.9	.780	20	.347	63	.621	27
	29.0	.634	14	.342	25	.279	16
	33.7	.630	23	.205	38	.355	16
	40.9	.266	24	.105	42	.239	18
	49.8	.215	17	.126	23	.243	16
	60.3	.131	17	.0965	25	.146	15
19...	15.6	1.20	12	1.10	19	.361	14
	18.9	.990	17	1.30	62	.391	24
	22.9	1.10	19	.370	55	.368	16
	29.0	.880	14	.230	33	.321	22
	33.7	.730	21	.200	63	.490	19
	40.9	.400	15	.150	62	.199	18
	49.8	.330	16	.180	71	.266	17
	60.3	.170	19	.0700	55	.112	17
20...	14.4	1.69	11	1.07	82	.984	15
	17.7	.676	10	.746	83	.587	17
	21.6	.710	23	.685	100	.669	16
	26.4	.527	17	.506	100	.515	16
	32.2	.408	17	.261	32+100	.368	13
	39.3	.217	19	.210	100	.209	16
	48.2	.297	16	.192	100	.208	14
	59.0	.151	12	.124	13+100	.141	13
21...	17.6	1.87	10	.840	82	1.22	21
	21.1	1.07	28	.710	50	.608	19
	25.2	.537	50	.393	100	.785	16
	30.2	.924	20	.645	62	.759	20
	36.2	.648	21	.531	71	.329	16
	43.3	.829	19	.386	25+120	.453	18
	51.8	.451	13	.241	82	.252	14
	62.1	.181	20	.157	14	.237	8
27...	7.57	4.48	8	-	-	1.13	22
	9.30	1.08	19	2.39	67	3.08	42
	11.3	1.80	22+42	1.38	19+26	.859	36
	13.8	1.91	30	1.25	76	1.06	17
	16.8	1.52	20	.744	24	.788	15
	20.3	1.54	22	.786	25	-	-
	24.6	.729	18	.504	17	.345	8
	29.7	.387	19	.228	11	.237	8

Table C-1. - Weaver Quarry, Alden, Iowa - Continued

Test	Scaled distance, $ft/lb^{1/2}$	Radial		Vertical		Transverse	
		Particle velocity, in/sec	Frequency, cps	Particle velocity, in/sec	Frequency, cps	Particle velocity, in/sec	Frequency, cps
32...	7.31	4.32	9	1.33	85	1.15	120+14
	8.74	1.80	11	-	-	0.835	17
	10.5	1.58	86+12	1.15	45	1.15	20
	12.6	1.79	16+80	1.37	45	0.849	19
	15.2	1.28	19	0.742	25	.988	18
	18.2	1.02	19	.522	27	.448	39
	21.9	1.04	15	.406	62	.438	19
	26.5	0.533	75+14	.328	62	.164	20

Table C-2. - Moberly Quarry, Webster City, Iowa

Test	Scaled distance, $ft/lb^{1/2}$	Radial		Vertical		Transverse	
		Particle velocity, in/sec	Frequency, cps	Particle velocity, in/sec	Frequency, cps	Particle velocity, in/sec	Frequency, cps
22...	7.38	-	-	1.36	28	-	-
	9.84	-	-	0.630	28	-	-
	13.2	-	-	.390	55	-	-
	17.9	-	-	.506	32	-	-
	23.9	-	-	.310	28	-	-
	31.8	-	-	.220	26	-	-
	41.6	-	-	.219	26	-	-
	51.9	-	-	.128	32	-	-
22...	16.3	-	-	0.629	28	-	-
	20.1	-	-	.440	28	-	-
	24.1	-	-	.327	11	-	-
	29.5	-	-	.223	17	-	-
	37.6	-	-	.120	28	-	-
	38.5	-	-	.107	21	-	-
	50.8	-	-	.0473	10	-	-
	60.4	-	-	.0498	14	-	-
25...	15.0	-	-	0.524	33	-	-
	17.5	-	-	.320	28	-	-
	21.0	-	-	.345	33	-	-
	26.5	-	-	.253	33	-	-
	33.0	-	-	.191	24	-	-
	41.5	-	-	.154	31	-	-
	52.3	-	-	.0643	36	-	-
	64.0	-	-	.0367	33	-	-
25...	23.8	-	-	0.164	28	-	-
	27.5	-	-	.0962	22	-	-
	32.0	-	-	.118	20	-	-
	37.8	-	-	.0797	22	-	-
	46.0	-	-	.0360	38	-	-
	47.5	-	-	.0390	72	-	-
	61.0	-	-	.0200	20	-	-
	71.8	-	-	.0255	21	-	-
26...	31.5	-	-	0.411	30	-	-
	33.3	-	-	.312	18	-	-
	36.1	-	-	.253	19	-	-
	42.0	-	-	.249	62	-	-
	51.1	-	-	.300	42	-	-
	64.4	-	-	.200	24	-	-
	82.6	-	-	.135	26	-	-
	103	-	-	.0899	62	-	-
26...	62.1	-	-	0.160	29	-	-
	69.4	-	-	.0857	31	-	-
	78.5	-	-	.110	17	-	-
	89.5	-	-	.0487	16	-	-
	105	-	-	.0465	26	-	-
	107	-	-	.0458	24	-	-
	132	-	-	.0220	25	-	-
	152	-	-	.0266	16	-	-

Table C-3. - P & M Quarry, Bradgate, Iowa

Test	Scaled distance, $ft/lb^{1/2}$	Radial		Vertical		Transverse	
		Particle velocity, in/sec	Frequency, cps	Particle velocity, in/sec	Frequency, cps	Particle velocity, in/sec	Frequency, cps
23...	20.8	-	-	0.164	62	-	-
	21.5	-	-	.176	83	-	-
	22.4	-	-	.172	62	-	-
	23.5	-	-	.143	83	-	-
	25.1	-	-	.122	71	-	-
	27.0	-	-	.166	36	-	-

Table C-3. - P & M Quarry, Bradgate, Iowa - Continued

Test	Scaled distance, $ft/lb^{1/2}$	Radial		Vertical		Transverse	
		Particle velocity, in/sec	Frequency, cps	Particle velocity, in/sec	Frequency, cps	Particle velocity, in/sec	Frequency, cps
23...	30.0	-	-	0.128	36	-	-
	33.6	-	-	.0679	14	-	-
	37.6	-	-	.0731	18	-	-
	43.3	-	-	.0390	13	-	-
	50.3	-	-	.0360	82	-	-
	61.3	-	-	.0200	17	-	-
24...	18.6	-	-	0.411	56	-	-
	19.2	0.529	30	.195	26	0.211	31
	21.4	-	-	.156	30	-	-
	23.0	-	-	.114	23	-	-
	25.0	-	-	.114	15	-	-
	27.4	-	-	.384	28	-	-
	30.8	0.252	16	.298	18	0.191	13
	34.8	-	-	.135	25	-	-
	39.2	-	-	.103	16	-	-
	45.2	-	-	.0712	24	-	-
	52.2	-	-	.0679	25	-	-
	63.2	-	-	.0617	21	-	-

Table C-4. - American Marietta Quarry, Ferguson, Iowa

Test	Scaled distance, $ft/lb^{1/2}$	Radial		Vertical		Transverse	
		Particle velocity, in/sec	Frequency, cps	Particle velocity, in/sec	Frequency, cps	Particle velocity, in/sec	Frequency, cps
28...	5.67	-	-	3.29	39	-	-
	6.95	-	-	2.64	45	-	-
	8.62	-	-	0.829	45	-	-
	10.6	-	-	1.05	56	-	-
	13.0	-	-	0.120	62	-	-
	15.5	-	-	.280	45	-	-
	24.9	-	-	.226	31	-	-
	31.0	-	-	.106	36	-	-
	38.2	-	-	.0596	33	-	-
	48.1	-	-	.0574	20	-	-
28...	6.27	-	-	1.14	55	-	-
	8.32	-	-	0.636	35	-	-
	11.0	-	-	.546	62	-	-
	14.6	-	-	.234	36	-	-
	24.1	-	-	.233	33	-	-
	27.8	-	-	.119	30	-	-
	31.9	-	-	.0768	31	-	-
	37.8	-	-	.0611	22	-	-
29...	18.0	-	-	0.439	41	-	-
	19.7	-	-	.368	40	-	-
	21.4	-	-	.342	32	-	-
	24.2	-	-	.123	33	-	-
	27.1	-	-	.321	32	-	-
	35.3	-	-	.167	26	-	-
	42.4	-	-	.0896	23	-	-
	49.5	-	-	.0850	40	-	-
	59.3	-	-	.0625	13	-	-
	71.2	-	-	.0672	23	-	-
	87.3	-	-	.0530	17	-	-
29...	20.6	-	-	0.420	27	-	-
	23.7	-	-	.326	31	-	-
	27.7	-	-	.290	28	-	-
	33.3	-	-	.181	34	-	-
	48.4	-	-	.137	38	-	-
	54.2	-	-	.171	26	-	-
	60.7	-	-	.140	31	-	-
	70.2	-	-	.119	42	-	-

Table C-5. - Marble Cliff Quarries, Shawnee, Ohio

Test	Scaled distance, $ft/lb^{1/2}$	Radial		Vertical		Transverse	
		Particle velocity, in/sec	Frequency, cps	Particle velocity, in/sec	Frequency, cps	Particle velocity, in/sec	Frequency, cps
30...	6.66	1.02	53	1.29	45	1.64	77
	8.41	-	-	0.973	53	-	-
	11.6	0.892	34	.508	56	0.806	42
	15.0	-	-	.207	53	-	-
	19.6	0.549	37	.272	59	0.179	43
	25.8	-	-	.303	50	-	-
	33.9	0.102	38	.0540	48	0.0569	50

Table C-5. - Marble Cliff Quarries, Shawnee, Ohio - Continued

Test	Scaled distance $ft/lb^{1/2}$	Radial		Vertical		Transverse	
		Particle velocity, in/sec	Frequency, cps	Particle velocity, in/sec	Frequency, cps	Particle velocity, in/sec	Frequency, cps
30...	10.5	-	-	1.10	48	-	-
	12.6	-	-	1.32	48	-	-
	14.9	-	-	0.527	50	-	-
	17.2	-	-	.473	30	-	-
	20.5	-	-	.375	24	-	-
	24.2	-	-	.232	33	-	-
	28.8	-	-	.314	45	-	-
31...	7.51	2.05	40	1.62	67	1.22	42
	9.44	-	-	1.06	56	-	-
	12.5	0.783	42	.552	50	.736	38
	16.3	-	-	.236	63	-	-
	20.9	.282	26	.177	42	.198	30
	27.3	-	-	.130	19	-	-
	34.0	.175	20	.0929	48	.127	19
31...	19.7	-	-	.238	36	-	-
	21.5	-	-	.208	50	-	-
	23.7	-	-	.120	14	-	-
	25.9	-	-	.182	50	-	-
	29.1	-	-	.135	40	-	-
	32.6	-	-	.118	31	-	-
	37.0	-	-	.101	24	-	-
	42.0	-	-	.126	22	-	-
81...	9.46	1.29	42	.733	48	.386	71
	11.1	1.09	40	.758	40	.680	45
	13.9	.488	27	.360	38	.301	19
	17.4	.324	26	.226	30	.176	29
	22.5	.334	21	.265	30	.147	29
	29.1	.283	20	.116	50	.130	32
	37.8	.212	21	.0620	40	.0912	22
	49.6	.0689	15	.0545	24	.0597	18
82...	6.89	1.80	48	.990	50	.878	48
	8.80	1.41	30	1.03	53	.867	30
	11.4	.743	33	.954	50	.668	33
	14.9	.835	20	.374	31	.560	21
	19.8	.687	20	.244	28	.249	21
	26.2	.265	14	.110	22	.116	19
	34.5	.204	45	.0681	53	.0733	91
	45.5	.112	16	.0468	38	.0609	50
83...	18.9	.478	10	.311	13	.448	27
	23.1	.560	32	.461	33	.292	33
	29.0	.379	32	.253	27	.285	40
	36.6	.210	26	.223	50	.269	23
	47.4	.257	24	.126	21	.206	19
	61.4	.170	19	.0746	36	.101	15
	80.2	.116	14	.0471	18	.0880	13
	105	.0617	16	.0303	16	.0448	12

Table C-6. - Hamilton Quarry, Marion, Ohio

Test	Scaled distance, $ft/lb^{1/2}$	Radial		Vertical		Transverse	
		Particle velocity, in/sec	Frequency, cps	Particle velocity, in/sec	Frequency, cps	Particle velocity, in/sec	Frequency, cps
33...	14.1	0.631	23	0.359	30	0.245	14
	16.4	-	-	.340	56	-	-
	19.1	.550	21	.189	71	-	-
	22.2	-	-	.164	16	-	-
	25.9	.257	23	.211	16	.245	14
	30.1	-	-	.164	16	-	-
	35.2	.217	25	.110	17	.161	11

Table C-7. - Flat Rock Quarry, Northern Ohio Stone Company, Flat Rock, Ohio

Test	Scaled distance, $ft/lb^{1/2}$	Radial		Vertical		Transverse	
		Particle velocity, in/sec	Frequency, cps	Particle velocity, in/sec	Frequency, cps	Particle velocity, in/sec	Frequency, cps
34...	7.55	-	-	3.25	56	1.53	34
	9.70	-	-	3.47	42	-	-
	12.4	2.19	19	4.26	42	-	-
	20.7	2.08	17	.736	30	.637	21
	26.6	-	-	.760	36	-	-
	34.0	.851	23	.827	31	.699	45
	44.4	-	-	.280	31	-	-

Table C-7. - Flat Rock Quarry, Northern Ohio Stone Company, Flat Rock, Ohio - Continued

Test	Scaled distance $ft/lb^{1/2}$	Radial		Vertical		Transverse	
		Particle velocity, in/sec	Frequency, cps	Particle velocity, in/sec	Frequency, cps	Particle velocity, in/sec	Frequency, cps
42...	4.87	-	-	5.74	21	5.10	14
	6.40	5.63	15	5.14	22	2.20	12
	8.30	5.58	15	3.67	20	1.65	26
	10.9	-	-	1.94	10	1.42	36
	14.4	2.57	16	.907	53	1.02	53
	18.8	1.68	18	.930	28	1.21	25
	24.6	1.20	16	.563	24	1.13	13
	32.3	.425	26	.672	9	.710	26
75...	7.09	2.17	25	1.79	37	2.19	36
	8.95	2.34	27	1.49	40	1.41	33
	11.4	2.19	42	1.14	48	1.68	45
	14.7	0.909	42	1.31	45	0.967	29
	19.2	.764	34	0.896	59	.560	33
	24.7	.794	40	.950	77	1.02	63
	32.7	.407	50	.401	40	.418	24
	42.8	.309	14	.0867	11	.348	14
78...	6.77	2.06	22	2.85	22	2.32	23
	7.96	2.19	26	1.86	24	1.67	26
	9.42	2.01	24	1.31	32	1.18	11
	11.5	1.72	23	0.912	30	0.861	45
	14.2	1.47	9	.786	17	.834	50
	17.5	1.09	34	.674	10	.788	20
	22.1	0.590	43	.373	43	.936	63
	27.9	.307	23	.278	20	.263	21
79...	22.9	0.401	31	0.611	26	0.395	18
	26.7	.384	30	.278	25	.334	21
	31.2	.341	29	.134	40	.251	21
	37.9	.287	26	.147	29	.246	21
	46.1	.235	23	.101	38	.261	24
	56.7	.152	20	.0806	32	.182	25
	71.0	.120	18	.0546	21	.156	18
	89.2	.0669	24	.0422	17	.0474	24

Table C-8. - France Stone Company, Bellevue, Ohio

Test	Scaled distance, $ft/lb^{1/2}$	Radial		Vertical		Transverse	
		Particle velocity, in/sec	Frequency, cps	Particle velocity, in/sec	Frequency, cps	Particle velocity, in/sec	Frequency, cps
35...	19.6	1.18	20	0.660	63	0.668	71
	27.3	.836	33	.765	48	-	-
	37.1	.385	28	.214	56	.215	53
	50.7	.594	25	.185	42	-	-
	69.8	.190	32	.0820	50	-	-
37...	145	-	-	0.0392	42	-	-
	162	-	-	.0265	33	-	-
	181	-	-	.0248	33	-	-
	206	-	-	.0144	45	-	-
	234	-	-	.0125	25	-	-
	270	-	-	.00705	45	-	-
	314	-	-	.00634	36	-	-
	368	-	-	.00672	33	-	-
37...	90.1	-	-	0.0977	31	-	-
	94.7	-	-	.0703	39	-	-
	102	-	-	.0421	29	-	-
	111	-	-	.0317	31	-	-
	122	-	-	.0387	31	-	-
	140	-	-	.0313	33	-	-
	161	-	-	.0281	23	-	-
	188	-	-	.0186	45	-	-
38...	141.0	-	-	0.0309	43	-	-
	159	-	-	.0234	56	-	-
	178	-	-	.0132	77	-	-
	203	-	-	.0101	53	-	-
	233	-	-	.00818	45	-	-
	269	-	-	.00658	37	-	-
	314	-	-	.00526	42	-	-
	369	-	-	.00412	59	-	-
38...	84.0	-	-	0.0799	37	-	-
	88.6	-	-	.0482	42	-	-
	96.8	-	-	.0415	71	-	-
	106.0	-	-	.0370	33	-	-
	117	-	-	.0368	56	-	-
	134	-	-	.0223	48	-	-
	155	-	-	.0206	42	-	-
	183	-	-	.0315	38	-	-

Table C-8. - France Stone Company Quarry, Bellevue, Ohio - Continued

Test	Scaled distance, $ft/lb^{1/2}$	Radial		Vertical		Transverse	
		Particle velocity, in/sec	Frequency, cps	Particle velocity, in/sec	Frequency, cps	Particle velocity, in/sec	Frequency, cps
39...	74.5	-	-	0.110	36	0.135	24
	79.0	0.151	26	.0541	63	.129	36
	85.8	.115	42	-	-	-	-
	94.8	-	-	.0588	71	.120	42
	106	.100	29	.061	45	.077	29
	122	.0606	29	.0328	48	.0750	16
	142	.0827	25	.0328	36	.0638	19
	170	.0708	14	.0241	42	.0416	17
40...	117	0.0600	26	0.0469	48	0.0608	44
	123	.0498	29	.0745	63	.0746	63
	140	.0586	50	.0571	56	.0438	36
	184	.0517	42	.0273	53	.0444	42
	248	.0210	33	-	-	.0185	26
	344	.0102	50	.00672	42	.0157	40
41...	18.3	-	-	0.888	48	-	-
	24.8	-	-	.970	45	-	-
	32.2	0.444	36	.539	67	0.292	42
	38.1	.521	29	.500	42	.353	40
	53.0	.415	37	.203	59	.171	62
	93.1	.147	42	.107	53	.0899	50
	150.0	.0771	56	.0583	67	.0492	48
	236.0	.0296	50	.0262	63	.0381	43

Table C-9. - France Company Quarry, Bloomville, Ohio

Test	Scaled distance, $ft/lb^{1/2}$	Radial		Vertical		Transverse	
		Particle velocity, in/sec	Frequency, cps	Particle velocity, in/sec	Frequency, cps	Particle velocity, in/sec	Frequency, cps
36...	6.04	4.92	22	2.58	24	2.34	20
	8.97	-	-	1.68	22	.810	29
	13.1	2.15	19	1.09	24	.884	28
	19.3	1.59	28	.613	25	.519	36
	28.3	.821	23	.323	29	.208	18
	41.4	.426	29	.200	31	-	-
43...	25.5	-	-	0.186	16	-	-
	30.9	-	-	.206	16	-	-
	38.5	-	-	.149	17	-	-
	48.0	-	-	.105	16	-	-
	59.7	-	-	.0532	20	-	-
	73.5	-	-	.0361	27	-	-
	91.6	-	-	.0268	23	-	-
76...	7.65	1.98	20	1.89	32	1.01	27
	9.68	1.97	24	1.25	33	.651	42
	12.2	1.73	30	.896	53	.618	42
	15.3	1.29	24	.549	25	.236	40
	19.3	.922	33	.533	50	.277	53
	24.4	.926	26	.327	26	.259	21
	31.1	.657	32	.303	32	.269	38
	42.7	.342	32	.143	27	.146	33
77...	28.7	0.732	30	0.493	45	0.243	45
	36.7	.738	36	.335	38	.420	48
	46.6	.534	36	.256	63	-	-
	58.5	.298	29	.127	45	.087	56
	74.2	.224	45	.107	53	.117	53
	94.2	.199	29	.0672	25	.0796	42
	120.0	.153	38	.0514	33	.042[illegible]	45
	166	.0856	43	.0291	28	.0194	40
80...	5.55	3.16	23	3.40	67	3.61	50
	9.25	1.23	20	1.55	15	2.01	10
	10.6	.896	29	.539	24	1.34	14
	12.0	.768	24	1.02	20	1.23	08
	12.9	.772	24	.794	14	1.06	23
	13.3	.773	22	.753	19	.830	25
	21.4	.265	14	.299	17	.382	16
	32.6	.232	16	.0790	20	.204	17

Table C-10. - Theodore Roosevelt Bridge Construction Site, Washington, D.C.

Test	Scaled distance $ft/lb^{1/2}$	Radial		Vertical		Transverse	
		Particle velocity, in/sec	Frequency, cps	Particle velocity, in/sec	Frequency, cps	Particle velocity, in/sec	Frequency, cps
44...	27.5	-	-	0.522	50	-	-
	37.2	-	-	.380	42	-	-
	51.0	-	-	.204	50	-	-
	70.8	-	-	.136	63	-	-
	96.4	-	-	.0715	83	-	-
	125	-	-	.0442	63	-	-
	157	-	-	.0319	50	-	-
45...	26.3	0.625	56	0.909	45	0.659	71
	47.7	.415	50	.404	36	.251	56
	89.8	.118	45	.133	31	.2	56
	116	.114	36	.0857	42	.0940	42
	145	.0531	29	.0690	45	.0339	26
46...	27.7	0.426	71	0.517	31	0.398	50
	37.2	.297	50	.347	38	.249	36
	50.8	.290	63	.207	31	.140	63
	70.6	.148	31	.114	29	.0834	83
	96.4	.110	36	.0685	71	.0857	33
	125	.0935	38	.0425	45	.0583	36
	157	.0294	56	.0396	45	.0301	31
47...	16.7	0.504	45	0.269	50	0.144	45
	25.7	.375	63	.237	38	.122	71
	38.8	.101	36	.139	125	.0657	100
	56.1	.0790	29	.0705	33	.0345	63
	74.9	.0464	38	.0319	36	.0382	36
	96.1	.0190	28	.0182	25	.0100	38
48...	23.0	1.25	45	0.922	56	0.379	42
	35.8	.413	38	.594	45	.158	33
	53.0	.355	29	.257	31	.130	29
	71.8	.153	23	.123	38	.144	31
	92.5	.0910	26	.0758	24	.0679	21
49...	21.8	0.521	50	0.342	38	0.122	63
	34.8	.181	45	.167	100	.0657	125
	51.9	.103	33	.0936	45	.0377	63
	70.7	.0551	36	.0382	29	.0404	31
	91.3	.0260	25	.0253	26	.0124	38
50...	21.0	1.27	50	1.04	42	0.389	38
	34.2	.405	38	.465	45	.184	36
	51.4	.264	31	.261	38	.159	38
	70.5	.155	21	.116	36	.137	33
	91.4	.0689	26	.0785	29	.0471	29
51...	27.8	0.344	50	0.373	28	0.291	36
	37.5	.348	45	.417	26	.278	38
	51.4	.373	42	.258	38	.170	38
	71.1	.186	36	.136	42	.0966	56
	97.0	.128	33	.0804	33	.0761	29
	126	.101	33	.0517	50	.0613	42
	158	.0366	50	.0417	45	.0335	26
52...	34.3	0.186	50	0.418	31	0.189	29
	44.9	.212	45	.242	33	.179	25
	60.0	-	-	.156	28	.0595	42
	81.6	.0878	36	.0803	125	.0658	50
	110	.0581	28	.0726	31	.0649	23
	141	.0477	33	.0380	29	.0477	31
	176	.0253	33	.0335	42	.0219	15
53...	28.9	0.282	83	0.361	45	0.331	26
	40.4	.242	63	.213	33	.200	45
	57.6	.113	33	.0995	100	.0938	28
	79.6	.0746	25	.0621	31	.119	33
	104	.0551	29	.0332	36	.0706	33
	131	.0269	25	.0286	25	.0306	22
54...	35.2	0.446	31	0.471	56	0.212	42
	50.0	.466	56	.334	38	.271	28
	71.8	.183	38	.210	45	.128	71
	100	.126	26	.128	63	.0739	50
	132	.0814	24	.0745	31	.0839	38
	167	.0560	25	.0489	42	.0309	25

Table C-11. - New York Trap Rock Corporation, Clinton Point Quarry, Poughkeepsie, N.Y.

Test	Scaled distance, $ft/lb^{1/2}$	Radial		Vertical		Transverse	
		Particle velocity, in/sec	Frequency, cps	Particle velocity, in/sec	Frequency, cps	Particle velocity, in/sec	Frequency, cps
55...	15.4	-	-	0.737	24	-	-
	18.7	-	-	.478	45	-	-
	22.1	-	-	.263	43	-	-
	26.5	-	-	.245	33	-	-
	37.5	-	-	.164	42	-	-
	56.4	-	-	.203	34	-	-
56...	27.4	-	-	0.347	27	-	-
	49.3	0.174	16	.0775	21	0.148	13
	52.0	.0716	48	.0560	56	.101	42
	54.6	.0537	53	.0457	56	.101	42
	58.2	.0768	23	.0746	38	.0891	33
	62.2	.0582	37	.0631	67	.0699	48
	67.3	.0571	32	.0499	36	.0953	38
	73.1	.0439	40	.0464	33	.0567	29
	81.3	.0909	34	.0861	34	.0862	28
57...	27.1	-	-	0.270	45	-	-
	41.6	-	-	.139	43	0.130	27
	44.9	0.254	48	.143	56	.120	50
	48.0	.152	42	.125	67	.207	48
	51.5	.411	16	.189	43	.270	19
	55.0	.176	28	.123	51	.193	30
	68.1	.152	32	.128	34	-	-
58...	28.7	0.618	45	0.637	14	0.480	19
	32.6	.562	21	.269	45	.523	45
	37.0	1.12	16	.410	40	.676	20
	42.2	.547	20	.448	43	.746	16
	47.1	.421	43	.610	13	-	-
	53.6	-	-	-	-	.225	38
	60.5	-	-	-	-	.328	42
59...	22.7	-	-	0.680	50	-	-
	35.0	0.452	29	.296	45	0.358	50
	39.7	.270	50	.228	50	.439	50
	44.2	.338	32	.215	53	.240	53
	49.3	.219	53	.913	16	.348	17
	56.5	.341	14	.230	48	.302	40
	63.5	.265	53	.327	16	.215	53
	72.8	.182	42	.226	45	.175	49
	82.0	.123	36	.176	42	-	-
62...	38.0	-	-	0.120	36	-	-
	38.0	-	-	.127	43	-	-
	52.4	0.120	56	.118	42	0.116	26
	55.5	.102	38	.0828	56	.116	32
	65.7	.102	32	.0911	56	.126	48
	73.3	.128	29	.139	42	.176	37
	78.0	.153	28	.124	33	.125	38
63...	8.49	1.24	18	1.34	42	-	-
	12.0	1.16	23	1.46	30	-	-
	17.0	.880	21	.835	34	-	-
	24.1	.588	23	.620	22	-	-
	34.0	.281	34	.344	42	-	-
	48.1	.194	50	-	-	-	-
63...	16.1	0.549	29	0.581	56	-	-
	21.8	.732	29	.618	23	-	-
	30.8	.228	23	.207	31	-	-
	38.3	.166	25	.245	33	-	-
64...	21.2	0.627	50	0.438	40	-	-
	28.3	.397	18	.303	34	-	-
	46.0	.101	50	.137	63	-	-
	55.2	.156	50	.0818	36	-	-
	77.1	.106	42	.0520	20	-	-
	106	.0322	56	.0357	15	-	-
64...	27.6	0.172	30	0.127	29	-	-
	35.4	-	-	.0517	-	-	-
	48.8	.0854	21	.0505	37	-	-
	60.1	.114	18	.0737	26	-	-
	83.4	.0332	-	.0351	-	-	-
	102	.0194	9	.0183	19	-	-
65...	8.00	0.657	40	0.705	33	-	-
	10.7	.658	17	.634	40	-	-
	17.3	.258	29	.202	30	-	-
	20.8	.258	18	.121	26	-	-
	29.1	.220	25	.124	24	-	-
	40.0	.177	36	.0676	53	-	-
65...	8.00	2.08	50	1.80	36	-	-
	16.0	.966	50	.760	38	-	-
	20.4	.718	26	.358	42	-	-
	29.1	.207	22	.125	27	-	-
	36.3	.133	28	.105	30	-	-

Table C-11. - New York Trap Rock Corporation, Clinton Point Quarry, Poughkeepsie, N.Y. - Continued

Test	Scaled distance, $ft/lb^{1/2}$	Radial		Vertical		Transverse	
		Particle velocity, in/sec	Frequency, cps	Particle velocity, in/sec	Frequency, cps	Particle velocity, in/sec	Frequency, cps
67...	8.01	1.49	30	1.63	37	1.46	25
	9.64	1.86	9	1.33	38	1.16	20
	12.0	.977	11	.676	33	.560	13
	14.7	.456	9	.518	43	.517	11
	18.3	.387	42	.311	37	.388	71
	22.7	.311	29	.211	38	.269	48
	28.0	.146	36	.158	36	.141	56
	34.8	-	-	.128	45	.124	50

Table C-12. - New York Trap Rock Corporation Quarry, West Nyack, N.Y.

Test	Scaled distance, $ft/lb^{1/2}$	Radial		Vertical		Transverse	
		Particle velocity, in/sec	Frequency, cps	Particle velocity, in/sec	Frequency, cps	Particle velocity, in/sec	Frequency, cps
60...	13.3	4.87	45	3.86	7	3.16	33
	16.9	3.27	42	-	-	-	-
	22.0	1.65	28	.896	45	1.26	29
	36.8	1.07	50	-	-	-	-
	49.1	-	-	.495	71	-	-
139...	10.8	1.47	63	3.59	38	1.73	50
	13.2	2.69	33	3.45	33	1.99	25
	14.5	2.27	33	3.39	36	2.59	29
	18.1	1.64	42	.686	36	.837	20
	18.6	4.42	33	2.76	50	1.46	50
	26.4	.786	45	1.05	50	1.64	45
	31.9	.972	50	.737	42	.624	50
	40.5	.631	50	.455	63	.558	50
	52.8	.679	50	.429	50	.363	63
	77.5	.551	45	.372	71	.339	56
140...	13.1	2.57	31	2.31	31	1.07	28
	16.0	2.05	29	1.96	31	.864	28
	22.0	1.07	23	1.52	42	.742	38
	25.4	1.78	31	1.63	45	1.05	36
	28.6	-	-	-	-	-	-
	34.8	1.27	45	.788	25	.490	56
	49.3	.632	71	.357	71	.413	63
	60.3	.351	83	.239	45	.214	71
	82.9	.556	56	.471	63	.400	63
141...	15.6	1.18	33	2.14	56	1.27	29
	19.4	2.07	33	3.09	42	2.29	28
	23.0	.985	50	.974	50	.527	50
	30.2	1.09	56	1.17	38	.797	42
	31.9	1.38	50	.936	63	.765	63
	37.7	1.03	45	.697	21	.380	50
	46.8	.467	56	.301	26	.279	63
	59.6	.339	42	.314	45	.212	63
	85.5	.411	56	.273	71	.307	63
142...	13.9	2.71	42	1.67	45	2.56	71
	19.0	1.54	36	1.11	45	1.07	31
	23.8	1.20	31	1.61	50	.696	29
	27.4	2.19	31	1.40	63	.852	28
	31.0	.824	33	.375	25	.405	50
	31.4	-	-	-	-	-	-
	37.7	1.43	71	.771	45	.837	63
	44.3	-	-	-	-	-	-
	44.9	1.01	50	.647	50	.427	50
	49.9	-	-	-	-	-	-
	53.8	.519	56	.253	38	.260	45
	66.1	.383	50	.160	71	.274	38
	91.1	.677	63	.479	56	.453	71
143...	13.1	1.57	42	2.79	63	1.64	38
	15.7	2.67	50	1.70	56	1.87	45
	18.7	2.07	50	1.62	50	4.47	66
	22.4	1.11	42	.909	71	.727	42
	26.7	.794	50	.680	50	.707	66
	32.1	1.38	45	1.61	56	.962	45
	37.3	.882	45	.806	83	.579	63
	46.0	1.28	38	1.04	83	.863	38
	54.8	1.03	56	.949	56	.714	50
	69.1	1.06	42	.901	26	.766	50

Table C-12. - New York Trap Rock Corporation Quarry, West Nyack, N.Y. - Continued

Test	Scaled distance, $ft/lb^{1/2}$	Radial		Vertical		Transverse	
		Particle velocity, in/sec	Frequency, cps	Particle velocity, in/sec	Frequency, cps	Particle velocity, in/sec	Frequency, cps
144...	20.4	0.897	56	0.924	42	0.579	42
	25.3	2.17	56	1.18	50	1.17	50
	27.9	2.07	56	1.45	56	3.08	56
	27.3	1.89	42	2.21	50	1.20	56
	31.2	.650	42	.526	71	.363	42
	34.8	.974	45	.746	42	.761	56
	39.5	.914	50	.950	56	.622	45
	44.0	.593	50	.467	63	.352	83
	51.6	.963	50	.983	56	.576	50
	59.3	.812	38	1.07	56	.994	42
	72.0	.905	56	.558	100	.493	45
145...	22.0	0.518	38	0.455	33	0.620	56
	26.8	.517	50	.805	63	.538	56
	30.8	.455	42	.557	42	.309	50
	35.2	1.52	38	.797	56	.821	38
	36.9	.579	38	.386	100	.376	42
	40.5	.303	38	.537	36	.437	45
	47.6	.306	83	.490	125	.463	63
	55.7	.403	31	.351	63	.358	56
	67.1	.503	63	.426	63	.415	45
146...	16.8	1.37	56	1.58	63	1.00	45
	19.5	.868	56	.659	56	.455	83
	23.6	.933	45	2.00	50	1.38	42
	27.6	1.31	56	1.18	33	1.33	63
	33.7	1.01	36	1.29	56	1.26	33
	40.5	.986	56	.642	50	.869	45
	48.4	.729	56	.504	63	.419	50
	57.9	.760	63	.869	63	.827	45
	76.3	.384	63	.317	100	.177	63
	82.8	-	-	.0852	100	.0644	83
147...	44.0	0.160	63	0.163	56	0.243	63
	61.7	.0631	50	.0476	36	.0631	56
	65.9	.0995	56	.0686	63	.0982	42
	71.1	.137	38	.109	50	.880	45
	84.1	.0478	42	.0498	45	.0608	42
	92.9	.608	50	.0400	100	.0461	45
	115	.0982	45	.0608	100	.0657	50
	129	.0560	100	.0480	56	.0785	56
	150	.0372	56	.0455	71	.0527	50
	316	.00846	56	.00935	58	-	-
148...	18.0	1.41	36	1.35	36	1.12	29
	24.2	.731	38	.615	38	.765	45
	27.3	.938	42	.645	63	.558	45
	29.6	1.18	38	.909	83	.590	42
	35.4	.381	42	.263	42	.325	42
	39.4	.610	45	.449	63	.229	45
	49.2	.608	42	.528	71	.535	42
	55.5	.785	38	.686	50	.910	38
	64.7	.596	42	.477	42	.478	38
	145	.0830	67	.0722	45	.0848	56
	145	.0808	100	.0604	56	.0684	42
149...	19.7	0.459	50	0.159	71	0.196	56
	36.0	.143	45	.102	45	.0897	56
	40.6	.162	45	.0808	56	.0833	36
	45.0	.207	38	.179	50	.118	42
	60.4	.0788	45	.0685	56	.0350	38
	70.2	.0496	45	.0170	33	.0645	50
	95.0	.0649	36	.0589	50	.0655	42
	111	.0685	42	.0791	56	.0977	42
	134	.0472	50	.0282	50	-	-
	322	.0121	-	.00919	-	.0128	-
	322	.0121	-	.00898	-	-	-
150...	48.8	0.0994	63	0.0830	83	0.0986	56
	68.5	.0400	50	.0328	42	.0409	56
	73.0	.0320	45	.0248	63	.0269	42
	85.3	-	-	.0160	63	.0130	63
	92.9	.0190	45	.0151	83	.0180	33
	103	.230	50	.0201	100	.0180	45
	127	.0244	63	.0295	56	.0432	63
	142	.0271	50	.0227	63	.0339	38
	165	.0288	63	.0198	83	.0134	36
	348	.00420	-	.00219	-	.00423	-
	348	.00256	-	.00262	-	.00314	-

Table C-13. - Littleville Dam Construction Site, Huntington, Mass.

Test	Scaled distance, $ft/lb^{1/2}$	Radial		Vertical		Transverse	
		Particle velocity, in/sec	Frequency, cps	Particle velocity, in/sec	Frequency, cps	Particle velocity, in/sec	Frequency, cps
68...	18.8	1.04	63	0.997	56	0.571	40
	28.5	.607	36	.513	48	.490	32
	36.8	.380	59	.575	30	.546	26
	51.4	.472	28	.475	22	-	-
	74.1	.102	13	.176	67	.0802	15
	106	-	-	-	-	.0547	28
69...	13.5	1.61	39	1.37	34	1.26	32
	20.3	.800	59	.790	63	.434	38
	29.3	.424	38	.409	45	.456	33
	37.2	.310	63	.424	33	.444	26
	51.0	.329	30	.261	48	.391	20
	72.7	.0822	12	.139	67	.0687	14
	103	-	-	.0621	59	.0433	17
70...	13.7	0.915	53	0.849	10	0.673	10
	20.4	.695	42	.560	45	.543	32
	26.2	.360	37	.740	30	.577	26
	36.2	.481	26	.570	42	.590	17
	51.9	.112	12	.219	63	.0970	16
	73.9	.104	20	.0835	10	.0590	22
71...	22.7	0.589	50	0.589	71	0.449	42
	33.4	.463	45	.341	43	.455	34
	43.1	.293	59	.469	30	.432	26
	59.7	.353	33	.369	40	.493	19
	85.7	.0849	13	.124	67	.0566	15
	122	-	-	.0611	34	.0464	22
72...	18.1	0.501	53	0.368	59	0.412	48
	26.6	.446	43	.268	50	.369	43
	34.1	.208	53	.285	40	.283	30
	47.3	.232	37	.228	48	.184	19
	67.8	.0461	11	.0772	63	.0294	33
	96.7	.0314	40	.0414	48	.0227	37
73...	24.5	0.880	53	0.840	53	0.539	45
	35.9	.659	38	.448	45	.554	31
	46.2	.310	56	.547	31	.522	50
	63.9	.483	28	.452	38	.582	23
	91.6	.0982	13	.132	13	.0645	14
	130	.0848	21	.0746	59	.0542	50
74...	20.1	0.314	67	-	-	0.253	67
	29.4	.309	67	0.147	71	.167	45
	37.5	.155	38	.227	36	.170	33
	51.9	.107	32	.131	43	.116	32
	74.4	.0328	13	.0487	48	-	-
	106	.0226	19	.0320	59	.0162	48

Table C-14. - Fairfax Quarries, Inc. Quarry, Centreville, Va.

Test	Scaled distance, $ft/lb^{1/2}$	Radial		Vertical		Transverse	
		Particle velocity, in/sec	Frequency, cps	Particle velocity, in/sec	Frequency, cps	Particle velocity, in/sec	Frequency, cps
86...	21.5	0.528	33	0.204	36	0.422	30
	23.5	-	-	-	-	.360	36
	25.9	-	-	.421	48	.705	40
	29.0	.273	45	.186	36	.232	59
	31.7	.165	37	.152	50	.242	36
	34.9	.157	36	.112	59	.220	59
	37.6	.204	40	.112	48	.172	43
87...	7.54	1.14	10	2.53	43	1.38	29
	9.35	1.41	48	2.45	34	1.79	36
	11.7	2.12	30	1.64	32	2.99	33
	14.7	.310	50	.634	34	.496	53
	17.9	.518	33	.432	83	.346	37
	22.2	-	-	.285	37	.244	59
	27.9	-	-	.235	67	.174	33
	34.9	.162	43	.139	31	.172	30
	43.4	.114	32	.106	29	.121	20
	54.7	.105	29	-	-	.0896	29
	67.9	.0772	11	.0450	23	.0796	13

Table C-14. - Fairfax Quarries, Inc. Quarry, Centreville, Va. - Continued

Test	Scaled distance, $ft/lb^{1/2}$	Radial		Vertical		Transverse	
		Particle velocity, in/sec	Frequency, cps	Particle velocity, in/sec	Frequency, cps	Particle velocity, in/sec	Frequency, cps
88...	8.13	1.47	42	1.94	48	1.27	48
	9.96	1.58	34	2.11	56	1.31	50
	12.6	1.33	42	1.61	59	.744	50
	15.8	1.14	43	.944	77	.937	53
	19.7	.818	71	.543	59	.352	12
	31.3	.292	59	.288	50	.273	50
	36.8	.413	42	.152	50	.152	37
	42.9	.347	45	.224	59	.235	43
	49.7	.153	50	.0730	50	.0796	50
	62.6	.0597	10	.0373	38	.0481	42
	80.1	.0249	91	.0241	50	.0219	67
89...	6.87	2.41	50	4.36	53	2.56	27
	8.16	1.33	31	2.46	56	1.61	27
	10.0	1.67	48	1.71	63	1.70	36
	12.3	.875	43	.909	67	1.24	37
	15.2	.788	31	-	-	-	-
	23.5	.982	13	.368	32	.712	32
	27.8	.474	38	.237	43	.214	43
	32.4	.558	45	.224	59	.211	56
	47.0	-	-	-	-	.155	50
	59.6	.0480	83	.0459	63	.0455	125
90...	7.15	2.82	36	3.21	53	1.93	53
	9.04	1.61	38	1.89	53	1.06	50
	11.7	1.64	71	2.11	59	.871	36
	14.9	1.63	43	1.06	59	.681	63
	18.9	1.06	45	.887	63	.808	48
	30.5	.585	42	.322	40	.365	42
	35.9	.460	42	.322	50	.228	53
	42.2	.440	45	.170	43	.293	43
	49.0	.186	14	.123	16	.126	13
	61.8	.112	12	.0758	17	.0827	17
	79.1	-	-	.0295	17	.0336	-
91...	6.78	-	-	4.65	26	4.83	26
	8.65	2.04	24	2.98	29	3.22	26
	10.3	1.26	29	1.61	59	-	53
	13.6	.936	33	1.73	83	1.70	30
	16.5	.773	48	1.08	56	1.48	27
	20.4	-	-	1.14	31	-	-
	30.6	.798	25	.261	77	.751	29
	37.0	.240	40	.167	53	.386	33
	44.8	.0932	13	.0833	20	.154	17
	55.0	.137	50	.148	48	.061	53
	67.0	.0673	43	.0700	59	.0647	56
94...	5.71	-	-	4.38	36	3.80	27
	7.32	3.41	56	2.48	50	2.23	31
	8.78	1.87	53	1.89	36	-	-
	11.6	1.81	63	2.52	56	.912	56
	14.1	1.48	36	1.14	59	1.16	50
	17.6	.867	32	1.10	56	.657	31
	27.0	.912	24	.511	67	.517	30
	32.5	.387	33	.178	83	.289	32

Table C-15. - W. E. Graham and Sons, Manassas Quarry, Manassas, Va.

Test	Scaled distance, $ft/lb^{1/2}$	Radial		Vertical		Transverse	
		Particle velocity, in/sec	Frequency, cps	Particle velocity, in/sec	Frequency, cps	Particle velocity, in/sec	Frequency, cps
92...	7.18	2.05	71	2.37	36	1.22	77
	11.0	1.22	63	1.60	59	0.936	43
	17.5	-	-	.556	23	-	-
	26.6	.685	10	.508	29	.640	10
	41.2	.281	12	.256	13	-	-
	63.5	.188	11	.123	50	.154	10
92...	12.2	1.03	45	1.06	53	0.702	59
	16.9	1.22	31	.676	59	.426	34
	23.8	-	-	.268	50	.347	43
	32.9	.669	19	.621	33	.421	36
	43.8	.338	28	.273	33	.224	38
	65.2	-	-	.143	71	.197	67

Table C-15. - W. E. Graham and Sons, Manassas Quarry, Manassas, Va. - Continued

Test	Scaled distance, $ft/lb^{1/2}$	Radial		Vertical		Transverse	
		Particle velocity, in/sec	Frequency, cps	Particle velocity, in/sec	Frequency, cps	Particle velocity, in/sec	Frequency, cps
93...	9.81	1.15	77	1.22	83	0.922	50
	14.3	1.58	56	1.48	67	1.10	43
	22.2	-	-	.781	24	-	-
	33.1	.431	19	.354	22	.337	36
	50.7	.149	34	.110	36	.134	22
	77.6	.163	22	.0878	31	.131	20
93...	12.0	1.61	67	1.12	71	1.95	46
	17.8	1.44	36	1.08	43	.781	56
	26.1	-	-	.495	43	.807	45
	37.0	.967	26	.486	40	.668	83
	50.2	.320	48	.380	28	.566	43
	75.8	-	-	.166	71	.281	50
95...	10.4	1.69	59	1.41	71	0.943	71
	15.4	.946	67	.875	67	.861	56
	20.8	-	-	.550	108	-	-
	27.0	.505	83	.647	139	.658	105
	41.4	.219	96	.168	113	-	-
	63.5	.257	66	.0874	148	.286	59
95...	7.11	2.20	71	2.05	59	1.83	45
	11.8	1.66	43	1.64	67	.821	45
	18.6	1.08	37	.729	53	.759	48
	27.8	1.16	29	.570	53	.821	42
	38.8	.504	48	.444	56	.456	30
	60.4	.244	53	.146	67	.149	50
117...	13.3	1.33	40	1.70	32	0.792	77
	16.6	-	-	.858	40	.863	50
	24.0	1.05	20	.691	40	-	-
	29.4	.564	30	.422	42	.248	37
	38.4	.487	20	.327	27	.245	53
	50.6	.577	23	.299	29	.333	26
117...	12.1	2.31	29	2.18	21	1.17	38
	18.1	-	-	.788	33	.770	45
	21.9	1.54	22	.774	15	.474	22
	26.0	-	-	.455	17	.273	24
	34.0	.992	17	.284	26	.172	41
	45.1	.211	36	.267	22	.164	41
118...	10.7	1.99	21	1.93	29	1.12	50
	13.9	-	-	1.20	33	.747	29
	20.3	1.09	30	.625	53	-	-
	25.0	.600	33	.730	36	.373	37
	32.7	.542	53	.451	31	.393	42
	43.1	.373	21	.347	27	.487	25
118...	10.5	2.74	32	2.46	34	1.46	33
	15.6	-	-	1.05	26	.501	59
	18.9	-	-	.648	-	.682	34
	22.4	-	-	.599	-	.318	21
	29.3	.726	-	.463	24	.348	-
	39.0	.318	-	.273		.170	34
120...	9.87	2.92	19	1.84	50	1.08	21
	13.5	1.54	29	.805	48	.778	36
	20.6	.926	38	.538	83	-	-
	25.8	.673	23	.545	56	-	-
	34.5	.564	21	.365	71	.405	33
	46.2	.387	26	.178	24	.243	25
120...	10.9	1.75	21	1.78	25	1.14	33
	15.7	1.49	25	1.10	34	.729	30
	19.3	1.06	23	-	-	-	-
	23.2	.697	17	.485	27	.458	23
	30.9	.711	18	.406	30	.401	20
	41.7	.251	27	.167	75	.217	50
121...	69.7	-	-	-	-	0.0807	56
	94.1	0.0360	46	-	-	-	-
	118	.0297	40	0.0243	31	.0334	50
	128	.0195	32	.0195	36	-	-
	263	-	-	.0526	111	.0437	53
	321	-	-	.0106	83	-	-
122...	68.3	0.0622	32	0.0346	59	0.0260	50
	80.5	.0439	53	.0306	56	.0154	48
	90.5	.0316	45	.0141	77	.0117	48
	113	.0168	34	.00847	40	.00797	48
	122	.0141	36	.0106	37	-	-
	143	.0142	38	.00848	38	.00656	38
	172	.0139	34	.00965	57	.00414	43
	208	.00599	28	.00318	49	.00253	68
	250	.00250	24	.00529	111	.00152	59
	304	-	-	.000922	83	.000808	34

Table C-15. - W. E. Graham and Sons, Manassas Quarry, Manassas, Va. - Continued

Test	Scaled distance, $ft/lb^{1/2}$	Radial		Vertical		Transverse	
		Particle velocity, in/sec	Frequency, cps	Particle velocity, in/sec	Frequency, cps	Particle velocity, in/sec	Frequency, cps
123...	10.0	2.63	33	2.58	38	2.11	36
	13.3	2.18	33	1.20	29	.889	29
	16.3	1.94	29	1.07	30	.848	23
	22.4	.708	33	.963	26	.366	28
	24.9	.725	22	.430	23	.432	22
	30.2	.758	15	.322	20	.536	14
	37.5	-	-	-	-	.243	27
	46.7	.544	21	.239	21	.219	43
	57.2	.211	22	.135	62	.0791	28
	70.8	.0737	31	.0847	33	.0656	26
125...	16.1	0.833	25	1.58	50	1.12	50
	25.3	.568	38	1.33	40	.528	31
	28.7	.705	48	.901	37	.311	42
	37.8	.604	32	.537	56	.506	30
	45.1	.487	26	.503	56	.386	42
	55.8	.244	-	.300	-	.159	-
	68.7	.318	-	.228	-	.170	-
	83.6	.325	-	.245	-	.197	-
	101	.156	30	.150	27	.139	31
	128	.149	30	.0971	29	.134	31
126...	6.71	2.71	26	2.30	50	2.07	50
	10.4	1.17	48	1.64	48	1.44	36
	11.7	.809	37	.995	63	.758	31
	15.4	.784	29	.731	36	1.26	36
	18.3	.771	50	.824	50	1.04	43
	22.6	.606	-	.374	-	.481	-
	27.8	.583	-	.339	-	.606	-
	33.8	.518	-	.298	-	.453	-
	40.9	.235	26	.196	29	.347	32
	51.5	.160	40	.105	32	.227	33

Table C-16. - Chemstone Corporation Quarry, Strasburg, Va.

Test	Scaled distance, $ft/lb^{1/2}$	Radial		Vertical		Transverse	
		Particle velocity, in/sec	Frequency, cps	Particle velocity, in/sec	Frequency, cps	Particle velocity, in/sec	Frequency, cps
96...	9.40	1.46	17	-	-	-	-
	12.1	.962	26	-	-	0.886	24
	13.9	1.39	21	1.54	25	1.62	25
	16.4	1.03	21	.683	25	-	-
	20.2	-	-	.423	19	.900	22
	24.8	.772	13	.334	23	.378	20
	30.6	.383	16	.314	17	.301	16
	38.6	.471	24	.159	83	.285	38
97...	7.55	1.84	13	2.04	20	1.16	24
	9.18	2.07	20	1.67	21	1.20	23
	12.0	.720	29	1.23	19	.481	25
	15.4	-	-	.999	17	.495	28
	22.5	.543	28	.632	16	.495	25
	25.6	.936	25	.535	26	.446	20
	33.4	.445	26	.246	72	.352	31
98...	17.0	1.61	33	1.76	56	1.67	36
	20.2	.679	26	.788	31	.794	31
	23.8	.829	33	.917	72	1.28	29
	28.0	.550	56	.346	42	.692	22
	33.5	.517	17	.233	45	.592	22
	39.7	.381	14	.142	17	.338	17
	48.0	.106	25	.929	42	.119	56
	56.1	.105	26	.991	20	.0788	50
99...	9.76	-	-	-	-	1.35	16
	12.6	1.85	29	1.67	28	1.92	21
	14.6	1.20	25	1.33	28	1.42	23
	17.3	.861	24	.628	50	1.53	23
	21.3	-	-	.824	31	.845	25
	26.3	.692	16	.406	20	.472	19
	32.5	.328	19	.342	17	.328	16
	41.2	.334	28	.215	36	.313	25
100...	15.8	1.31	36	0.529	42	0.538	56
	25.3	1.06	26	.693	36	.611	25
	29.2	.328	20	.267	25	.380	31
	33.4	.573	24	.173	28	.328	33
	38.1	.442	20	.230	17	.409	25
	44.6	.333	20	.121	25	.293	25
	51.8	.258	15	.178	19	.204	17
	71.1	.0640	25	.0484	17	-	-

Table C-16. - Chemstone Corporation Quarry, Strasburg, Va. - Continued

Test	Scaled distance, $ft/lb^{1/2}$	Radial		Vertical		Transverse	
		Particle velocity, in/sec	Frequency, cps	Particle velocity, in/sec	Frequency, cps	Particle velocity, in/sec	Frequency, cps
101...	9.70	1.64	31	1.81	26	1.90	24
	11.3	1.09	20	1.14	26	1.57	22
	13.6	1.17	19	1.02	29	2.25	26
	16.8	-	-	.714	29	.764	16
	20.7	.946	15	.461	26	.616	20
	25.8	.938	14	.340	17	.434	15
	32.5	.358	16	.198	42	.347	28
102...	25.8	0.672	31	0.281	42	0.280	31
	30.3	.246	33	.185	28	.211	36
	35.2	.430	25	.136	31	.469	29
	40.9	.196	26	.113	20	.261	24
	48.4	.173	23	.0579	23	.153	24
	56.7	.110	12	.0484	17	.0681	28
	79.4	.0306	36	.0285	42	.0299	31
103...	11.1	2.02	7	2.61	19	1.27	10
	14.7	.840	17	1.09	38	1.25	25
	17.2	.773	45	.580	26	1.09	22
	20.7	.602	42	.500	63	1.01	24
	25.9	.765	26	.243	17	.474	21
	32.3	.346	18	.318	19	.493	23
	40.5	.223	14	.249	17	.232	15
	51.9	.195	25	.0929	72	.353	23
104...	8.50	-	-	1.24	20	-	-
	10.3	0.558	14	1.04	23	1.89	24
	12.7	.786	19	.863	42	1.38	25
	16.3	2.01	22	.456	22	1.10	29
	20.6	.634	16	.434	22	.860	23
	26.0	.296	11	.285	20	.276	16
	33.7	.384	23	.129	42	.535	23
105...	8.37	-	-	2.47	-	1.37	-
	11.5	-	-	2.65	-	1.10	-
	22.7	0.995	17	1.15	28	.536	29
	27.5	.873	25	.00178	63	.497	28
	30.2	.581	20	.424	36	.421	19
	34.1	.598	19	.283	18	.464	20
	38.4	.310	14	.217	17	.240	18
106...	7.70	2.08	15	1.40	15	-	-
	9.42	1.98	25	1.42	25	2.00	21
	11.8	.922	29	1.09	38	1.61	17
	15.2	2.60	25	.600	33	1.58	28
	19.5	.566	28	.529	20	1.18	25
	24.8	.435	13	.384	20	.348	19
	32.3	.323	20	.161	36	.363	19
107...	11.9	1.05	-	0.812	-	0.608	-
	15.2	1.21	-	.746	-	-	-
	26.8	.483	28	.670	29	.552	26
	29.1	.253	19	.278	28	.248	36
	31.7	.549	26	.216	63	.403	31
	34.5	.323	22	.257	28	.341	23
	36.2	.435	20	.173	22	.280	22
	38.5	.347	20	.366	20	.235	16
	43.0	.161	7	.130	20	.140	17
	48.9	.171	56	.0571	18	-	-
108...	6.25	1.42	22	1.43	17	2.17	28
	7.88	1.52	20	2.01	26	1.44	21
	10.0	1.13	21	.959	42	1.41	31
	13.3	3.34	23	.727	28	.657	25
	15.1	1.02	20	.977	22	1.70	21
	17.3	.711	19	.448	24	.628	25
	22.2	.387	15	.263	15	.338	14
	29.0	.270	18	.124	38	.392	19
109...	7.28	2.19	26	1.55	31	1.26	20
	9.45	1.09	25	1.12	25	1.85	22
	12.3	.736	50	.766	21	1.29	23
	16.6	2.19	24	.373	33	.597	25
	18.9	.863	26	.800	20	.958	24
	21.9	.387	20	.334	23	.628	25
	28.7	.223	17	.264	19	.240	16
	38.1	.273	25	.105	50	.286	24
110...	11.2	1.10	24	1.06	42	1.14	29
	14.7	.420	48	.472	38	1.09	-
	26.2	.680	27	-	-	-	-
	29.9	.484	27	.283	13	.345	26
	34.6	.245	11	.144	26	.235	33
	44.9	.181	11	.0847	17	.112	48
	59.6	.124	43	.120	33	.142	23

Table C-16. - Chemstone Corporation Quarry, Strasburg, Va. - Continued

Test	Scaled distance, ft/lb$^{1/2}$	Radial		Vertical		Transverse	
		Particle velocity, in/sec	Frequency, cps	Particle velocity, in/sec	Frequency, cps	Particle velocity, in/sec	Frequency, cps
111...	10.4	1.12	31	1.01	36	1.45	29
	13.8	.465	50	.712	50	1.23	33
	18.3	.539	31	.581	45	.627	28
	25.1	.871	30	.518	42	.420	28
	28.7	.570	28	.278	17	.285	28
	33.4	.290	16	.211	24	.328	33
	43.7	.155	13	.0884	15	.143	25
	57.9	.280	19	.121	36	.195	24

Table C-17. - Chantilly Crushed Stone Company Quarry, Chantilly, Va.

Test	Scaled distance, ft/lb$^{1/2}$	Radial		Vertical		Transverse	
		Particle velocity, in/sec	Frequency, cps	Particle velocity, in/sec	Frequency, cps	Particle velocity, in/sec	Frequency, cps
114...	10.3	0.808	-	0.713	-	0.606	-
	12.5	.455	-	.540	-	-	-
	14.3	.357	-	.289	-	-	-
	17.1	.277	-	-	-	-	-
	21.0	-	-	.170	56	.235	28
	28.5	.196	36	.118	36	.156	19
115...	23.3	-	-	0.218	42	0.364	33
	31.4	0.253	67	.177	57	.346	31
	45.9	.100	33	.0816	31	.141	29
116...	16.3	0.678	21	0.284	45	0.862	22
	21.6	.461	-	.223	-	.950	-
	26.8	.258	-	.170	-	.253	-
	32.0	-	-	.151	-	-	-
	37.3	.235	-	.111	-	-	-
119...	14.5	1.22	23	0.734	36	0.997	21
	20.6	.789	-	.443	-	.705	-
	26.7	.374	-	.451	-	.940	-
	32.8	.378	-	.134	-	.434	-
	39.0	.267	-	.174	-	.334	-

Table C-18. - Culpeper Crushed Stone Company Quarry, Culpeper, Va.

Test	Scaled distance, ft/lb$^{1/2}$	Radial		Vertical		Transverse	
		Particle velocity, in/sec	Frequency, cps	Particle velocity, in/sec	Frequency, cps	Particle velocity, in/sec	Frequency, cps
124...	79.8	0.0879	17	0.0812	38	-	-
	89.3	.0862	21	.0393	17	0.106	19
	107	.0498	38	.0357	63	.0794	16
	121	.0429	31	.0259	56	.0780	17
127...	4.94	2.49	29	2.86	28	3.06	17
	7.16	1.84	25	1.83	42	2.44	17
	10.5	1.82	36	1.26	45	1.25	17
	15.4	.952	38	.793	42	.973	38
	23.1	.385	42	.250	45	.579	42
	33.9	.189	22	.113	26	.179	28
	45.2	.204	26	.205	33	.139	28
129...	5.70	2.31	22	2.18	36	3.51	18
	8.70	1.93	23	1.27	42	2.64	21
	13.0	.960	38	.758	50	.848	20
	19.8	.442	42	.235	56	-	-
	29.5	.279	20	.145	16	.304	19
	39.5	.196	21	.0771	29	.162	18
129...	16.2	0.476	-	0.329	-	0.331	-
	19.1	-	-	.306	-	-	-
	23.4	.197	-	.379	-	-	-
130...	8.41	2.32	24	1.76	28	1.16	18
	9.69	2.78	42	1.37	38	-	-
	15.9	1.60	29	1.47	42	.745	33
	20.5	1.06	23	.667	23	.818	25
	27.3	.585	33	.480	28	.679	23
	36.0	.380	18	.196	50	.446	23
	45.4	.285	17	.165	25	.250	24
	102	.0412	40	.0437	56	-	-
	126	-	-	-	-	.0877	38

Table C-18. - Culpeper Crushed Stone Company Quarry, Culpeper, Va. - Continued

Test	Scaled distance, ft/lb$^{1/2}$	Radial		Vertical		Transverse	
		Particle velocity, in/sec	Frequency, cps	Particle velocity, in/sec	Frequency, cps	Particle velocity, in/sec	Frequency, cps
132...	5.58	1.78	14	3.27	31	2.71	24
	6.75	2.18	36	2.14	29	2.71	25
	8.58	3.09	16	1.73	28	2.75	19
	12.4	1.94	31	1.29	42	1.15	45
	16.8	.960	23	.968	19	.741	28
	23.0	.634	28	.731	45	.537	26
	31.1	.453	29	.288	50	.461	28
	76.5	.0955	9	.0413	18	-	-
	93.1	.0429	14	.0340	14	.0366	18
	116	.121	8	.0253	9	.0727	8
133...	5.54	3.00	23	2.87	29	2.27	28
	6.76	3.33	50	2.14	56	2.15	45
	8.74	3.65	31	2.47	56	1.75	19
	12.7	2.48	29	1.62	56	1.47	33
	17.1	1.28	29	.954	45	.994	24
	23.6	1.08	38	.701	50	.848	45
	31.9	.667	33	.471	38	.575	25
	54.9	.111	24	.0893	42	.154	28
135...	7.17	3.77	23	2.24	50	2.80	23
	11.2	1.71	19	1.88	45	1.67	28
	15.9	1.07	25	1.01	45	1.07	28
	19.2	1.15	-	.837	-	.704	-
	22.6	.771	29	.691	50	.745	28
	31.3	.617	31	.405	50	.533	28
	43.2	.424	-	.169	-	.340	-
	64.1	.109	24	.0480	42	.187	42
138...	13.8	1.27	24	0.862	36	1.11	24
	16.0	.842	33	.809	50	.960	29
	19.3	.727	28	-	-	-	-
	24.3	.308	42	.295	36	.535	42
	32.0	.314	28	.169	56	.568	45
	43.1	.118	29	.136	33	.298	45
	54.4	.102	38	.0806	56	.238	42

Table C-19. - General Crushed Stone Company Quarry, Doswell, Va.

Test	Scaled distance, ft/lb$^{1/2}$	Radial		Vertical		Transverse	
		Particle velocity, in/sec	Frequency, cps	Particle velocity, in/sec	Frequency, cps	Particle velocity, in/sec	Frequency, cps
152...	6.86	1.18	38	1.03	100	-	-
	13.3	.705	24	.706	28	0.806	38
	23.4	.300	9	.144	17	.281	13
	24.9	.231	8	.105	18	.186	11
	26.7	.207	10	.187	15	.312	13
	29.0	.210	14	.143	13	.288	13
	32.1	.167	8	.132	10	.245	10
	35.7	.0992	13	.105	14	.0909	16
	41.4	.0858	38	.0673	16	.127	8
	53.3	.208	10	.0924	9	.167	17
	59.0	.151	9	.150	11	.180	12
	77.7	.0606	24	.0515	15	-	-
153...	6.72	2.19	20	2.42	16	1.98	25
	7.71	1.19	14	1.98	17	1.31	28
	9.08	1.38	33	1.41	19	1.11	29
	10.8	1.06	25	.942	17	.694	25
	12.9	1.25	22	1.73	18	.729	17
	15.5	1.17	16	1.01	17	1.07	21
	19.2	.683	14	.649	20	.364	13
	23.2	.588	19	.353	25	.304	20
	29.7	.459	18	.431	18	.264	24
	43.3	.313	10	.234	23	.523	20
	49.8	.306	25	.302	25	.337	11
	71.0	.206	11	.180	14	.115	13
154...	3.97	6.14	16	5.13	36	4.00	13
	4.85	2.87	25	2.74	26	1.67	28
	5.95	2.27	24	1.38	23	1.39	19
	7.63	1.39	45	1.48	23	1.02	26
	9.54	1.38	12	1.34	22	1.18	18
	11.9	.974	13	.836	21	.852	19
	15.3	.478	18	.533	20	.354	15
	19.1	.461	22	.253	12	.339	18
	25.2	.314	16	.460	17	.218	19
	37.9	.301	17	.219	29	.353	14
	44.1	.357	24	.421	24	.322	23
	63.9	.103	11	.0710	12	-	-

Table C-20. - Riverton Lime and Stone Company Quarry, Riverton, Va.

Test	Scaled distance, ft/lb$^{1/2}$	Radial		Vertical		Transverse	
		Particle velocity, in/sec	Frequency, cps	Particle velocity, in/sec	Frequency, cps	Particle velocity, in/sec	Frequency, cps
137	7.56	3.54	25	3.35	24	3.79	29
	13.7	2.52	31	1.29	33	1.06	36
	19.5	3.46	22	2.53	31	1.09	29
	23.6	-	-	1.17	26	-	-

Table C-21. - Southern Materials Corporation, Jack Stone Quarry, Petersburg, Va.

Test	Scaled distance, ft/lb$^{1/2}$	Radial		Vertical		Transverse	
		Particle velocity, in/sec	Frequency, cps	Particle velocity, in/sec	Frequency, cps	Particle velocity, in/sec	Frequency, cps
164	6.41	1.31	17	1.64	21	1.36	19
	8.58	1.26	20	1.37	17	1.40	17
	9.48	1.13	19	1.14	29	-	-
	10.8	.862	-	.663	-	1.07	-
	12.2	.584	28	.476	18	.822	16
	15.4	.480	15	.400	21	.713	15
	17.8	.306	12	.413	20	.568	20
	21.3	.372	13	.353	20	.558	15
	25.1	.205	-	.213	-	.270	-
	28.8	.141	-	.273	-	.252	-
	34.1	.141	14	.263	16	.288	17
165	4.01	1.82	24	1.82	33	1.18	25
	5.04	2.69	23	2.41	36	1.88	21
	5.93	2.31	22	2.75	31	1.11	31
	7.30	1.67	-	2.00	-	1.24	-
	9.03	1.10	33	1.40	20	.964	33
	11.8	.758	24	.545	36	1.20	24
	14.2	.986	28	.779	56	.781	33
	17.5	.409	19	.409	33	-	-
	20.9	.423	-	.406	-	.203	-
	26.8	.192	-	.179	-	.125	-
	33.7	.177	9	.145	13	.0909	38
166	4.66	2.67	21	1.49	26	1.38	25
	5.65	2.77	25	1.72	13	1.52	24
	6.83	1.28	13	1.11	17	-	-
	8.39	1.26	-	1.04	-	1.14	-
	10.3	1.03	25	.909	33	1.00	23
	13.0	.661	20	.673	17	.556	29
	15.4	.496	25	.652	22	.473	28
	19.0	.345	20	.400	14	.351	24
	23.1	.305	-	.426	-	.319	-
	29.1	.201	-	.324	-	.182	-
	36.4	.120	13	.125	13	.155	14
167	4.29	3.58	22	2.71	23	2.63	20
	5.44	2.13	16	1.30	15	1.89	21
	6.26	2.36	20	1.91	17	1.94	18
	7.66	2.36	20	1.37	23	1.45	16
	9.48	1.44	19	.787	22	.248	29
	11.9	1.07	19	.709	13	1.01	16
	14.3	1.47	20	1.43	19	1.00	23
	17.2	.487	-	.795	-	.462	-
	21.3	.603	-	.563	-	.551	-
	26.3	.362	-	.640	-	.255	-
	33.4	.275	13	.327	19	.155	26
168	12.4	0.649	26	0.926	-	0.417	56
	17.1	.743	36	1.10	50	.487	50
	21.2	.661	38	1.35	42	.284	56
	27.1	-	-	.613	-	-	-
	35.1	.300	42	.320	50	.183	56
	47.4	.229	45	.0942	50	.284	72
	58.0	.259	33	.312	83	.218	83
	72.9	.103	38	.186	72	.0889	83
	90.1	.101	-	.137	-	.115	-
	114	.0435	-	.0551	-	.0300	-
	145	.0254	72	.0560	72	.0290	83

Table C-22. - Superior Stone Company, Buchanan Quarry, Greensboro, N.C.

Test	Scaled distance, ft/lb$^{1/2}$	Radial		Vertical		Transverse	
		Particle velocity, in/sec	Frequency, cps	Particle velocity, in/sec	Frequency, cps	Particle velocity, in/sec	Frequency, cps
155	18.0	0.595	23	1.15	25	0.484	25
	20.6	.509	33	.469	28	.399	33
	22.0	.351	29	.346	16	.270	29
	25.4	.261	55	.182	11	.361	18
	30.3	.170	23	.172	18	.200	17
	36.1	.194	18	.145	22	.135	28
	43.0	.188	19	.120	25	.245	28
	51.3	.132	24	.0926	31	.0893	24
	59.0	.0847	84	.0800	55	.0621	51
	67.3	.0475	70	.0813	81	.0430	81
	78.9	.0496	63	.0702	63	.0519	36
	88.9	.0298	26	.0372	14	.0360	13
156	15.1	0.714	25	0.766	33	0.321	29
	16.8	.820	42	.909	28	.710	29
	19.9	.421	25	.410	15	.451	38
	22.7	.933	14	.462	9	.278	9
	25.6	.160	31	.204	22	.120	26
	28.1	.198	42	.236	31	.227	31
	40.2	.231	28	.244	26	.200	21
	46.3	.136	18	.137	24	.121	29
	54.2	.0920	8	.0853	8	.0539	19
	61.8	.163	11	.154	23	.0967	13
	74.0	.0510	38	.0936	71	.0434	45
	86.2	.0565	25	.0588	14	.0494	29
157	16.4	0.758	18	1.78	30	0.783	38
	19.0	.607	26	.679	14	.406	30
	20.6	.600	19	.526	18	.448	22
	23.8	.487	91	.283	12	.442	58
	28.8	.242	21	.247	17	.209	16
	34.8	.198	22	.205	26	.0962	28
	41.3	.175	21	.203	23	.143	-
	47.9	-	-	.125	19	-	-
	56.2	.133	64	.115	64	.0907	8
	64.3	.0987	91	.0993	58	.0516	14
	78.8	.0451	47	.0936	16	.0422	25
	89.0	.0351	20	.0490	38	.0321	17
158	31.2	0.103	33	0.822	31	0.385	36
	34.2	.345	50	.327	28	.303	38
	39.5	.172	36	.151	15	.152	28
	44.8	.404	8	.128	10	.133	26
	54.2	.0848	28	.103	31	.0800	56
	64.6	.0631	25	.0603	33	.0472	71
	76.0	.0638	29	.124	28	.105	33
	86.9	.0621	24	.0437	24	.0518	25
	101	.0549	8	.0323	10	.0379	25
	115	.0523	8	.0446	14	.0421	7
	137	.0218	50	.0361	63	.0231	56
	157	.0235	17	.0223	13	.0255	45
159	17.0	0.393	23	0.713	23	0.403	28
	19.2	.658	33	.321	23	.461	31
	20.7	.372	25	.326	20	.175	28
	23.5	.273	11	.380	64	.245	8
	27.7	.242	17	.241	13	.187	20
	32.8	.116	23	.147	18	.111	23
	38.6	.220	19	.162	25	.132	21
	43.6	-	-	.115	17	-	-
	50.6	.109	30	.0673	22	.118	38
	57.5	.124	8	.175	18	.0760	7
	68.4	.0621	42	.0735	56	.0450	15
	78.6	-	-	.0583	14	.0481	38

Table C-23. - Superior Stone Company, Hi-Cone Quarry, Greensboro, N.C.

Test	Scaled distance ft/lb$^{1/2}$	Radial		Vertical		Transverse	
		Particle velocity, in/sec	Frequency, cps	Particle velocity, in/sec	Frequency, cps	Particle velocity, in/sec	Frequency, cps
160	8.34	1.30	63	2.10	63	2.42	56
	10.1	1.33	45	1.22	36	1.03	45
	12.2	.847	-	1.61	-	.893	-
	16.3	.758	29	.517	56	.624	20
	22.3	.599	33	.558	24	.858	50
	27.3	.413	29	.531	34	-	-
	34.4	.470	-	.250	-	.232	-
	42.1	.148	-	.162	-	.151	-
	52.8	.0788	100	.0962	125	.0800	56
	64.9	.109	19	.0661	19	.100	26

Table C-23. - Superior Stone Company, Hi-Cone Quarry, Greensboro, N.C. - Continued

Test	Scaled distance $ft/lb^{\frac{1}{2}}$	Radial		Vertical		Transverse	
		Particle velocity, in/sec	Frequency, cps	Particle velocity, in/sec	Frequency, cps	Particle velocity, in/sec	Frequency, cps
161...	9.73	1.63	31	1.16	45	2.02	42
	11.7	.957	36	1.67	33	2.03	29
	13.8	.881	50	1.49	50	1.47	33
	16.6	.967	-	.853	-	.933	-
	21.6	.702	36	.564	33	.387	33
	26.8	.539	28	.381	36	.553	31
	32.0	.289	21	.196	23	-	-
	38.4	.268	-	.207	-	.191	-
	47.5	.119	-	.139	-	.177	-
	58.9	.101	36	.0535	50	.101	45
	72.5	.118	26	.0439	29	.0727	36
162...	6.83	1.76	45	2.61	45	1.64	42
	8.51	1.60	50	2.06	45	1.46	45
	10.4	1.64	-	2.08	-	1.31	-
	14.0	1.47	36	.800	36	.579	45
	19.5	.933	36	.776	31	.696	38
	24.0	.702	36	.393	29	-	-
	30.4	.545	-	.346	-	.328	-
	37.3	.147	17	.176	28	.188	33
	46.9	-	-	.0943	125	.0719	50
	57.7	.126	-	.0833	-	.124	-
163...	6.83	1.73	38	3.22	56	3.80	63
	8.47	1.31	45	1.40	33	1.50	50
	10.5	.997	-	1.28	-	1.28	-
	14.3	-	-	.622	36	-	-
	19.8	.947	42	.462	22	.870	50
	24.5	.693	36	.652	28	.652	45
	31.0	.555	-	.249	-	.309	-
	38.1	.185	-	.193	-	.162	-
	47.9	.0897	83	.0847	125	.0709	100
	59.1	.164	33	.0776	56	.0835	38

Table C-24. - Warner Company Quarry, Union Furnace, Pa.

Test	Scaled distance, $ft/lb^{\frac{1}{2}}$	Radial		Vertical		Transverse	
		Particle velocity, in/sec	Frequency, cps	Particle velocity, in/sec	Frequency, cps	Particle velocity, in/sec	Frequency, cps
151...	3.39	4.85	11	8.73	19	6.94	12
	4.57	15.0	13	13.8	31	3.61	22
	6.22	6.79	10	7.46	28	5.48	14
	8.63	5.76	17	5.49	56	2.62	38
	11.9	3.68	33	2.19	71	2.68	38
	16.1	1.72	16	.954	42	.842	45
	20.2	1.67	14	1.04	50	.771	38
	69.0	.304	-	.195	-	.181	-
171...	3.39	6.77	10	10.2	30	6.67	-
	4.40	13.2	11	20.9	16	7.47	20
	6.04	9.26	20	8.85	19	5.60	28
	8.24	5.68	25	4.40	38	4.71	71
	11.1	6.67	22	4.17	31	2.24	38
	14.9	5.15	36	2.98	29	3.05	36
	20.3	2.07	24	1.56	38	1.48	42
	66.6	.127	-	.0799	-	.160	-

Appendix D.—Geology Description

A brief description of the geologic condition, face height, and overburden thickness at each site follows:

Site 1.—Weaver Quarry, Alden, Iowa. The quarry is in the Gilmore City Limestone. As exposed at the face, the rock is light tan, argillaceous, and loosely jointed. The floor of the quarry consists of a massive, oölitic limestone. There is no structural dip. The face height was 30 feet with 6 feet of overburden.

Site 2.—Webster City Quarry, Webster City, Iowa. The quarry is in a light brown, loosely jointed, dolomitic limestone of the Spergen Formation. There is no structural dip. The face height was 10 feet with 56 feet of overburden.

Site 3.—P & M Quarry, Bradgate, Iowa. The quarry is in the same geological setting as site 1. The face height was 24 feet with 2 to 12 feet of overburden.

Site 4.—Ferguson Quarry, Ferguson, Iowa. The quarry is in the same geologic setting as site 1. The face height ranged from 15 to 20 feet with 15 to 20 feet of overburden.

Site 5.—Shawnee Quarry, Shawnee, Ohio. The quarry is in the Columbus Limestone, in the general area of the Columbus Formation-type section. The Columbus Formation is typically a hard, flat-lying, thickly bedded, gray limestone, often slightly fractured and weathered in the upper levels, and hard and unfractured in the lower levels. The face height was 25 feet with 15 feet of overburden.

Site 6.—Hamilton Quarry, Marion, Ohio. The quarry was in both the Columbus and Delaware Formations (see site 5). The Delaware varies from an argillaceous, cherty, blue limestone to a very pure limestone and is flat-lying. The face height was 20 feet with 10 feet of overburden.

Site 7.—Flat Rock Quarry, Flat Rock, Ohio. The quarry in the Columbus Limestone (see site 5) had a face height of 50 to 55 feet with 9 feet of overburden.

Site 8.—Bellevue Quarry, Bellevue, Ohio. The quarry in the Columbus Limestone (see site 5) had a face height of 18 feet with 2 to 12 feet of overburden.

Site 9.—Bloomville Quarry, Bloomville, Ohio. Operating in both the Columbus and Delaware Formations, (see sites 5 and 6), the quarry had a face height ranging from 18 to 32 feet with 17 feet of overburden.

Site 10.—Washington, D.C.—The rock at the east approach of the Theodore Roosevelt Bridge over the Potomac River was a dark, greenish-gray, gneissoid diorite. The bedrock dips eastward away from the site. The overburden thickens from 5 feet at the working area to 50 feet at the end of the gage array.

Site 11.—Poughkeepsie Quarry, Poughkeepsie, N.Y. The quarry was in the Stockbridge Group, a tilted, jointed dolomite. The face height varied from 28 to 104 feet with overburden thickness ranging from 2 to 50 feet.

Site 12.—West Nyack Quarry, West Nyack, N.Y. The quarry is in the Palisade Diabase of Upper Triassic age. The face height varied from 20 to 45 feet with little or no overburden as the result of stripping.

Site 13.—Littleville Dam Site, Huntington, Mass. This test was the sinking of a 16½ by 21 foot shaft to a depth of 50 feet. The rock was a quartz-sericite schist with a pronounced foliation that dipped 60° to the west. The surface was irregular and ranged from exposed bedrock to 5 feet of glacial till.

Site 14.—Centreville Quarry, Centreville, Va. The quarry is on diabase of Triassic age and had a face height of 30 to 50 feet with 10 feet of overburden.

Site 15.—Manassas Quarry, Manassas, Va. In the Triassic diabase, the quarry had a face height of 22 to 45 feet with 6 feet of overburden.

Site 16.—Strasburg Quarry, Strasburg, Va. The quarry is in the New Market Limestone overlying the Beekmantown Formation which is quarried elsewhere but not utilized in this quarry. The New Market consists of thick-bedded, bluish-gray, fine- to medium-grained, crystalline dolomite, and compactly textured, blue- or dove-colored, coarsely fossiliferous limestone. The beds strike N. 75° E. and dip 30° to the southeast. The face height varied from 4 to 20 feet with 6 feet of overburden.

Site 17.—Chantilly Quarry, Chantilly, Va. This quarry in the Triassic diabase, had a face height of 34 to 45 feet with 4 feet of overburden.

Site 18.—Culpeper Quarry, Culpeper, Va. This quarry is in the Manassas Sandstone of Triassic age. The rock is a medium-bedded, fine-grained, red and gray sandstone composed mainly of quartz and feldspar and dips 6° to 8° to the northwest. There are three distinct sets of vertical joints that strike N 45° E, N 15° E, and east. The face height varies from 30 to 45 feet with 1 to 5 feet of overburden.

Site 19.—Doswell Quarry, Doswell, Va. This quarry is in the Baltimore granite-gneiss which is a fine- to medium-grained, light- to dark-gray gneiss. In places, the gneiss is coarse-grained with large phenocrysts. The gneissic structure strikes N 45° E and dips 45° to the southeast. The rock is highly jointed with the most prominent joint set striking N 55° W and dipping 70° NE. The height of the working face is 50 feet with 20 to 30 feet of overburden.

Site 20.—Riverton Quarry, Riverton, Va. This quarry is in the Beekmantown Formation and consists of medium- to thick-bedded, fine-grained, gray dolomites, interbedded with thick-bedded, fine-grained, gray limestones with calcite-filled fractures. The beds dip from 25° to 45° in an easterly direction. The only shot recorded was a toe shot with little or no overburden.

Site 21.—Jack Quarry, Petersburg, Va. This quarry is in the Baltimore granite-gneiss and is similar to the rock at site 19. Details on the structure and jointing were not available. The face height varied from 40 to 80 feet with 30 feet of overburden.

Site 22.—Buchanan Quarry, Greensboro, N.C. This quarry is in a granite diorite complex showing moderate to strong gneissic structure. Grain size varies from fine to coarse. The rock is moderately jointed and deeply weathered. The height of the working face varied from 27 to 50 feet with 30 feet of overburden.

Site 23.—Hi-Cone Quarry, Greensboro, N.C. This quarry is in a granite-gneiss similar to the rock at site 22. The height of the working face is 50 feet with 30 feet of overburden.

Site 24.—Union Furnace Quarry, Union Furnace, Pa. This quarry is operating in the Beekmantown Formation and the overlying strata, in the Rodman, Lowville, and Carlin. The Beekmantown contains thick-bedded dolomites with chert and thin-bedded, blue limestones. The overlying beds are dark, fine-grained, nearly pure limestones. The limestones have been folded and faulted with individual beds overturned. Joints are numerous and closely spaced. Only one large shot is fired annually with a face height of 185 to 200 feet. Overburden thickness ranges from 2 to 10 feet.

☆ U.S. GOVERNMENT PRINTING OFFICE: 1970 O—400-881